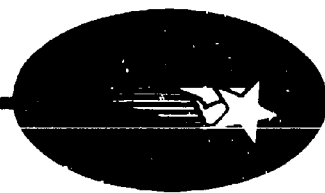


3-27-67-1 • VOL. 4 • NOVEMBER 1967



3-27-67-1 • VOL. 4 • NOVEMBER 1967

AD 664496

DASA 1917-4

# THERMAL RADIATION PHENOMENA

VOL. 4

## EXCITATION AND NON-EQUILIBRIUM PHENOMENA IN AIR

DISTRIBUTION  
OF THIS DOCUMENT  
IS UNLIMITED

FEB 2 1968

A 306

Reproduced by the  
CLEARINGHOUSE  
for Federal Scientific & Technical  
Information Springfield Va. 22151

DASA 1917-4  
3-27-67-1 Vol. 4  
November 1967

**THERMAL RADIATION PHENOMENA**

**Excitation and Non-Equilibrium  
Phenomena in Air**

by

**R. K. Landshoff and J. L. Magee**

Edited by

**John L. Magee and Henry Aroeste**

**Work performed under contract**

**DA-49-146-XZ-198**

## FOREWORD

"Thermal radiation" is electromagnetic radiation emitted by matter in a state of thermal excitation. The energy density of such radiation in an enclosure at constant temperature is given by the well known Planck formula. The importance of thermal radiation in physical problems increases as the temperature is raised; at moderate temperatures (say, thousands of degrees Kelvin) its role is primarily one of transmitting energy, whereas at high temperatures (say, millions of degrees Kelvin) the energy density of the radiation field itself becomes important as well. If thermal radiation must be considered explicitly in a problem, the radiative properties of the matter must be known. In the simplest order of approximation, it can be assumed that the matter is in thermodynamic equilibrium "locally" (a condition called local thermodynamic equilibrium, or LTE), and all of the necessary radiative properties can be defined, at least in principle. Of course whenever thermal radiation must be considered, the medium which contains it inevitably has pressure and density gradients and the treatment requires the use of hydrodynamics. Hydrodynamics with explicit consideration of thermal radiation is called "radiation hydrodynamics".

In the past twenty years or so, many radiation hydrodynamic problems involving air have been studied. In this work a great deal of effort has gone into calculations of the equilibrium properties of air. Both thermodynamic and radiative properties have been calculated. It has been generally believed that the basic theory is well enough understood that such calculations yield valid results, and the limited experimental checks which are possible seem to support this hypothesis. The advantage of having sets of tables which are entirely calculated is evident: the calculated quantities are self-consistent on the basis of some set of assumptions, and they can later be improved if calculational techniques are improved, or if better assumptions can be made.

The origin of this set of books was in the desire of a number of persons interested in the radiation hydrodynamics of air to have a good source of reliable information on basic air properties. A series of books dealing with both theoretical and practical aspects was envisaged. As the series materialized, it was thought appropriate to devote the first three volumes to the equilibrium properties of air. They are:

The Equilibrium Thermodynamic Properties of Air,  
by F. R. Gilmore

The Radiative Properties of Heated Air,  
by B. H. Armstrong and R. W. Nicholls

Tables of Radiative Properties of Air,  
by Lockheed Staff

The first volume contains a set of tables along with a detailed discussion of the basic models and techniques used for their computation. Because of the size of the related radiative tables and text, two volumes were considered necessary. The first contains the text, and the second the tables. It is hoped that these volumes will be widely useful, but because of the emphasis on very high temperatures it is clear that they will be most attractive to those concerned with nuclear weapons phenomenology, reentry vehicles, etc.

Our understanding of kinetic phenomena, long known to be important and at present in a state of rapid growth, is not as easy to assess as are equilibrium properties. Severe limitations had to be placed on choice of material. The fourth volume is devoted to general aspects of this topic. It is:

Excitation and Non Equilibrium Phenomena in Air,  
by Landshoff, et al.

It provides material on the more important processes involved in the excitation of air, criteria for the validity of LTE and special radiative effects.

A discussion of radiation hydrodynamics was felt to be necessary and the fifth volume which deals with this topic is:

Radiation Hydrodynamics of High Temperature Air,  
by Landshoff, Hillendahl, et al.

It reviews the basic theory of radiation hydrodynamics and discusses the application to fireballs in the atmosphere.

The choice of material for these last two volumes was made with an eye to the needs of the principal users of the other three volumes.

Most of the work on which these volumes are based was supported by the United States Government through various agencies of the Defense Department and the Atomic Energy Commission. The actual preparation of the volumes was largely supported by the Defense Atomic Support Agency.

We are indebted to many authors and organizations for assistance and we gratefully acknowledge their cooperation. We are particularly grateful to the RAND Corporation for permission to use works of F. R. Gilmore and H. L. Brode and to the IBM Corporation for permission to use some of the work of B. H. Armstrong. Most of the other authors are employed by the Lockheed Missiles and Space Company, in some cases as consultants.

Finally, we would like to acknowledge the key role of Dr. R. E. Meyerott of LMSC in all of this effort, from the initial conception to its realization. We are particularly grateful to him for his constant advice and encouragement.

Criticism and constructive suggestions are invited from all readers of these books. We understand that much remains to be done in this field, and we hope that the efforts represented by this work will be a stimulus to its development.

The Editors

J. L. Magee

H. Aroeste

R. K. M. Landshoff

## EXCITATION AND NON-EQUILIBRIUM PHENOMENA IN AIR

### Table of Contents

Chapter 1.	Introduction (J.L. Magee, R.K. Landshoff, and D.H. Holland)	1
Chapter 2.	Interaction of Photons and Charged Particles with Air Molecules (R.K. Landshoff)	
2.1	Absorption and scattering of X-rays and $\gamma$ -rays	11
2.2	Auger electrons	14
2.3	Heavy particle collision phenomena	16
2.4	Collision phenomena of fast electrons	27
2.5	Collision phenomena of slow electrons	34
Chapter 3.	Secondary Processes Following Excitation of Air (R.K. Landshoff, J.L. Magee, M. Scheibe)	
3.1	Disposition of the energy lost by primary electrons	62
3.2	Atmospheric fluorescence	67
3.3	Thermalization and capture of subexcitation electrons	72
3.4	Secondary molecular processes	77
3.5	Chemical contaminants resulting from absorption of radiation	92
Chapter 4.	X-ray Heating of Air (R.K. Landshoff)	
4.1	Introduction	110
4.2	Energy deposition in the stripping region	112
4.3	Energy deposition at large distances	125
4.4	Asymptotic approximation for the energy deposition	127
Chapter 5.	Shock Heating of Air (R.K. Landshoff)	
5.1	Standard hydrodynamic approach	130
5.2	Very strong shocks	133
5.3	Radiative preheating	138

<b>Chapter 6.</b>	<b>The Approach to Composition Equilibrium in Air</b> (J.L. Magee, M. Scheibe, H. Aroeste)	
6.1	Introduction	143
6.2	Remarks on notation	149
6.3	The system of equations	151
6.4	Linear form of equations	154
6.5	The low-temperature reactions of air	159
6.6	The relaxation of air at low temperatures	164
6.7	The high temperature reactions of air	165
6.8	The relaxation of air at high temperatures	169
6.9	Composition relaxation of air following a sudden change in energy content	171
<b>Chapter 7.</b>	<b>Adiabatic, Near Equilibrium Cooling of Air</b> (M. Scheibe and J.L. Magee)	
7.1	The linear equations and their solution	175
7.2	Relation of temperature and density changes	178
7.3	The relaxation process	180
7.4	The criterion for LTE	183
<b>Chapter 8.</b>	<b>Non-Equilibrium Radiative Transport</b> (D.H. Holland)	
8.1	Introduction	195
8.2	The transport equation	197
8.3	Non-equilibrium occupation numbers	201
8.4	Non-equilibrium transport equation	205
8.5	Collision limited radiation from an optically thin gas	209
8.6	Radiation from a semi-infinite slab	214
8.7	Radiation from a finite slab	222
8.8	Spectrum of emitted radiation	224
8.9	Resonant scattering	226
8.10	Summary and conclusions	230

<b>Chapter 9.</b>	<b>Radiation in Tenuous Air at High Temperatures (A.E. Kingston)</b>	
9.1	Introduction	233
9.2	Properties of a large sphere of hot hydrogen	234
9.3	Model for sphere of hot air	249
9.4	Conclusions	255
<b>Chapter 10.</b>	<b>Radiation in Tenuous Air with Contaminants at Low Temperatures (M. Scheibe)</b>	
10.1	Radiation of air at low temperatures	264
10.2	Collision excitation mechanisms	266
10.3	Collision limiting of emitted radiation	272
10.4	Excitation by electron recombination	276
10.5	Conclusions	
<b>Appendix A.</b>	<b>The Approach to Equilibrium of a Displaced System (J.L. Magee)</b>	282
<b>Appendix B.</b>	<b>Table of the States and Spectra of the Metallic Monoxides (R.W. Nicholls)</b>	289

Work on this volume has been carried out under the guidance of R. K. Landshoff and J. L. Magee. The actual authorship, which they share with several other members of the Lockheed (LMSC) Staff, is indicated in the Table of Contents. Particular thanks are due to Dr. A. E. Kingston, a temporary LMSC staff member now at Queen's University, Belfast, for writing Chapter 9.

## Chapter 1. INTRODUCTION

This volume originated as part of a comprehensive study of nuclear fireballs. Its primary objectives are to determine the conditions under which equilibrium assumptions provide a valid basis for fireball calculations, and to derive alternative formulations for use in situations where equilibrium does not obtain. Our attention is accordingly directed almost exclusively to the interactions which occur in air, and frequently to an energy flux so large that only a nuclear detonation could have produced it.

In spite of the specific nature of the problems attacked, however, we hope that the development is sufficiently general to be of use to workers in other fields. In particular, much of the information contained herein is directly applicable to the study of ionization and contaminants produced in the ionosphere under naturally occurring conditions, and can also be applied to the environment of re-entry vehicles. Furthermore, various laboratory plasmas and shock tubes produce situations which closely resemble certain regimes encountered in the atmospheric response to a nuclear detonation. Indeed, one can with some justification view a nuclear detonation as a large-scale experiment to obtain information of general physical interest.

The general problem discussed in the following pages is the response of a system to changes in its energy content. We characterize all processes other than heat conduction by which the energy of the system is increased as "excitation". Excitation processes considered in detail include energy deposition by energetic atomic particles, x-rays, thermal radiation, and hydrodynamic shock waves. The energy loss mechanisms considered are

mechanical work on its surroundings performed by the system during an adiabatic expansion, and radiative energy loss from the system.

Two classes of the general problem are discussed in the following chapters. In the first we imagine a sudden change in the energy of a system. As a result the system is displaced from equilibrium. The return to equilibrium, with no further energy change, is the process of relaxation. Study of relaxation in air from states produced by various initial stimuli constitutes a substantial portion of the succeeding development.

The second class of problems involves the continuous gain or loss of energy by the system, with both gain and loss mechanisms simultaneously operative in some cases. In such situations the system will generally assume a non-equilibrium configuration which may be slowly varying. We characterize such a situation as a quasi-steady state, and sometimes speak of the system as being in equilibrium with the source (or sink) of energy. This situation is not to be confused with true thermodynamic equilibrium, and in practice little danger of confusion arises from the terminology.

The organization of the material presented here is based on another classification of problems. We can summarize it as follows:

- (a) Problems which must be discussed in terms of individual collision processes and detailed bookkeeping procedures. The best example of this class is x-ray absorption in air. Chapters 2, 3, and 4 are devoted to various aspects of these problems.
- (b) Problems which are best discussed with reference to local thermodynamic equilibrium (LTE). Particle collision rates are high and all displacements from LTE are relatively small. Chapters 5, 6, and 7 are devoted to problems of this type.

- (c) Problems which involve the thermal radiation field in an important way. In such cases particle collision rates are relatively low, or the system is small with respect to important radiative mean free paths. Chapters 8, 9, and 10 are devoted to consideration of such matters.

Now we shall proceed to describe in somewhat more detail the material presented here, based on the chapter organization.

Absorption of x- or  $\gamma$ -rays in air produces conditions which vary with the energy density of the deposit. At low energy densities air is displaced from equilibrium in a manner which requires very long times for relaxation to true equilibrium. For such small increases of energy density there is no change in equilibrium molecular composition of air; the only change is a slight increase in temperature. On the other hand, the absorption of x-rays creates many extraneous high-energy intermediates such as free electrons, positive and negative ions, and atoms. These intermediates react in various ways to produce molecular products such as  $O_3$ ,  $NO$ , which must be decomposed into  $O_2$  and  $N_2$  before equilibrium is attained, and because of the low temperature of the system, the time required is very long. The description of the behavior of air under such conditions requires a great deal of information on the interaction of the air molecules with a variety of particles. Almost all of the interactions of interest occur between the particles and air molecules in their ground states. Some of the required data on cross sections, mechanisms, etc. are discussed in Chapters 2 and 3. Generally speaking, in such cases one is interested in displaced states which are far from equilibrium and a great deal of bookkeeping is involved.

At the other extreme are problems involving absorption of x-rays at high energy density, or x-ray heating of air. In this case, because of the substantial increase in energy density, the equilibrium composition of air is changed. Electrons and ions formed in the x-ray absorption and particle impact processes are also present at equilibrium, reaction rates are high, and such air relaxes in very short times. Here a problem of great importance is the maximum energy which can be absorbed from a flux of x-rays. As absorption continues, each atom will absorb several photons and it is clear that after all electrons are removed from the atoms, further absorption cannot occur. The magnitude of the energy density in the air when saturation is reached depends upon a number of parameters, such as photon energy, air density, and flux density. These problems are discussed at some length in Chapter 4 along with some detailed considerations of the energy deposit in air from point x-ray sources. The latter is a specific problem of great interest in the study of fireballs formed by nuclear weapons.

The formation and growth of a nuclear fireball is essentially a problem in radiation hydrodynamics. The basis for a great deal of radiation hydrodynamics is the older "standard" form of hydrodynamics which neglects radiation. This theory is reviewed briefly in Chapter 5 and is followed by a discussion of the modifications to the theory required for the inclusion of effects of thermal radiation. Two principal effects are discussed. The first is the weakening of very strong shocks by radiation losses, and the second is the occurrence of radiation waves as precursors of strong shocks. It should be emphasized that the role of thermal radiation here is relatively minor in the sense that LTE is almost maintained in the air under such conditions.

A question of extreme importance in radiation hydrodynamics is whether or not LTE is a valid approximation in a given case. The principal purpose of Chapters 6 and 7 is to investigate this question in as systematic a manner as possible. In this discussion conditions are such that particle collision rates are high and effects of thermal radiation are neglected. Relative to each other, the relaxation rates of various collision processes show considerable differences. It is instructive to make this comparison in terms of the number of collisions required for each type.

Displacements from LTE can occur in energy distribution as well as in composition. For a given composition of the system, energy is distributed among four forms: translational, rotational, vibrational, and electronic. The most rapid adjustment in energy distribution occurs in the translational form, and it is frequently said that this requires only one collision time. Rotational relaxation is also known to be fast and is a few collision times for diatomic molecules in the temperature ranges of interest here. The situation with vibrational energy is more complicated and is reviewed briefly in Chapter 6. The point of principal concern is that vibrational relaxation is faster than composition relaxation. Finally, electronic energy relaxation is only of concern in special cases. Usually, the amount of energy involved in electronic excited states of a system is negligible and the numbers of excited species small enough to be unimportant. Of course, it is understood that our classification of electronic excitation does not include ionization which is a composition change; very large amounts of energy can be involved in the latter.

A great deal of attention has recently been given to composition relaxation in air. Two types of studies have been made:

- (1) Numerical studies of the rate equations for displaced systems with specific initial conditions
- (2) General studies of the relaxation of small displacements from equilibrium.

In all of this work it is assumed that, except for composition, the system is completely relaxed. In (1) it is found that as a practical matter only certain of the rate processes are important at any time and many of the concentrations are in "steady states". It can usually be understood why the equations depend more upon certain of the constants than others. On the other hand, the set of equations must actually be solved for each initial condition of interest, and there is usually a very significant sensitivity of the computed results to the rate constants used.

In (2) there is the advantage that the system of equations can be treated in general because for small displacements they become linear. In this case precise meaning can be given to "relaxation time". As before, however, there is sensitivity to the rate constants used and, of course, there is a very definite limit on the magnitude of displacement which can be considered in this manner. As a practical matter, calculations in hydrodynamics and radiation hydrodynamics must at the present state of the art be based on LTE with non-equilibrium effects considered as perturbations. For this reason it is of great importance to have a means for estimating the extent of deviations from LTE in the most general manner possible. We have attempted to use method (2) for this purpose. Criteria for validity of the use of LTE are developed in Chapters 6 and 7.

The first type of situation in which the adequacy of LTE is questionable occurs in air which has been heated suddenly by the addition of energy, such as in x-ray absorption or shock heating. If LTE is to be considered adequate, the relaxation time must be shorter than other times of significance in the particular situation. The study of relaxation times in this context is made in Chapter 6.

Another situation in which a criterion for the applicability of LTE is needed occurs when a parcel of air is subjected to a continuous change, such as in cooling during expansion following passage of a shock wave. Here the system is displaced slightly from LTE, the magnitude of the displacement depending upon the superimposed rate of change. Formulation of a criterion for this case is considered in Chapter 7.

Most of the non-equilibrium phenomena so far mentioned have not involved thermal radiation explicitly. In almost all of the cases of interest to us, the total amount of energy in the thermal radiation field is very small, negligible for such purposes as energy balance. This is certainly true for all cases in which the temperature is low enough so that molecules exist. However, radiative processes can have large effects on systems of interest, and in Chapters 8, 9, and 10 we shall be concerned with several special problems. These involve systems in which certain radiative mean free paths are large compared with the dimensions of the system and cases where the collisional excitation rate is too low to maintain LTE.

The optical properties of a gas are determined jointly by the occupation numbers of the various states of the atomic particles which constitute the gas, the optical transition probabilities among these states, and the profiles of the lines corresponding to these transitions. Implicitly the state of the

thermal radiation field is involved through these variables. In many situations the occupation numbers have the values corresponding to thermodynamic equilibrium at some temperature, and hence can be expressed according to the laws of statistical mechanics in terms of temperature, density and the statistical weights and energy levels of the states. In this case, the only additional information required to write down the transport equation governing the flow of radiation in the gas is knowledge of the various transition probabilities and the corresponding line shapes.

Most conventional treatments of radiation transport are based on the assumption of LTE. Such calculations have been used with considerable success to interpret radiative transport phenomena occurring under a wide range of conditions, e.g., in stars, nuclear fireballs, and laboratory plasmas. In a tenuous gas, however, the rate of collisions which excite the upper states may be so small compared to the rate at which the excited states radiate that the equilibrium occupation numbers cannot be maintained. The populations of the upper states may then be smaller than the equilibrium value, and depend on the frequency of exciting collisions, the optical transition probabilities, and the light intensity. Indeed, since the interaction between light and matter is essentially a scattering process under these conditions, the very concept of occupation numbers is of questionable validity in describing the system.

One might expect, therefore, that in some situations the rate of radiation from a tenuous gas is smaller than that predicted on the basis of the assumption of equilibrium, and is determined at least partially by the rate of collisional excitation. If this is the case, the radiation is said to be

collision limited, and the assumption of LTE is invalid. Within the last few years, various astrophysicists have come to realize that there is no general a priori justification for the assumption of LTE, and that in many cases of interest the conditions for LTE are not satisfied. As a result, a whole school devoted to the study of non-LTE transport has come into being.

In Chapter 8 the non-LTE theory of radiative transport is briefly presented in an elementary manner. Various features of non-LTE radiation are developed and illustrated through example calculations.

In Chapter 9 a particular problem of considerable interest is discussed, the radiative cooling of a tenuous sphere of hot gas. This is a non-LTE problem of a different type from that discussed in Chapter 8. The gas loses energy by radiation, causing a decrease in the population of the excited states. At the same time the excited states are being repopulated by recombination of free electrons, and this supplies the energy for further radiation. Thus the recombination of electrons plays a dominant role in determining the rate of radiation and composition of the gas. Under these conditions the rate of radiation is found to be larger than the rate from a gas in LTE with the same energy content, density, and dimensions.

The gas of most interest for the present work is, of course, air. However, first the simpler problem of the cooling of a sphere of hydrogen is studied. Scaling laws are derived which make possible use of the results found for hydrogen in calculations for cooling of a sphere of nitrogen. Under the conditions of interest, the behavior of a sphere of nitrogen provides a good approximation to that of hot air. This work furnishes a detailed example of a system with a quasi-steady displacement from its LTE energy distribution.

In Chapter 10 the emission of radiation from tenuous air under non-LTE conditions at relatively low temperatures is discussed. Since the emissivity of air decreases sharply with decreasing temperature, the possible contribution from impurities is also considered. Some of the results of Chapter 8 are applied to this case. In addition, the effect on the radiation by the electron recombination mechanism discussed in Chapter 9 is treated.

## Chapter 2. INTERACTION OF PHOTONS AND CHARGED PARTICLES WITH AIR MOLECULES

### 2.1 Absorption and scattering of X-rays and gamma-rays

The photon energies covered in this section are much larger than those which lead to the excitation of a bound electron to another bound state and smaller than those which lead to pair production. In that energy range the processes of concern are photoelectric absorption and Compton and Rayleigh scattering.

The photoelectric and the Compton interaction both liberate bound electrons. In the first mentioned process the photon transfers its entire energy to the electron and disappears in the act and in the latter it transfers only part of its energy. Photoelectric absorption dominates below 50 keV and Compton scattering takes over at higher energies. In contrast to the incoherent Compton scattering, Rayleigh scattering is coherent and the photons don't transfer any energy to the electrons. At low photon energies Rayleigh scattering outweighs Compton scattering and at high energies the balance changes around. In air the cross-over point is at about 12 keV.

In the analysis of energy deposition by X-rays and gamma-rays, scattering processes play a double role. On the one hand the partial energy transfer by Compton collisions must be added to the energy transfer by photoelectric processes. On the other hand the directional changes due to scattering delay the escape of photons from a given region of space and increase the probability that they will deposit their energy in that region.

For numerical calculations of the energy deposition by X-rays and gamma-rays one needs certain cross-sections and related quantities as follows.

1) The cross-sections  $\sigma_{P.E.}$ ,  $\sigma_C$  and  $\sigma_R$  for photoelectric, Compton and Rayleigh collisions. The latter two are averaged over the possible directions of the scattered photon. In place of the cross-sections which are expressed in units like, e.g.,  $\text{cm}^2/\text{atom}$ , one can also use absorption and scattering coefficients per unit mass or volume, i.e.  $K = \frac{N\sigma}{A} \frac{\text{cm}^2}{\text{g}}$  or  $\mu = \rho K \text{ cm}^{-1}$  where  $N$  is Avogadro's number,  $A$  the average atomic weight and  $\rho$  the density.

2) The average energy transfer  $\overline{\Delta h\nu}$  in the Compton collision of a photon.

In addition it is useful to introduce certain combinations of these quantities which enter directly into the calculations. These are:

3) The Compton absorption coefficient

$$K_{C.A.} = \frac{\overline{\Delta h\nu}}{h\nu} K_C \quad (2.1-1)$$

4) The total absorption coefficient

$$K_{Abs} = K_{P.E.} + \frac{\overline{\Delta h\nu}}{h\nu} K_C \quad (2.1-2)$$

5) The total scattering coefficient

$$K_S = K_C + K_R \quad (2.1-3)$$

6) The total attenuation coefficient

$$K_{Att} = K_{P.E.} + K_S \quad (2.1-4)$$

Figs. 2-1 to 2-3 show the energy dependence of the coefficients  $K_{P.E.}$ ,  $K_A$ ,  $K_C$  and  $K_S$  in N, O and air. The data for  $K_{P.E.}$  have been taken from a compilation by Gilmore (1959). The remaining data come from recent calculations by Veigele et al. (1965) which treat the scattering from bound electrons. Fig. 2-4 shows the ratios  $K_{P.E.}/K_S$ , the average fractional energy transfer per Compton collision  $\frac{\Delta h\nu}{h\nu}$  and the average fractional energy transfer for combined photoelectric and scattering processes  $K_{Abs}/K_{Att}$ .

An ejected electron acquires that part of the energy which is not used to overcome its binding energy. For energies exceeding the K shell binding energy  $h\nu_K$ , removal of the K electron is about 20 times more probable than removal of an L electron. In either case the liberated electron has the kinetic energy  $h\nu - h\nu_n$ , where the binding energies  $h\nu_n$  are given in Table 2.1. The structure of the K absorption edges shows a few discrete lines followed by a continuum. The onset of the continuum which determines  $h\nu_K$  is not sharp enough to be measured directly and must be evaluated by an extrapolation procedure. The edge structure of  $N_2$  and  $O_2$  has been recently measured by Hartmann and Chun (1964) and the listed values  $h\nu_K$  represent their interpretation of these data. These values are larger than earlier listings by Fine and Hendee (1955). The emission lines  $h\nu_{KL}$  whose determination is more straightforward are taken from the compilation by Fine and Hendee. The ionization energies  $h\nu_L$  are known from spectroscopic data and are taken from the potential energy curves presented by Gilmore (1965). We note that they differ from the ionization energies 14.55 eV and 13.61 eV for atomic N and O.

Table 2.1 X-Ray Absorption Edges and K Emission Lines in eV

	$h\nu_K$	$h\nu_{KL}$	$h\nu_L$
$N_2$	410	392	15.6
$O_2$	541	523	12.1

## 2.2 Auger electrons

A vacancy created in the K shell by photoelectric absorption can be filled with the simultaneous emission of an X-ray quantum ( $K\alpha$ ) which carries away the energy difference  $h\nu_{KL}$ . This is, however, a relatively rare process which occurs with only about 1% probability.

Much more frequently the transition of one of the electrons to the K shell is accompanied by ejection of another one of the electrons - the so-called "Auger effect". In the case of  $N_2$  and  $O_2$  an experimental study by Mehlhorn (1960) of the energy distribution of these Auger electrons shows them to occur in two groups whose average energies are listed in Table 2.2. If  $E_A$  is the energy carried away by the liberated electrons the doubly ionized molecules are left behind with the energy  $h\nu_K - E_A$ . From the Auger spectra one can therefore identify two levels of  $N_2^{++}$  as

Table 2.2 Energies of Auger Electrons in eV

	$E_{A1}$	$E_{A2}$
$N_2^+ \rightarrow N_2^{++} + e$	360	336
$O_2^+ \rightarrow O_2^{++} + e$	490	463

well as of  $O_2^{++}$ . Levels of these ions can also be reached by electron bombardment of the neutral molecules. To discriminate the doubly charged molecular ions from other ions Dorman and Morrison (1963) have made a mass spectroscopic analysis of the isotopic molecules  $N^{14}N^{15}$  and  $O^{16}O^{17}$  and have determined the appearance potentials. The ion  $N_2^{++}$  has two closely spaced levels whose average energy lies 43 eV above the ground state of the neutral molecule and  $O_2^{++}$  has a level at 36 eV. Using the binding energies listed in Table 2.1 the calculated levels  $h\nu_K - E_{A_1}$  of  $N_2^{++}$  and  $O_2^{++}$  lie somewhat higher than the observed appearance potentials. This may be due to the presence of a number of excited states of these ions. The existence of such states has been demonstrated theoretically by Hurley (1962) who obtained the potential curves of such ions by adding the Coulomb repulsion of two positive charges to the known potential curves of the isoelectronic neutral molecules. The energy spread of the observed Auger electrons is sufficiently wide to hide most of the level structure and make the levels blend into broad groups whose centers lie above the ground state energies.

It is important to note that recent experiments by Carlson and Krause (1965) have shown that a single photon can remove as many as 5 electrons from a neon atom. The probability for this is small but 25% of the atoms had three or more electrons removed. The additional electrons have much less energy than the photoelectron and the fast Auger electron. Such experiments have not been performed with  $N_2$  or  $O_2$  but it is quite likely that one would in that case also find additional ionization processes.

The practical significance of the release of two or even more electrons per photon is not that it would result in more ionization because ordinarily the direct ionization by X-ray absorption accounts only for a small fraction of the final amount of ionization. The bulk of the ionization is caused subsequently when the fast primary electrons collide with the air molecules. The true practical significance arises in regions of where the X-ray flux is so intense that it produces complete stripping with less than 1 photon per electron. This mechanism will be discussed in section 4.

### 2.3 Heavy particle collision phenomena

In this section the different mechanisms contributing to the stopping power of the atmosphere for neutral and ionized heavy particles are reviewed. The slowing down of a heavy particle is due to its elastic and inelastic collisions with the ambient atoms, and of the latter collisions we consider those giving rise to ionization, electron capture, and electron loss.

Elastic collisions dominate the energy loss for particle velocities below about  $5 \times 10^7$  cm/sec. The loss rate of the kinetic energy  $K_1$  is governed by the transport cross section  $\sigma_{tr}$  according to the law

$$\frac{dK_1}{dx} = -n_2 \sigma_{tr} K_1 \quad (2.3-1)$$

where  $n_2$  is the number density of atoms in the ambient air. If  $R$  is the impact parameter for a collision where  $K_1$  is reduced by  $\Delta K_1$  the transport cross section is calculated by the formula

$$\sigma_{tr} = \frac{2\pi}{K_1} \int |\Delta K_1| R dR \quad (2.3-2)$$

Designating the ambient particle with the index 2, the energy loss in an individual collision is

$$\Delta K_1 = - \left[ \frac{M_2}{M} |\Delta E| + \frac{2M_1 M_2}{M^2} K_1 (1 - r \cos \theta) \right] \quad (2.3-3)$$

where  $|\Delta E|$  is the inelastic loss and  $\theta$  the scattering angle in the center of mass system of the two colliding particles. We also have introduced  $M = M_1 + M_2$  and  $r = \sqrt{1 - \frac{M}{M_2} \frac{|\Delta E|}{K_1}}$ . Expanding  $r$  leads to the approximate expression

$$\Delta K_1 = - \frac{2M_1 M_2}{M^2} K_1 (1 - \cos \theta) + \frac{M_2 + M_1 \cos \theta}{M} \Delta E \quad (2.3-4)$$

Since small angle collisions dominate the inelastic part can be further simplified by setting  $\cos \theta$  in the second term equal to unity which leads to

$$\Delta K_1 = - \frac{2M_1 M_2}{M^2} K_1 (1 - \cos \theta) + \Delta E \quad (2.3-5)$$

Entering this into Eq. (2.3-2) one obtains

$$\sigma_{tr} = \sigma_{el} + \sigma_{inel} \quad (2.3-6)$$

with

$$\sigma_{el} = \frac{4\pi M_1 M_2}{M^2} \int (1 - \cos \theta) R dR \quad (2.3-7)$$

$$\sigma_{inel} = \frac{2\pi}{K_1} \int |\Delta E| R dR \quad (2.3-8)$$

The cross sections for these two types of collisions have been calculated with the assumption that the colliding particles can be represented by the Thomas-Fermi model of the atom. In that theory the electron distributions of different species of atoms are given by the same universal distribution function of the radius as measured in units of the scaling length

$$a = 0.8853 a_0 Z^{-1/3} = 4.685 \times 10^{-9} Z^{-1/3} \text{ cm} \quad (2.3-9)$$

where  $a_0$  is the Bohr radius and where the charge  $Z$  entering the scaling length is

$$Z = (Z_1^{2/3} + Z_2^{2/3})^{3/2} \quad (2.3-10)$$

This choice combines the effect of the two colliding atoms as suggested by Bohr (1948).

With Thomas-Fermi scaling the integral in Eq. (2.3-7) becomes

$$\int (1 - \cos \theta) R dR = a^2 \sigma_{el}^*(\epsilon) \quad (2.3-11)$$

where

$$\epsilon = \frac{1}{2} \frac{M_1 M_2}{M_1 + M_2} \frac{a v^2}{Z_1 Z_2 e^2} \quad (2.3-12)$$

is a dimensionless measure of the energy in the center of mass system.

For numerical work it is more convenient to rewrite  $\epsilon$  as

$$\epsilon = 1.63 \times 10^{-14} \frac{A_1 A_2}{A_1 + A_2} \frac{v^2}{Z_1 Z_2 Z^{1/3}} \quad (2.3-13)$$

or as

$$\epsilon = 32.5 \frac{A_2}{A_1 + A_2} \frac{\bar{K}_1}{Z_1 Z_2 Z^{1/3}} \quad (2.3-14)$$

where  $A_1$  and  $A_2$  are atomic weights,  $v$  the velocity in cm/sec and  $\bar{K}_1$  the kinetic energy of the moving particle in keV.

Published results for  $\sigma_{el}^*$  by Firsov (1958) and by Lindhard et al. (1963) differ somewhat. We have repeated the calculation without making the mathematical approximations of the above authors and obtained results by and large intermediate between the older ones. The applications described below are based on Firsov's cross section because at the time it was the only one available. That cross section can be fitted by the expression

$$\sigma_{el}^* = \frac{1}{2\epsilon^2} \ln(1 + 0.7 \epsilon) \quad (2.3-15)$$

Actually the difference between this expression and the more accurate results arise only in the low energy region where the distance of closest approach between the collision partners is large and where the Thomas-Fermi potential does not drop off rapidly enough. To make a significant improvement one should use a more realistic potential for the cross section calculations.

To obtain the energy loss due to excitation and ionization, Firsov (1959) assumes that there is a friction-like force between the orbital electrons of the two atoms while they are passing each other. The resultant conversion of the kinetic energy of relative motion into excitation energy, is due to the transfer of momentum by electrons from one particle to the other in the region where the electronic shells overlap. The energy lost to electron excitation or ionization at a given impact parameter  $R$  and velocity  $v$  is

$$|\Delta E| = \frac{0.35 (Z_1 + Z_2)^{5/3} \hbar v / a_0}{(1 + 0.16 (Z_1 + Z_2)^{1/3} R / a_0)^5} \quad (2.3-14)$$

where  $a_0 = \hbar^2 / m e^2$ . Entering this into Eq. (2.3-8) leads to

$$\sigma_{inel} = 7.15 (Z_1 + Z_2) \frac{E_0}{K_1} \frac{\hbar v}{e^2} a_0^2 \quad (2.3-15)$$

where  $E_0 = e^2 / a_0$  has been introduced to make the dimensions evident.

The inelastic cross section does not scale in the same manner as the elastic one, but it is nevertheless convenient to take out the factors appearing in Eqs. (2.3-7) and (2.3-11) and to write the cross section in the form

$$\sigma_{inel} = 4\pi a^2 \frac{M_1 M_2}{M^2} \sigma_{inel}^* \quad (2.3-16)$$

Doing this, Firsov's result can be expressed by writing

$$\sigma_{inel}^* = \frac{K}{\sqrt{\epsilon}} \quad (2.3-17)$$

with

$$K = K_F = 0.0225 \left( \frac{Z}{Z_1 Z_2} \right)^{1/2} (Z_1 + Z_2) \left( \frac{A_1 + A_2}{A_1 A_2} \right)^{3/2} A_2 \quad (2.3-18)$$

The inelastic cross section has also been evaluated by Lindhard et al. In this instance the model is entirely different and is based on an idea by Fermi and Teller (1947). Essentially one calculates the momentum and energy transfer from the incoming charged particle to the individual electrons of the target atom by classical mechanics assuming a Coulomb interaction. Then one excludes those orbits where the final state of the electron would be one which is already occupied. This amounts to keeping the impact parameter below a certain limit at which the energy transfer is large enough to be possible. Fortunately the maximum impact parameter occurs inside a logarithm so that the precise way of choosing it does not have a very large effect on the final result. The cross section based on this model has the same energy dependence as that obtained by Firsov so that one can also use Eqs. (2.3-16) and (2.3-17) but with a different factor  $K$ . Details of Lindhard's calculation are not available in published form but from the final result quoted in the article to which we have referred, we obtain

$$K = K_L = 0.08 \left( \frac{Z_1 Z_2}{Z} \right) \left( \frac{A_1 + A_2}{A_1 A_2} \right)^{3/2} A_2 Z_1^{1/6} \quad (2.3-19)$$

A list of coefficients calculated for various ions passing through air is given in Table 2.3.

Table 2.3 The Coefficient K Entering Eq. (2.3-17) for the Inelastic Cross Section as Calculated by Firsov and Lindhard

	Li	N	Al	Fe	W	U
$K_F$	.300	.153	.125	.138	.242	.278
$K_L$	.195	.132	.111	.104	.110	.113

After combining the elastic and inelastic cross sections as in Eq. (2.3-6) the resulting transport cross section can be entered into Eq. (2.3-1) to find the particle range. The integrated form of that equation is

$$\int_{x_0}^{x_1} n dx = \frac{(A_1 + A_2)^2}{4\pi a^2 A_1 A_2} \left( L(\epsilon_0) - L(\epsilon_1) \right) \quad (2.3-20)$$

$$L(\epsilon) = \int_0^{\epsilon} \frac{d\epsilon'}{\epsilon' \sigma^*(\epsilon')} \quad (2.3-21)$$

where

$$\epsilon \sigma^*(\epsilon) = K\sqrt{\epsilon} + \frac{1}{2\epsilon} \ln(1 + 0.7 \epsilon) \quad (2.3-22)$$

The function  $\frac{L(\epsilon)}{\epsilon}$  is presented graphically in Fig. 2.5. To obtain the range of a particle travelling in a horizontal direction or at a low enough altitude the particle density  $n$  can be taken out of integral in Eq. (2.3-20). At high altitudes and for a particle travelling at an angle  $\zeta$  with the vertical

we find the altitude at the end point from the relation

$$\int n dx = 4.2 \times 10^{22} \frac{|p_1 - p_0|}{g \cos \zeta} \quad (2.3-22)$$

where the pressures are in dynes/cm<sup>2</sup>.

To account for the energy which is spent in inelastic collisions one has a large variety of processes in which the incoming or the target particle or maybe both are being raised to excited states. Firsov (1959) has interpreted the area  $\pi R^2$ , where the energy loss given by Eq.(2.3-14) exceeds the ionization energy  $E_1$  of the gas atoms, as the cross section for their ionization by fast ions. With this interpretation he is led to the ionization cross section formula

$$\sigma = \sigma_0 \left[ (v/v_0)^{1/5} - 1 \right] \quad (2.3-23)$$

with

$$\sigma_0 = \frac{32.7}{(Z_1 + Z_2)^{2/3}} 10^{-16} \text{ cm}^2 \quad (2.3-24)$$

and

$$v_0 = \frac{23.3 E_1}{(Z_1 + Z_2)^{5/3}} 10^6 \text{ cm/sec} \quad (2.3-25)$$

$E_1$  in (eV) being the first ionization potential of the gas atom. The cross section formula is intended to apply only when the incoming particles are ions so that their further ionization is much less probable than the ionization

of the target particles. The formula is also limited to velocities of the incoming particle below the orbital velocity of the electron to be ejected. In the vicinity of that velocity the cross section reaches a maximum and at still larger velocities it falls off roughly as  $1/v$ . A modified version of Eq. (2.3-23)

$$\sigma = \frac{\sigma_0 \left[ (v/v_0)^{1/5} - 1 \right]}{1 + \frac{.06\sqrt{E_1}}{(Z_1 + Z_2)^{5/3}} \frac{v}{v_0}} \quad (2.3-26)$$

extends the validity to higher velocities.

A comparison of the predictions of Eq. (2.3-23) with experiment has been carried out by Fedorenko (1959). The velocity range of the colliding ions varied from  $7 \times 10^6$  to  $9 \times 10^7$  cm/sec, and in this region there is agreement between theory and experiment to within a factor of 2.

In the course of colliding repeatedly with the particles of the ambient gas the ionization of the incoming particle keeps on changing. Nikolaev et al. (1961) have measured the equilibrium distribution of the various states of ionization for elements whose nuclear charges range from  $Z = 5$  to 36. The probability  $\phi_i$  of finding the ion to have a charge  $i$  is approximately of the form

$$\phi_i \approx \frac{1}{\sqrt{2\pi} \sigma} \exp \left[ -\frac{(i - \bar{i})^2}{2 \sigma^2} \right] \quad (2.3-27)$$

Their data on the average charge can be fitted by the expression

$$\bar{I} = 0.4 \frac{h\nu}{2e} Z^{1/2} = 1.83 \times 10^{-9} \nu Z^{1/2} \quad (2.3-28)$$

differing somewhat from the  $Z^{1/3}$  law given by Bohr. The width of the distribution function  $\bar{q}_1$  lies in the interval  $0.6 < \sigma < 1.1$ . In another series of papers Nikolaev et al. (1963) present cross sections for changing the charge of an ion by either attaching or stripping off electrons. Typical examples of these cross sections, say for Al traveling with a speed of  $2.6 \times 10^8$  cm/sec in air are  $\sigma_{01} = 1.2 \times 10^{-15} \text{ cm}^2$ ,  $\sigma_{12} = 3.5 \times 10^{-16} \text{ cm}^2$ ,  $\sigma_{10} = 4 \times 10^{-17} \text{ cm}^2$  and  $\sigma_{21} = 2.7 \times 10^{-16} \text{ cm}^2$  where the first and second index denote the charge of the ion before and after the collision. Eq. (2.3-23) is even useful for the lighter atoms, where one finds it to agree to within a factor of 3. A comparison of the theory with the experimental data of Van Eck and Kistemaker (1960) for electron loss cross sections for lithium in helium:  $\text{Li} + \text{He} \rightarrow \text{Li}^+ + \text{He} + \bar{e} + \Delta E$  is made in Table 2.4.

Table 2.4 Electron Loss Cross Sections for Lithium in Helium

$\nu$ (cm/sec)	$\sigma(\text{cm}^2 \times 10^{-16})$ (Firsov)	$\sigma(\text{cm}^2 \times 10^{-16})$ (expt)
$4 \times 10^7$	1.45	0.6
$6 \times 10^7$	2.52	1.0
$8 \times 10^7$	3.54	1.3

The cross section for electron capture (charge transfer) is more difficult to estimate. For lack of sufficient theoretical or experimental data, it is necessary to rely on empirical rules. From an examination of available experimental data on charge transfer reactions, Hasted (1960) has observed that the maximum charge-transfer cross section occurs at a velocity  $v_m$  of the incident particle given by

$$\frac{a \Delta E}{v_m h} \approx 1 \quad (2.3-29)$$

where  $\Delta E$  is the energy defect and "a" has the dimension of length. Hasted claims the best fit is given by  $a = 8A$ . If we express  $\Delta E$  in eV, this choice of  $a$  leads to the expression

$$v_m = 1.9 \times 10^7 \Delta E \text{ cm/sec} \quad (2.3-30)$$

For velocities in the adiabatic region, the charge transfer cross section varies according to

$$\sigma = c \exp (-k a \Delta E/v) \quad (2.3-31)$$

where  $c$  and  $k$  are constants for any particular reaction. There is, at present, no rigorous theoretical basis for Eq. (2.3-30). For velocities greater than that for which  $\sigma_{\max}$  occurs,  $\sigma$  falls off with increasing energy as some inverse power of  $v$ .

For a typical reaction  $D^+ + A \rightarrow D + A^+$  the energy difference will be of the order of 7 eV, so that the velocity at which  $\sigma_{\max}$  occurs is approximately  $1.3 \times 10^8$  cm/sec. Rapp and Francis (1962) have investigated the applicability of the simplest type of theory in charge transfer considerations and have presented a very general correlation of cross sections in terms of molecular parameters.

## 2.4 Collision phenomena of fast electrons

Only a small part of the energy of X-rays and gamma rays which are absorbed in air appears directly as ionization and excitation energy. The bulk of the energy is carried by electrons in the keV and MeV range, and after one has ascertained the energy deposited at some point in space one does not commit too much of an error by considering it to be entirely in the form of fast primary electrons. Information on the collision processes of such electrons, i.e., of processes leading to the production of secondary electrons and of various types of ions and excited molecules or atoms is therefore essential for predicting thermal and radiative properties of irradiated air.

Effects of Primary Electrons. When fast electrons collide with atoms or molecules they can produce many different changes in their collision partners. To keep track of these changes one needs, in principle, to know the cross sections of the various processes and the energy distribution of the secondary electrons. Below we review briefly what one can infer about these quantities from experimental data and theoretical considerations. For more detail the reader is referred to the review articles by Kieffer and Dunn (1966) and by Burgess (1966).

The most reliable collision cross section data are those for the total ionization cross section

$$\sigma_i = \sigma_1 + 2\sigma_2 + \dots \quad (2.4-i)$$

The first term  $\sigma_1$  combines the processes which liberate one secondary electron;  $\sigma_2$  measures processes which produce 2 secondary electrons, etc. Total ionization cross sections for  $O_2$  and  $N_2$  have been measured by Tate and Smith (1932) up to 700 eV. Measurements of the same type have recently been repeated by Rapp and Englander-Golden (1965). The new data essentially confirm the earlier ones and extend them to 1000 eV. A good analytical fit to the experimental results is obtained by writing

$$\sigma_i = A \frac{E - E_i}{E^2} \log \left( \frac{\frac{E}{E_i} + p \sqrt{\frac{E_i}{E}}}{1 + p} \right) \quad (2.4-2)$$

with constants as listed in Table 2.5.

Table 2.5 Constants for Fitting Total Ionization Cross Sections by Eq. 2.4-1

	$E_i$ (eV)	$10^{16} A$ (eV cm <sup>2</sup> )	$p$
$N_2$	15.6	625	1
$O_2$	12.2	840	3

This expression is made to approach zero at the threshold and at high energies it blends into the type of formula which one would expect from the Born approximation. It is therefore reasonable to use the above formula even beyond 1000 eV.

In Figs. 2.6 and 2.7 we present for  $N_2$  and  $O_2$  respectively, the experimental data on ionization and excitation cross sections. Curve 1 in Fig. 2.6 represents the total ionization cross section for  $N_2$  of Rapp and Englander-Golden, and curve 2 is the cross section for formation of  $N^+$  ions with kinetic energy  $> 0.25$  eV of Rapp et al. (1965). Curve 3 gives the data of Hagstrum and Tate (1941) for formation of  $N_2^+$ . Curve 4, which is the calculated difference between

curves 1 and 3, rises slowly above curve 2. Up to about 50 eV the two curves coincide, which agrees with the expectation that low energy electrons produce at most singly charged ions. The part of curve 4 which rises above curve 2, for electron energies above 50 eV, is indicative of the production of multiply charged ions.

There are 3 curves labeled 5 (a, b and c) which represent somewhat conflicting data on the excitation of the lowest vibrational level ( $v = 0$ ) of the  $B^2\Sigma_u^+$  state\* of  $N_2^+$ . These data are obtained by measuring the emission of bands in the first negative system ( $B^2\Sigma_u^+ \rightarrow X^2\Sigma_g^-$ ). Curve 5a represents data of Stewart (1956) which extend up to 200 eV, of Sheridan, Oldenburg and Carleton (1961) for the whole range, and of Hayakawa and Nishimura (1964) from 400 eV on up. Curve 5b which lies roughly a factor 2.4 higher represents data of Latimer and McConkey (1965) up to 300 eV and of Holland (1966) from 100 eV on up. To resolve this discrepancy McConkey, Woolsey and Burns (1967) recalibrated the intensity of this band and confirmed their earlier results. We feel at this time that curve 5b is the more reliable one. Curve 5c is a relative measurement by Zapesochnyi and Kishko (1961) where the emphasis was put on resolving the structure at low electron energies. This curve has been arbitrarily normalized so that its smooth high energy section coincides with curve 5b.

Curve 6a is the cross section for exciting the  $C^3\Pi_u$  state of  $N_2$  from an experiment by Stewart and Gabathuler (1958). This cross section combines collisions leading to the three lowest vibrational levels in the proportion 0.57 : 0.31 : 0.12. Curve 6b represents excitation of the same state but is based on measurements of transport coefficients in an electric

---

\* The energy levels mentioned in this section are shown in the potential energy curves on pp. 53-57 of DASA 1917-1 and in the diagrams on pp. 346-350 of DASA 1917-2.

field. The maximum of curve 6b is about 3.5 times larger than that of curve 6a. The interpretation by Engelhardt et al. (1964) that this peak belongs to the  $C^3\Pi_u$  levels may have to be revised in view of recent experimental data by Zapesochnyi and Skubenich (1966) and Brongersma and Oosterhoff (1967) which show a strong excitation of the  $B^3\Pi_g$  levels by electrons in this energy range. The maximum found by Zapesochnyi and Skubenich is about  $1.3 \times 10^{-16} \text{ cm}^2$ , which is even higher than curve 6b.

Points 7, 8, and 9 give data derived from Silverman and Lassetre (1965) for the excitation of the  $a^1\Pi_g$ ,  $b^1\Sigma_u^+$ , and  $b^1\Pi_u$  states, respectively, of  $N_2$ . The dashed curves through these points are based on the Born approximation as developed by Bethe. Curves 10 and 11 are cross sections for the excitation of the  $a^1\Pi_g$  and  $A^3\Sigma_u^+$  states, respectively, of  $N_2$ , obtained simultaneously with the cross section 6b by Engelhardt et al. Curve 12 is the total vibrational excitation cross section of  $N_2$  as obtained by Schulz (1964) but normalized to a larger absolute value by Engelhardt et al. This is discussed in section 2.5.

Fig. 2-7 gives in curves 1 and 2 analogous data of Rapp, Englander-Golden and Briglia for  $O_2$  ionization cross sections\*. The curves 3 and 4 are the data of Stewart and Gabathuler for partial excitation cross-sections of the second vibrational level of the  $A^2\Pi_u$  and  $^4\Sigma_g$  states, respectively, of  $O_2^+$ . Point 5 gives the data of Silverman and Lassetre (1964) for the excitation of the Schumann-Runge continuum of  $O_2$  and the dashed curve through the point represents the theoretical energy dependence of this cross section if the Born approximation is valid. This curve lies decidedly higher than curve 6 which has been obtained by Phelps and Kasner (1966) for the same process. This as well as curve 7 which is the cross section for exciting

\* Note that if the data of Craggs, Thorburn, and Tozer (1957) for the cross section for the formation of  $O_2^+$  were normalized to the ionization cross section at 40 eV and plotted on Fig. 2-7, the low energy part of that curve would coincide closely with curve 1 in much the same manner as the Hagstrum-Tate data for  $N_2^+$ .

the continuum associated with the  $A^3 \Sigma_u^+$  level has been obtained from transport coefficients in an electric field using the technique employed by Engelhardt et al.

Grün (1957) has measured the energy loss rate  $-\frac{1}{n} \frac{dE}{dx}$  of electrons in air for energies ranging from 6 to 30 keV. These values lie about 2% below the values calculated from Bethe's formula (1933)\*. To extrapolate Grün's values to the somewhat lower energies of interest to us we use Fig. 2.8 which is a graph of  $-\frac{E}{n} \frac{dE}{dx}$  versus  $\log E$  to facilitate a comparison with Bethe's formula  $-\frac{dE}{dx} = \frac{2\pi e^4}{E} nZ \ln \frac{E}{I}$ . In the interval from 100 eV to the starting point of Grün's data this should be approximately a straight line. Above 6 keV a slight upward curvature sets in because of relativity effects and below 100 eV the curve levels off and begins to head towards zero at the ionization energies of nitrogen and oxygen. In the vicinity of  $E = 500$  eV Silverman and Lassetre (1964; 1965) have measured energy loss spectra of electrons colliding with  $O_2$  and  $N_2$ . These have been used to calculate  $\frac{1}{n} \frac{dE}{dx}$  for that value of  $E$ . The resulting  $\frac{E}{n} \frac{dE}{dx}$  has also been entered in Fig. 2.8.

Energy Distribution of Secondary Electrons. A certain fraction of the energy which is used in ionizing an air molecule reappears as kinetic energy of the secondary electron. These secondary electrons can in turn excite and ionize other molecules. In order to evaluate the number of such processes one has to know the energy distribution of the secondary electrons.

\* op cit. page 521. For calculations see report NBS 577.

Attempts to measure the energy distribution of secondary electrons produced in air have not produced satisfactory results because of the appearance of tertiary electrons, particularly at low energies. This depends in a complicated manner on the geometry of the experiment and cannot be readily corrected for. Nevertheless, the experiments affirm what one would also expect on theoretical grounds, that the distribution depends only very little on the energy of the primary electrons and on the type of the gas.

Because of the mentioned difficulties with the experimental data we feel that theoretical results are more trustworthy, even though such calculations have not been carried out for air.

In the estimates made below we have used the results of Bethe (1933)<sup>\*</sup> who has calculated the distribution of various types of collisions for high-velocity impacts of electrons in a gas of H atoms. It can be seen that all quantities except the absolute cross section are reasonably insensitive to the energy of the primary electrons.

The fraction of secondaries whose energy lies above  $E$  is well represented by

$$F_s(E) = \left( 1 + \frac{4}{3} \frac{E}{I} \right)^{-\frac{4}{3}} \quad (2.4-3)$$

$I$  being the ionization energy of the H atom. This relation fits Bethe's results for 1 keV primaries very closely. The average energy of secondary electrons with this distribution is  $\bar{E} = \frac{9}{4} I$ .

---

\* op. cit. page 517

Recently K. Omidvar (1965) has determined the energy distribution of secondary electrons ejected from excited states of the hydrogen atom. Since the electrons ejected from N and O come from the L shell it seems most appropriate to use Omidvar's results for  $n = 2$ . This leads to a ratio  $\bar{E}/I$  which has been estimated to lie between 3.5 and 4.0, i.e., somewhat larger than the above value of 2.25. Unfortunately these results depend rather critically on the high energy tail of the distribution and a more careful study is indicated. The analysis below, which was carried out before Omidvar's results had appeared, was not repeated with the new data because this would still have been just a preliminary effort. A more conclusive evaluation will be possible with data applying directly to O and N which are expected to be forthcoming in the near future.

## 2.5 Collision phenomena of slow electrons.

The processes whereby fast electrons lose their energy are those which lead to ionization or other forms of electronic excitation. For an electron whose energy drops lower than about 7 eV such processes become impossible. Following Platzmann (1955) we call electrons which have too little energy to be degraded by producing electronic excitation "subexcitation electrons". Actually the oxygen molecule has several levels which lie below the 7 eV value mentioned above but according to Schulz and Dowell (1962) the cross sections for exciting these levels are negligibly small. Another inelastic process which takes place above 5 eV is the dissociative capture  $O_2 + e \rightarrow O + O^-$ . This reaction has a cross section rising to a maximum of  $1.3 \times 10^{-18} \text{ cm}^2$  but it, as well as direct attachment, which occurs at much lower energies, capture the electron rather than slowing it down. These processes will be discussed later.

Once in the subexcitation region, further degradation of electrons is slower than at higher energies. The loss rate can be written as

$$-\frac{dE}{dt} = \lambda \nu E \quad (2.5-1)$$

where  $\lambda$  is the fraction of energy lost per collision. The collision rate  $\nu$  is proportional to the number density  $n$  of the molecules and is related to the total collision cross section  $\sigma$  by

$$\nu = n \sigma v \quad (2.5-2)$$

where  $v$  is the electron velocity. Both  $\lambda$  and  $\sigma$  depend on the energy of the electron. In Fig. 2.9 we show the cross sections for  $N_2$  and  $O_2$  as determined by Engelhardt, Phelps and Risk (1964) and by Phelps and Kasner (1966). These cross sections were selected to give a consistent description of the effect of d.c. electric fields on electron drift velocities. Drift data relate to swarms of electrons subjected to an electric field to accelerate them. The energies which are reached under the competing effects of that acceleration and of the deceleration by collisions with the gas molecules are statistically distributed and not sharp as in beam experiments. The energies which are quoted in such experiments are therefore average energies. The quantities actually measured can be expressed as average cross sections weighted with the velocity distribution function of the electrons.

In earlier attempts at interpreting drift data, which are described in detail by Huxley and Crompton (1962), velocities were assumed to follow either a Maxwell or a Druvesteyn distribution law. Engelhardt et al. improved this by calculating the distribution function which has been made possible by the use of theoretical data on rotational excitation due to Gerjouy and Stein (1955) and experimental data by Schulz (1964). The assignment of cross sections made in this manner is not unique but the authors believe their results on  $N_2$  to be accurate to  $\pm 10\%$  or better. In the case of  $O_2$  they assign an accuracy of  $\pm 20\%$ . Fig. 2.9 also shows a cross section per air molecule using weight factors 0.8 and 0.2 for  $N_2$  and  $O_2$ .

The fractional energy loss per collision is made up of parts  $\lambda_1$  depending on whether the loss is due to elastic momentum transfer or

rotational or vibrational excitation of the molecules. We note that these fractions are not defined per collision of type 1 but are based on collisions of all types, so that  $\lambda = \Sigma \lambda_i$ .

The fractional energy loss of an electron of mass  $m$  colliding elastically with a molecule of mass  $M$  (at rest) is on the average  $\lambda_e = 2m/M$ . The fractions  $\lambda_r$  and  $\lambda_v$  going into the excitation of rotational and vibrational energy are generally larger than  $\lambda_e$ .

Using the theory of Gerjouy and Stein (1955) the rotational part of the fractional energy loss is

$$\lambda_r = \frac{32 Q^2}{15} \frac{B}{E} \frac{\pi a_0^2}{\sigma_t} \left( 1 - \frac{kT}{E} \right) \quad (2.5-3)$$

where  $Q$  is a dimensionless measure of the quadrupole moment of the molecule,  $B$  the factor in formula  $E_r = B J(J+1)$  for the rotational energy of the molecule and  $\sigma_t$  the total collision cross section per gas molecule. Recently attempts have been made, for example by Takayanagi and Geltman (1965), to extend the theory of Gerjouy and Stein by using more realistic interaction potentials, but these have not yet been used to evaluate  $\lambda_r$ . For nitrogen the energy constant is  $B = 0.249 \times 10^{-3}$  eV. On the basis of electron drift data Engelhardt, Phelps and Risk (1964) suggest to use  $Q = -1.04$ . For  $O_2$  the two constants are  $B = 0.180 \times 10^{-3}$  eV and  $Q = +0.30$ . The ratio  $\lambda_r/\lambda_e$  for air (i.e., using the weight factors 0.8 and 0.2 for calculating  $Q^2 B$  and  $\sigma_t$  in Eq. (2.5-3) at 300°K is shown in Fig. 2-10.

The cross sections for exciting the vibrational levels of  $N_2$  as determined by Schulz (1964) are shown in Fig. 2.11. We note that these cross sections are appreciable only above 1.7 eV whereas it takes only 0.288 eV to go from the groundstate ( $v = 0$ ) to the first excited state ( $v = 1$ ). This result confirms and extends earlier experiments by Haas (1957) and to interpret their results both authors postulate that the excitation proceeds via an intermediate state with the electron temporarily tied to a negative ion  $N_2^-$ . The data of Schulz are taken at a scattering angle of  $72^\circ$  and one would have to know the angular dependence to obtain total cross sections. Lacking this information Engelhardt et al. (1964) have normalized the total vibrational cross section  $\sigma_{vt} = \Sigma \sigma_v$  to be  $5.5 \times 10^{-16} \text{ cm}^2$  at its maximum, i.e., at  $E = 2.2 \text{ eV}$ . To agree with the data of Haas one would have to make the maximum equal to  $3.8 \times 10^{-16} \text{ cm}^2$ . Using the first alternative we have calculated

$$\lambda_v = 0.8 \frac{\Sigma \sigma_v \Delta E_v}{\sigma_t E} \quad (2.5-4)$$

which is the fractional energy loss for exciting the vibrations of the  $N_2$  molecules present in air. The corresponding quantity for  $O_2$  can at present not be obtained but it is evidently much smaller. The ratio  $\lambda_v/\lambda_e$  is shown in Fig. 2.10. Harries (1927) determined the energy loss of monoenergetic electrons of 5.2 eV in  $N_2$  to be  $3.65 \times 10^{-3} \text{ eV}$  per collision. This is not the value published in the original paper but a corrected one given in a footnote by Harries and Hertz (1927). The quoted value amounts to a fractional loss of  $6.3 \times 10^{-4}$  per collision in air. The corresponding value  $\lambda_v/\lambda_e = 16$  is also entered in Fig. 2.10.

For energies ranging from 0.1 eV to 1.5 eV we have calculated  $\lambda$  from the electron drift velocity  $W$  and the Townsend factor  $k_1$  as obtained by Lowke (1963) and Jory (1965), respectively. To calculate  $\lambda$  we use the formula  $\lambda = 1.8 \times 10^{-14} W^2/k_1$  developed by Huxley and Crompton (1962) assuming a Maxwellian distribution for the electrons. The electrons in a swarm are of course not monoenergetic but since  $\lambda$  does not change violently in this interval it is not a serious error to plot that quantity against the mean energy  $\bar{E} = \frac{3}{2} k_1 (T/11,600)$ .

Fig. 2.12 shows the product  $n_0 \sigma \lambda$ , i.e., the fractional energy loss of an electron per unit path length in atmosphere air, which has been calculated from the data in Figs. 2.9 and 2.10. It is of interest to note that this quantity stays nearly constant from an energy of 0.8 eV down to 0.08 eV.

#### Dissociative Attachment

In addition to elastic and inelastic collision processes, electrons also undergo capture processes. The first one of those is the dissociative capture in  $O_2$



This is an endothermic process which removes electrons as they slow down from 10 eV to the threshold which lies at 3.6 eV. Fig. 2.13 shows the cross section of this reaction as measured by Buchelnikova (1959) and Schulz (1962). The same shape but larger absolute values were found by Craggs et al. (1957).

Below the threshold for dissociative attachment the predominant capture process for electrons is their attachment to the oxygen molecule which has a stable negative ion. The electron affinity, i.e., the binding energy of the electron in the  $O_2^-$  ion, is not very accurately known. A value of 0.43 eV obtained by Pack and Phelps (1966) from electron attachment and

detachment rates represents a reasonable compromise. The values published by various other authors range from 0.15 eV obtained by identifying it with a measured threshold for photodetachment to 0.9 eV based on thermochemical data. The difficulty of obtaining a definitive result arises probably because the  $O_2^-$  ion is not necessarily in its ground state.

The energy which is liberated when an electron is attached must somehow be carried away for example, by a photon or by a third particle. Radiative attachment is a two-body reaction



and its rate is governed by the equation

$$\frac{dn_e}{dt} = -\beta_r n_e n_{O_2} \quad (2.5-7)$$

The rate constant can be calculated from measured values of the cross section for photodetachment of  $O_2^-$  - the reverse processes - by utilizing the principle of detailed balancing. Results of such a calculation depend on the electron affinity and three curves are presented by Branscomb (1962)\*. Interpolating to the quoted value of 0.43 eV one obtains a radiative attachment rate which is approximately given by the expression

$$\beta_r = 8 \times 10^{-17} E_e^{5/2} \text{ cm}^3 \text{ sec}^{-1} \quad (2.5-8)$$

---

\* op. cit. p. 134

where  $E_e$  is the electron energy. At thermal energies radiative attachment is an extremely slow process and can not be counted on to explain the data. To fill this need Bloch and Bradbury (1935) suggested the two-step process



where a vibrationally excited negative ion is formed and almost instantly deactivated by a molecule  $M$  (either  $O_2$  or  $N_2$ ). This mechanism was invoked to explain a strong attachment which increased with energy and whose rate coefficient indicated a two-body process.

Recent findings by Chanin et al. (1962) have completely changed this interpretation. By means of drift experiments where the average electron energy ranges from a few down to a few hundredths electron volt these authors find that the attachment of low energy electrons does not obey a two-body law as had been claimed in earlier work. Two-body attachment predominates only when the average electron energy is greater than about 1 eV and it is largely due to dissociative attachment of electrons in the high energy tail of the velocity distribution. In 1935 it was thought that  $O_2$  could not undergo dissociative attachment and for this reason Bloch and Bradbury specifically dismissed the possibility of that process. The new data show that the attachment ceases to be a two-body reaction when the energy drops below 1 eV and that its rate now obeys a three-body law. One can still

invoke the Bloch-Bradbury sequence of excitation and deactivation to explain this but it would require that the deactivation rate should be quite small in contrast to the original hypothesis. It is actually not necessary to use the concept of an intermediate state and instead one can regard the capture as a true three-body reaction



where the molecule  $\text{M}$  carries away the excess energy which has been released by the capture of the electron. The attachment frequency per electron  $\nu_a$  is proportional to the product of the two densities  $n_{\text{O}_2}$  and  $n_{\text{M}}$  and it depends on the temperature of the gas and on the energy of the electron. The detachment frequency  $\nu_d$  per  $\text{O}_2^-$  ion is proportional to  $n_{\text{M}}$  and depends very strongly on temperature because the collision partners have to supply the energy of 0.43 eV binding the electron to the ion.

Chanin et al. and more recently Pack and Phelps (1966) have investigated the reaction (2.5-11) for pure oxygen by observing current wave forms when short bursts of electrons are drifting through an electric field  $\epsilon$ . In Fig. 2.14 we show the temperature dependence of  $\nu_d/n_{\text{O}_2}$  and of  $\nu_a/(n_{\text{O}_2})^2$  as obtained by them. The latter quantity depends also on the average energy of the electron swarm which depends in turn on  $\epsilon/n_{\text{O}_2}$  but the graph shows only the thermal limit which is reached when the electric field is zero.

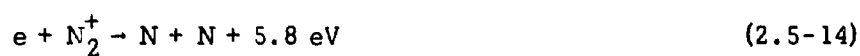
One can compare this coefficient with one obtained by an entirely different technique which has been developed by Van Lint et al. (1963). After the gas is ionized by a short pulse of high energy electrons from a linear accelerator one observes the time dependence of the propagation of micro-waves through the gas sample. From these data one can calculate the density and average collision frequency of the electrons. The coefficient describing the observed attachment rate is approximately  $3 \times 10^{-30} \text{ cm}^6/\text{sec}$  in very good agreement with the result of Pack and Phelps.

In air or any other mixture of  $\text{O}_2$  and  $\text{N}_2$  the attachment frequency can be expressed as

$$\nu_a = (K_a n_{\text{O}_2} + K_b n_{\text{N}_2}) n_{\text{O}_2} \quad (2.5-12)$$

where  $K_a$  is the rate coefficient as measured for pure oxygen. For drifting electrons of 0.1 eV Chanin et al. (1962) found the ratio of the coefficients to be about  $\frac{K_b}{K_a} = 0.027$ . Van Lint (1963) finds a similar ratio  $\frac{K_b}{K_a} = 0.031$  for thermal electrons. The much larger effectiveness of  $\text{O}_2$  as a third-body is not unreasonable because one would expect two  $\text{O}_2$  molecules to keep an electron going back and forth between them for a much longer time than between an  $\text{O}_2$  and an  $\text{N}_2$  molecule which does not form a stable negative ion. By keeping the electron longer in the vicinity of the two molecules one would obviously increase the probability of eventual capture.

In air which contains a significant population of positive ions capture occurs by the processes



and other less effective reactions. The rate of electron disappearance in these cases is of the form

$$-\frac{dn_e}{dt} = \alpha n_e n_{ion} \quad (2.5-17)$$

Values for  $\alpha$  including temperature dependence have been suggested by Bortner (1966). They are part of a large list of reaction rate constants representing the consensus of the participants at a meeting of the IAEA Atomic and Molecular Processes Panel (January 5, 1966) which was organized for this purpose. The rate constants are fitted by the expression

$$\alpha = a T^b e^{-10^3 c/T} \quad (2.5-18)$$

with  $c = 0$  for exothermic reactions like the ones listed above. As known from statistical mechanics, the constants  $a$ ,  $b$  and  $c$  for the reverse reactions are related in a simple manner to those for the forward reactions and Bortner lists both sets. He furthermore recommends two choices designated as low and high temperature numbers. The first are intended for use in temperature regions where the reactions go predominantly in the exothermic direction and the others when endothermic reactions predominate. In Table 2.7 we list the recommended low temperature set of constants  $a$  and  $b$  ( $c$  being zero) for the above electron capture processes. This list should be regarded as tentative and the A and M Panel plans to issue improved lists at intervals. The constants for the radiative recombination with  $O^+$  have been taken from an earlier report by Bortner and Galbraith (1965). This report as well as a publication by Whitten and Popoff (1964) also contain detailed discussions on the use of such constants in deionization calculations.

Table 2.7 Parameters for Rate Constants

Capturing Ion	a	b
$NO^+$	$1.5 \times 10^{-4}$	-1
$N_2^+$	$9 \times 10^{-5}$	-1
$O_2^+$	$6 \times 10^{-5}$	-1
$O^+$	$2.25 \times 10^{-5}$	-0.75

## References

- Bates, D.R., Atomic and Molecular Processes, Acad. Press, 1962.
- Bethe, H.A., Handbuch der Physik I, 24, 1933.
- Bloch, F. and N. Bradbury, Phys. Rev. 48, 689, 1935.
- Bohr, N., Mat. Fys. Medd. Dan. Vid. Selsk 18, (8), 1948.
- Bortner, M.H. and H.J. Galbraith, DASA Report 1667, 1965.
- Bortner, M.H., Private Communication, Feb. 3, 1966.
- Branscomb, L.M.,: see Bates (1962), 1962.
- Brongersma, H.H. and L.J. Oosterhoff, Chem. Phys. Let. 1, 169, 1967.
- Buchelnikova, I.S., JETP 8, 783, 1959.
- Burgess, A., Rev. Mod. Phys. (in preparation).
- Carlson, T.H. and M.O. Krause, Phys. Rev. 140, A1057, 1965.
- Chanin, L.M., A.V. Phelps and M. Biondi, Phys. Rev. 128, 219, 1962.
- Craggs, J.D., R. Thorburn and B.A. Tozer, Proc. Roy. Soc. A240, 473, 1957.
- Dorman, F.H., and J.D. Morrison, J. Chem. Phys. 39, 1906, 1963.
- Engelhardt, A.G., A.V. Phelps and C.G. Risk, Phys. Rev. 135A, 1566, 1964.
- Fedorenko, N.V., Soviet Physics, Uspekhi, 2, 526, 1959.
- Fermi, E., and E. Teller, Phys. Rev. 72, 399, 1947.
- Fine, S. and C.F. Hendee, Nucleonics 13, 3, 36, 1955.
- Firsov, O.B., Soviet Physics, JETP 6, 534, 1957.
- Firsov, O.B., Soviet Physics, JETP 7, 308, 1958.
- Firsov, O.B., Soviet Physics, JETP 9, 1076, 1959.
- Gerjouy, E. and S. Stein, Phys. Rev. 97, 1671, 1955.
- Gilmore, R., RAND Report RM-2367-AEC, 1959.

- Gilmore, F.R., JQSRT 5, 369, 1965.
- Grün, A.E., Zs. f. Naturf, 12a, 89, 1957.
- Haas, R., Zs. Phys. 148, 177, 1957.
- Hagstrum, H.D. and J.T. Tate, Phys. Rev. 59, 354, 1941.
- Hartmann, H. and H.K. Chun, Theor. Chim. Acta 2, 1, 1964.
- Harries, W., Zs. f. Phys. 42, 26, 1927.
- Harries, W. and G. Hertz, Zs. f. Phys. 46, 177, 1927.
- Hasted, J.B., Advances in Electronics and Electron Physics, Vol. 13, Academic Press, Inc., 1960.
- Hayakawa, S. and H. Nishimura, J. Geomag. Geoelect. 16, 72, 1964.
- Holland, R. (private communication), 1966.
- Eurley, A.C., J. Mol. Sp. 9, 18, 1962.
- Huxley, L.G.H. and R.W. Crompton: see Bates (1962), 1962.
- Jory, R.L., Austral. J. Phys. 18, 235, 1965.
- Kieffer, L.J. and G.H. Dunn, Rev. Mod. Phys. 38, 1, 1966.
- Latimer, I.D. and J.W. McConkey, Proc. Phys. Soc. 86, 463, 1965.
- Lindhard, Scharff and Scholtz, Kgl. Danske. Vid. Selsk. Mat. fys. Medd. 33, 14, 1, 1963.
- Lowke, J.J., Austral. J. Phys. 16, 115, 1963.
- McConkey, J.W., J. M. Woolsey and D.J. Burns, Planet. Space Sci. 15, 1332, 1967.
- Mehlhorn, W., Zs. f. Phys. 160, 247, 1960.
- NBS Circular 577, July, 1956.
- Nikolaev, Dimitriev, Fateeva and Teplova, JETP 6, 1019, 1958; 12, 627, 1961. 13, 695, 1961; 14, 67, 15, 11, 1962; 16, 259, 1963.
- Omidvar, K., Phys. Rev. 140A, 26, 1965.
- Pack, J.L., and A.V. Phelps, J. Chem. Phys. 44, 1870, 1966.

- Phelps, A.V. and W.H. Kasner, Report AFWL-TR-66-34, 1966.
- Platzmann, R.L., Radiation Res. 2, 1, 1955.
- Rapp, D. and W.E. Francis, J. Chem. Phys. 37, 2631, 1962.
- Rapp, D., P. Englander-Golden, and D.D. Briglia, J. Chem. Phys. 42, 4081, 1965.
- Rapp, D., and P. Englander-Golden, J. Chem. Phys. 43, 1464, 1965.
- Schulz, G.J. and J.T. Dowell, Phys. Rev. 128, 174, 1962.
- Schulz, G.J., Phys. Rev. 128, 178, 1962.
- Schulz, G.J., Phys. Rev. 125, 229, 1962; 135, 988, 1964.
- Sheridan, W.F., O. Oldenberg, and N.P. Carleton, Second Intl. Conf. on Phys. of Electronic and Atomic Coll., Boulder, Colo., p. 159, 1961.
- Silverman, S.M. and E.N. Lassettre, J. Chem. Phys. 40, 2922, 1964.
- Silverman, S.M. and E.N. Lassettre, J. Chem. Phys. 42, 3420, 1965.
- Stewart, D.T., 1956 Proc. Phys. Soc. A69, 437, 1956.
- Stewart, D.T. and E. Gabathuler, Proc. Phys. Soc. 72, 287, 1958.
- Takayanagi, K., and S. Geltman, Phys. Rev. 138, A1003, 1965.
- Tate, J.T., and P.T. Smith, Phys. Rev. 39, 270, 1932.
- Van Eck, J. and J. Kistemaker, Physica 26, 629, 1960.
- Van Lint, RTD TDR-63-3076, AFWL (Gen. Atomic), 1963.
- Veigele, Wm. J., E.M. Henry and M.E. Donaldson, Kaman Report KN-65-119 (R), 1965.
- Whitten, R.C. and I.G. Poppoff, J. Atm. Sci. 21, 117, 1964.
- Zapesochnyi, I.P. and S.M. Kishko, Doklady 5, 1008, 1961.
- Zapesochnyi, I. P. and V.V. Skubenich, Opt. and Spectrosc. 21, 83, 1966.

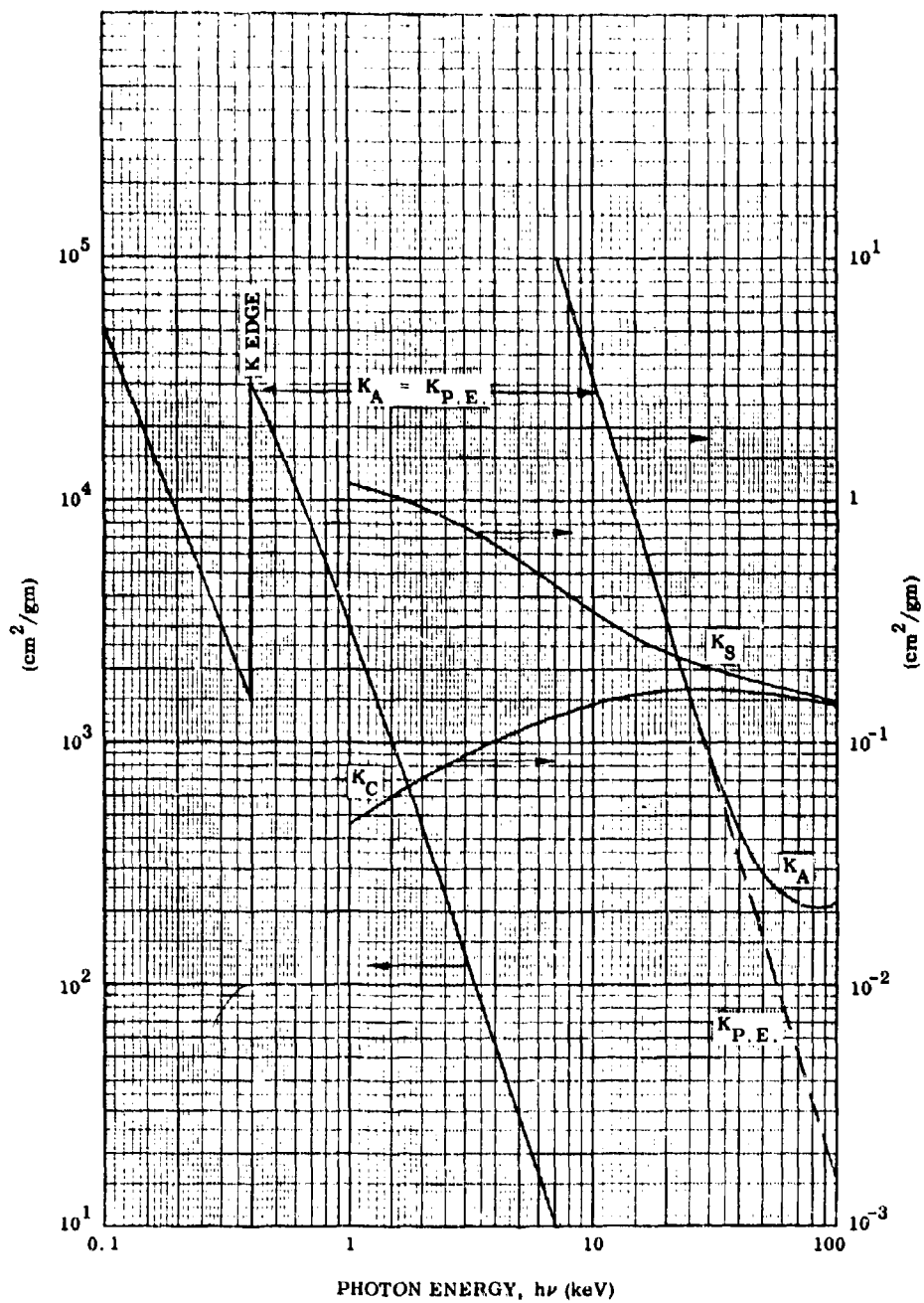


FIG. 2-1 X-RAY ABSORPTION AND SCATTERING COEFFICIENT IN NITROGEN.

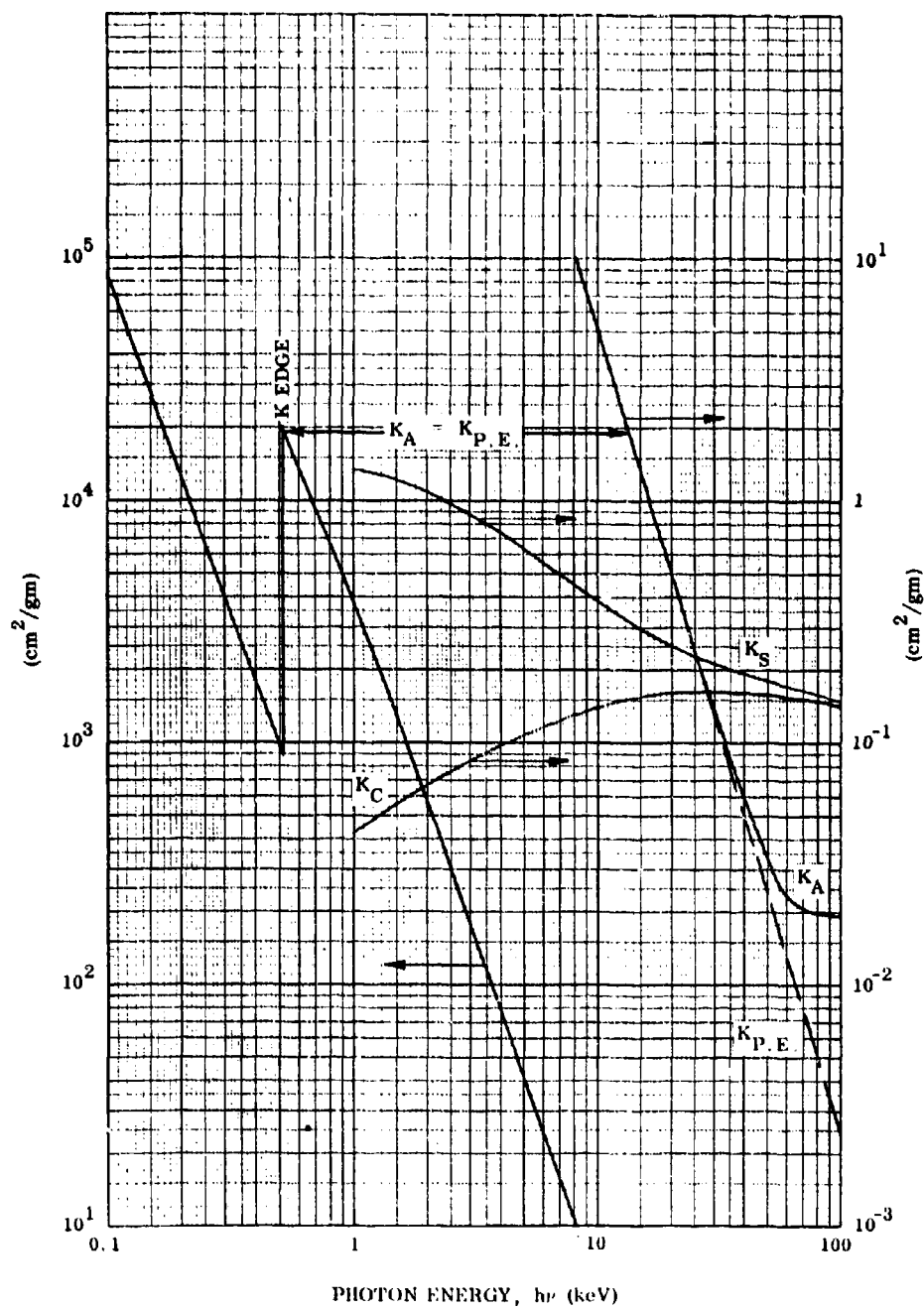


FIG. 2-2 X-RAY ABSORPTION AND SCATTERING COEFFICIENT IN OXYGEN.

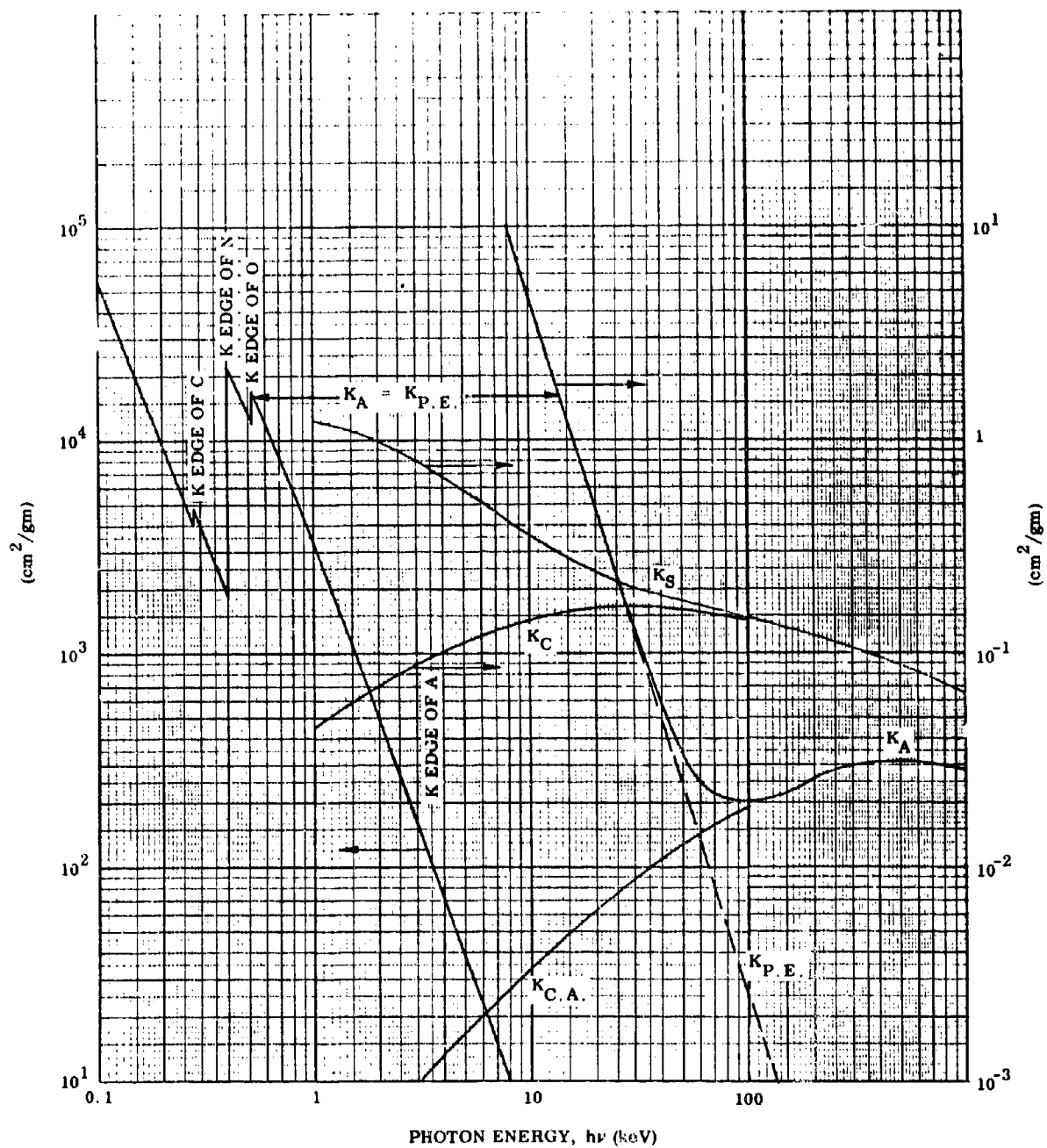


FIG. 2-3 X-RAY ABSORPTION AND SCATTERING COEFFICIENTS IN AIR.

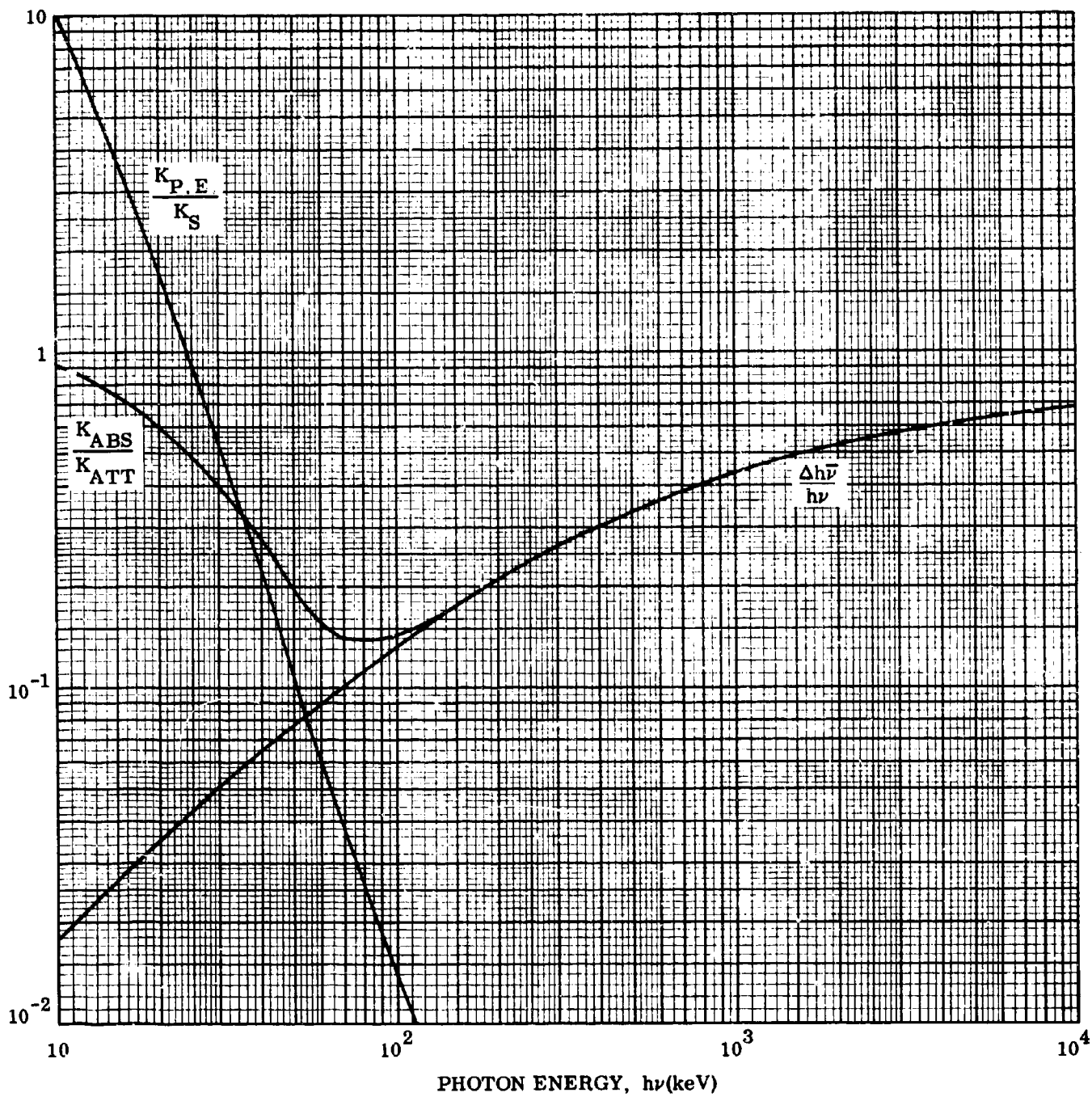


FIG. 2-4 SOME RATIOS PERTAINING TO THE ENERGY LOSS OF X-RAY AND GAMMA QUANTA.

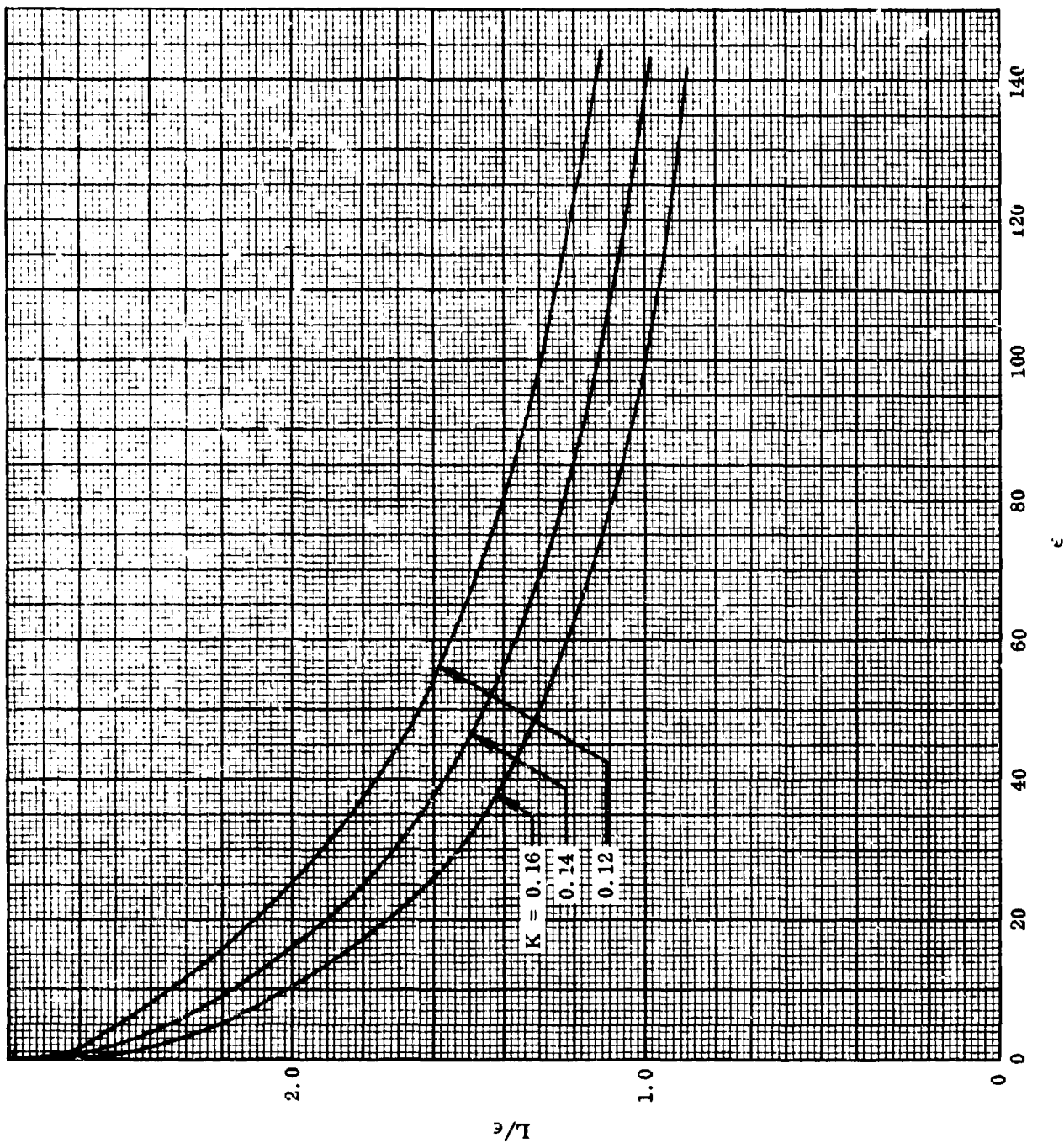


FIG. 2-5 FUNCTION TO BE USED IN CALCULATING THE RANGE OF FAST HEAVY PARTICLES (SEE EQ. 2.3-20)

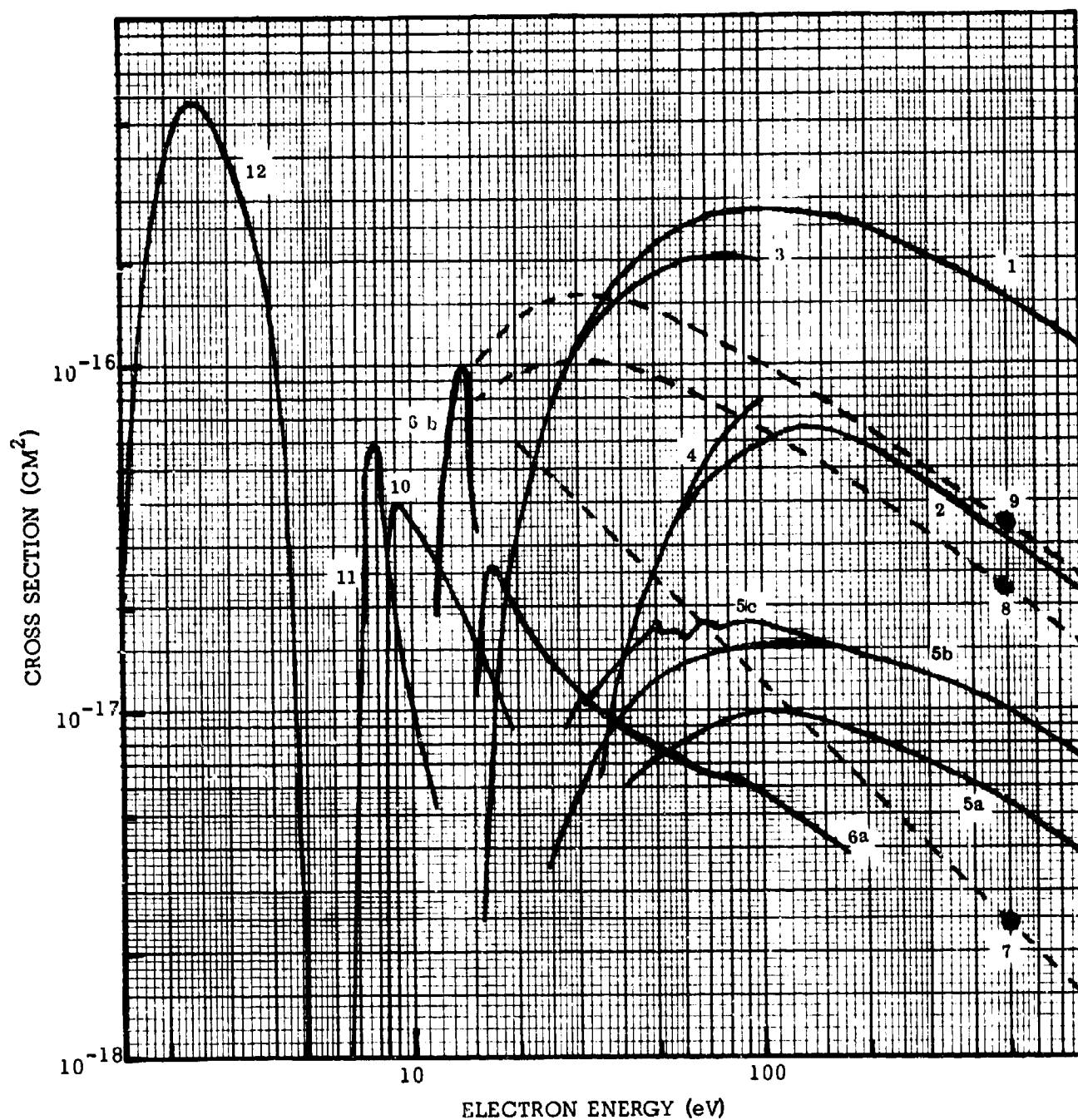


FIG. 2-6 ENERGY DEPENDENCE OF SEVERAL CROSS SECTIONS IN  $N_2$   
(For details see pp. 28 to 30.)

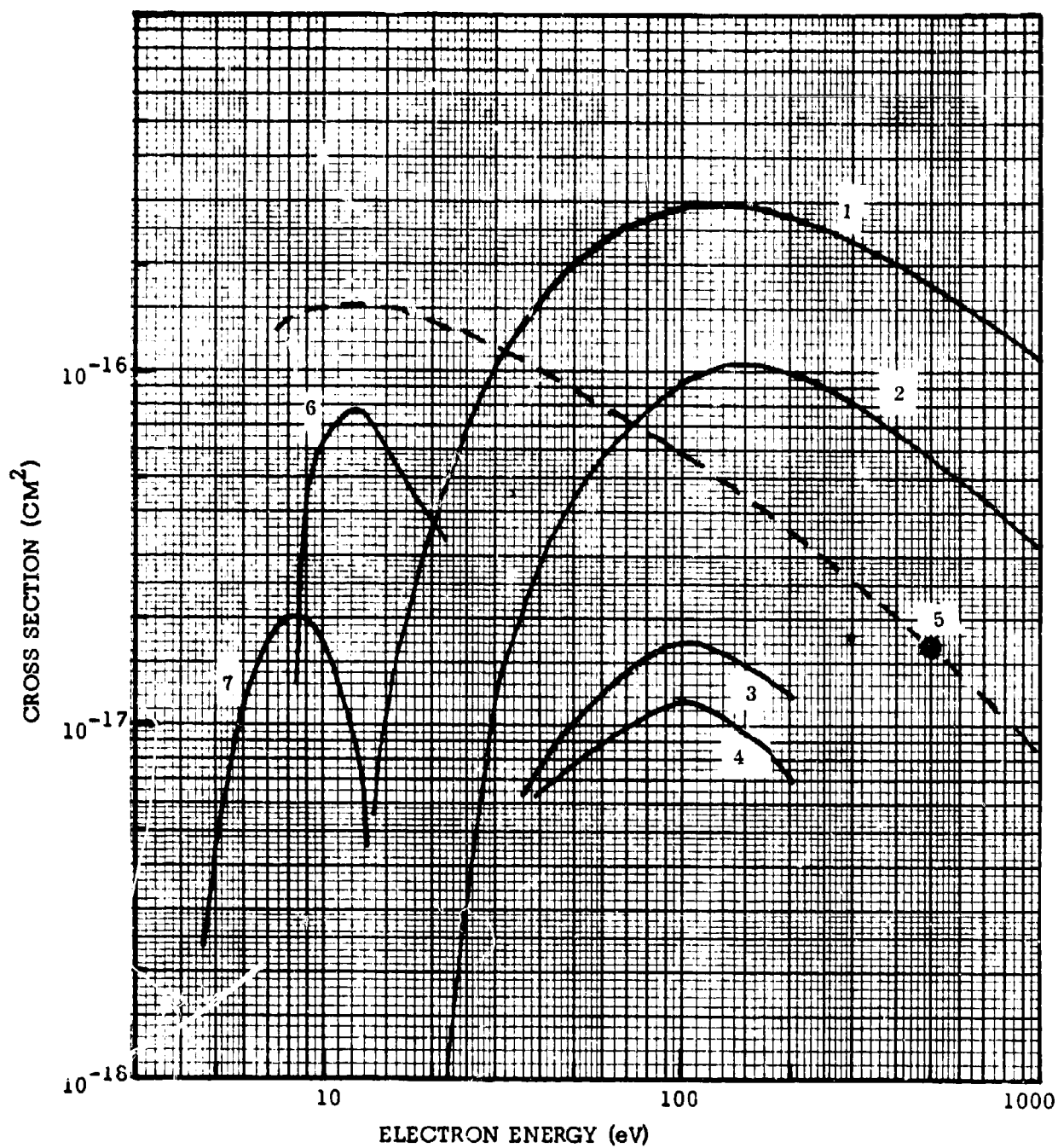


FIG. 2-7 ENERGY DEPENDENCE OF SEVERAL CROSS SECTIONS IN  $O_2$   
(For details see pp. 30 and 31.)

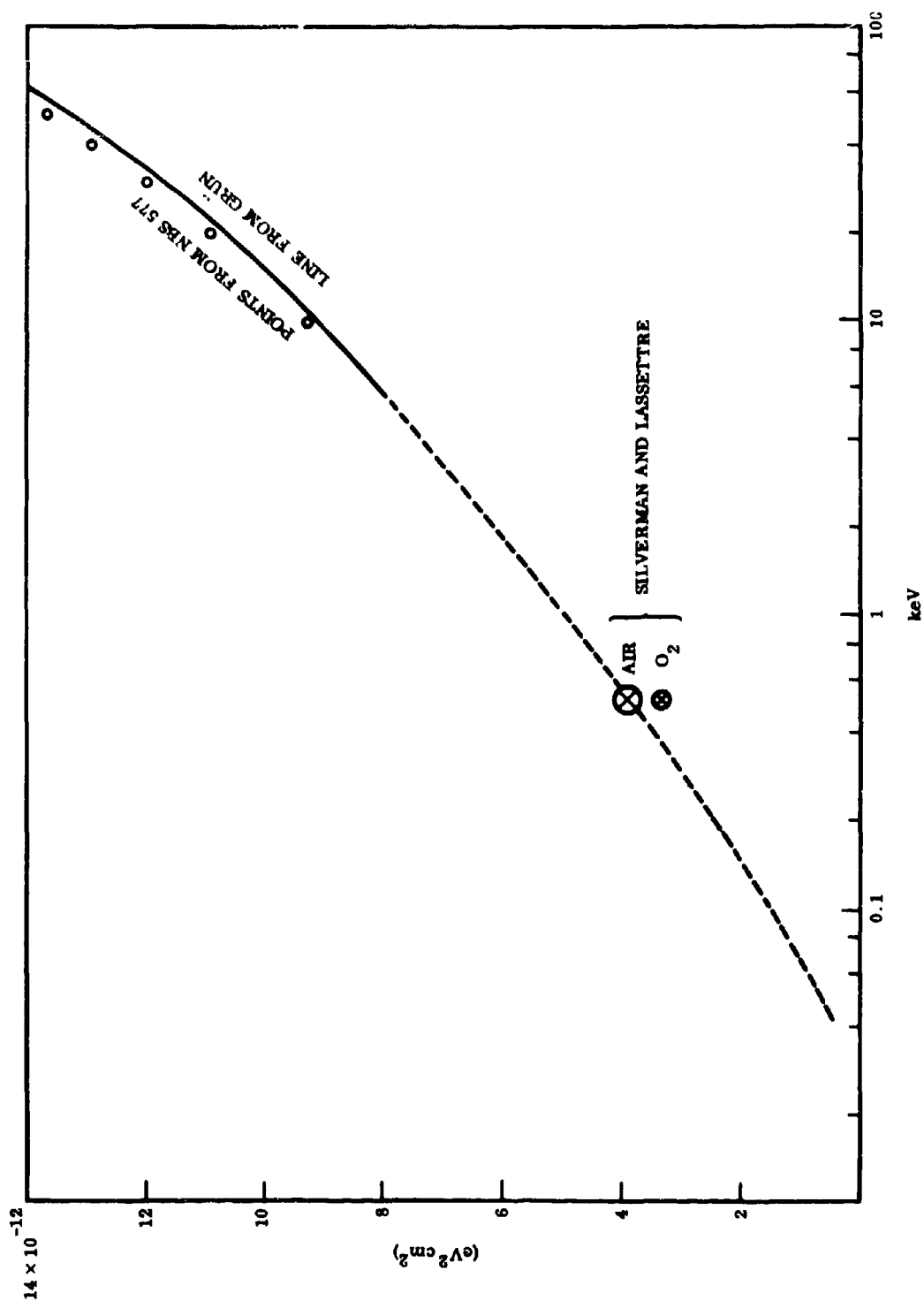


FIG. 2-8' -  $\frac{E}{n} \frac{dE}{dx}$  vs.  $\log E$

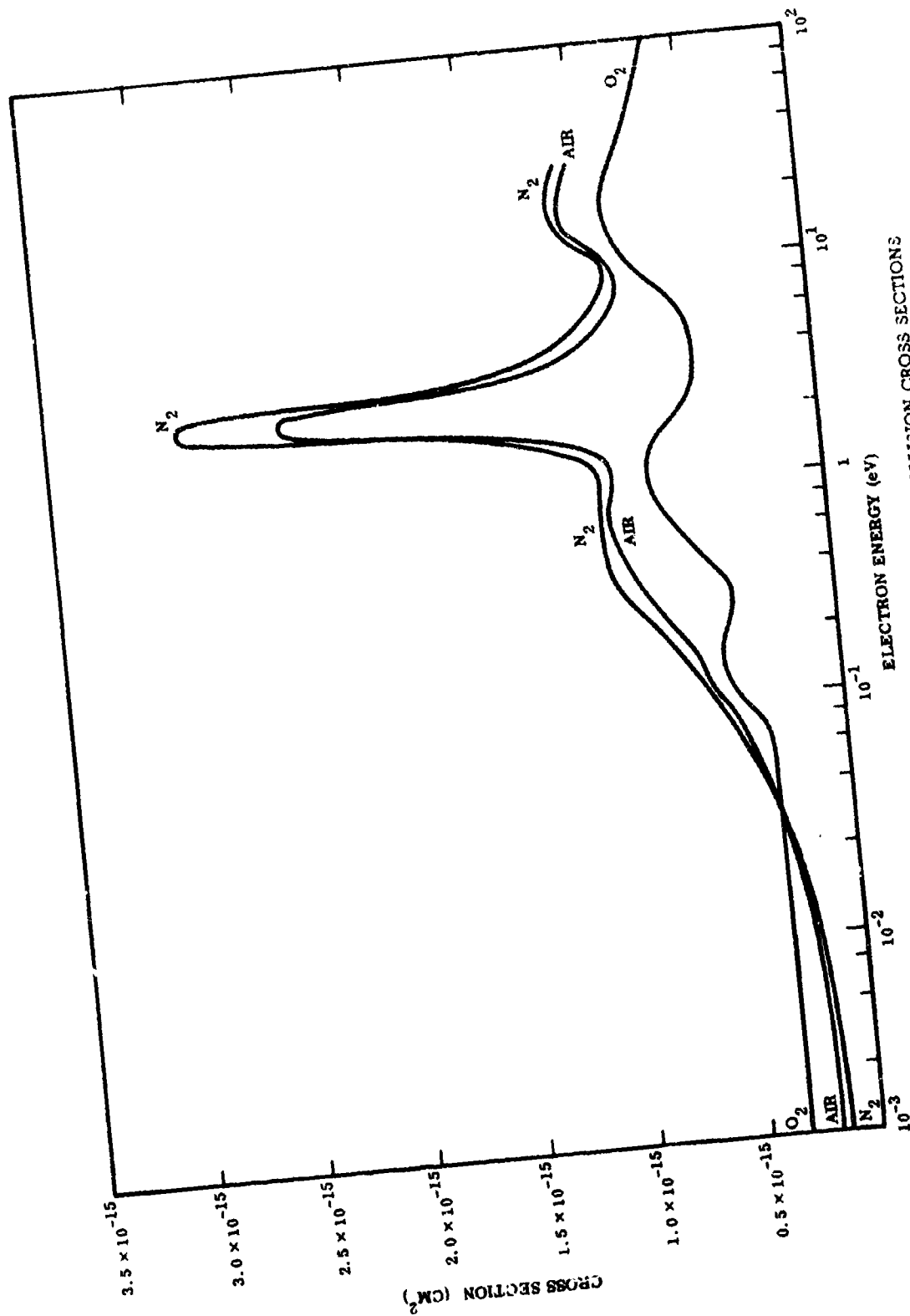


FIG. 2-9 ENERGY DEPENDENCE OF ELECTRON COLLISION CROSS SECTIONS IN N<sub>2</sub>, O<sub>2</sub> AND AIR BELOW 100 eV.

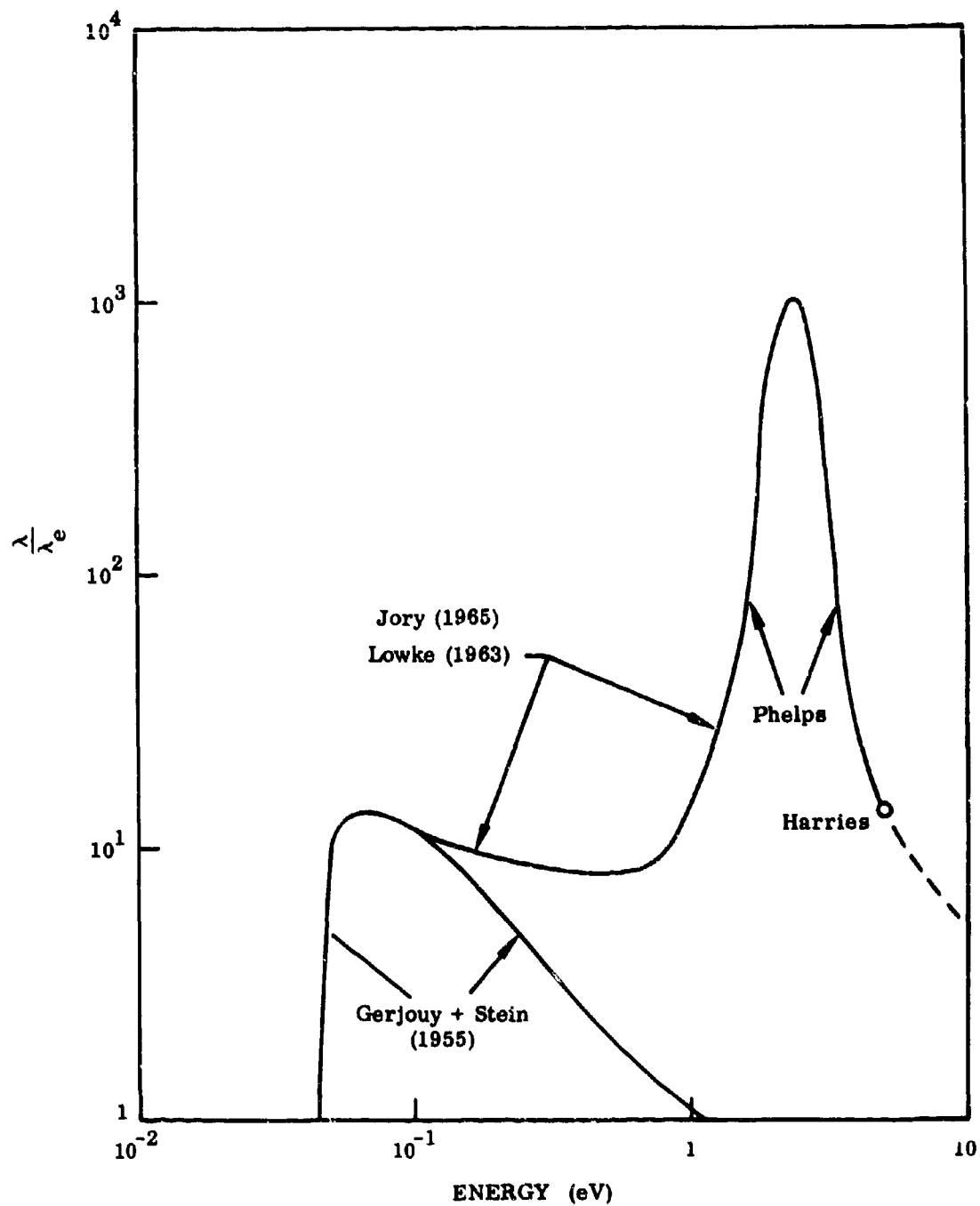


FIG. 2-10 ENERGY LOST EXCITING ROTATIONAL AND VIBRATIONAL ENERGY RELATIVE TO ENERGY LOST IN ELASTIC COLLISIONS (FOR AIR).

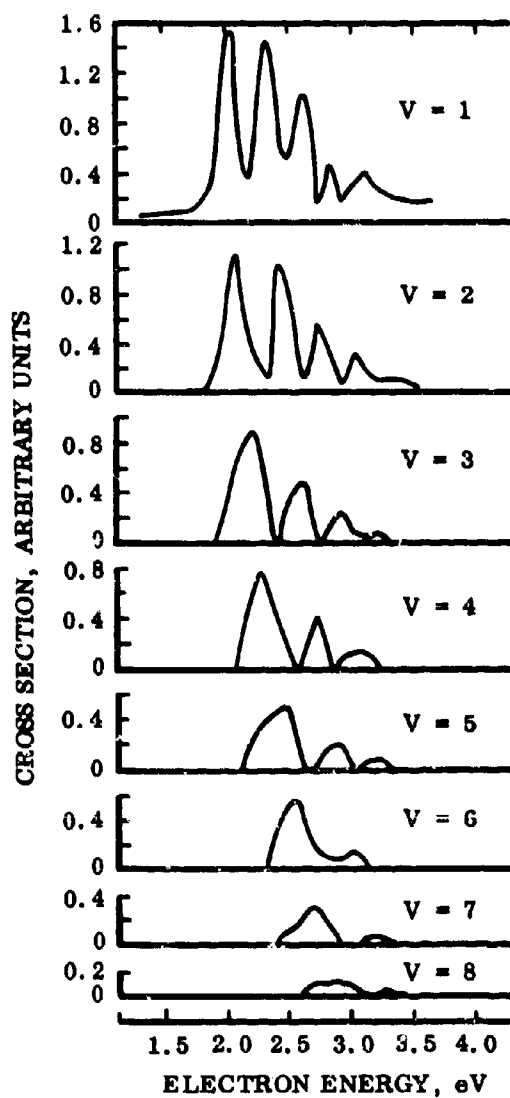


FIG. 2-11 ENERGY DEPENDENCE OF VIBRATIONAL CROSS SECTION OF NITROGEN BY ELECTRON COLLISION

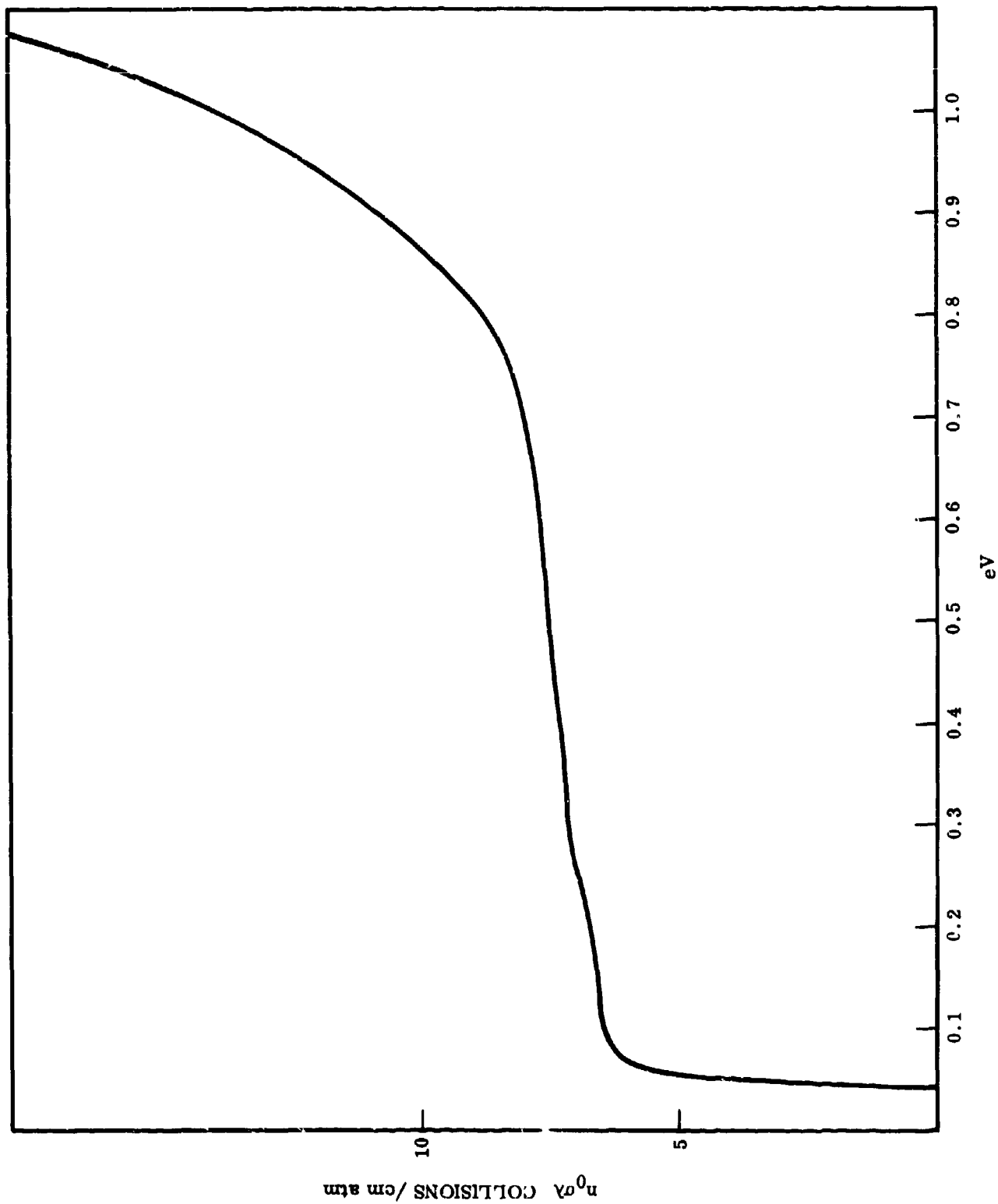


FIG. 2.12 FRACTIONAL ENERGY LOSS OF ELECTRON PER UNIT PATH LENGTH IN AIR AT ATMOSPHERIC PRESSURE. (See Eq. (6.39))

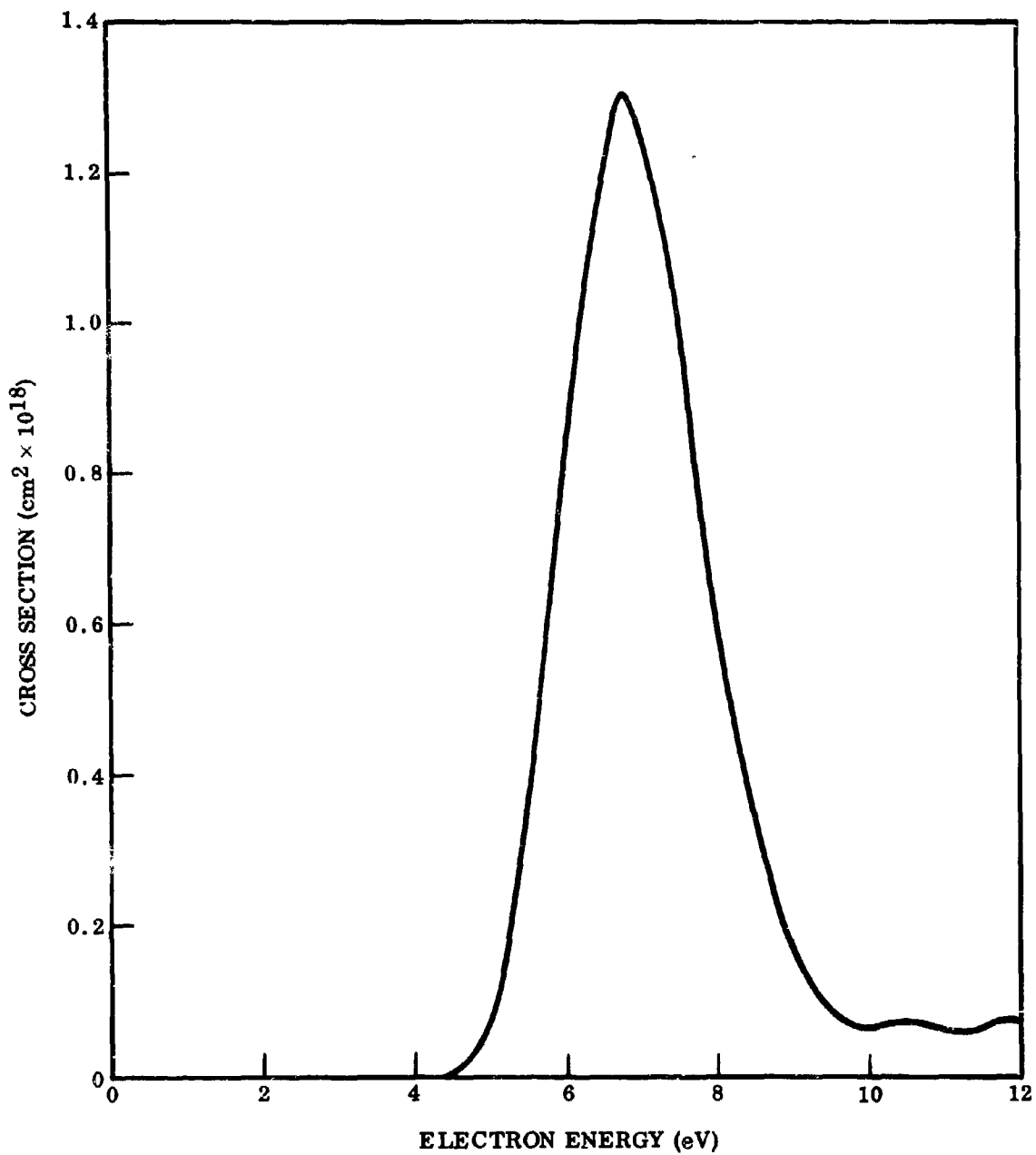


FIG. 2-13 ENERGY DEPENDENCE OF CROSS SECTION  
FOR THE PROCESS  $e + O_2 \rightarrow O + O^-$

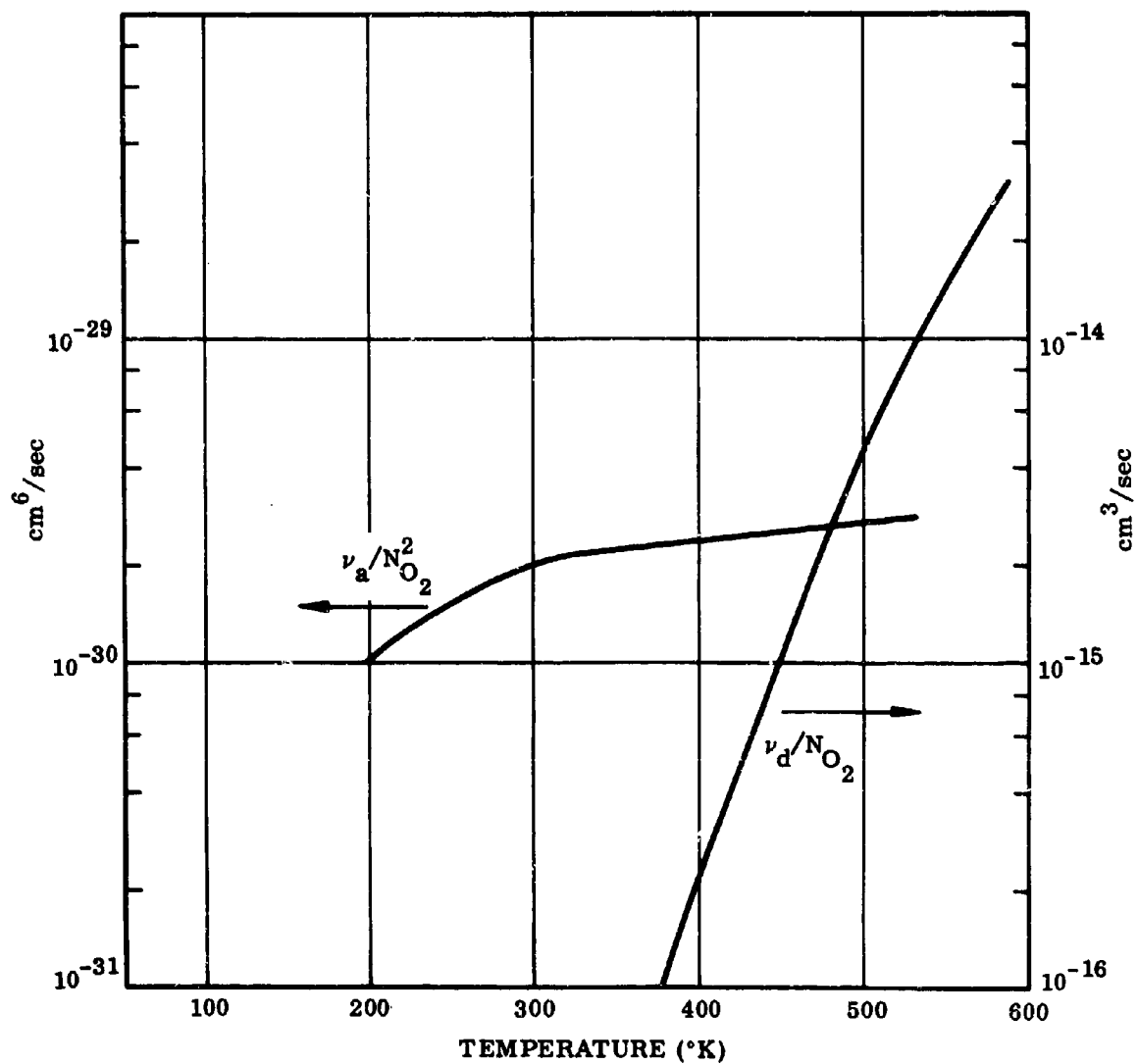


FIG. 2.14 RATE COEFFICIENTS FOR ELECTRON ATTACHMENT AND DETACHMENT ON  $O_2^-$  IN PURE OXYGEN.

## Chapter 3. SECONDARY PROCESSES FOLLOWING EXCITATION OF AIR

### 3.1 Disposition of the energy lost by a primary electron

To keep track of how the primary energy redistributes itself and how much of it appears as fluorescent radiation in various bands and lines, how much of it is used up for ionization, dissociation etc., is a complicated job of bookkeeping. Since only some of the relevant cross sections are known one has to make judicious use of all available information and make model assumptions to guess where one has not enough information. Such an attempt was made by the authors in a report (Lockheed, LMSD-48361) which appeared in 1958. Since that time many new experimental and theoretical data have become available so that it is possible to make these assignments somewhat better now. One of the most accurately measured quantities which have to do with the slowing down of electrons is the energy per ion pair,  $W = E/J$  where  $J$  is the total number of electrons liberated by the slowing down of an electron of energy  $E$ . For sufficiently large  $E$ , say above 20 keV, this quantity is essentially independent of  $E$ . Whyte reports (1953) a weighted average of several independent measurements of this energy as  $W_{\text{air}} = 33.73 \pm 0.15$  eV. For the components of air one finds  $W_{\text{N}_2} = 34.6 \pm 0.3$  eV and  $W_{\text{C}_2} = 30.8 \pm 0.3$  eV. Gerbes (1937)

presents evidence that  $W$  increases somewhat as the primary energy decreases. The high energy limit of Gerbes lies slightly below the more recent value of  $W_{\text{air}}$ . Normalizing his results to the currently adopted value one obtains

$$W_{\text{air}} = \left( 33.73 + \frac{175}{\sqrt{E - E_1}} \right) \text{ eV/ion pair } (E \text{ in eV}) \quad (3.1-1)$$

For  $E_1$  one can use an average value, say 15 eV.

Another quantity of interest is the differential energy loss per ion pair  $\gamma = \frac{dE}{dJ} = \frac{W^2}{W - E \frac{dW}{dE}}$ . This formula leads approximately to

$$\gamma_{\text{air}} = \left( 33.73 + \frac{87.5}{\sqrt{E - E_1}} \right) \text{ eV/ion pair} \quad (3.1-2)$$

To account for the energy which is lost by a primary electron we consider the example of a 1 keV electron as it passes through a layer of air where it produces on the average one ion pair. The particular value of 1 keV lies in the range of interest for the problems with which we are concerned and it is to be expected that the manner in which the energy loss of the

primary is distributed will be representative of a wide range of primary energies. To evaluate the thickness of the one ion pair (o.i.p.) layer we note from Eq. (3.1-2) that it takes on the average  $\gamma_{\text{air}} = 36.5$  eV to produce one ion pair. The energy loss rate of a 1 keV electron is taken from Fig. 2.8 to be  $\frac{1}{n} \frac{dE}{dx} = 50.4 \times 10^{-16}$  eV cm<sup>2</sup>/molecule and dividing this into  $\gamma_{\text{air}}$  we find that the o.i.p. layer contains  $n\Delta x = 0.725 \times 10^{16}$  molecules/cm<sup>2</sup>. The ionization cross section of air at 1 keV is  $\sigma_i = 0.95 \times 10^{-16}$  cm<sup>2</sup>/molecule so that the primary electron produces  $\sigma_i n\Delta x = 0.69$  secondary electrons while it is passing through the o.i.p. layer. It is clear that the remaining 0.31 negative charge carriers must also be electrons which are produced either by the secondary electrons or by the excited molecules which have been left behind. Before we account for the missing electrons we shall go through an energy check to account for the initial distribution of the 36.5 eV which the primary electron left behind. We expect this energy to be used up in producing various kinds of ions, excited molecules and atoms and in transferring some amount of kinetic energy to the secondary electrons. We have not enough information to distinguish between the formation of the X, A and B states of  $N_2^+$ . In our account we lump these states together and assign them the ionization energy of the X state - admitting that the true value should be somewhat larger. The relative probabilities of forming  $N_2^+$  or  $N + N^+$  are taken from Fig. 2.6 and so are the probabilities for exciting the two major singlet states of  $N_2$ . For  $O_2$  we do essentially the same except that the dominant non-ionizing collision is taken to be the dissociative transition to the Schumann-Runge continuum. The numerical details of the above

accounting scheme are listed in Table 3.1. The energy assigned to secondary electrons was so chosen that the total would come to 36.5 eV. Since we have left out some minor recipients of energy and have underestimated the energy for forming  $N_2^+$  ions the nominal average energy of secondaries is likely to be a little larger than the true value.

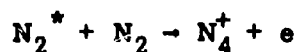
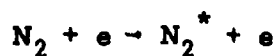
Table 3.1 Distribution of Energy Caused Directly  
by Primary Electrons in o.i.p. Layer.

Recipient	Number	Energy for one (eV)	Required Energy (eV)
$N_2^+$	.435	15.6	6.78
$N + N^+$	.102	24.3	2.48
$O_2^+$	.109	12.2	1.33
$O + O^+$	.044	18.7	0.82
$N_2$ b $i\Pi$	.12	12.85	1.54
$N_2$ h $^1\Sigma$	.08	14.01	1.12
$O + O$	.05	8.44	0.42
e	.69	31.9	22.01
			36.50

The nominal average energy of 31.9 eV per secondary electron can be compared to the energy  $E = \frac{9}{4} I = 33.8$  eV which follows from Eq. (2.4-3) if one uses an average ionization energy of  $I = 15$  eV. This is a small discrepancy which may easily arise from applying a calculation performed for H atoms to  $O_2$  and  $N_2$  molecules. Nevertheless, it shows that there is not much room for assigning additional amounts of energy to excitation.

To account for the 0.31 electrons which must still be produced we consider first ionizations due to the secondary electrons. One secondary

electron would produce  $\int_1^{500} \frac{E}{W_{\text{air}}} \left| \frac{dF_s}{dE} \right| dE$  additional electrons. In the low energy range, where most of the secondaries are, the energy per ion pair is of course not very well known. Lacking better information we take the expression given in Eq. (3.1-1). The factor  $\frac{dF_s}{dE}$  was taken from Eq. (2.4-3). The upper limit of 500 eV was taken because one counts an electron emerging from an electron collision with more than half the energy of the incoming electron as the primary electron. The value of the integral was found to be 0.29 and from the 0.69 secondary electrons one obtains therefore 0.20 additional electrons. If the average number of  $(n+1)^{\text{st}}$  generation electrons produced by one  $n^{\text{th}}$  generation electron were to remain at the same value of 0.29 the sum of all third and higher generation electrons would be  $(0.69)(0.29)/(1-0.29) = 0.28$  bringing the total up to 0.97 i.e. just .03 short of the one electron required by the definition of the o.i.p. layer. It is clear that the ratio 0.29 cannot be maintained since subsequent generations have less and less energy. Assuming that the ratio is cut in half at each step the sum of third and higher generation electrons reduces to 0.23 and the total to 0.92 so that one has to account for 0.08 more. It is clear that any explanation of this number will have to involve excited states of the  $N_2$  molecule. One possibility seems to be photoionization of  $O_2$  by quanta which are emitted from the  $b^1\Pi_u$  and the  $h^1\Sigma_u^+$  levels of  $N_2$ . Przybylski (1962) presents experimental evidence for this process but the observed yield is quite low giving only  $2 \times 10^{-3}$  ionizing quanta per ionizing collision. Another possible source of electrons is suggested by the work of Curran (1963) who observed  $N_4^+$  ions in a mass spectrometer which appear for electron energies above  $15.04 \pm 0.05$  eV. He assigns these ions to the sequence of collisions



From the work on electron impact spectra in  $N_2$  (Silverman and Lassettre, 1965) one knows that there are several excited states of  $N_2$  which might be responsible for this or similar reactions. The cross sections associated with these states are about of the right order of magnitude.

### 3.2 Atmospheric fluorescence

When high-energy electrons are stopped in air, a fraction of the molecules, atoms, and ions are left in excited states and will radiate in a time determined by the life of the optical state in question ( $\sim 10^{-8}$  sec). We refer to this type of emission as fluorescence.

The observed light intensity is determined by the initial population of the excited levels, collisional de-excitation, self-absorption, and perhaps by the production of intermediary states. The initial population of the excited levels is proportional to the energy deposited per unit volume but is insensitive to the initial energy of the primary electrons. The collisional de-excitation and self-absorption effects to be discussed later are reduced with increasing altitude and may be unimportant in many cases. The production of intermediate states could lead to an increase in fluorescence if it could be shown that intermediate states with long lives could be excited to higher levels from the ground states of the molecules. Examples of possible important intermediate states\* are the ground state of  $N_2^+$ , the  $A^3\Sigma_u^+$  and the  $a^1\Pi_g$  states of  $N_2$ . The radiative lifetime of the triplet state is about 1 sec (Carleton and Oldenberg, 1962); that of the singlet state is  $1.7 \times 10^{-4}$  sec (Lichten, 1957).

---

\* See footnote on p. 29.

Some of the spectra observed in fluorescence are:

$N_2^+$	First negative bands
$N_2$	Second positive bands
$O_2$	Schumann-Runge bands

It is likely that the  $N_2$  first positive bands, the  $N_2^+$  Meinel bands, and the  $O_2^+$  first negative bands should also be observable.

The excitation of these band systems may be by either the high-energy primary electron or by the secondary, tertiary, etc., electrons produced by the primary electron. Frankenthal et al. (1966) include also excitation by Auger electrons which appear when the primary electrons kick out K electrons.

The energy distribution of the electrons from Eq. (2.4-3) has been used, with the cross sections for  $N_2$  and  $O_2$  wherever known, to make estimates of the fluorescence intensity. It can be seen that the energy distribution is insensitive to the primary energy, so that in the first approximation one does not have to take account of the slowing down of the primary electrons.

a) The  $N_2^+$  First Negative Band System. For energies somewhat in excess of the threshold, it can be seen from Fig. 2.6 that the cross section ( $\sigma_5$ ) for exciting the  $v = 0$  level of the upper state of the  $N_2^+$  first negative bands is roughly proportional to the total ionization cross section for  $N_2$  and  $O_2$ . The ratio of the cross section for exciting the (0-0) transition at  $3914\text{\AA}$  to the ionization cross section for air stays at a nearly constant value, say  $f$ , regardless of the electron energy. This holds reasonably well for the secondary electrons as well as the primary ones to

within the accuracy considered here. Since the energy to produce an ion pair from both primary and secondary electrons is  $W \approx 34$  eV, the total number of (0-0) transitions in the  $N_2^+$  first negative system should be  $fE_p/W$  where  $E_p$  is the energy of the primary. Since the energy of the photon emitted is about  $h\nu \approx 3$  eV, the fraction of the total energy radiated in this band (i.e., the fluorescence efficiency for this band) is  $\eta = fh\nu/W$ .

We have two choices for  $f$  which are obtained from the cross section curves 5a and 5b in Fig. 2.6. They are  $f = 0.02$  and  $f = 0.048$  and they lead respectively to the fluorescence efficiencies  $\eta \approx 1.8 \times 10^{-3}$  and  $\eta \approx 4.2 \times 10^{-3}$ . An experimental determination by Hartman (1964) at pressures between  $10^{-1}$  and  $10^{-2}$  mm Hg leads to  $\eta = 3.3 \times 10^{-3}$ . Bennett (1965)\* quotes a value  $\eta = 10^{-2}$  from observations of a series of high altitude nuclear explosions.

b) The  $N_2$  Second Positive Bands. The cross sections for excitation of some of the  $v = 0$  level of the  $C^3\Pi_u$  state of  $N_2$  by electron impact from the ground state of  $N_2$  is also shown in Fig. 2.6. This shows a maximum somewhat above the threshold and thereafter a rather rapid decrease with energy, characteristic of an inter-combination (singlet-triplet) excitation function. Since this excitation function differs so radically in shape from the ionization cross section, it is necessary to consider the excitation by primary and secondary electrons separately. The number excited directly by primary electrons is only about  $10^{-3}$  of the number of ions formed by these electrons. The estimate for secondary electrons is based on a comparison with the number of ionizing collisions which we estimated in the preceding section to be about 0.2 per secondary electron. About 50% of these take place above 25 eV where the cross section for exciting  $N_2$  to the

---

\* op. cit. page 15.

$C^3\Pi_u$  level is quite small compared to the ionization cross section. Below 25 eV the two cross sections cross over and their average values are roughly the same leading to an estimate of 50% of 0.2 or 0.1 excitation processes per secondary electron in nitrogen. In air this is further reduced to 0.08. This is of course a very crude result but it is sufficiently much larger than the number  $10^{-3}$  estimated for primary electrons to indicate that most of the  $N_2$  second positive fluorescence produced by high energy electrons in air is due to the secondary electrons. This is in agreement with the qualitative observations of C.Y. Fan (1956). The fluorescence efficiency for the  $N_2$  second positive system is thus of the order  $0.08 (4/34) \approx 10^{-2}$  where 4 eV is the approximate energy of photons in this system. This is 3.5 times as large as the efficiency evaluated for the  $N_2^+$  first negative system  $(1 + 0.31 + 0.1) \times 2 \times 10^{-3}$ . This relative result agrees sufficiently well with the lower pressure (5 Torr) results of Davidson and O'Neil (1964a) for 50 keV electrons where this ratio is 2:1 if measured in air and 2:9 if measured in  $N_2$ .

c) The  $N_2$  First Positive Bands. Unfortunately no absolute cross sections for the excitation of the  $N_2$  first positive band exist, so that it is difficult to make intensity estimates. However, Davidson and O'Neil (1964a) report that the fluorescence efficiency of the  $N_2$  first positive bands is about half the  $N_2^+$  first negative results at 5 Torr.

At higher pressures it becomes necessary to consider the possibility of quenching by collisional deactivation. For example, at 600 Torr Davidson and O'Neil (1964a) give the efficiency of quenching of the  $N_2$  second positive transitions as about  $10^2$  that of the  $N_2^+$  first negative

ones, whereas at 5 Torr this factor is only 3. By comparing results at high and low pressures Davidson and O'Neil (1964b) can derive a value of the cross section for deactivation of excited  $N_2^+$  ions by collisions with  $N_2$  molecules as  $\sim 10^{-15} \text{ cm}^2$ .

One may expect considerable alteration in the relative intensities of the various band systems due to self-absorption. The  $N_2^+$  first negative bands and Meinel bands terminate on the ground state of the  $N_2^+$  molecule. In regions of high ion density, self-absorption effects will be important. On the other hand, the  $N_2$  second positive bands terminate on a short-lived excited state, so that self-absorption effects are not likely to be important. A similar situation arises in the case of the  $O_2$  Schumann-Runge bands. The Franck-Condon factors are such that transitions to high vibration states of the ground electronic state are favored. Since these are not populated at ambient temperature, self-absorption effects on this system should be less important than on the  $N_2^+$  systems.

### 3.3 Thermalization and capture of subexcitation electrons

The slowing down of electrons is a very rapid process until their energy drops below the lowest electronic excitation threshold. Most of the time required for thermalization is spent in losing the remainder of the energy. Entering the collision rate as given by Eq. (2.5-2) into Eq. (2.5-1) and setting  $n = n_0/p$ , i.e., dividing the sea level value  $n_0 = 2.68 \times 10^{19} \text{ cm}^{-3}$  by the pressure in atmospheres one obtains

$$-\frac{dE}{dt} = \frac{n_0 \sigma \lambda v E}{p} \quad (3.3-1)$$

The energy dependence of  $n_0 \sigma \lambda$  is shown in Fig. 2.12. From 0.8 eV down to slightly above the thermal energy  $\frac{3}{2} kT \approx 0.04 \text{ eV}$  this product is nearly constant. Assuming it to be exactly constant one can integrate Eq. (3.3-1) and obtain

$$t = \frac{2p}{n_0 \sigma \lambda v} \left( 1 - \sqrt{\frac{E}{E_0}} \right) \approx \frac{2p}{n_0 \sigma \lambda v} \quad (3.3-2)$$

where  $v = 1.2 \times 10^7 \text{ cm/sec}$  is approximately the thermal speed of electrons and  $E_0$  is large enough to ignore  $\sqrt{E/E_0}$  compared to 1. From Fig. 2.12 we take  $n_0 \sigma \lambda = 7 \text{ coll/cm atm}$  and find for the slowing down time

$$t \approx \frac{1.2 \times 10^{-8}}{p} \text{ sec} \quad (p \text{ in atm}) \quad (3.3-3)$$

The whole slowing down process takes about  $2/\lambda$  collisions where  $\lambda$  is an average value and a measure of the distance of electron travel is given by

$$\sqrt{r^2} = \frac{\sqrt{2/\lambda}}{n \sigma} = \frac{2 \times 10^{-3}}{p} \text{ cm} \quad (3.3-4)$$

Not all subexcitation electrons reach thermal energy because of various capture processes which may take place. The rate at which electrons are captured by these reactions is

$$\frac{dn_e}{dt} = - 0.2 n n_e \sigma_{\text{capt}} v \quad (3.3-5)$$

where  $0.2 n$  is the number density of oxygen molecules in air. Combining this equation with Eq. (2.5-1) one is led to

$$\frac{dn_e}{n_e} = 0.2 \frac{\sigma_{\text{capt}}}{\sigma} \frac{dE}{\lambda E} \quad (3.3-6)$$

The first possibility of attachment arrives when the electrons are in the dissociative capture region, i.e. in the energy interval from 10 eV down to 4 eV. Integrating Eq. (3.3-6) we find that the fraction

$$- \frac{\Delta n_e}{n_e} = 0.2 \int_4^{E_0} \frac{\sigma_{\text{capt}}}{\sigma} \frac{dE}{\lambda E} \quad (3.3-7)$$

of the electrons with a starting energy  $E_0$  are captured by this process. Using the data in Figs. 2.9, 2.10 and 2.13 we find that about 1.5% of the electrons starting with 7 eV are lost by dissociative capture. If one assumes - following Platzman (1955) - a distribution function

$$N(E) = \frac{2 I^2 (I + E_x)^2}{E_x (2I + E_x)} \frac{1}{(I + E)^3} \quad (3.3-8)$$

for the starting energy in the subexcitation region which cuts off at  $E_x = 7$  eV one finds that only 0.125% of the electrons attach in this manner. The electrons which survive the dissociative capture process are by and large thermalized before the remaining capture processes take place. In this context "thermalizing" means that the electrons acquire a Maxwell distribution at the temperature of the ambient air. The electron density, on the other hand, is still very much larger than the thermal equilibrium value. The prediction of the rate at which the electron density diminishes is of great importance because this density determines the propagation of electromagnetic waves in air. In calculations of this nature one must keep track of the various species which are able to capture electrons such as  $O_2$  and positive ions. One also has to keep track of negative ions from which electrons can be detached and which can recombine and remove positive ions.

At a large enough distance from the source of the ionizing radiation the concentrations of the ambient neutral molecules  $O_2$  and  $N_2$  change only by very small amounts which can be ignored. It remains, nevertheless, a formidable task to integrate the host of differential equations for the remaining species concentrations. The main features of the solution can

often be recognized by lumping some of the species together. Such a theory is for example presented by Latter and LeLevier (1963), who follow the densities  $n$  and  $N$  of electrons and negative ions. Because of charge conservation the positive ion density is  $n + N$  and one does not need to follow it separately. The major negative ion species is  $O_2^-$  but there may be others such as  $O^-$  and  $O_3^-$ . The major positive ion species are  $NO^+$ ,  $N_2^+$  and  $O_2^+$ . The model leads to two coupled differential equations

$$\frac{dn}{dt} = -\beta n - \alpha(n + N) N \quad (3.3-9)$$

$$\frac{dN}{dt} = \beta n - \gamma(n + N) N \quad (3.3-10)$$

with an initial value  $N = 0$  for the negative ion density. The initial electron density  $n_0$  is considered to be known. The coefficient  $\beta$  is the attachment frequency in air and is identical to  $\nu_a$  as given by Eq. (2.5-12). From the data in Fig. 2.14 one obtains

$$\beta = 0.65 \times 10^8 p^2 \text{ sec}^{-1} \quad (3.3-11)$$

where  $p$  is the pressure in atmospheres. The coefficient  $\alpha$  describes the recombination of electrons with positive ions and it should be some average for the mixture of the three major species of concern. Entering the coefficients from Table 2.7 into Eq. (2.5-18) and assuming an ambient temperature of  $300^\circ\text{K}$

the three values of  $\alpha$  range from  $2 \times 10^{-7} \text{ cm}^3/\text{sec}$  to  $5 \times 10^{-7} \text{ cm}^3/\text{sec}$ .

LeVier (1964) concludes from fitting high-altitude nuclear explosion data that  $\alpha$  must lie between  $3 \times 10^{-7} \text{ cm}^3/\text{sec}$  and  $7 \times 10^{-7} \text{ cm}^3/\text{sec}$ .

This range results from the uncertainty in the negative-positive ion recombination coefficient  $\gamma$ . He suggests a "best fit" where  $\alpha = 4 \times 10^{-7} \text{ cm}^3/\text{sec}$  and  $\gamma = 3 \times 10^{-8} \text{ cm}^3/\text{sec}$ . This value lies in the range suggested by the lab data.

The rate equations, Eqs. (3.3-9) and (3.3-10), can be integrated analytically if  $\gamma$  is assumed to be equal to  $\alpha$ . With this assumption one overestimates the lifetime of the free electrons but only by a small amount because the solutions of the rate equations are fairly insensitive to the exact value of  $\gamma$ . Setting  $\gamma = \alpha$  the solution becomes

$$n = \frac{n_0}{1 + \alpha n_0 t} e^{-\beta t}$$

and

$$N = \frac{n_0}{1 + \alpha n_0 t} (1 - e^{-\beta t}) .$$

At late times one obtains from this the asymptotic solution  $n = e^{-\beta t}/\alpha t$  and  $N = 1/\alpha t$  which is independent of the initial density  $n_0$ .

The statement made earlier in this section that electrons are thermalized before they are captured is not altogether correct. Near sea-level densities where attachment dominates over recombination the capture time

for electrons is  $\rho^{-1}$ . Using Eqs. (3.3-3) and (3.3-11) the ratio of slowing down to capture time is  $\beta t_s = 0.8 p$ . At sea-level, therefore, the two processes go essentially at the same rate. For discussions of thermal and blackout phenomena it is not really necessary to worry about this because both processes are essentially over after  $10^{-8}$  sec. Such details may, however, be of importance if one discusses electromagnetic pulse shapes.

### 3.4 Secondary molecular processes

The molecular processes discussed in this section include all thermal processes involving atoms, molecules, positive and negative ions. The primary action of ionizing radiation produces four kinds of positive ions ( $N_2^+$ ,  $N^+$ ,  $O_2^+$  and  $O^+$ ) and two kinds of atoms (N, O). The collision processes of secondary electrons produce the same ions and atoms and, in addition, two negative ions ( $O^-$  and  $O_2^-$ ). These intermediates react further in a variety of exothermic reactions which we shall now consider.

Under conditions of interest here all intermediates can be considered as thermal in kinetic energy content. Energy given them in their formation is not more than is commonly given to reaction products in exothermic chemical reactions. Furthermore, we are considering only cases in which the energy deposit of the ionizing radiation is small so that the ambient temperature is not increased. We shall actually take the temperature to be  $300^\circ\text{K}$  in quantitative considerations.

We are concerned here only with mechanisms and rate constants. The description of chemical effects in specific cases requires appropriate bookkeeping procedures. This problem is discussed in the next section.

### 3.4.1 Ion-molecule reactions

It has long been recognized that ions in the gas phase have very special properties, as contrasted with neutral molecules. Langevin (1905) presented an analysis of the collision of an ion with a neutral molecule, and Thomson (1924) discussed the mechanism of the neutralization reaction of positive and negative ions. Both of these processes have unusually large cross sections. Another important property of ions is the formation of clusters, and Lind (1928) postulated that many of the chemical reactions induced by ionizing radiation occurred in clusters. The role of clusters in the radiation chemistry of gases has not been clarified; Magee and Funabashi (1959) have discussed the problem.

Ion-molecule reactions have been studied experimentally in mass spectrometry (Gioumousis and Stevenson, 1958; Hamill, et al, 1962) and more recently in a variety of techniques (Ferguson, et al, 1956). The simple general treatment of Langevin (1905) makes the large cross sections understandable and gives an approximately valid formula for their magnitudes. It is a classical treatment which we shall summarize briefly because of its central position in discussions of ion-molecule reactions.

Consider the interaction between a singly-charged ion and a molecule which has a polarizability  $\alpha$ . If both particles are small compared with their separation,  $r$ , the magnitude of the force between them can be given to a good approximation as

$$F(r) = -\frac{2\alpha e^2}{r^5} \quad (3.4-1)$$

and the potential as

$$V(r) = - \frac{1}{2} \frac{\alpha e^2}{r^4} \quad (3.4-2)$$

It is assumed in this treatment that the molecule has no dipole, or higher electric moments.

Langevin called attention to the fact that for each value of the relative energy  $E$  there is a critical impact parameter for which the trajectories degenerate into spirals and the collision partners come very close. This phenomenon can be understood in terms of the radial motion of the pair in the "effective" potential which includes the ion-polarizability term of Eq. (3.4-2) and a contribution from the angular momentum. For a particular value of the angular momentum  $L$  this effective potential is

$$V_L(r) = \frac{L^2}{2\mu r^2} - \frac{\alpha e^2}{2r^4} \quad (3.4-3)$$

where  $\mu$  is the reduced mass. In terms of the impact parameter  $b$  and the velocity  $v$  at infinite separation the angular momentum is

$$L = \mu v b \quad (3.4-4)$$

Fig. 3.1 shows a set of effective potential curves for several values of the angular momentum. A feature of these curves is that each has a single maximum. If the energy is fixed at  $E = \frac{1}{2} \mu v^2$ , the

different angular momenta will correspond to different impact parameters. Let us consider the motion of the pair for the highest angular momenta of the figure,  $L_4$  and  $L_3$ . The two particles will approach until they reach the separations designated as  $P_4$  and  $P_3$  respectively and turn back. The value of  $L_2$  was chosen so that precisely at the maximum of the potential energy curve the relationship

$$V_{L_2}(r^*) = 1/2 \mu v^2 \quad (3.4-5)$$

is valid. Of course at this point the pair come to rest, but then the motion continues to small separations. At this energy, motion for all angular momenta smaller than  $L_2$  also continue to very small separations. The trajectories for values of  $r$  smaller than the value at potential maximum are spirals.

This analysis shows that the trajectories are divided into two classes: those with impact parameters greater than  $b^* = \frac{L_2}{\mu v}$ , which turn at large distances; and those with impact parameters less than  $b^*$ , which approach to small separations, or "collide". The "collision" cross section is given by

$$\sigma = \pi b^{*2} \quad (3.4-6)$$

Use of elementary analysis gives the relationship

$$\sigma_L = \pi \sqrt{\frac{2ae^2}{E}} \quad (3.4-7)$$

which is called the "Langevin" cross section. This can also be

written

$$\sigma_L = 2\pi \sqrt{\frac{\mu}{v}} \frac{a}{v} \quad (3.4-8)$$

and it is seen to have a typical  $1/v$  dependence on velocity.

For reaction of ions in air with molecules of air,  $a = 1.6 \times 10^{-24} \text{ cm}^3$  for both  $\text{O}_2$  and  $\text{N}_2$ , and we get

$$\sigma_L = \frac{8 \times 10^{-10}}{v} \text{ cm}^2 \quad (3.4-9)$$

If we make the assumption that some particular reaction occurs on every ion-molecule collision, we get for the ion-molecule rate constant for air molecules

$$k_{im} = \overline{v\sigma_L} = 8 \times 10^{-10} \text{ cm}^3/\text{sec} \quad (3.4-10)$$

At this point we should note that the effective potential curves for an actual ion-molecule pair will have the form shown in Fig. 3.2 rather than 3.1. At small distances the potential must be repulsive because of exchange interactions. The difference between the sets of curves in these two figures actually has very little to do with the estimated ion-molecule collision rate, because at the calculated distances of the critical potential maximum, the form of the potential given by Eq. (3.4-3) is adequate. The assumption that any particular chemical reaction occurs at every ion-molecule reaction is more questionable. There are no general principles which prevent activation energies for such reactions, even if they are exothermic. If different channels are possible, Eq. (3.4-10) gives the maximum value of the sum of the rate constants.

Experimental measurements verify that many ion-molecule reactions have rate constants of the estimated magnitude. On the other hand, there are important exceptions.

#### 3.4.2 Reactions of ions

The most abundant initially formed positive ions of air are  $N_2^+$ ,  $N^+$ ,  $O_2^+$  and  $O^+$  (see Table 3.1). In addition other species, such as  $NO$ ,  $NO_2$ ,  $O_3$ ,  $O_2^-$ , and  $O^-$ , are formed in secondary reactions. The possibly important reactions of the ion with the neutral species are summarized in Tables 3.2 and 3.3. In systems at low temperature it is only the exothermic processes which are important. The rate constants were taken from several sources. Two of the primary sources were unpublished lists which represented what was believed to be the best values at the times of compilation (Sparks and Pennington, 1965; Bortner, 1966). Also used were Bortner (1965), Ferguson, et al, (1966), and Ferguson (1966). The latter two represent the most recent data on certain of the reactions. In the case of some rates, marked by an asterisk, the values are estimates made by the authors in accord with the most recent data on similar reactions. We should emphasize that many of the rates in Tables 3.2 and 3.3 are subject to drastic change as more experimental data is obtained.

The exothermic heats of the reactions,  $\Delta E$ , are given in electron volts. The rate constants are given in  $cm^3/sec$ . A temperature of  $300^\circ K$  is assumed.

Table 3.2 EXOTHERMIC REACTIONS OF POSITIVE AIR IONS

Reaction	$\Delta E$	Rate Constant
$N_2^+ + O_2 \rightarrow O_2^+ + N_2$	3.5	$1 \times 10^{-10}$
$N_2^+ + O_2 \rightarrow NO^+ + NO$	4.4	$1 \times 10^{-16}$
$N_2^+ + NO \rightarrow NO^+ + N_2$	6.3	$4 \times 10^{-10}$
$O_2^+ + N_2 \rightarrow NO^+ + NO$	0.9	$5 \times 10^{-16}$
$O_2^+ + NO \rightarrow NO^+ + O_2$	2.8	$7 \times 10^{-10}$
$N^+ + O_2 \begin{cases} \rightarrow O_2^+ + N \\ \rightarrow NO^+ + O \end{cases}$	$\begin{cases} 2.5 \\ 6.7 \end{cases}$	$1 \times 10^{-9}$
$N^+ + O_2 \rightarrow O^+ + NO$	2.3	$1 \times 10^{-12}$
$N^+ + NO \rightarrow N_2^+ + O$	2.2	$3 \times 10^{-12}$
$N^+ + NO \rightarrow O^+ + N_2$	4.2	$1 \times 10^{-12}$
$N^+ + NO \rightarrow NO^+ + N$	5.3	$8 \times 10^{-10}$
$O^+ + O_2 \rightarrow O_2^+ + O$	1.5	$2 \times 10^{-11}$
$O^+ + N_2 \rightarrow NO^+ + N$	1.1	$3 \times 10^{-12}$
$O^+ + NO \rightarrow NO^+ + O$	4.3	$2 \times 10^{-11}$
$O^+ + NO \rightarrow O_2^+ + N$	0.2	$3 \times 10^{-12}$
$N_2^+ + N \rightarrow N^+ + N_2$	1.0	$5 \times 10^{-11}^*$
$N_2^+ + O \rightarrow O^+ + N_2$	2.0	$1 \times 10^{-10}$
$N_2^+ + O \rightarrow NO^+ + N$	3.1	$2 \times 10^{-10}$
$O_2^+ + N \rightarrow NO^+ + O$	4.2	$2 \times 10^{-10}$
$N^+ + O \rightarrow O^+ + N$	0.9	$5 \times 10^{-12}$

Table 3.3 EXOTHERMIC REACTIONS OF NEGATIVE AIR IONS

Reaction	$\Delta E$	Rate Constant
$O_2^- + O \rightarrow O^- + O_2$	1.0	$1 \times 10^{-11}$
$O_2^- + NO \rightarrow NO_2^- + O$	1.6	$1 \times 10^{-12}$
$O_2^- + O_3 \rightarrow O_3^- + O_2$	2.4	$2 \times 10^{-10}$
$O_2^- + NO_2 \rightarrow NO_2^- + O_2$	3.6	$1 \times 10^{-9}$
$O_2^- + NO_2 \rightarrow O_3^- + NO$	0.4	$1 \times 10^{-11} *$
$O^- + O_3 \rightarrow O_2^- + O_2$	3.0	$1 \times 10^{-11}$
$O^- + O_3 \rightarrow O_3^- + O$	1.4	$7 \times 10^{-10}$
$O^- + NO_2 \rightarrow NO_2^- + O$	2.5	$1 \times 10^{-9}$
$O_3^- + NO_2 \rightarrow NO_2^- + O_3$	1.1	$1 \times 10^{-9}$
$O_3^- + N_2 \rightarrow NO_2^- + NO$	1.3	$1 \times 10^{-20}$
$O_3^- + NO \rightarrow NO_2^- + O_2$	3.1	$1 \times 10^{-12} *$
$O_3^- + O \rightarrow O_2^- + O_2$	1.6	$1 \times 10^{-11}$
$NO^- + O_2 \rightarrow O_2^- + NO$	**	$1 \times 10^{-9}$
$NO^- + O \rightarrow O^- + NO$	**	$1 \times 10^{-11}$
$NO^- + O_3 \rightarrow O_3^- + NO$	**	$1 \times 10^{-9} *$
$NO^- + NO_2 \rightarrow NO_2^- + NO$	**	$1 \times 10^{-9} *$

\*\* The electron affinity of NO is uncertain. The value for the reaction  $NO^- + O_2 \rightarrow O_2^- + NO$  (Ferguson, 1966) indicates that it is less than the affinity of  $O_2$ .

Three body reactions have not been included in Tables 3.2 and 3.3 although they may be important at high pressures. For positive ion-neutral association, i.e.,



where  $A^+$  and  $B$  may be atoms or molecules and  $M$  is any third body, the rate is estimated to be of the order of  $10^{-29} \text{ cm}^6/\text{sec}$ . When  $A^+$  and  $AB^+$  are replaced by  $A^-$  and  $AB^-$  the rate is estimated to be an order of magnitude lower (Sparks and Pennington, 1965; Bortner, 1965).

Examination of Table 3.2 shows that  $NO^+$  is the end product of several reaction sequences. Since  $NO$  has the lowest ionization potential (9.3 eV) of any possible air species,  $NO^+$  is to be expected in abundance. For a more detailed discussion of the charge transfer reactions reference can be made to Hasted (1960) and Rapp and Francis (1962).

If we estimate the lifetime of the primary ions using Eq. (3.4-10) we obtain a value

$$\tau_{A^+} = \frac{1}{k_{im}N_B} = \frac{5 \times 10^{-11}}{p} \text{ sec.} \quad (3.4-11)$$

where  $p$  is the pressure in atmospheres. Since many of the reactions rates in Table 3.2 do not have the maximum value given by Eq. (3.4-10), the time given by Eq. (3.4-11) is a minimum time. The actual conditions which exist in any situation will depend on the rate constants in a more complicated manner than indicated by Eq. (3.4-11).

Table 3.3 has included many reactions involving  $O_3$  and  $NO_2$  even though these species are present in only small quantities. This has

been done because of their large electron affinities, 2.9 and 4.0 eV respectively.  $\text{NO}_2^-$  in particular could be important because of its relative stability.

Table 3.3 does not include any reactions involving negative ions and nitrogen atoms. No estimates of these reactions were available, probably because N is not an important constituent of the normal atmosphere and is important only at very early times following intense ionization impulses (Branscomb and Le Levier, 1964). In one case, namely collisions between  $\text{O}_2^-$  and N, the main channels taken involve the production of free electrons (Ferguson, 1966; see also Section 3.4.5). Thus the charge transfer or atom transfer type channels would have rate constants which are small and could possibly be neglected even when the N concentration is appreciable.

#### 3.4.3 Reactions of atoms

It is clear that the primary processes in the ionization of air produces atoms. Table 3.1 reveals that 17 percent of ionizations yield N atoms and 6.3 percent yield O atoms. In addition to the reactions of the atoms with ions there are reactions with the air molecules, the important of which are shown in Table 3.4. The three body reaction rates are expressed as two body rates but are pressure dependent. The reference is Bortner (1966).

Table 3.4 EXOTHERMIC REACTIONS OF ATOMS IN AIR

Reaction	$\Delta E(\text{eV})$	Rate Constant
$\text{N} + \text{O}_2 \rightarrow \text{NO} + \text{O}$	1.4	$3 \times 10^{-17}$
$\text{N} + \text{NO} \rightarrow \text{N}_2 + \text{O}$	3.3	$3 \times 10^{-11}$
$\text{N} + \text{NO}_2 \rightarrow \text{NO} + \text{NO}$	3.4	$5 \times 10^{-12}$
$\text{N} + \text{N} \rightarrow \text{N}_2$	9.8	$5 \times 10^{-13}_p$
$\text{N} + \text{O} \rightarrow \text{NO}$	6.5	$7 \times 10^{-13}_p$
$\text{O} + \text{NO} \rightarrow \text{NO}_2$	3.1	$2 \times 10^{-12}_p$
$\text{O} + \text{O}_2 \rightarrow \text{O}_3$	1.1	$1 \times 10^{-14}_p$
$\text{O} + \text{O} \rightarrow \text{O}_2$	5.1	$7 \times 10^{-14}_p$
$\text{O} + \text{O}_3 \rightarrow \text{O}_2 + \text{O}_2$	4.0	$5 \times 10^{-15}$
$\text{O} + \text{NO}_2 \rightarrow \text{NO} + \text{O}_2$	2.0	$5 \times 10^{-12}$

The first two reactions of Table 3.4, which would be most important at low pressures, suggest that nitrogen atoms recombine in a sequence of two bimolecular reactions with the production of oxygen atoms. Thus, when three-body recombination is not rapid, atomic oxygen will be an important constituent for long times. These first two reactions will also control the formation of NO which in turn controls the formation of  $\text{NO}_2$ . A detailed discussion of the role of oxygen atoms in the nitrogen oxide production can be found in Franscomb and LeLevier (1964).

The reactions which require third bodies, and which are important at high pressures, have rate constants of the magnitude

$$k' \approx 10^{-11} (2.5 \times 10^{19} \text{ Vp}) \text{ cm}^3 \text{ sec}^{-1} \quad (3.4-12)$$

where  $p$  is the pressure in atmospheres, and  $V$  is the volume in which an air molecule is an effective third body. We can estimate  $V$  as

$$V \approx \frac{4\pi}{3} (6 \times 10^{-8})^3 = 9.1 \times 10^{-22} \text{ cm}^3$$

which gives

$$k' \approx 2 \times 10^{-13} p \text{ cm}^3 \text{ sec}^{-1} \quad (3.4-13)$$

The rate constants given in Table 3.4 for three-body recombination are in general agreement with Eq. (3.4-13).

#### 3.4.4. Positive-negative ion recombination

The reaction of positive and negative molecular (or atomic) ions has the largest rate of any process of chemical interest, owing to the long-range Coulomb force between the ions. In the pressure-dependent region, we can estimate the rate constant as follows (see Thomson, 1924): assume that oppositely charged ions recombine if they approach each other within a distance  $r_C \approx e^2/kT$ , and if one of them then loses its kinetic energy by collision with a neutral molecule. If we write the rate of recombination as

$$-\frac{dN}{dt} = k'' N n_{\text{air}} \quad (N = \text{ion density}) \quad (3.4-14)$$

the rate constant  $k''$  is approximately the rate constant given by Eq. (3.4-10) for collision of an ion with a neutral molecule multiplied by the number  $VN$  of ions of opposite charge within the volume  $V = (4\pi/3)r_C^3$ . Expressing  $n_{\text{air}}$  by the pressure  $p$  in atmospheres

and substituting numerical values gives

$$-\frac{dN}{dt} = k N^2 \quad (3.4-15)$$

with

$$k = 1 \times 10^{-5} p \left( \frac{300}{T} \right)^3 \text{ cm}^3 \text{ sec}^{-1} \quad (3.4-16)$$

This value is much higher, at 300°K, than the value suggested in Sparks and Pennington (1965) and Bortner (1965), which is

$$k = 5 \times 10^{-8} p \left( \frac{300}{T} \right)^{3/2} \text{ cm}^3 \text{ sec}^{-1} \quad (3.4-17)$$

Not only is the magnitude in disagreement but the temperature dependence as well. The use of a lower value of the rate constant for ion-neutral molecule reaction, as indicated by some of the reactions in Table 3.3, would mitigate this disagreement.

Eq. (3.4-16) is valid for pressures up to 0.1 atm., after which it increases less rapidly with increasing pressure. Near 1 atm. the mean free path for ion-molecule collisions drops below  $r_c$ , and  $k$  reaches a maximum of  $2.3 \times 10^{-6}$ , after which it decreases approximately as  $1/p$ .

It is clear that  $k$  cannot decrease below the rate constant for mutual neutralization in the absence of third bodies. This is given in the above mentioned references as

$$k = 3 \times 10^{-8} \left( \frac{300}{T} \right)^{1/2} \text{ cm}^3 \text{ sec}^{-1} \quad (3.4-18)$$

### 3.4.5 Secondary molecular processes which create free electrons

In many problems of great interest the free electron concentration is the most important property of a disturbed atmosphere. It has been realized for a long time that electrons can be detached from negative ions by exothermic chemical processes, but only recently has much progress been made in measurements of rate constants of such processes. Table 3.5 lists exothermic detachment reactions which can occur in ionized air. The reference is Ferguson (1966).

Table 3.5 EXOTHERMIC DETACHMENT REACTIONS OF  
NEGATIVE IONS OF AIR

Reaction	$\Delta E$	Rate Constant
$O^- + O \rightarrow O_2 + e$	3.7	$3 \times 10^{-10}$
$O^- + N \rightarrow NO + e$	5.0	$3 \times 10^{-10}$
$O_2^- + N \begin{cases} \rightarrow NO + O + e \\ \rightarrow NO_2 + e \end{cases}$	$\begin{cases} 1.0 \\ 4.1 \end{cases}$	$5 \times 10^{-10}$
$O_2^- + O \rightarrow O_3 + e$	0.6	$5 \times 10^{-10}$
$O_3^- + O \rightarrow O_2 + O_2 + e$	1.2	$1 \times 10^{-10}$
$O_3^- + N \rightarrow O_2 + NO + e$	2.6	$1 \times 10^{-10} *$
$O^- + NO \rightarrow NO_2 + e$	2.7	$5 \times 10^{-10}$
$O^- + O_3 \rightarrow O_2 + O_2 + e$	2.6	$1 \times 10^{-10} *$

Such reactions are relatively unimportant in many situations because they involve minor constituents. On the other hand, they may play a critical role in determination of the electron concentration.

#### 3.4.6 Exothermic reactions between radiation products

Several molecular products have been formed in the reactions presented above, for example,  $\text{NO}$ ,  $\text{NO}_2$ , and  $\text{O}_3$ . Although reactions of ionic and atomic intermediates with such products are faster than their reactions with each other, under some conditions the latter reactions are important. For example, the reaction sequence



is known to occur in irradiated air (Harteck and Dondes, 1958).

In the absence of ozone the  $\text{N}_2\text{O}_5$  will decompose into  $\text{NO}_2$  and  $\text{O}_2$ . This process is catalysed by  $\text{NO}$  as Hisatsune et al (1957) have shown in the reaction sequence



All radiation products are unstable and will decompose eventually with formation of oxygen and nitrogen. Ozone is very unstable and will re-form oxygen relatively rapidly by thermal reactions at ordinary temperature. This process is also catalysed by ultraviolet radiation (McGrath and Norrish, 1957). Nitrogen dioxide is the most stable of all the radiation products. Its lifetime with respect to re-formation of  $\text{N}_2$  and  $\text{O}_2$  at ordinary temperatures is essentially infinite.

### 3.5 Chemical contaminants resulting from absorption of ionizing radiation in air

In this section we are concerned with chemical effects in air produced by relatively small deposits of ionizing radiation. Our knowledge of this field comes from two types of investigations which have been carried on rather extensively: (a) studies of the ionosphere and the "disturbed atmosphere" following x-ray deposits at high altitudes; (b) studies of the radiation chemistry of air. Under (a), the principal concern is the persistence of free electron concentration, total ionization is frequently less than one molecule in a million, and the density of the air is of the order of  $10^{-2}$  to  $10^{-5}$  normal sea level density. Under (b) the principal concern is the chemical contaminants themselves, total ionization is usually considerably larger than that of (a) and densities of the irradiated air are almost always sea level density or greater.

#### 3.5.1 Contaminants in the upper atmosphere

Models have been constructed for the study of the upper atmosphere. The complicated nature of the problem can be appreciated by noting that the bookkeeping procedure commonly employed involves fifteen species and 145 to 200 different elementary reactions (Bortner, 1965; Keneshea, 1963). The transient electron concentration is computed for various sets of initial conditions by solving the rate equations simultaneously on a digital computer using a code developed by Keneshea (1963). In a general way this problem is understood, but the relative effects of various processes are not known (Bortner, 1965). At the present time accurate predictions cannot be made. This situation will improve as more reliable rate constants become available.

It is perhaps of more interest for us to consider in some detail a typical problem of the upper atmosphere: the events which follow a sudden, intense pulse of ionizing radiation which does not deposit enough energy to raise the temperature appreciably. This problem was discussed by Branscomb and LeLevier(1964) for the region of the atmosphere between 30 and 80 km. These authors pointed out that following initial absorption of radiation there are several distinct time periods in which different processes are important.

1. Electron disappearance. For initial fractional ionization levels greater than about  $10^{-7}$ , recombination of electrons to  $N_2^+$  and  $O_2^+$  dominates attachment to  $O_2$ , and we consider this case only. This recombination involves dissociation and the production of atoms.

2. Nitrogen atom reaction. Initially the only possible reaction is



but as NO builds up, the reaction



competes. At the end of this time period the principal constituents of the disturbed air are  $N_2$ ,  $O_2$ , NO and O.

3. Ozone formation. At first the oxygen atoms combine with  $O_2$  in a three-body process to form ozone.



As the ozone builds up, the reaction



competes.

4. Nitrogen dioxide formation. All of the nitric oxide (NO) which survived the nitrogen atom period is ultimately converted to  $\text{NO}_2$ . The reactions are



According to Branscomb and LeLevier, the disturbed air ultimately contains  $\text{O}_3$  and  $\text{NO}_2$  as contaminants in proportions that depend upon the individual rate constants. For smaller initial fractional ionizations, relatively less contaminants are formed because electron attachment to  $\text{O}_2$  occurs and the molecular ion neutralization process produces fewer atoms than the dissociative capture neutralization mechanism.

A principal reason for the importance of the chemical contaminants in the atmosphere formed by ionizing radiation is that these small constituents alter the electron decay properties for additional ionization produced later. During the time when oxygen atoms still exist in abundance, for example, the following reaction can enhance the free electron concentrations and thus alter the observed attachment rate:



There is evidence of a different type which bears on the negative ions of the upper atmosphere. It is known (Kircher, et al, 1960) that in the steady-state irradiation of pure oxygen (either gas or liquid) the steady-state concentration of ozone is extremely small, a few parts per million. The initial production rate of ozone is known to be rather large, approximately one molecule per sixteen electron volts of absorbed energy in the system as a whole. The low steady-state concentration can only mean that there is a very effective decomposition of ozone in irradiated oxygen. After a careful study, Fueki and Magee (1963, 1964) proposed that ozone is decomposed in the following negative ion chain



Estimated chain lengths for this decomposition are as high as ten thousand.

Harteck et al. (1965) have considered the significance of this chain decomposition of ozone with respect to the radiolysis of air. They point out in the early stages of a steady irradiation of air ozone builds up to a concentration of several orders of magnitude greater than it is able to do in pure oxygen. The only reasonable explanation of this fact seems to be that the radiation-induced decomposition chain reaction

is stopped. The most likely chain-breaking step is one or the other of these reactions:



or



If this explanation is correct, it may be that most of the negative charge in a contaminated atmosphere is normally found in  $\text{NO}_2^-$  ions.

### 3.5.2 The radiation chemistry of air

Now let us turn to the evidence to be obtained from radiation chemistry. The radiation chemistry of air has long been of interest, partly because it was known rather early that the oxides of nitrogen were produced and it was thought that ionizing radiations might furnish a practical way for "fixation of nitrogen". Early work in this field has been described by Lind (1928, 1961) and more recent efforts by Harteck and Dondes (1964, 1957) and Farteck et al. (1965).

What follows is a very brief summary of the situation as known from irradiation of air at relatively high pressures. The complexity of the reactions increases with time in air under steady irradiation and after relatively little decomposition, the reaction products start competing for the intermediates. At relatively high pressures (atmospheric and above) it has been verified that a radiation-stationary state is reached. In this state only  $\text{NO}_2$  and  $\text{N}_2\text{O}$  occurs as reaction products. The situation is illustrated in Fig. 3.3 given by Harteck and Dondes (1964). In this figure various mixtures of oxygen and nitrogen have been irradiated to

a stationary state and the relative proportions of  $N_2$ ,  $N_2O$ ,  $NO_2$  and  $O_2$  are given by the segments of vertical lines in the figure. It is interesting that ozone never occurs in a stationary-state of irradiated oxygen and nitrogen mixtures. In the approach to the stationary-state, ozone and nitrogen pentoxide ( $N_2O_5$ ) are known to occur in a complicated interplay which has been described by Harteck and Dondes (1958), Harteck et al. (1965), and mentioned briefly in Section 3.4.6. Fig. 2.4 shows the variation in these species with time in air under steady irradiation given by Harteck et al. (1965).

In the early days of radiation chemistry, yields were expressed in terms of numbers of product molecules formed per ion pair created by the ionizing radiation. More recently the custom has been to use the amount of product per one hundred electron volts of energy absorbed (this is the "G value"). The latter system is preferable because in many conditions of interest it is impossible to know how many ion pairs were created. In such cases any use of absorbed energy to calculate a number of ion pair produced is artificial and is avoided by use of "G values" for products.

The radiation yield of  $NO_2$  in air for relatively small irradiations is a "G value" of around six. It is believed that the sequence of reactions



is the simplest (and oversimplified) description of the  $NO_2$  formation mechanism. Harteck and Dondes (1964) say that approximately twelve N atoms would be produced if all the  $N_2^+$  were neutralized by the reaction



but it appears that if very little  $O_2$  is present, the charge exchange reaction



occurs and reduces the yield of N atoms to a "G value" of around six. Of course the yield is reduced even further as the irradiation is continued by reaction of NO and  $NO_2$  with intermediates, and at the stationary-state it is zero, since the products are decomposed at the same rate at which they are formed.

It should be emphasized that no mechanism for the radiation chemistry of air has been proposed which can claim to be more than exploratory. The roles of many intermediates such as  $N_3^+$ ,  $N_4^+$ , etc. have not even been considered. There is no model of the radiation chemistry of air corresponding to the models of Keneshea, Bortner and others of the upper atmosphere.

### 3.5.3 Contaminants formed by radiation in lower atmosphere

In all of this section we have considered only dry air. In the upper atmosphere there is no moisture and in laboratory experiments moisture is deliberately excluded. However, in the lower atmosphere, moisture does occur and it can have a rather dominating influence on the chemical contaminants, at least when the total chemical yields are small.

The  $H_2O$  molecule is known to cluster with ions (Phelps and Kasner, 1966). In considering its role in the radiation chemistry of air, let us start with an estimate of its effectiveness in formation of clusters. The equilibrium constant for the reaction of any ion of air  $X^\pm$  with

water



can be estimated as

$$K = \frac{[\text{XH}_2\text{O}]^\pm}{[\text{H}_2\text{O}][\text{X}^\pm]} \approx v \exp(-E_B/kT) \quad (3.5-18)$$

where the brackets indicate concentrations. The quantity  $v$  is obtained rigorously as a function of the partition functions, but is certainly of the general magnitude of  $10^{-23} \text{ cm}^3$ ; the binding energy  $E_B$  is expected to be of the order of an electron volt if  $\text{X}^\pm$  is a positive ion, because a one-electron chemical bond can be formed.

If we take  $E_B = 1$ ,  $kT = 1/40$ , we get

$$K \approx 10^{-23} e^{40} \approx 10^{-6} \quad (3.5-19)$$

and this gives as the ratio of clustered to unclustered positive ions

$$\frac{[\text{XH}_2\text{O}]^+}{[\text{X}^+]} = 10^{-6} [\text{H}_2\text{O}] \quad (3.5-20)$$

For average sea level conditions

$$[\text{H}_2\text{O}] \approx 10^{17}$$

and the clustering ratio is estimated to be

$$\frac{[\text{XH}_2\text{O}]^+}{[\text{X}^+]} \approx 10^{11}$$

It is quite clear that the clustering tendency is very great; the important question is whether the ions survive neutralization long enough to form clusters. The clustering reaction must have a three-body mechanism, and its rate is given by

$$-\frac{d[X^+]}{dt} = k' [X^+] [H_2O] [M] \quad (3.5-21)$$

where  $[M]$  is the third body concentration. We can estimate the magnitude of rate constant  $k'$  as the product of an ion-molecule reaction rate constant ( $10^{-9} \text{ cm}^3/\text{sec}$ ) and the volume for effective action of a third body ( $10^{-20} \text{ cm}^3$ ). The resulting constant ( $10^{-29} \text{ cm}^6/\text{sec}$ ) is much larger than the corresponding constant for neutral atom recombination ( $10^{-32} \text{ cm}^6/\text{sec}$ ) because of the longer range of ion-molecule interactions.

We estimate the clustering time of an ion at sea level as follows:

$$-\frac{1}{[X^+]} \frac{d[X^+]}{dt} = \frac{1}{\tau_c} = 10^{-29} \times 10^{17} \times 3 \times 10^{19} \approx 3 \times 10^7 \quad (3.5-22)$$

or the clustering time is approximately  $3 \times 10^{-8} \text{ sec}$ .

The lifetime of an ion under steady irradiation at sea level is given by

$$\tau_i \approx \sqrt{\frac{10^6}{I}} \quad (3.5-23)$$

where we have taken the ion-ion recombination rate coefficient as  $10^{-6} \text{ cm}^3/\text{sec}$ , and  $I$  is the rate of formation of ions per  $\text{cm}^3$ . The two lifetimes  $\tau_c$  and  $\tau_i$  are equal when

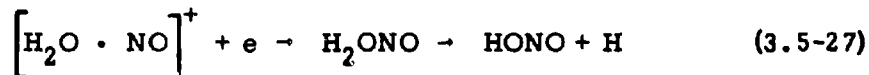
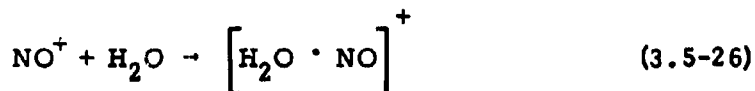
$$\sqrt{\frac{10^6}{I}} = 3 \times 10^{-8}$$

or

$$I \approx 10^{21} \quad (3.5-24)$$

For almost all sea level irradiations in which chemical contaminants are of interest, ions will have time to cluster.

As a specific example of an effect of moisture let us consider the formation of HONO in irradiated, moist air. It has been known from the earliest nuclear weapons tests that large amounts of this molecule are formed at very early times, less than a microsecond. Three molecules are required for its formation:  $N_2$ ,  $O_2$ , and  $H_2O$ . A mechanism consistent with the discussion presented here starts with the primarily formed  $N^+$  ion. It is



The unstable molecule  $H_2ONO$  formed on neutralization of the clustered  $NO^+$  ion has another exothermic decomposition mechanism.



Thus, we have another mechanism for formation of  $NO_2$ , catalysed by moisture, in irradiated air. This mechanism is much faster than the reaction sequence given in Eqs. (3.5-13) and (3.5-14), which is so slow that it could not account for  $NO_2$  formed at early times.

One other effect of moisture is that its reactions lead to the production of H atoms which would react with oxygen to form  $\text{HO}_2$  and OH . These intermediates also must have significant effects in contaminated atmospheres.

## References

- Bennett, E.W., Report LA-3439-MS, TID-4500, 1965.
- Bortner, M.H., Research Directed Toward an Investigation of the Chemical Kinetics of Atmospheric Deionization, AFCRL-65-392, Air Force Cambridge Research Lab., Bedford, Mass., 1965.
- Bortner, M.H., Tentative Suggested Standard Rate Constants, General Electric Co., Philadelphia, Penn., 1966.
- Branscomb, L.M. and R.E. LeLevier, Changes in the Chemical Composition of the Atmosphere Following Intense Ionization Impulses, RM-4364-PR, The RAND Corp., Santa Monica, Calif., 1964.
- Carleton, N.P. and O. Oldenberg, J. Chem. Phys. 36, 3460, 1962.
- Curran, R.K., J. Chem. Phys. 38, 2974, 1963.
- Davidson, G. and R. O'Neil, J. Chem. Phys. 41, 3946, 1964a.
- Davidson, G. and R. O'Neil, Report AFCRL-64-466, 1964b.
- Fan, C.Y., Phys. Rev. 103, 1740, 1956.
- Ferguson, E.E., F.C. Fehsenfeld, A.L. Schmeltekopf, P.D. Goldan and H.I. Schiff, J. Chem. Phys. 44, 4087, 1966; J. Chem. Phys. 44, 4095, 1966; F.C. Fehsenfeld, A.L. Schmeltekopf and E.E. Ferguson, J. Chem. Phys. 44, 4537, 1966.
- Ferguson, E.E., Private communication to R. Gunton, 1966.
- Frankenthal, S., O.P. Manley and Y.M. Treve, J. Chem. Phys. 44, 257, 1966.
- Fueki, K. and J.L. Magee, Discussions Faraday Soc. 36, 19, 1963; J. Phys. Chem. 68, 2901, 1964.
- Gerbes, W., Ann. d. Phys. 30, 169, 1937.
- Gloumousis, G. and D.P. Stevenson, J. Chem. Phys. 29, 294, 1958.
- Hamill, W.J. and N. Boelrijk, J. Amer. Chem. Soc. 84, 730, 1962; L.P. Theard and W.J. Hamill, J. Amer. Chem. Soc. 84, 1134, 1962; T.S. Moran and W.J. Hamill, J. Chem. Phys. 39, 1413, 1963.

- Harteck, P. and S. Dondes, J. Chem. Phys. 27, 546, 1957.
- Harteck, P. and S. Dondes, J. Chem. Phys. 28, 975, 1958.
- Harteck, P. and S. Dondes, Science 146, 30, 1964.
- Harteck, P., S. Dondes and B. Thompson, Science 147, 393, 1965.
- Hartman, P.L., Los Alamos Report, LA-3147-MS, 1964.
- Hasted, J.B., Inelastic Collisions between Atomic Systems, Advances in Electronics and Electron Physics 13, Ed. by L. Marton, Academic Press, N.Y., 1960.
- Hisatsune, I.C., B. Crawford, Jr. and R.A. Ogg, Jr., J. Amer. Chem. Soc. 79, 4648, 1957.
- Keneshea, T.J., A Solution to the Reaction Rate Equation in the Atmosphere below 150 Kilometers, AFCRL-63-711, Air Force Cambridge Research Lab., Bedford, Mass., 1963.
- Kircher, J.F., J.S. McNulty, J.L. McFarling and A. Levy, Radiation Res. 13, 452, 1960.
- Langevin, P., Ann. Chem. Phys. 5, 245, 1905.
- Latter, R., and R.E. LeLevier, J. Geophys. Res. 68, 1643, 1963.
- LeLevier, R.E., J. Geophys. Res. 69, 481, 1964.
- Lichten, W., J. Chem. Phys. 26, 306, 1957.
- Lind, S.C., Chemical Effects of Alpha Particles and Electrons, The Chemical Catalog Co., N.Y., 1928.
- Lind, S.C., Radiation Chemistry of Gases, Rheinhold, N.Y., 1961.
- McGrath, W.D. and R.G.W. Norrish, Proc. Roy. Soc. A242, 265, 1957.
- Phelps, A.V. and W.H. Kasner, Studies and Experimental Work on Atomic Collision Processes Occurring in Atmospheric Gases, AFWL-TR-66-34, Air Force Weapons Lab., Kirtland Air Force Base, N.M., 1966.

ics of the Ionization Processes in Air, Lockheed Report LMSD-48361,  
1958 (now out of print).

Platzmann, R.L., Radiation Res. 2, 1, 1955.

Przybylski, A., Zs. f. Phys. 168, 504, 1962.

Rapp, D. and W.E. Francis, J. Chem. Phys. 37, 2631, 1962.

Silverman, S.M. and E.N. Lassettre, J. Chem. Phys. 42, 3420, 1965.

Sparks, D.C. and R.H. Pennington, A Preliminary Survey of Selected Rates  
for Atmospheric Reactions, Air Force Weapons Lab., Kirtland Air  
Force Base, N.M., 1965.

Thomson, J.J., Phil. Mag. 47, 337, 1924.

Whyte, C.N., Radiation Research 18, 265, 1963.

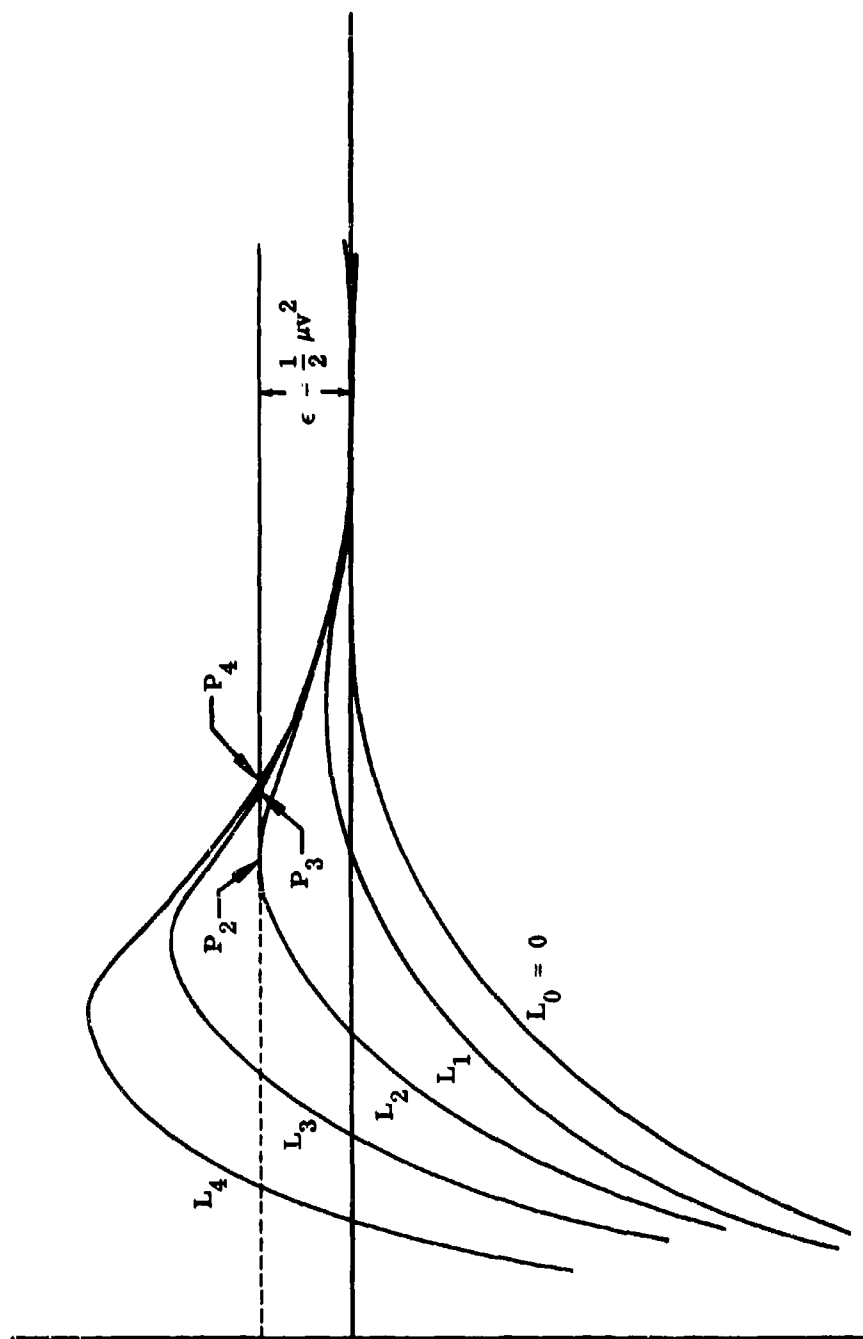


FIG. 3-1 EFFECTIVE POTENTIAL CURVES FOR ION-MOLECULE PAIR

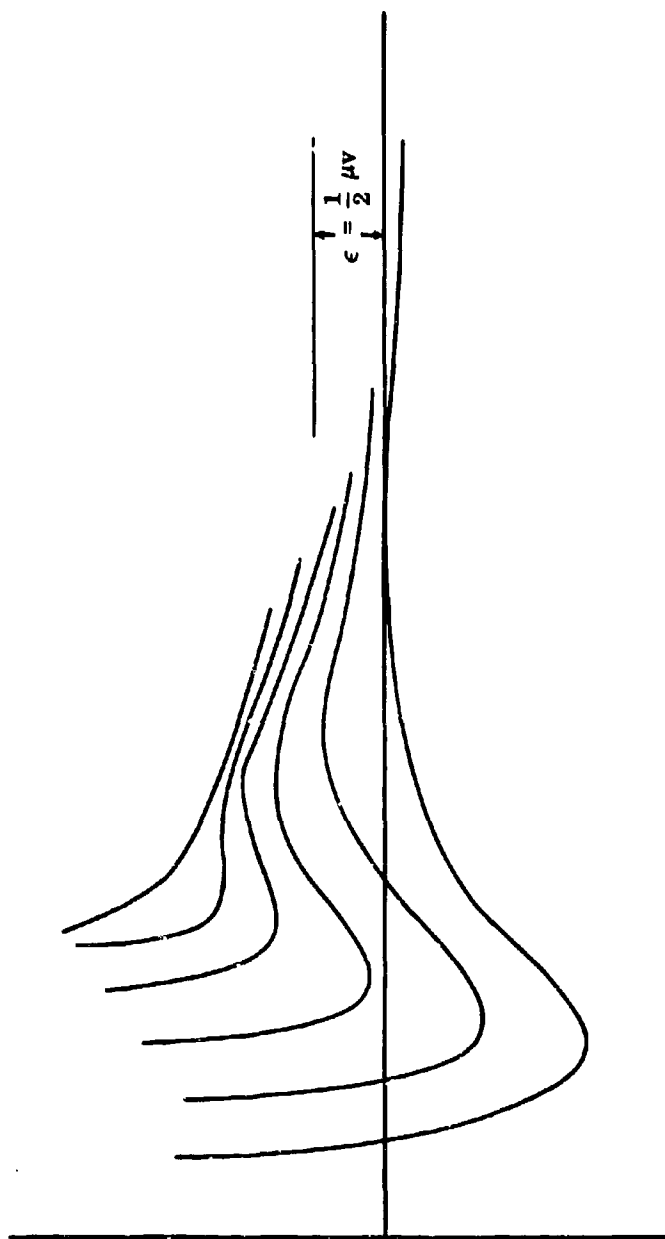


FIG. 3-2 ACTUAL POTENTIAL CURVES FOR ION-MOLECULE PAIR

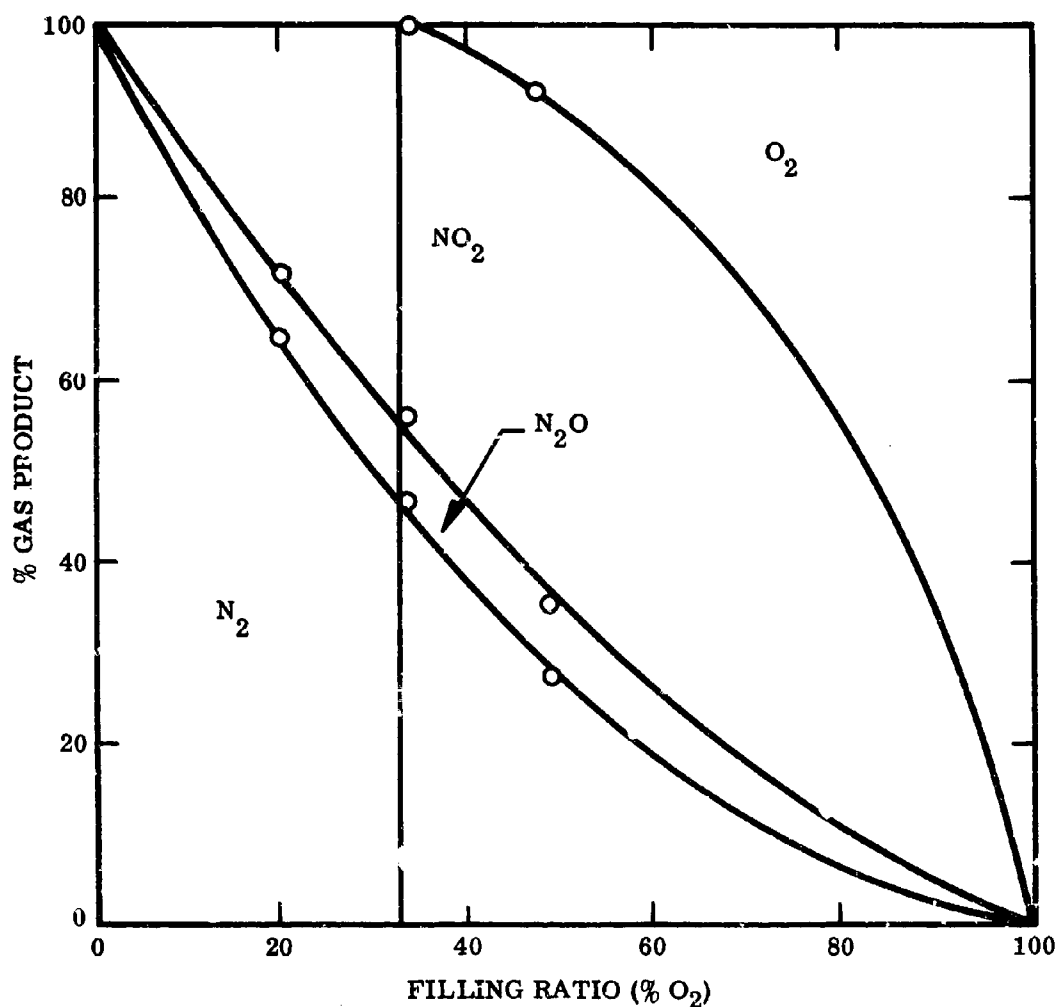


FIG. 3-3 KINETIC RADIATION EQUILIBRIUM DIAGRAM FOR  $\text{N}_2\text{-O}_2$  SYSTEM AT HIGH PRESSURE AND  $80^\circ\text{C}$ . A VERTICAL LINE AT THE PROPER FILLING RATIO WILL BE DIVIDED INTO SEGMENTS THAT ARE PROPORTIONAL TO THE PARTIAL PRESSURES OF THE FOUR GASEOUS COMPONENTS OF THE MIXTURE. THE SAMPLE LINE SHOWS THE SITUATION FOR 33 PERCENT  $\text{O}_2$ .

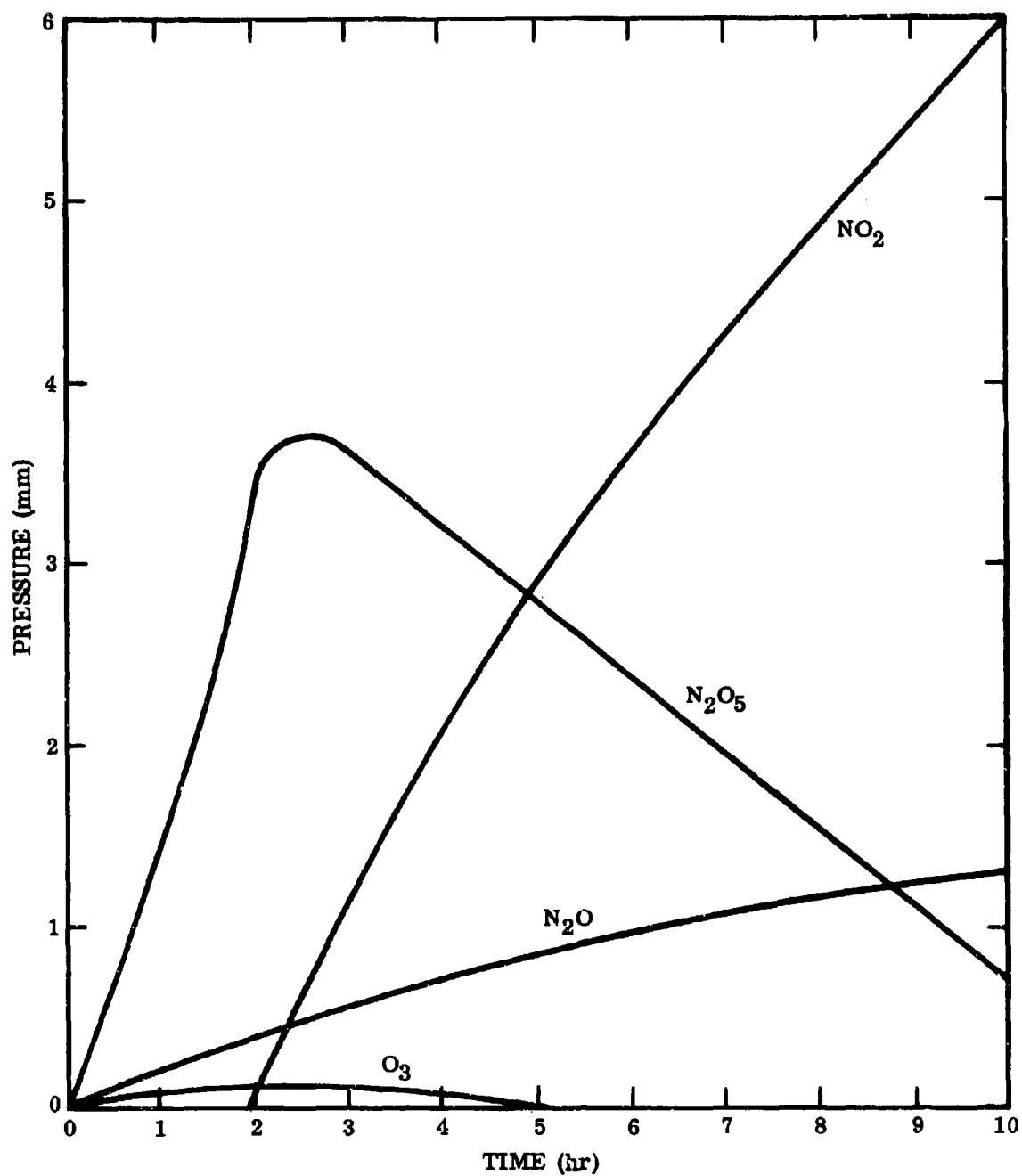


FIG. 3-4 CHANGE OF PRODUCT CONCENTRATION IN THE POLONIUM-210 IRRADIATION OF AIR.

## Chapter 4. X-RAY HEATING OF AIR

### 4.1 Introduction

We focus our attention on the heating produced by a short but very intense burst of X-rays from a point source. The total radiation energy usually lies above  $10^{20}$  erg and nearly all the photons have energies above the K edges of O and N.

If the spectral intensity of the X-rays  $I_\nu(r, t)$  and the spectral absorption coefficient of the air  $k_\nu(r, t)$  are known functions of position and time one can calculate the energy deposition per unit mass

$$E = \iint k_\nu(r, t) I_\nu(r, t) d\nu dt \quad (4.1-1)$$

Before the burst arrives at the point  $r$  the absorption coefficient there is of course that of cold air as given in Chapter 2. As soon as ionization sets in, however,  $k_\nu(r, t)$  changes. Near the source the radiation is sufficiently intense to strip all electrons off the air molecules and at that stage  $k_\nu$  reduces to zero (except for a minute contribution due to Compton collisions) so that the photons can no longer deposit any energy in that region. Moving further away from the source it takes somewhat longer to produce complete stripping because the photon stream is thinning out (like  $r^{-2}$ ) and the just liberated photoelectrons, as well as the Auger electrons, also get a chance to contribute to the ionization. With this competing process it takes fewer photons than before to strip off all electrons and this means that the energy deposition per atom becomes smaller.

The statistics of the complete stripping process depends on the unknown cross sections of photons and electrons for removing electrons from the variously charged ions of O and N. In section 4.2 we estimate the number of photons used up per atom and their energy by means of a model of the chain of processes which lead to complete stripping. We also estimate the radius of the stripped region.

In the above-mentioned model we worry only about the change of  $k_\nu$  but not about the change of  $I_\nu$  during the deposition period. At larger distances this is no longer permissible because absorption begins to matter. Being frequency dependent, this changes the character of the spectral distribution by cutting out the photons near the edges and letting those at higher energies pass. In section 4.3 we outline a model which accounts for this hardening as well as for some change in  $k_\nu$ . In section 4.4 we present an asymptotic theory which introduces additional simplifications and permits the derivation of an analytic formula. In section 4.5 finally, we evaluate the effect of Compton scattering, which delays the escape of photons from the vicinity of the source. This, of course, increases the number of photons absorbed near the source and decreases it at large distances. The effect is, however, quite small unless the photons have energies above 20 keV.

#### 4.2 Energy deposition in the stripping region

At the source the spectral distribution of the radiated power is assumed to be that of a blackbody of temperature  $T$ . In general,  $T$  and the total radiated power  $P_0$  are functions of time. The spectral intensity at a distance  $r$  and a time  $t$  is

$$I_\nu(r, t) = \frac{b_\nu(T(t)) P_0(t)}{4\pi r^2} \quad (4.2-1)$$

where

$$b_\nu = \frac{B_\nu(T(t))}{B(T(t))} \quad (4.2-2)$$

is the Planck distribution function normalized to unity, i.e., with

$$B(T) = \int_0^\infty B_\nu(t) d\nu \quad (4.2-3)$$

Eq. (4.2-1) neglects absorption which is only permissible at small distances from the source. In practice we shall always make the simplifying assumption that  $P_0$  and  $T$  remain constant for the entire duration of the burst and are zero before and afterwards.

To start with we assume that the X-ray flux is so large that the entire ionization of an atom is over before any of the photoelectrons have had a chance to participate by the ejection of a secondary electron. This is obviously the situation where the ionization requires a maximal number of photons and which leads to a maximum amount of energy transfer. It is evident from the height of the K edges as shown in Figs. 2.1 and 2.2 that the ejection of a K electron is about 20 times more probable than the ejection of an L electron and for simplicity we ignore the latter possibility. Thus L electrons disappear not by photoeffect but by filling the vacancies created in the K shell and by the simultaneous emission of Auger electrons which carry away the excess energy (see Section 2.1). This sequence of removing two electrons from the L shell follows the creation of a K shell vacancy within about  $10^{-14}$  sec, i.e., practically instantly. The complete ionization of an N or O atom therefore takes five photons. The first three of these cause the disappearance of the 5 (or 6) electrons from the L shell and the other two remove the remaining electrons from the K shell.

To determine the energy deposited by these photons one has to know the average energy per photon. For the first photon which goes to work on the neutral molecules this average energy is

$$h\bar{\nu} = \frac{\sum c_i \nu_K \int_1^{\infty} b_{\nu}^k \nu_i d\nu}{\sum c_i \nu_K \int_1^{\infty} \frac{b_{\nu}^k \nu_i d\nu}{h\nu}} \quad (4.2-4)$$

where  $c_i$  are the fractions of species  $i$  and the  $k_{\nu_i}$  their spectral absorption coefficients. For our calculation it is sufficiently accurate to assume  $c_{O_2} = 0.2$ ,  $c_{N_2} = 0.8$  and no other constituents. It is known empirically from the work of Henke, White and Lundberg (1957) that  $K$  absorption coefficients of various species can be expressed in terms of a "universal" absorption coefficient which has the form

$$k_{\nu} = \frac{\lambda_K}{A} f(\lambda/\lambda_K) \quad (4.2-5)$$

where  $A$  is the atomic weight and  $\lambda_K$  is the wavelength of the  $K$  edge. Recently the coefficients of the pure species have been remeasured by Ogier, Lucas and Park (1964) and by Bearden (1966). For the purpose of this calculation we have fitted these results in the form

$$k_K = \frac{\lambda_K}{A} \left( 2.68 \left( \frac{\lambda}{\lambda_K} \right)^3 - 1.11 \left( \frac{\lambda}{\lambda_K} \right)^4 \right) \times 10^4 \frac{\text{cm}^2}{\text{g}} \quad (4.2-6)$$

where  $\lambda_K$  is expressed in  $\text{\AA.U.}$  Entering this expression into Eq. (4.2-4), the Planck means of  $k_{\nu}$  and  $(k_{\nu}/h\nu)$  in the numerator and the denominator can be written as

$$\bar{k}_{\nu} = \frac{15}{\pi^4} \sum c_i \frac{\lambda_{K_i}}{A_i} \left[ 2.68 f_0 \left( \frac{h\nu_{K_i}}{kT} \right) - 1.11 f_1 \left( \frac{h\nu_{K_i}}{kT} \right) \right] \quad (4.2-7)$$

$$\left(\frac{k}{h\nu}\right) = \frac{1}{kT} \frac{15}{\pi^4} \sum c_i \frac{\lambda_{K_i}}{A_i} \left[ 2.68 f_1\left(\frac{h\nu_{K_i}}{kT}\right) - 1.11 f_2\left(\frac{h\nu_{K_i}}{kT}\right) \right] \quad (4.2-8)$$

where we have set

$$f_n(\nu) = \int_{\nu}^{\infty} (e^u - 1)^{-1} \frac{du}{u^n} \quad (4.2-9)$$

For  $n = 0$  this integral is

$$f_0(\nu) = \ln (1 - e^{-\nu})^{-1} \quad (4.2-10)$$

For the higher values of  $n$  one obtains

$$f_n(\nu) = \frac{1}{u^{n-1}} \sum_{k=1}^{\infty} E_n(k\nu) \quad (4.2-11)$$

The functions obtained by summing these series were fitted in the form

$$f_n = f_0 / (\nu + \Delta_n)^n \quad (4.2-12)$$

$$\Delta_1 = \frac{0.316 \sqrt{\nu + 1.35 \nu}}{1 + 0.428 \sqrt{\nu + 1.35 \nu}} \quad (4.2-13)$$

$$\Delta_2 = \frac{0.132 \sqrt{\nu + 1.13 \nu}}{1 + 0.373 \sqrt{\nu + 1.13 \nu}} \quad (4.2-14)$$

The average energy given by Eq. (4.2-4) can be fitted by the expression \*

$$h\bar{\nu} = 0.97 kT^{1/4} \text{ keV} \quad (4.2-15)$$

The denominator, which will be used later on in this section was fitted by

$$\left(\frac{k_y}{h\nu}\right) = \frac{1200}{(kT)^2 (kT + 1.0)} \frac{\text{cm}^2}{\text{g keV}} \quad (4.2-16)$$

Subsequent photons deliver somewhat larger average energies because the removal of two or more L electrons raises the binding energy  $h\nu_K$  of the K electrons. A calculation of these changes was carried out with the aid of the absorption coefficient given by Eq. (4.2-6).

The ionization energies for ions which have only two or one of their electrons left were taken from Allen (1963). In nitrogen the average energy of photon number 4 which removes the first of these two electrons is approximately  $1.26 h\bar{\nu}$  and the last one takes  $1.48 h\bar{\nu}$ . These two factors are nearly independent of the source temperature. For photons number 2 and 3 we interpolate between photons number 1 and 4. Thus the energy deposited

---

\* In all numerical formulas given in this chapter  $kT = \frac{T}{1.16 \times 10^7}$  expresses the temperature in keV.

in removing the L shell is  $3.26 h\bar{\nu}$  and the total energy for all five photons is  $6 h\bar{\nu}$ . With the proper conversion factor the maximum energy deposition in the immediate vicinity of the source is therefore

$$E_0 = 3.9 \times 10^{14} (kT)^{1/4} \frac{\text{ergs}}{\text{gm}} \quad (4.2-17)$$

When this energy is thermalized the resulting temperature is

$$T_{\text{air}} = \left( 5.65 (kT)^{1/4} - 1.43 \right) \times 10^6 \text{ } ^\circ\text{K} \quad (4.2-18)$$

To discuss the effect of electrons we have to compare the rates of ionization by collision and by photoeffect. As a measure of the first we introduce an average value  $n \bar{\sigma}_0 \bar{v}$  where  $n$  is the number of atoms per unit volume,  $\sigma_0$  the cross section for ionizing a neutral atom (or half molecule) and where the averaging refers to the energy distribution of the photoelectrons. As a measure of the rate of photoionization we use the reciprocal of the average time  $\tau$  for producing one photoelectron per atom.

To calculate the deposited energy we have to know the average number of photons absorbed per atom while the L shell is removed. This number, which we designate by the letter  $x$ , depends on the ratio of the above two rates, i.e., on the quantity

$$a = n \bar{\sigma}_0 \bar{v} \tau \quad (4.2-19)$$

A small number  $a$  means that collisions are not very important and in that limit  $x$  approaches, as we have argued above, the value three.

At the other end of the  $a$  scale collisions dominate and every primary electron quickly loses its energy contributing to the further ionization of the gas. The secondary electrons also cause ionization and the gas rapidly approaches a state of thermal equilibrium at a temperature  $T_g$  where its internal energy is equal to the energy deposited by the X-rays. Collisional ionization stops almost completely when the L shell has been removed. To estimate the number of photons used up at that point we equate the deposited energy  $x h\bar{\nu}$  with the internal energy which is essentially the sum of ionization and kinetic energy. The energy per atom for stripping the L shells from a 4:1 mixture of N and O is 300 eV and with the kinetic energy of 5.2 electrons added to that of the ions one obtains

$$x = (0.3 + 9.3 kT_g) / h\bar{\nu} \quad (4.2-20)$$

Typical values of the gas temperature at which ions have lost their L shells but retain their K shells range from 0.02 to 0.04 keV. Entering  $kT_g = 0.03$  into Eq. (4.2-20) and using Eq. (4.2-15) our estimate for the lower limit of  $x$  for very large  $a$  becomes  $x \approx 0.6 (kT)^{-1/4}$ .

To determine  $x$  for intermediate values of  $a$ , where neither mode of ionization outweighs the other one, one has to follow the ionization history of the atoms step by step and take into account that ionization by electron collision gets more difficult every time another electron has been removed. The relevant ionization cross sections are not actually

known but can be obtained approximately by scaling down the known cross section for the neutral atoms. The proper scaling law for ions of charge  $i$  is

$$\sigma_i = \frac{5-i}{5} \left( \frac{E_0}{E_i} \right)^2 \sigma_0 (E/E_i) \quad (4.2-21)$$

where  $E_i$  is the ionization potential. Such a scaling law is known to apply to the classical formula of J.J. Thomson and to the quantum theoretical formula of Bethe which has been derived in the Born approximation. These cross sections are energy dependent and in order to evaluate the ionization processes one should, in principle, know the energy distribution of the fast electrons starting from the time at which they are ejected and following this through the various stages where they lose energy by collisions which ionize or otherwise excite the air atoms. What really matters are the averages  $\overline{\sigma_i v}$  for this energy distribution. Fortunately the energy dependence of  $\overline{\sigma_0 v}$  is not very pronounced and one can make a fairly reliable estimate of  $\overline{\sigma_0 v}$  for a combination of photo and Auger electrons. The value used below is  $\overline{\sigma_0 v} = 2 \times 10^{-7} \text{ cm}^3/\text{sec}$ . Corresponding estimates for the  $\overline{\sigma_i v}$  applying to the higher stages of ionization are less accurate but they have fortunately less effect on the final result.

An integration following the successive ionization processes step by step was carried to the point where the L shell is gone. This was done

numerically for various values of  $a = n \tau \sigma_0 V$  and the resulting values of  $x$  are listed in Table 4.1.

Table 4.1 Number of Photons for Removing the L Shell of a Nitrogen Atom

$a =$	.2	.5	1	2	5	10	20	50	100
$x =$	2.94	2.88	2.79	2.65	2.42	2.20	1.90	1.56	1.30

As the quantity  $a$  becomes still larger  $x$  approaches the limit given by Eq. (4.2-20). To use the above results for determining  $x$  at some point in the vicinity of a specified source the average time  $\tau$  for ejecting the first photoelectron must be expressed in terms of the distance  $r$  of that point and of the variables describing that source. The number density of photons absorbed in cold air rises initially at the rate

$$\dot{n}_{ph} = \rho \int \frac{I_v}{h\nu} k_v dv \quad (4.2-22)$$

To obtain  $\tau$  we divide this into the number density of atoms  $\frac{N_0}{A}$ . To evaluate the integral in Eq. (4.2-22) we make the simplifying assumption that the intensity can be expressed in the form

$$I_v = \frac{b_v(T) Y(r)}{4\pi r^2 t} \quad (4.2-23)$$

where  $t$  is the total duration of the X-ray burst. In this relation  $Y(r)$  is assumed to be the X-ray yield attenuated by the absorption within the sphere of radius  $r$  which accounts for conservation of energy but not for the hardening of the spectrum.

Entering the assumed expression for  $I_v$  into Eq. (4.2-22) leads to the deposition rate

$$\dot{n}_{ph} = \frac{\rho Y(r)}{4\pi r^2 t} \left( \frac{k_v}{h\nu} \right) \quad (4.2-24)$$

and in turn to

$$\tau = \frac{N_0}{A \dot{n}_{ph}} = \frac{N}{A} \frac{4\pi r^2 t}{Y(r)} \left( \frac{k_v}{h\nu} \right) \quad (4.2-25)$$

The ratio  $\frac{N}{A} = 4.2 \times 10^{22} \text{ g}^{-1}$  is the reciprocal of the mass per air atom.

To obtain the attenuated value of  $Y$  for Eq. (4.2-25) one has to reduce the unattenuated energy which is radiated at the origin by the amount deposited within the sphere. This leads to the expression

$$Y = Y_0 - 4\pi \rho \int E r^2 dr \quad (4.2-26)$$

The factor  $r^2$  in the integrand weighs the outer edge more heavily and one can approximately set

$$Y = Y_0 - \frac{4\pi}{3} \rho r^3 E \quad (4.2-27)$$

where  $E$  is taken at  $r$  itself. Entering this expression and  $\left( \frac{k_v}{h\nu} \right)$  as given by Eq. (4.2-16) into Eq. (4.2-25) one finds

$$\tau = \frac{4\pi \times 10^{11}}{1.8} \frac{(kT)^2 (kT + 1.0)}{Y_0 - \frac{4\pi}{3} \rho r^3 E} r^2 t \quad (4.2-28)$$

To obtain  $a = n \bar{\sigma}_0 \bar{v} \tau$  we multiply  $\tau$  by  $n = 5.4 \times 10^{19} \frac{\rho}{\rho_0} \text{ cm}^{-3}$  and  $\bar{\sigma}_0 \bar{v} = 2 \times 10^{-7} \text{ cm}^3/\text{sec}$  leading to

$$a = 7.5 \times 10^{24} \frac{(kT)^2 (kT + 1.0)}{Y_0 - \frac{4\pi}{3} \rho r^3 E} \frac{\rho}{\rho_0} r^2 t \quad (4.2-29)$$

This formula contains 3 parameters which characterize the source: its total energy  $Y_0$ , its temperature  $T$  and the duration time  $t$ . In place of the last parameter it is often useful to introduce the radius  $R$  of the source which is related to the other three by the Stefan-Boltzmann law

$$\frac{Y_0}{4\pi R^2 t} = \sigma T^4 \quad (4.2-30)$$

Making this substitution leads to the alternative expression

$$a = \frac{(0.56) (kT + 1.0)}{(kT)^2 \left(1 - \frac{4\pi}{3} \frac{\rho r^3 E}{Y_0}\right)} \frac{\rho}{\rho_0} \left(\frac{r}{R}\right)^2 \quad (4.2-31)$$

The number of photons  $x$  corresponding to the rate ratio  $a$  is generally less than three. The energy of removing the L shell is therefore reduced by a factor of approximately  $\frac{x}{3}$ . The subsequent removal of the K shell is not aided by collision processes and it still takes two photons and the same amount of energy as before. The total energy deposition for complete stripping is therefore

$$E = (1.8 + 0.7 x) \cdot 10^{14} (kT)^{1/4} \text{ ergs/gm} \quad (4.2-32)$$

which agrees with Eq. (4.2-17) if  $x$  assumes the value three. Entering this expression for  $E$  into Eq. (4.2-31) and solving for  $\rho/\rho_0$  one is led to the relation

$$\rho/\rho_0 = \left( \frac{(kT + 1.0) (.56) \left(\frac{r}{R}\right)^2}{(kT)^2 a(x)} + (1 + 0.36x) 9.7 \times 10^{11} \frac{R^3}{Y_0} (kT)^{1/4} \left(\frac{r}{R}\right)^3 \right)^{-1} \quad (4.2-33)$$

which can be inverted to obtain the number  $x$  of absorbed photons as a function of the distance  $r$  from the source.

The above considerations apply only within a sphere where the deposited X-ray energy is large enough for stripping off all electrons. In order to estimate the radius of that sphere we evaluate the combined time for stripping the L shell and then absorbing two more photons to remove the K shell. We then set this time, which depends on the X-ray flux density and therefore on the radius, equal to the duration of the pulse.

The deposition time for the first photon is given by Eq. (4.2-25). For subsequent photons the deposition time becomes somewhat larger. These increases were calculated like the corresponding energies per photon, i.e., by entering the universal absorption coefficient for the appropriate ion into the integral of Eq. (4.2-22). For the last photon the absorption coefficient was multiplied by  $1/2$  since there is only one electron left in the K shell. In the calculation of the energy per photon this factor  $1/2$  does not matter because it occurs in the nominator as well as the denominator. The calculated time for removing the L shell without

the aid of collisions, i.e., using three photons can be fitted by the expression

$$\tau_L = \frac{2.97 + 2.73 kT}{1 + kT} \tau \quad (4.2-34)$$

With the aid of collisions this time is reduced by approximately a factor  $\frac{x}{3}$ . The additional time for removal of the K shell is

$$\tau_K = \frac{2.8 + 2kT}{1 + kT} \tau \quad (4.2-35)$$

To obtain the stripping radius we set

$$\left( \frac{x}{3} \frac{\tau_L}{\tau} + \frac{\tau_K}{\tau} \right) = \frac{t}{\tau} \quad (4.2-36)$$

and take  $t/\tau$  from Eq. (4.2-28) and express  $E$  by means of Eq. (4.2-32).

The resulting relation

$$\rho/\rho_0 = \frac{10^{-12} \frac{Y_0}{r^3} - 0.72 \frac{(kT)^2}{r} [2.8 + .99x + (2 + .91x) kT]}{(1 + .36x) (kT)^{1/4}} \quad (4.2-37)$$

permits a calculation of the stripping radius. To perform this calculation one must find that distance  $r$  for which one calculates the same  $x$  from both this and the preceding relation Eq. (4.2-33). This  $r$  is the radius of the stripping region where one is permitted to determine  $x$  from Eq. (4.2-33).

### 4.3 Energy deposition at large distances

The ionization produced by X-rays at large distances from the center of the burst has very little effect on the spectral absorption coefficient. In calculating the integral of Eq. (4.1-1) which gives the energy deposition, any change of  $k_v$  from its cold air value can be ignored. One does, however, have to pay attention to the hardening of the spectral distribution which results from the selective absorption along the entire path. In the calculation of this hardening one should properly allow for the absence of absorption in the stripping region.

In this section we describe a fairly simple model for performing a calculation. It is based on the observation that ionization does not produce a very significant change of the absorption coefficient above the K edge as long as the K shell vacancies are being refilled. After the ionization has reached the point where the K shell disappears permanently this changes and  $k_v$  drops sharply. To evaluate the total absorption at some distant point, it is sufficiently accurate to regard the total X-ray path as consisting of an inner part with no absorption and an outer part with the full amount of cold air absorption. The dividing point should lie close to the stripping radius  $r_s$  which increases while the deposition takes place. To follow  $r_s$  as a function of time one can take advantage of the results which have been obtained in section 4.2. The suggested model uses the following procedure. One first considers that part of the burst which is emitted prior to  $t' < t$  i.e., an amount  $Y'_0 = \frac{t'}{t} Y_0$  and calculates the energy deposition as if  $k_v$  remained at its cold air value. This part of the calculation is concerned

with points near enough to the burst so that one can ignore the attenuation of  $I_v$  and one obtains therefore

$$E_o(t') = \frac{t'}{t} \frac{Y_o \overline{k_v}}{4\pi r^2} \quad (4.3-1)$$

Having ignored the decrease of  $k_v$  due to stripping, this expression is not bounded, and as one approaches the center it rises above the maximum  $E(r)$  predicted in section 4.2. In our model the radius where the two curves intersect is used as the stripping radius to express the spectral intensity in the form

$$I_v = \frac{Y_o}{4\pi r^2 t} e^{-\rho k_v (r-r_s)} \quad (4.3-2)$$

One can now calculate the energy deposition at larger radii

$$E = \frac{Y_o}{4\pi r^2 t} \int_0^t dt' \int b_v k_v e^{-\rho k_v (r-r_s(t'))} dv \quad (4.3-3)$$

and we repeat at this point that  $k_v$  stands for the cold air value.

#### 4.4 Asymptotic approximation for the energy deposition

The evaluation of  $E$  by Eq. (4.3-3) is clearly a machine operation but there is an approximate method at large enough distances which leads to a very simple analytic result. To start with one replaces  $r_s(t')$  by an average so that one gets rid of the time integral in Eq. (4.3-3). This leads to

$$E = \frac{Y_o}{4\pi r^2} \int b_\nu k_\nu e^{-\rho k_\nu (r-\bar{r}_s)} d\nu \quad (4.4-1)$$

Next we replace the frequency  $\nu$  by the dimensionless variable  $u = \frac{h\nu}{kT}$  and write the distribution function in the form

$$b_\nu d\nu = \frac{15}{\pi} u^3 (e^u - 1)^{-1} du \quad (4.4-2)$$

For  $k_\nu$  we use the approximation

$$k_\nu = k_1/u^3 \quad (4.4-3)$$

$$k_1 = 4.5 \times 10^3 (kT)^{-3} \text{ cm}^2/\text{gm} \quad (4.4-4)$$

This leads to

$$E = \frac{15 k_1 Y_o}{4\pi^5 r^2} \int e^{-\frac{\rho k_1 (r-\bar{r}_s)}{u^3}} (e^u - 1)^{-1} du \quad (4.4-5)$$

For large values of  $r$ , low-lying frequencies do not contribute significantly to this integral and it can be replaced by

$$\int_0^\infty e^{-\left(\frac{\rho k_1 (r-r_s)}{u^3}\right) + u} du \quad (4.4-6)$$

The integrand has a sharp maximum at

$$u_m = \left(3\rho k_1 (r-r_s)\right)^{1/4} \quad (4.4-7)$$

and by the saddle point method one obtains approximately

$$\int_0^\infty e^{-\left(\frac{\rho k_1 (r-r_s)}{u^3}\right) + u} du \approx \sqrt{\frac{\pi u_m}{2}} e^{-\frac{4}{3} u_m} \quad (4.4-8)$$

If this is entered into Eq. (4.4-5) one obtains

$$E = 69 \frac{\sqrt{u_m} e^{-\frac{4}{3} u_m}}{r^2 (kT)^3} Y_0 \text{ ergs/gm} \quad (4.4-9)$$

where  $Y_0$  is given in eigs and  $r$  in cm.

### References

- Allen, C.W., Astrophysical Quantities, University of London,  
The Athlone Press, 1963.
- Bearden, A.J., J. Appl. Phys. 37, 1681, 1966.
- Henke, B.L., R. White, and B. Lundberg, J. Appl. Phys. 28, 98, 1957.
- Ogier, W.T., G.J. Lucas and R.J. Park, Appl. Phys. Let. 5, 146, 1964.
- Veigele, Kaman Nuclear KN-65-116 (R), 1965.

## Chapter 5. SHOCK HEATING OF AIR

### 5.1 Standard hydrodynamic approach

A shock wave is a hydrodynamic disturbance which spreads conditions of high density, pressure and temperature. Quite often these changes take an exceedingly short time and in that case it is convenient to picture the shock as a sharp front across which the density  $\rho$ , the pressure  $p$  and the velocity  $v$  undergo discontinuous changes which obey the conservation laws of mass, momentum and energy. If the shock front travels with a speed  $D$  and the fluid ahead of and behind the front travels with velocities  $v_1$  and  $v_2$  the mass flow through the shock is

$$F = \rho_1 (D - v_1) = \rho_2 (D - v_2) \quad (5.1-1)$$

This is the conservation law of mass. Those for momentum and energy are

$$G = p_1 + F (D - v_1) = p_2 + F (D - v_2) \quad (5.1-2)$$

and

$$H = h_1 + \frac{F}{2} (D - v_1)^2 = h_2 + \frac{F}{2} (D - v_2)^2 \quad (5.1-3)$$

In the last equation we have introduced  $h = e + \frac{p}{\rho}$  the enthalpy per unit mass which is a function of  $p$  and  $\rho$ . Eqs. (5.1-1), (5.1-2) and (5.1-3) which are known as the Hugoniot relations relate a total of seven variables, i.e. the six state variables  $\rho_1$ ,  $p_1$ ,  $v_1$  and the shock speed  $D$ . If conditions ahead of the shock ( $\rho_1$ ,  $p_1$ ,  $v_1$ ) are known the remaining four variables are still unknown and with three relations between them one has a one parameter family of solutions. To settle on one particular

solution one has to pin down one more item of information, for example, the pressure  $p_2$  or the velocity  $v_2$  behind the shock. One is, however, limited by the condition that the entropy should be larger behind the front than ahead of it. For any reasonable equation of state this is equivalent with having a higher pressure and density behind the front.

The Hugoniot relations are simplified considerably for an ideal gas, i.e. if one can approximate the equation of state by a  $\gamma$  - law

$e = \frac{1}{\gamma-1} \frac{p}{\rho}$  or the equivalent  $h = \frac{\gamma}{\gamma-1} \frac{p}{\rho}$ . Introducing the pressure ratio  $\xi = \frac{p_2}{p_1}$  one can solve in that case for the compression ratio

$$\frac{\rho_2}{\rho_1} = \frac{(\gamma+1)\xi + (\gamma-1)}{(\gamma-1)\xi + (\gamma+1)} \quad (5.1-4)$$

For very strong shocks this ratio approaches the value  $\frac{\gamma+1}{\gamma-1}$ .

The velocity with which a shock overtakes the fluid

$$D - v_1 = \sqrt{1 + \frac{\gamma+1}{2\gamma} (\xi - 1)} c_1 \quad (5.1-5)$$

is always larger than the sound velocity

$$c_1 = \sqrt{\gamma \frac{p_1}{\rho_1}} \quad (5.1-6)$$

ahead of the shock. Relative to the fluid behind the shock front its velocity can be expressed in the form

$$D - v_2 = \sqrt{1 + \frac{\gamma+1}{2\gamma} (\xi^{-1} - 1)} c_2 \quad (5.1-7)$$

which is clearly less than the sound velocity

$$c_2 = \sqrt{\gamma \frac{p_2}{\rho_2}} \quad (5.1-8)$$

in that region of the fluid. These two statements, i.e. that the shock front is supersonic with respect to the fluid ahead of and subsonic with respect to the fluid behind the front are generally true and not just for fluids obeying a  $\gamma$  - law .

If a shock runs into an ideal gas at rest it accelerates that gas to a velocity

$$v_2 = (\xi - 1) \sqrt{\frac{2}{(\gamma + 1) \xi + (\gamma - 1)} \frac{p_1}{\rho_1}} \quad (5.1-9)$$

This equation can be turned around to calculate the pressure ratio which develops when a piston pushes the gas with a velocity  $v_2$  . For a piston velocity which is large compared to the sound speed ahead of the shock one can derive the approximate relation

$$e_2 = \frac{1}{\gamma - 1} \frac{p_2}{\rho_2} \approx \frac{v_2^2}{2} \quad (5.1-10)$$

according to which the internal and the kinetic energy density behind a strong shock front are equal. At energy densities where the air is completely ionized the temperature which corresponds to this relation is approximately given by equating

$$\frac{\Delta v^2}{2} = \frac{3}{2} s N k T \quad (5.1-11)$$

Here and below we have dropped the index 2 . For air with a mixture of 0.79 nitrogen and 0.21 oxygen atoms the average atomic weight is  $A = 14.41 \frac{\text{gm}}{\text{mole}}$  and the number of particles per atom-counting the electrons -is  $s = 8.21$  . These numbers lead to

$$T = 7 \cdot 10^{-9} v^2 \text{ } ^\circ\text{K} \quad (5.1-12)$$

or

$$kT = 6 \cdot 10^{-16} v^2 \text{ keV} \quad (5.1-13)$$

with  $v$  measured in cm/sec.

## 5.2 Very strong shocks

In a shock one has conservation of mass, momentum and energy but, as stated earlier, the entropy rises. To understand the physical processes which bring this rise about, the oversimplified picture of a discontinuous change must be replaced by the more realistic one that the high and the low pressure region are connected by a transition region whose width is of the order of several mean free paths of the gas particles. During the very rapid changes which take place in the transition region the gas is not in thermodynamic equilibrium. The various nonequilibrium processes are of a dissipative nature and are responsible for the increase in entropy.

If a shock is driven by a very fast "piston" moving with a speed like  $10^8$  cm/sec or more, Eq. (5.1-13) predicts temperatures above 6 keV. At these temperatures air is almost completely ionized and the hydrodynamic approach to shock theory is beset with two major objections which make its application highly suspect. On the one hand the rate of equilibration

becomes too slow and on the other one, radiation may be too rapid. It seems worthwhile to make some crude order of magnitude estimates of the importance of these effects and to formulate some of the questions which arise even though we have at present no definitive answers to them.

With air being completely ionized, the individual particles interact with cross sections given by Rutherford's formula for Coulomb collisions. The magnitude of the Rutherford cross-section decreases with the square of the energy and at energies corresponding to  $10^8$  cm/sec it is very small. In the classical theory one relies on collisions to transfer the momentum and energy of the particles behind the shock front to those ahead of it and to establish thermal equilibrium. When the cross sections become too small that is no longer possible. The least efficient collisions are those between particles with a large mass ratio. For collisions between ion and electrons the cross section is  $2\sqrt{\frac{m}{M}}$  times smaller than for collisions between two particles with the same mass, i.e. two ions or two electrons. Because of this strong reduction (to 1/80 in the case of air) one can often use the approximation of regarding the plasma as a mixture of an ion gas and an electron gas with each one having its own temperature. Using that model one can describe the weak interaction in terms of a very small frictional drag and of a very slow exchange of heat energy between the two gases. The near absence of drag forces does not imply, however, that the two components move independently because they are coupled together by strong electrostatic fields which rapidly equalize the two streaming velocities. Without that equilization ions and electrons would run apart and one can show that such a separation of

charges cannot exceed the Debye length  $l_D = \sqrt{\frac{kT}{8\pi n e^2}}$  which is always very much smaller than collisional mean free paths. In a steady state shock wave electrostatic forces can only transfer momentum but not heat energy from the ion gas to the electron gas and the latter transfer remains determined by collisions. Calculations made with this model of a plasma lead to a relatively narrow transition region for the fluid velocity and for the ion temperature which is imbedded in a much wider transition region for the electron temperature (Jaffrin and Probst, 1964). With the Rutherford cross section formula this width is of the order

$$l = \frac{1}{\lambda} \sqrt{\frac{M}{m}} \left( \frac{kT}{Ze^2} \right)^2 \frac{1}{n} \quad (5.2-1)$$

where  $T$  is not necessarily a true temperature but a measure of the particle energy. The dimensionless factor  $\lambda$  depends logarithmically on  $T$  and the electron density but the variation introduced by this is so insignificant that one can use a constant value  $\lambda \approx 30$ . The values of  $\lambda$  adopted by different authors may lie a factor 2 above or below this one, depending on the definition adopted for the cross section, but in an argument of a qualitative nature this does not matter.

Entering appropriate values for air and expressing  $n$  in terms of air density relative to sea-level the width of the electron temperature wave is

$$l \approx 0.1 \left( \frac{\rho}{\rho_0} \right)^{-1} (kT)^2 \text{ cm} \quad (5.2-2)$$

Expressing the final temperature  $T$  in terms of the piston velocity by means of Eq. (5.1-13) this becomes

$$\ell \approx 3.6 \times 10^{-32} \left( \frac{\rho}{\rho_0} \right)^{-1} v^4 \text{ cm} \quad (5.2-3)$$

The velocity of a strong shock is just slightly above the piston velocity so that one can estimate that it takes about a time  $\ell/v$  to bring the electrons in a parcel of shocked air into equilibrium. At the end of that time the electron gas supposedly reaches the final temperature  $T$  and with it a fraction  $(Z/Z + 1)$  of the internal energy as given by Eq. (5.1-10). The approximate heating rate of the electron gas is therefore  $Q_{\text{heat}} = \rho v^3 / 2\ell$  or, with the aid of Eq. (5.2-3),

$$Q_{\text{heat}} = 1.8 \times 10^{28} \left( \frac{\rho}{\rho_0} \right)^2 v^{-1} \frac{\text{erg}}{\text{cm}^3 \text{ sec}} \quad (5.2-4)$$

Intuitively such large temperatures as predicted by Eq. (5.1-13) seem unrealistic and the question naturally arises if there are loss mechanisms which prevent that much heating. There are three modes of radiation which might contribute to this, i.e. Bremsstrahlung, radiative recombination and line radiation. Artsimovich (1964) quotes an approximate formula and presents graphs giving this radiation as a function of the electron temperature  $T_e$ . In the units used in this chapter we obtain for air near  $kT_e = 1 \text{ keV}$

$$Q_{\text{rad}} \approx 10^{18} \left( \frac{\rho}{\rho_0} \right)^2 \left( 5.5 (kT_e)^{1/2} + \frac{10}{(kT_e)^{1/2}} + \frac{10}{(kT_e)^{3/2}} \right) \frac{\text{erg}}{\text{cm}^3 \text{sec}} \quad (5.2-5)$$

The three halves power law in the line radiation term enters because the population of bound states, as given by the Saha equation, decreases as the inverse of the available phase space of the electrons. In the temperature range of interest the Boltzmann factor varies slowly and is therefore not included. Equating  $kT_e$  with the equilibrium value one obtains for  $v = 10^8$  cm/sec where  $kT = 6$  keV a rate

$$Q_{\text{rad}} = 1.8 \times 10^{19} \left( \frac{\rho}{\rho_0} \right)^2 \text{ erg/cm}^3 \text{sec} \text{ as compared to } Q_{\text{heat}} = 1.8 \times 10^{20} \left( \frac{\rho}{\rho_0} \right)^2 .$$

This is not quite enough to reduce the final temperature by an appreciable amount.

While the electron temperature is still rising the loss rate as calculated from Eq. (5.2-5) is larger and may be enough to cut the final temperature more effectively. At this stage one can't draw any more definite conclusions because there are as yet many unresolved questions. It is, for example, extremely doubtful whether the Saha equation applies where the electron gas is not in equilibrium. Even if the electrons have a Boltzmann velocity distribution it is almost certain that the population of bound states is not determined by the electron temperature. The reason for this is that radiative mean free paths, even at the center of a line, are so large that practically all photons escape. The states which contribute to the line radiation are therefore under-populated and there will be less of this type of radiation than under equilibrium conditions; just how much less is hard to predict. The other two radiation terms

in Eq. (5.2-5) depend only on the velocity distribution so that they probably remain valid. One must also consider that the air ahead of the shock may have been preheated by X-rays. It is furthermore possible that the equilibration is not brought about by individual particle collisions but by an instability of some kind. In that case the heating rate could be much larger and there would be less time for radiation losses. Other problems may arise if the piston material and the air get mixed up either because of Taylor instability or because the mean free paths are large.

Whether the temperature of the shock heated air does or does not reach the value predicted by Eq. (5.1-13) it is reasonably certain that it will indeed be extremely hot and that it will get rid of its energy by the emission of X-rays. There are too many unresolved questions however, to predict the spectral distribution of these X-rays.

### 5.3 Radiative pre-heating

From debris driven shocks travelling with speeds like  $10^8$  cm/sec or more we now turn to shocks originating near the surfaces of fireballs. Again classical shock theory as presented in the beginning of this section oversimplifies the picture but for a different reason. The classical theory does not include radiative energy transfer which may play an important role. For a proper understanding of this one must remember the characteristic temperature dependence of the air opacity which has a pronounced maximum when  $kT$  lies in the vicinity of 5 eV and drops by many orders of magnitude below and above that temperature. There are several different situations which arise because of this variation and which depend on the temperatures  $T_1$  and  $T_2$  ahead of and behind the shock front. In the course of the fireball expansion these temperatures drop and the character of radiation effects changes.

We are mainly concerned with the phase during which  $T_2$  is still high enough and  $K(T_2)$  large enough to make the shocked air opaque whereas  $T_1$  has already dropped low enough to make the air somewhat more transparent. In that situation the shock front radiates like a black body and sends a radiant heat flux  $\sigma T_1^4$  into the unshocked region. This flux preheats a layer whose width is of the same magnitude as the radiative mean free path. While a given portion of air lies within this layer its temperature gradually rises until the shock front arrives. At that time hydrodynamic heating takes over and raises the temperature suddenly to a much higher value. This heating mechanism leads to a temperature toe which protrudes ahead of the much larger shock induced temperature rise.

In the toe, hydrodynamic heating is insignificant and to calculate the temperature rise one can therefore use the energy equation at constant density

$$\rho \frac{\partial e}{\partial t} = - \frac{\partial \mathcal{J}}{\partial x} \quad (5.3-1)$$

where  $\mathcal{J}$  is the radiant heat flux. If the toe passes rapidly so that there is not enough time for changing major features of the shock such as its speed, one can approximate the problem by assuming steady state conditions. This implies that the toe moves with the same speed as the shock and that it maintains a constant shape. One can therefore write

$$\mathcal{J} = \mathcal{J}(x - Dt) \quad (5.3-2)$$

and

$$\frac{\partial \mathcal{J}}{\partial x} = - \frac{1}{D} \frac{\partial \mathcal{J}}{\partial t} \quad (5.3-4)$$

so that

$$\rho \frac{\partial e}{\partial t} = \frac{1}{D} \frac{\partial \mathcal{J}}{\partial t} \quad (5.3-5)$$

To integrate this equation we note that  $\mathcal{J}$  is zero until the heating wave arrives and that it rises to the  $\sigma T_2^4$  at the point where the toe touches the shock front. One is thus led to the relation

$$\rho_1 \Delta e = \sigma T_2^4 / D \quad (5.3-6)$$

for the energy rise at the back of the toe. The presence of this toe is very significant because it determines how far one can see into the fireball.

There is a distinct phase during the evolution of a fireball where the radiation observed on the outside comes from some point on this toe. As overall temperatures drop, the air becomes more transparent and the observed radiation comes from points further back in the toe and eventually from the region behind the shock front.

Immediately behind the shock front the temperature profile overshoots and then drops back to the normal shock value. This blip is very narrow corresponding to the short radiative mean free path in this very opaque region. In the volume "Radiation Hydrodynamics of High Temperature Air" we will see that one can treat the net flux as the difference of the fluxes carried by an outgoing and an ingoing stream. Applying that method to this case we find that the blip structure has hardly any effect on the outgoing stream whose flux remains essentially at the value  $\sigma T_2^4$

The ingoing stream on the other hand starts at the front with a flux which is orders of magnitude smaller since it comes from the cooler region outside the shock. Travelling inwards, however, it rises very rapidly to the same  $\sigma T_2^4$  at which point the net flux, which is the difference, has dropped to zero. The energetics in the blip is exactly the reverse of that in the toe. There is a net flux  $\sigma T_2^4$  leaving at the front and no flux entering at the rear, which leads to a cooling of the region. The energy change across the blip is given by the same equation (Eq. (5.3-6))<sup>1</sup> derived for the toe, except for the sign and replacing  $\rho_1$  by  $\rho_2$ .

To find the blip in numerical calculations one would have to make a division into very narrow zones. This would be an expensive proposition and is generally not done particularly since the blip has virtually no practical significance.

The whole topic of the effect of radiative transfer on shock structure has in recent years been studied quite extensively from various points of view. A good review of the current status has been presented by Vincenti and Kruger (1965).

### References

- Artsimovich, L.A., Controlled Thermonuclear Reactions, Gordon and Breach Sci. Publ., New York, 1964.
- Jaffrin, M.Y. and F. Probst, Structure of a Plasma Shock Wave, Phys. Fluids 7, 1658, 1964.
- Vincenti, W.G., and C.H. Kruger, Jr., Introduction to Physical Gas Dynamics, John Wiley and Sons, Inc., 1965.

## Chapter 6. THE APPROACH TO COMPOSITION EQUILIBRIUM IN AIR

### 6.1 Introduction

In this chapter we shall be concerned with departures from equilibrium which are limited in some definite way and, for the most part, small. It is convenient to discuss such departures by defining a relaxation time  $\tau$  such that

$$-\frac{dA}{dt} = \frac{1}{\tau} (A - A_0) \quad (6.1-1)$$

where  $A$  is some variable dependent on the time  $t$ , and  $A_0$  is that variable's equilibrium value. One can also define a number

$$Z = \tau/\tau_c \quad (6.1-2)$$

where  $\tau_c$  is the time between collisions. Thus,  $Z$  is the number of collision times required for relaxation.

A system such as air can have non-equilibrium in various energy distributions, as well as in composition. Later in this section we review the known energy distribution relaxation phenomena of air. Generally, it will be seen that the number  $Z$  for energy distribution relaxation is small compared with the  $Z$  for composition relaxation. Therefore, when considering times of the order of the composition relaxation time, it may be a justifiable approximation to assume that all degrees of freedom other than composition are already relaxed, but care should be exercised in this regard. We actually make this assumption in our treatment.

We have already noted in Chapter 1 that the usual treatments of radiative transfer assume that any system under consideration is in LTE. The same assumption is made in most treatments of hydrodynamics and radiation-hydrodynamics. In many cases of interest for thermal radiation phenomena, significant deviations from LTE occur, and it is therefore desirable from a practical point of view to have a set of criteria to determine the adequacy of the LTE assumption under any set of conditions. In the remainder of this chapter we are concerned with one of the situations which illustrates the possible inadequacy of the LTE assumption: a system receives a deposit of energy suddenly, for example through absorption of radiation or by the passage of a shock wave. The normal LTE assumption is that the system immediately attains the appropriate final state, whereas it actually requires a finite time to relax. The validity of an approximation which neglects the relaxation time depends upon the magnitudes of other significant time constants of the system. The basic problem is the relaxation

of a complex system which has a finite displacement from equilibrium.

The principles governing chemical reactions are quite well understood. Of course, this is not to say that the relevant parameters, such as reaction rate coefficients, are known. Nevertheless, in complex systems a principal difficulty in calculation arises from the complicated nature of the "bookkeeping" problem, i.e., keeping all conditions satisfied simultaneously. This problem is stressed, and thus the material of this section is more mathematical than chemical in content. However, comments will be made later in the chapter regarding the reliability of the reaction rate coefficients, etc.

#### Energy Distribution Relaxation.

Without change of species, energy may be distributed in four forms: translation, rotation, vibration, and electronic. Although electronic relaxation times may be close to the order of magnitude of chemical or ionization relaxation times, one can generally ignore the energy in the electronic form, as it constitutes a relatively small fraction of the total energy when chemical or ionization phenomena are also involved. In Chapters 8, 9 and 10, however, it will be seen that in certain cases the energy distribution in electronic states is important, and consideration of electronic relaxation is deferred until that section.

The most rapid adjustment in energy distribution occurs in the translational form. It has been shown theoretically (Kohler, 1948) that the number of collision times necessary for translational relaxation is

$$Z_{tr} = (\tau_{tr}/\tau_c) = 1.271 \quad (6.1-3)$$

This result is derived for an ideal gas with rigid spherical molecules, but is generally expected to be approximately valid for more realistic cases. Although early experiments on monatomic gases were not in agreement with the above result, recent experiments show (Greenspan, 1956) that prior experimental results were in error, and theory and experiment are now in concordance. The data for polyatomic gases presents other difficulties in interpretation (Greenspan, 1963), and therefore, comparison between theory and experiment has been largely confined to monatomic gases.

The relaxation time for rotation is almost as rapid as for translation. Measurements of ultrasonic wave absorption for air (Evans and Bazley, 1956) indicate that the number of collision times required for rotational relaxation,  $Z_{\text{rot}}$ , at 30°C is about 10. This is determined from the theoretical formula (Herzfeld and Litovitz, 1959)

$$\alpha/\alpha_{\text{cl}} = 1 + 0.067 Z_{\text{rot}} \quad (6.1-4)$$

where  $\alpha$  and  $\alpha_{\text{cl}}$  are the measured and classical absorption coefficients. Unfortunately, an error of about 0.2 in  $\alpha/\alpha_{\text{cl}}$  gives rise to an error of a factor of 3 in  $Z_{\text{rot}}$ , and it is difficult to measure  $\alpha$  that precisely. It is, however, justifiable for our purposes to assume that rotational relaxation is very rapid at temperatures  $\geq 300^\circ\text{K}$ .

The relaxation time for vibration is much longer than for rotation and translation, and indeed, it approaches the times required for chemical

relaxation. A theoretical formula for  $Z_{\text{vib}}$  has been given (Herzfeld and Litovitz, 1959) as

$$Z_{\text{vib}} = 1.017 Y(2,2) \left( \frac{r_0}{r_c} \right)^2 \left[ (\bar{Q})_{\text{av}} (1 - e^{-\theta/T}) \right]^{-1} \quad (6.1-5)$$

where  $Y(2,2)$  is a function correcting for attractive forces (Hirschfelder, et al., 1954),  $r_0$  is the usual Lennard-Jones parameter,  $r_c$  is the collision radius,  $(\bar{Q})_{\text{av}}$  is the appropriate deactivation cross section, and  $\theta$  is the characteristic temperature for vibration.

Comparison of theory and experiment for air molecules (Herzfeld, 1963) is shown in Table 6.1. There are two columns for theoretical results because of two different choices in the steric factor entering into  $(\bar{Q})_{\text{av}}$ . The second column involves a steric factor computed on the basis of spherical molecules, and the third column is obtained with a steric factor for elongated molecules.

Similar difficulties occur in the measurements for NO vibrational relaxation, where the low temperature (Robben, 1959) and high temperature (Wray, 1962) data do not agree by a factor of about 3 at the point of overlap, and the early theory is not easily reconcilable with either of the experimental results. New theoretical calculations (Herzfeld, 1963) have not been performed for NO, but the experimental data at least indicate that the NO relaxation time is closer to that for  $\text{O}_2$  than for  $\text{N}_2$ .

Table 6.1 Comparison of Theory and Experiment  
for Vibrational Relaxation in Air Molecules

Molecules	T(°K)	Z <sub>theor</sub> <sup>(a)</sup>	Z <sub>theor</sub> <sup>(b)</sup>	Z <sub>exp</sub>
O <sub>2</sub> - O <sub>2</sub>	288	4.2 x 10 <sup>7</sup>	2.0 x 10 <sup>7</sup>	1.6 x 10 <sup>7</sup>
	323	2.4 x 10 <sup>7</sup>	1.2 x 10 <sup>7</sup>	1.0 x 10 <sup>7</sup>
	1372	15,000	7,200	36,000
	1953	4,100	2,000	12,000
	2912	1,000	480	1,800
	4000	370	180	780
	6000	140	65	190
O <sub>2</sub> - N <sub>2</sub>	323	2.8 x 10 <sup>7</sup>	1.4 x 10 <sup>7</sup>	4 x 10 <sup>6</sup>
	1953	3,800	1,900	5,000
N <sub>2</sub> - N <sub>2</sub>	475	2.1 x 10 <sup>9</sup>	1.1 x 10 <sup>9</sup>	> 8 x 10 <sup>8</sup>
	558	8.2 x 10 <sup>8</sup>	4.3 x 10 <sup>8</sup>	1.1 x 10 <sup>8</sup>
	778	7.0 x 10 <sup>7</sup>	3.6 x 10 <sup>7</sup>	6.5 x 10 <sup>6</sup>
	1168	4.7 x 10 <sup>6</sup>	2.4 x 10 <sup>6</sup>	2.3 x 10 <sup>6</sup>
	2450	75,000	39,000	150,000
	3640	11,600	6,000	24,000
	4630	4,300	2,200	8,000

On the basis of the results in this table, the relaxation time of N<sub>2</sub> is about an order of magnitude longer than for O<sub>2</sub>, and it would also seem that O<sub>2</sub> is more effective in deactivation of N<sub>2</sub> than N<sub>2</sub> itself. However, at higher temperatures not reported in the table for O<sub>2</sub> - N<sub>2</sub>, this effect apparently does not persist (Blackman, 1955), and thus, doubt is cast on the validity of the lower temperature data.

## 6.2 Remarks on notation

Consider a chemical reaction of a complex system:



where the  $X_i$ 's are chemical species. This reaction proceeds in both directions, and at equilibrium the rates are equal. The rate of change in concentration of the species involved, due to this step alone, is given by:

$$\frac{dC_m}{dt} = \frac{dC_n}{dt} = - \frac{dC_p}{dt} = - \frac{dC_q}{dt} = -k_{mn,pq} C_m C_n + k_{pq,mn} C_p C_q \quad (6.2-2)$$

Here the  $C_i$ 's are concentrations in molecules per  $\text{cm}^3$ , and the  $k_{mn,pq}$  are rate constants in  $\text{cm}^3$  per second. It is understood that concentrations and rate constants can be given in various units. Chemists most often use moles per liter or pressure in atmospheres for concentrations and the appropriate rate constants. In the system adopted here the rate constant is related simply to the cross section for the process

$$k_{mn,pq} = \bar{v}_{mn} \sigma_{mn,pq} \quad (6.2-3)$$

where  $\bar{v}_{mn}$  is the average relative velocity of the pair  $mn$ .

At equilibrium there is no net chemical change, and we have:

$$k_{mn,pq} C_m^0 C_n^0 = k_{pq,mn} C_p^0 C_q^0 \quad (6.2-4)$$

where the  $C_i^0$ 's are equilibrium concentrations, the  $k$ 's are related through the equilibrium constant:

$$K_{mn,pq} = \frac{k_{mn,pq}}{k_{pq,mn}} = \frac{C_p^0 C_q^0}{C_m^0 C_n^0} \quad (6.2-5)$$

It is convenient to introduce a symbol for the equilibrium rate:

$$R_{mn,pq} = R_{pq,mn} = k_{mn,pq} C_m^0 C_n^0 = k_{pq,mn} C_p^0 C_q^0 \quad (6.2-6)$$

Since we shall be interested primarily in systems which are near equilibrium, we introduce another measure of concentration of a component:

$$\eta_m = \frac{C_m}{C_m^0} \quad (6.2-7)$$

which is clearly dimensionless, and becomes unity at equilibrium. For the isothermal case we can write equations equivalent to (6.2-2) as follows:

$$\frac{d}{dt} (C_m^0 \eta_m) = - R_{mn,pq} (\eta_m \eta_n - \eta_p \eta_q) \quad (6.2-8a)$$

$$\frac{d}{dt} (C_n^0 \eta_n) = - R_{mn,pq} (\eta_m \eta_n - \eta_p \eta_q) \quad (6.2-8b)$$

$$\frac{d}{dt} (C_p^0 \eta_p) = - R_{mn,pq} (\eta_p \eta_q - \eta_m \eta_n) \quad (6.2-8c)$$

$$\frac{d}{dt} (C_q^0 \eta_q) = - R_{mn,pq} (\eta_p \eta_q - \eta_m \eta_n) \quad (6.2-8d)$$

### 6.3 The system of equations

The net rate of change of composition in a complex system which has been displaced from equilibrium involves terms of two types:

- a) The net effect of all elementary chemical reactions.
- b) A source term which gives the numbers of molecules introduced per unit volume per unit time by other processes. An example of such a term is the creation or destruction of species by ionizing radiation.

The equations which give the rates of change in a complex system of  $N$  constituents are:

$$\frac{d}{dt} C_m^0 \eta_m = Q_m - \sum_{n,p,q} R_{mn,pq} (\eta_m \eta_n - \eta_p \eta_q) \quad (6.3-1)$$

$$m = 1, 2, \dots, N$$

where  $Q_m$  is the source term and the summation runs over all possible elementary reactions.

The cases of most interest come in two categories:

- a) There is a sudden displacement of equilibrium of the system after which external influences cease.

This is essentially the description of shock heating where a high temperature suddenly occurs, and then conditions remain essentially constant for a while. The system finds itself in a displaced condition because the composition is that of a much lower temperature. Another example is a high flux of radiation which creates species far from equilibrium. For these cases the  $Q_m$  terms in (6.2-1) are zero.

- b) A system at equilibrium is slowly displaced from equilibrium by a constant external stimulus.

For shock-heated air which has come to equilibrium at a high temperature there is an application of this case. As a parcel of air cools because of adiabatic expansion it is constantly displaced from equilibrium by the decreasing temperature. If the rate of cooling is too fast, the high temperature condition is retained or "frozen" in. Another example of this case is a system with a relatively small and constant external source of ionizing radiation. For these cases the source terms  $Q_m$  are not zero.

There is no simple way to enumerate the number of possible elementary reactions of a system; this is a complicated function of the physical and chemical properties of the constituent atoms and molecules. In any case

of interest it is a finite number, perhaps of the order of one hundred. For the sake of convenience let us say that this number is  $P$ . These reactions can be ordered in a standard way (which is arbitrary), and their equilibrium rates designated as  $R_j$ , where  $j$  runs from 1 to  $P$ . Each reaction will have a standard direction which may, for example, be chosen as the exothermic direction.

Reaction (6.2-1) may, for example, be called number  $s$  in the sequence and we could then have

$$R_s = R_{mn,pq}$$

The basic equation (6.3-1) can be written in this new notation, featuring explicitly the contribution of the reactions as

$$\frac{d}{dt} C_m^0 \eta_m = Q_m - \sum_{j=1}^P \delta(j,m) R_j f_j(\vec{\eta}) \quad (6.3-2)$$

where  $\delta(j,m)$  is a quantity which has the following properties:

$\delta(j,m) = 1$  if species  $m$  appears as reactant in  $j$ th reaction,

$\delta(j,m) = -1$  if species  $m$  appears as product in  $j$ th reaction,

$\delta(j,m) = 0$  if species  $m$  does not appear in  $j$ th reaction,

and  $f_j(\vec{\eta})$  is the appropriate function of  $\eta_1, \eta_2, \dots, \eta_N$  which goes with the  $j$ th reaction. In the following we shall have occasion to use both forms of the basic equation.

#### 6.4 Linear form of equations

Many of the situations of particular interest involve only slight displacements from equilibrium. The  $\eta_m$ 's are all near unity and we can make the substitution

$$\eta_m = 1 + \epsilon_m \quad (6.4-1)$$

where by hypothesis  $\epsilon_m$  is much less than unity. Equations (6.2-1) can be written with neglect of square terms to yield

$$\frac{d}{dt} C_m^0 \eta_m = Q_m + \sum_{j=1}^N A_{mj} \epsilon_j \quad (6.4-2)$$

$m = 1, 2, 3 \dots N$

and the  $A_{mn}$  are linear combinations of the  $R_{mn,pq}$

$$A_{mj} = \sum_{n,q} (R_{mn,jq} - R_{mj,nq}) \quad (j \neq m) \quad (6.4-3a)$$

$$A_{mm} = - \sum_{p,q} R_{mm,pq} \quad (j = m) \quad (6.4-3b)$$

In the notation in which the  $P$  reactions are indicated explicitly we can write (6.4-2) as

$$\frac{d}{dt} C_m^0 \eta_m = Q_m - \sum_{j=1}^P \delta(j,m) R_j f_j(\xi) \quad (6.4-4)$$

where  $f_j(\vec{e})$  is the function obtained from  $f_j(\vec{\eta})$  by means of the substitution (6.4-1).

It is quite clear that these equations can be written in matrix form

$$\frac{d}{dt} \vec{C} = \frac{d}{dt} C^0 \vec{\eta} = \vec{Q} + A \vec{e} \quad (6.4-5)$$

where it is understood that the quantities without vector signs are matrices.

We shall have several vector quantities and matrices associated with the concentrations

$$\begin{aligned} \vec{C} &= \begin{bmatrix} C_1 \\ C_2 \\ \vdots \\ C_N \end{bmatrix} & \vec{C}^0 &= \begin{bmatrix} C_1^0 \\ C_2^0 \\ \vdots \\ C_N^0 \end{bmatrix} & (\vec{C}^0)^{1/2} &= \begin{bmatrix} (C_1^0)^{1/2} \\ (C_2^0)^{1/2} \\ \vdots \\ (C_N^0)^{1/2} \end{bmatrix} \\ C^0 &= \begin{bmatrix} C_1^0 & & & \\ & C_2^0 & & \\ & & \ddots & \\ & & & C_N^0 \end{bmatrix} & (C^0)^{1/2} &= \begin{bmatrix} (C_1^0)^{1/2} & & & \\ & (C_2^0)^{1/2} & & \\ & & \ddots & \\ & & & (C_N^0)^{1/2} \end{bmatrix} \end{aligned} \quad (6.4-6)$$

For the remainder of this section we shall limit our attention to the case that all  $Q_m$  are zero and the temperature and density are constant. The basic linear equation can then be written as

$$C^0 \frac{d\vec{\epsilon}}{dt} = A\vec{\epsilon} \quad (6.4-7)$$

Because of the constancy of temperature and density,  $C^0$  is independent of time and can be put to the left of  $\frac{d\vec{\epsilon}}{dt}$ . The matrix  $A$ , with elements defined in (6.4-3), is symmetric.

A more convenient equation can be obtained in terms of a new column matrix  $\vec{\delta}$  defined in terms of the relation

$$\vec{\epsilon} = (C^0)^{-1/2} \vec{\delta} \quad (6.4-8)$$

where  $(C^0)^{-1/2}$  is a diagonal matrix whose elements are the reciprocals of the square roots of the concentrations. The equation in  $\vec{\delta}$  is

$$\frac{d\vec{\delta}}{dt} = (C^0)^{-1/2} A (C^0)^{-1/2} \vec{\delta} = B\vec{\delta} \quad (6.4-9)$$

where the matrix  $B$  is defined by the equation. It is quite evident that the matrix  $B$  is symmetric, since both  $A$  and  $C^0$  are.

The solution to equation (6.4-9) is easy to obtain. Consider the eigenvalue problem

$$B\vec{\delta} = \lambda \vec{\delta} \quad (6.4-10)$$

Since the matrix  $B$  is real and symmetric, there is a set of eigenvalues

$$\lambda_1, \lambda_2, \lambda_3, \dots, \lambda_N$$

which are all real. Let us designate the corresponding set of eigenvectors

$$\vec{\delta}^1, \vec{\delta}^2, \vec{\delta}^3, \dots, \vec{\delta}^N$$

In terms of these quantities we can write the general solution to equation (6.4-7) as

$$\vec{\delta} = \sum_{k=1}^N a_k \vec{\delta}^k e^{\lambda_k t} \quad (6.4-11)$$

where the  $a_k$  are arbitrary constants. The displaced concentrations are given by  $\vec{\delta}$ , which can be obtained from (6.4-11) by means of the transformation (6.4-8)

In any real system of  $N$  chemical species there must be a number of conservation conditions which introduce linear dependences into the system of equations which (6.4-5) represents. The technique for solving the equations described here is not invalidated by these linear dependences; for each of them a zero value of  $\lambda_k$  appears automatically in the eigenvalue problem (6.4-10)

It is clear from equation (6.4-11) that if an initially displaced system is to approach equilibrium, all of the  $\lambda_k$ 's must be zero or negative. We feel intuitively that this must be true, but it would be desirable to have a

general mathematical proof that such a result comes from the solution. Such a proof, suggested by J. Uretsky, can be obtained as follows.

Let us consider the relation

$$B \vec{\delta}^k = \lambda_k \vec{\delta}^k \quad (6.4-12)$$

which the  $k^{\text{th}}$  eigenvector obviously satisfies. Transform this equation by multiplication with the matrix  $(C^0)^{1/2}$ , and we get

$$A \vec{\epsilon}^k = \lambda_k C^0 \vec{\epsilon}^k \quad (6.4-13)$$

Comparison of (6.4-2) and (6.4-4) shows that we have an alternative way of writing (6.4-13) as a set of linear equations

$$- \sum_{j=1}^P \delta(j, m) R_j f_j(\vec{\epsilon}^k) = \lambda_k C_m^0 \epsilon_m^k \quad (6.4-14)$$

$m = 1, 2, 3 \dots N$

where by  $\epsilon_m^k$  is meant the magnitude of  $\epsilon_m$  in the  $k^{\text{th}}$  eigenvector. Of course, only the relative values of the displacements  $\epsilon_1^k, \epsilon_2^k, \epsilon_N^k$  are determined, and so the absolute magnitude of this quantity is not fixed.

Let us now multiply equation (6.4-14) by  $\epsilon_m^k$  and sum over all  $m$

$$- \sum_{m=1}^N \epsilon_m^k \sum_{j=1}^P \delta(j, m) R_j f_j(\vec{\epsilon}^k) = \lambda_k \sum_{m=1}^N C_m^0 (\epsilon_m^k)^2 \quad (6.4-15)$$

It can be shown that the double sum on the left side of (6.4-15) reduces to a single sum. Each  $f_j(\vec{e}^k)$  is a linear combination of the several  $e_m^k$ 's which are involved in the  $j^{\text{th}}$  reaction. A particular term  $R_j^m f_j(\vec{e}^k)$  will appear in the double sum once for each of the  $e_m^k$  involved in the reaction and will be multiplied by each of them. We can therefore collect the first sum into a single sum over the reactions in the form

$$- \sum_{j=1}^P R_j f_j(\vec{e}^k) \mathcal{L}_j(\vec{e}^k)$$

where the factor  $\mathcal{L}_j(\vec{e}^k)$  is a linear factor containing each of the  $e_m^k$ 's which belong to the  $j^{\text{th}}$  reaction. In  $\mathcal{L}_j(\vec{e}^k)$  each of the reactants and products has a term; the reactants have positive signs, and the products have negative signs according to our convention. The function  $\mathcal{L}_j(\vec{e}^k)$  is therefore precisely the same as  $f_j(\vec{e}^k)$  in every case, and we can write

$$- \sum_{j=1}^P R_j \left[ f_j(\vec{e}^k) \right]^2 = \lambda_k \sum_{m=1}^N C_m^0 (e_m^k)^2 \quad (6.4-16)$$

All quantities in this sum other than  $\lambda_k$  are essentially positive quantities. Therefore,  $\lambda_k$  must either be negative or zero.

## 6.5 The low temperature reactions of air

At low temperatures (say below 6000°K) air is composed principally of molecules and atoms, and these species dominate the composition relaxation processes. In this section we use the system of equations discussed above. In Table 6.2 we list the species which have been included, and in Table 6.3 we list the reactions which have been used.

Table 6.2

## Species List

Species Number	Species Name
1	$N_2$
2	$O_2$
3	$NO$
4	$N$
5	$O$
6	$N_2O$
7	$NO_2$
8	$O_3$

In Table 6.3 the listed rate coefficient is for the forward reaction. A reverse rate coefficient is used in each case to be in agreement with the appropriate equilibrium constant. Unfortunately, no claim for great accuracy can be made for these rate expressions. Neither the absolute magnitude or the temperature dependence is well known. In some cases measurements of the rates have only been made at one temperature, and the temperature dependence has been guessed. The references indicated in the last column are as follows:

- a) Bortner, 1963
- b) Sparks and Pennington, 1965
- c) Kaufman, 1961.

These are essentially survey articles and should be consulted for the reference to individual rate measurements.

Table 6.3  
Reactions and Rate Coefficients

<u>Reaction</u>	<u>Rate Coefficient</u>	<u>Reference</u>
1. $O + O + O \rightleftharpoons O_2 + O$	$2 \times 10^{-31} T^{-1/2}$	a, b
$O + O + O_2 \rightleftharpoons O_2 + O_2$	$6 \times 10^{-32} T^{-1/2}$	
$O + O + M \rightleftharpoons O_2 + M$	$1 \times 10^{-32} T^{-1/2}$	
2. $N + N + N \rightleftharpoons N_2 + N$	$3 \times 10^{-29} T^{-1}$	a
$N + N + N_2 \rightleftharpoons N_2 + N_2$	$6 \times 10^{-30} T^{-1}$	
$N + N + M \rightleftharpoons N_2 + M$	$3 \times 10^{-30} T^{-1}$	
3. $N + O + M \rightleftharpoons NO + M$	$2 \times 10^{-31} T^{-1/2}$	a, b
4. $N + O_2 \rightleftharpoons NO + O$	$3 \times 10^{-16} T^{3/2} \exp(-3000/T)$	a, b
5. $N + NO \rightleftharpoons N_2 + O$	$5 \times 10^{-13} T^{1/2}$	a, b
6. $NO + NO \rightleftharpoons N_2 + O_2$	$2 \times 10^{-11} \exp(-40000/T)$	a
7. $O + N_2O \rightleftharpoons NO + NO$	$2 \times 10^{-10} \exp(-14000/T)$	a, b
8. $O + N_2 + M \rightleftharpoons N_2O + M$	$2 \times 10^{-30} T^{-1} \exp(-10000/T)$	b
9. $N + NO + M \rightleftharpoons N_2O + M$	$1 \times 10^{-30} T^{-1} \exp(-10000/T)$	b
10. $NO + O + M \rightleftharpoons NO_2 + M$	$2 \times 10^{-29} T^{-1}$	a, b, c
11. $N + O_2 + M \rightleftharpoons NO_2 + M$	$3 \times 10^{-31} T^{-1} \exp(-3000/T)$	a, b
12. $O + O_2 + M \rightleftharpoons O_3 + M$	$2 \times 10^{-31} T^{-1}$	a, b, c

Table 6.3 (cont'd)

<u>Reaction</u>	<u>Rate Coefficient</u>	<u>Reference</u>
13. $O + O_3 \rightleftharpoons O_2 + O_2$	$2 \times 10^{-11} T^{1/2} \exp(-2750/T)$	b, c
14. $O + N_2O \rightleftharpoons N_2 + O_2$	$5 \times 10^{-11} \exp(-13500/T)$	a, b, c
15. $O + NO_2 \rightleftharpoons NO + O_2$	$3 \times 10^{-13} T^{1/2}$	b, c
16. $N + NO_2 \rightleftharpoons N_2 + O_2$	$2 \times 10^{-13} \exp(-7000/T)$	a, b
17. $N + NO_2 \rightleftharpoons NO + NO$	$1 \times 10^{-11} \exp(-5000/T)$	a, b
18. $N + NO_2 \rightleftharpoons N_2O + O$	$4 \times 10^{-11} \exp(-4000/T)$	a, b
19. $N + N_2O \rightleftharpoons NO + N_2$	$8 \times 10^{-13} \exp(-5000/T)$	a
20. $N + O_3 \rightleftharpoons NO + O_2$	$8 \times 10^{-12} \exp(-5000/T)$	a
21. $N + O_3 \rightleftharpoons NO_2 + O$	$8 \times 10^{-13} \exp(-3000/T)$	a
22. $NO + O_3 \rightleftharpoons O_2 + NO_2$	$8 \times 10^{-13} \exp(-1250/T)$	a, b
23. $NO + N_2O \rightleftharpoons N_2 + NO_2$	$4 \times 10^{-10} \exp(-25000/T)$	a
24. $N_2 + O_3 \rightleftharpoons O_2 + N_2O$	$2 \times 10^{-11} \exp(-1500/T)$	a
25. $NO_2 + O_3 \rightleftharpoons O_2 + O_2 + NO$	$2 \times 10^{-12} \exp(-1250/T)$	a
26. $N_2O + O_3 \rightleftharpoons O_2 + O_2 + N_2$	$2 \times 10^{-11} \exp(-4000/T)$	a
27. $NO + NO + NO \rightleftharpoons N_2O + N_2O$	$1 \times 10^{-35} \exp(-5000/T)$	a
28. $N_2 + NO + NO \rightleftharpoons N_2O + N_2O$	$1 \times 10^{-34} \exp(-5000/T)$	a

Table 6.3 (cont'd)

<u>Reaction</u>	<u>Rate Coefficient</u>	<u>Reference</u>
29. $\text{N}_2\text{O} + \text{N}_2\text{O} \rightleftharpoons \text{N}_2 + \text{N}_2 + \text{O}_2$	$2 \times 10^{-12} \exp(-10000/T)$	a
30. $\text{N}_2\text{O} + \text{NO}_2 \rightleftharpoons \text{O}_2 + \text{N}_2 + \text{NO}$	$2 \times 10^{-12} \exp(-15000/T)$	a
31. $\text{O}_3 + \text{O}_3 \rightleftharpoons \text{O}_2 + \text{O}_2 + \text{O}_2$	$2 \times 10^{-11} \exp(-7000/T)$	a
32. $\text{N}_2\text{O} + \text{O}_3 \rightleftharpoons \text{O}_2 + \text{NO} + \text{NO}$	$3 \times 10^{-12} \exp(-13000/T)$	a
33. $\text{NO} + \text{NO}_2 \rightleftharpoons \text{O}_2 + \text{N}_2\text{O}$	$2 \times 10^{-12} \exp(-30000/T)$	a
34. $\text{N}_2 + \text{O}_3 \rightleftharpoons \text{NO} + \text{NO}_2$	$1 \times 10^{-12} \exp(-36000/T)$	a
35. $\text{NO}_2 + \text{NO}_2 \rightleftharpoons \text{N}_2 + \text{O}_2 + \text{O}_2$	$2 \times 10^{-13} \exp(-30000/T)$	a
36. $\text{N}_2\text{O} + \text{O}_3 \rightleftharpoons \text{NO}_2 + \text{NO}_2$	$2 \times 10^{-13} \exp(-30000/T)$	a
37. $\text{O}_2 + \text{NO} + \text{NO} \rightleftharpoons \text{NO}_2 + \text{NO}_2$	$1 \times 10^{-40} \exp(-4000/T)$	b

## 6.6 The relaxation of air at low temperatures

We solve the eigenvalue problem (6.4-8) for low temperature air. There are eight eigenvalues of which two are zero, because of the two conservation conditions.

$$2C_1 + C_3 + C_4 + 2C_6 + C_7 = \text{const (conservation of nitrogen atoms)} \quad (6.6-1a)$$

$$2C_2 + C_3 + C_5 + C_6 + 2C_7 + 3C_8 = \text{const (conservation of oxygen atoms)} \quad (6.6-1b)$$

The range of conditions considered was from 2000°K to 6000°K and from ten times normal air density to  $10^{-6}$  normal density. Eigenvalues and eigenvectors were obtained using an IBM 7094 computer.

Solutions of the time dependent displacements using equation (6.4-11) were examined for several cases in which initial values of  $\epsilon_3$  through  $\epsilon_8$  were equal, and the initial values of  $\epsilon_1$  and  $\epsilon_2$  were obtained from conservation conditions (6.6-1). It was found that the subsequent behavior of all the  $\epsilon$ 's (or the  $\delta$ 's) was determined to the largest extent by the term involving the smallest non-zero eigenvalue, which we denote by  $\lambda_6$ . In other words, the value of  $a_6$  in equation (6.4-11) is almost always greater than any of the other  $a$ 's ( $a_7$  and  $a_8$  are always zero since the  $\delta$ 's must go to zero as  $t \rightarrow \infty$ ). In the few cases where  $a_5$  is larger than  $a_6$ ,  $\lambda_5$  is about equal to  $\lambda_6$ . In many cases the largest eigenvalue,  $\lambda_1$ , is many orders of magnitude larger than  $\lambda_6$ , but the value of  $a_1$  is always negligible compared to  $a_6$ . Thus, it is the longest relaxation

time which is the most significant in the determination of the relaxation process. Even though only one or two species are directly controlled by the reaction or reactions which give rise to this eigenvalue, the other species controlled by faster reactions are in pseudo-equilibrium and are tied to the slowly changing species. Of course, it may be possible by a special choice of initial displacements to decouple some of these dependencies, but in general it will not be possible.

In Fig. 6.1 the behavior of the smallest eigenvalue is summarized as a function of the temperature and density parameters. The large temperature dependence at the lowest temperatures is due to the exponential terms in many of the rates listed in Table 6.3. At the higher temperatures these terms become less important, and the terms of the type  $T^n$ , where  $n$  takes on values from 1.5 to -1.0, become dominant in many cases. Thus, as we increase the temperature, the variation with temperature decreases and may even reverse. Another reason for the seemingly irregular behavior of  $\lambda_6$  (or  $\frac{1}{\lambda_6}$ ) is that at different densities the value of  $\lambda_6$  may be determined primarily by different sets of rates. For example, one would expect the three-body reactions to be most important at the highest densities, and the two-body reactions to be most important at the lowest densities.

#### 6.7 The high temperature reactions of air

The situation in air at high temperatures (12,000° and above) is much simpler than at the low temperatures. Except at the highest densities all the molecular species concentrations have decreased to

chemically negligible proportions. We need deal only with atoms and singly and possibly multiply ionized ions. To simplify matters even further, we can assume that only the nitrogen atoms and ions are important. This can be done on the basis that the electron-ion recombination rates for oxygen are much the same as for nitrogen. The reactions we have considered are



The effective two-body rate coefficients for reaction (6.7-1) were taken from Bates, et al., 1962, and are shown in Table 6.4. They were derived for hydrogen plasmas which were optically thick towards the Lyman lines but should not be strongly dependent on the chemical species.

Table 6.4

## Effective Two-Body Recombination Coefficient

Electron density ( $n_e$ ) $\text{cm}^{-3}$	Temperature deg K			
	4000	8000	16,000	32,000
$10^8$	$9 \times 10^{-13}$	$5 \times 10^{-13}$	$2 \times 10^{-13}$	$6 \times 10^{-14}$
$10^9$	$1 \times 10^{-12}$	$5 \times 10^{-13}$	$2 \times 10^{-13}$	$6 \times 10^{-14}$
$10^{10}$	$1 \times 10^{-12}$	$5 \times 10^{-13}$	$2 \times 10^{-13}$	$6 \times 10^{-14}$
$10^{11}$	$2 \times 10^{-12}$	$6 \times 10^{-13}$	$2 \times 10^{-13}$	$5 \times 10^{-14}$
$10^{12}$	$3 \times 10^{-12}$	$7 \times 10^{-13}$	$2 \times 10^{-13}$	$5 \times 10^{-14}$
$10^{13}$	$9 \times 10^{-12}$	$7 \times 10^{-13}$	$1 \times 10^{-13}$	$5 \times 10^{-14}$
$10^{14}$	$4 \times 10^{-11}$	$8 \times 10^{-13}$	$1 \times 10^{-13}$	$5 \times 10^{-14}$
$10^{15}$	$2 \times 10^{-10}$	$3 \times 10^{-12}$	$2 \times 10^{-13}$	$6 \times 10^{-14}$
$10^{16}$	$2 \times 10^{-9}$	$3 \times 10^{-11}$	$1 \times 10^{-12}$	$8 \times 10^{-14}$
limit $n_e \rightarrow \infty$	$2 \times 10^{-25} n_e$	$2 \times 10^{-27} n_e$	$9 \times 10^{-29} n_e$	$3 \times 10^{-30} n_e$

The rate coefficient for reaction (6.7-4), which was important in relatively small regions up to 24,000°K, were obtained from a table similar to that above in Bates, et al., 1962, for the optically thin case. They were decreased arbitrarily by a factor of 2 for the case of optically thick resonance lines.

The rate coefficients for reactions (6.7-2) and (6.7-3) (Sparks and Pennington, 1965) were  $5 \times 10^{-26} T^{-3/2} \text{ cm}^6/\text{sec}$  and  $2 \times 10^{-10} T^{-0.7} \text{ cm}^3/\text{sec}$ , respectively. The analogous reactions for the doubly charged ion, reactions (6.7-5) and (6.7-6), were assumed to have

rate coefficients four times the rates for the singly charged ion.

In certain of the high density regions the rate of recombination of  $N^+$  and electrons via the reactions



was comparable to the largest of the reactions (6.7-1) through (6.7-6). The rates for these reactions are  $3 \times 10^{-5} T^{-2} e^{-13000/T}$  for the charge exchange reaction (Bortner, 1963) and  $9 \times 10^{-5} T^{-1}$  for the dissociative recombination reaction (Sparks and Pennington, 1965). However, since these reactions never dominated the recombination, they were ignored in the interest of simplicity.

In the intermediate region from  $6000^\circ$  to  $12000^\circ$  and perhaps higher (at the high densities) the situation is more complicated. At the low temperature end the molecular reactions will dominate the general reaction processes in air. As we increase the temperature the molecular species concentrations will decrease, and the degree of ionization will increase. At some point the ionization and electron recombination will dominate the reaction processes. This point will, of course, be dependent on the density.

It is in the region that the molecular reactions dominate that the dominant ion is not  $N^+$  but  $NO^+$ . The recombination of  $NO^+$  and electrons is very rapid, having a rate coefficient of about  $5 \times 10^{-8}$  at  $3000^\circ K$  (Sparks and Pennington, 1965). When  $NO$  is the prime contributor of electrons, the ionization will in general, be tied to the neutral molecular reactions.

## 6.8 The relaxation of air at high temperatures

The characteristic relaxation times of air at high temperatures were not obtained by detailed calculations analogous to those for the low temperature molecular region. For selected temperatures and densities, only a three component system was used. These three species were the dominant ion, electrons, and the neutral atom formed by recombination. In addition, only one reaction was used, i.e., that recombination reaction, (6.7-1) to (6.7-6), yielding the maximum rate of ion depletion. The  $B$  matrix then becomes a three by three matrix each of whose elements involves only one reaction rate. Since there are still two conservation equations, one for heavy nuclei and one for total charge, there is only one non-zero eigenvalue, which is the sum of the diagonal elements of  $B$ .

In practice the dominant reaction at the high temperatures is reaction (6.7-1) or (6.7-4). The non-zero eigenvalue when  $N^+$  is the dominant ion is

$$\lambda = - \left( 2 + \frac{N_e}{N_N} \right) k_a N_{N^+} \quad (6.8-1)$$

where  $N_e$ ,  $N_{N^+}$ , and  $N_N$  are the electron, ion, and neutral atom concentrations, and  $k_a$  is the rate coefficient for reaction (6.7-1).

Similarly, when  $N^{++}$  is the dominant ion we have

$$\lambda = - \left( 3 + \frac{N_e}{N_{N^{++}}} \right) k_d N_{N^{++}} \quad (6.8-2)$$

where  $k_d$  is the rate coefficient for reaction (6.7-4) and  $N^{++}$  is the doubly ionized ion concentration.

We see that for a high degree of single ionization the time constant can become very small (or  $\lambda$  very large). However, before  $\lambda$  gets too large, the degree of double ionization will become important and this will determine  $\lambda$ . Similar consideration would apply to even higher temperatures where triple ionization becomes important, as well in the lower temperature region, where the molecular species disappear.

Using Eq. (6.8-1) and (6.8-2),  $\lambda$  was computed for the high temperature region. In the intermediate region, i.e., above 6000° and where the molecular species are still important, the values of the relaxation time were estimated and are basically extrapolations of the behavior of  $\lambda$  below 6000°K. It was assumed that when the molecular species began to disappear  $\lambda$  would increase rapidly until the ionization and recombination reactions dominate. The resulting time constants for temperatures above 6000° are shown in Fig. 6.1, together with those for temperatures below 6000°K. It should be emphasized, however, that the values above 6000°K are far more approximate than the values below 6000°K and involve considerable guesswork.

## 6.9 Composition relaxation of air following a sudden change in energy content

The relaxation times for air shown in Fig. 6.1 are estimates of the times required for approach to composition equilibrium following a sudden change in energy content. It has been assumed in making the calculations that all degrees of freedom other than composition are completely relaxed.

This figure is useful as a general guide, but it should be remembered that quantitative considerations always require more accurate specifications of criteria. For example, if the energy is added by means of shock heating air at a density of  $\rho = 10^{-1} \rho_0$  to a temperature of  $2000^\circ\text{K}$ , the estimate of the relaxation time from the figure is approximately 0.3 second. Under such conditions the non-equilibrium condition which is relaxing is primarily the formation of the equilibrium amount of the nitrogen oxides,  $\text{NO}$  and  $\text{NO}_2$  which amount to only one percent or so of the total number of molecules. If only pressures and densities are of interest in a particular case, this relaxation may be completely unimportant, and the relaxation of real interest is the energy distribution relaxation, which requires somewhat less time. On the other hand if certain optical properties are of importance, the nitrogen oxide composition may be of dominating significance.

In use of this figure it is also well to remember that the method of adding the energy is important. In connection with the same example mentioned above, the sudden addition of energy such that air approaches equilibrium at  $2000^\circ\text{K}$  at a density of  $0.1 \rho_0$ , consider the case of energy addition by X-ray deposit. Here the composition is displaced in the direction of more extraneous molecules, such as nitrogen oxides, ozone, etc.,

than should exist at equilibrium. Again, the usefulness of the figure depends upon the quantitative nature of the problem.

Fig. 6.1 was obtained by two different sets of calculations, as described above. It has an interesting transition region between low and high temperatures which varies with the density. Near  $\rho/\rho_0 = 1$  we find that the estimated relaxation time for temperatures from 6000°K to 8000°K are the same; as the density ratio decreases to  $10^{-2}$  the region is between temperature of 4000°K to 6000°K; as the density ratio decreases further to  $10^{-4}$  the region is between 3000°K to 5000°K. This transition region has an interesting feature that the estimated relaxation time actually doubles back on itself at certain densities; i.e. there are conditions for which the relaxation time is longer for the higher of two temperatures. This feature seems to be the result of a complicated interplay of many reactions which have various temperature dependences and to the rapid appearance and disappearance of certain species in certain regions. It is not a result of the separation of high and low temperature regimes using different techniques and approximations in the computations.

The results of this study cannot be presented as a definitive description of the composition relaxation in air. The authors believe that the techniques used are valid and that as more reliable data on reaction rates become available the quantitative features can be improved. On the other hand, the effects of temperature are extremely complicated and the reliability of the rate constants is difficult to assess. In spite of these short-comings the general relaxation picture is most likely given quite well by Fig. 6.1.

### References

- Bates, D.R., A.E. Kingston and R.W.P. McWhirter, Proc. Roy. Soc. A 267, 297 (1962) and 270, 155 (1962).
- Blackman, V.H., Vibrational Relaxation in O<sub>2</sub> and N<sub>2</sub>, Tech. Rept. II-20 ori-105II, Princeton Univ., Princeton, N.J. (1955).
- Bortner, M.H., Chemical Kinetics in a Re-entry Flow Field, R63SD63, General Electric, King of Prussia, Pa. (1963).
- Evans, E.J. and E.N. Baxley, Acustica 6, 238 (1956).
- Greenspan, M., J. Acoust. Soc. Am. 28, 664 (1956).
- Greenspan, M., Dispersion and Absorption of Sound by Molecular Processes, ed. by D. Sette, Academic Press, New York (1963).
- Herzfeld, K., Dispersion and Absorption of Sound by Molecular Processes, ed. by D. Sette, Academic Press, New York (1963).
- Herzfeld, K. and T. Litovitz, Absorption and Dispersion of Ultrasonic Waves, Academic Press, New York (1959).
- Hirshfelder, J., C. Curtiss, and R. Bird, Molecular Theory of Gases and Liquids, Wiley, New York (1954).
- Kaufman, F., Progress in Reaction Kinetics 1, ed. by G. Porter, Pergamon Press, New York (1961).
- Kohler, M., F. Physik. 125, 715 (1948).
- Robben, F., J. Chem. Phys. 31, 420 (1959).
- Sparks, D.C. and R.H. Pennington, A Preliminary Survey of Selected Rates for Atmospheric Reactions, AFWL, Kirtland Air Force Base, New Mexico (1965).
- Wray, K., J. Chem. Phys. 36, 2597 (1962).

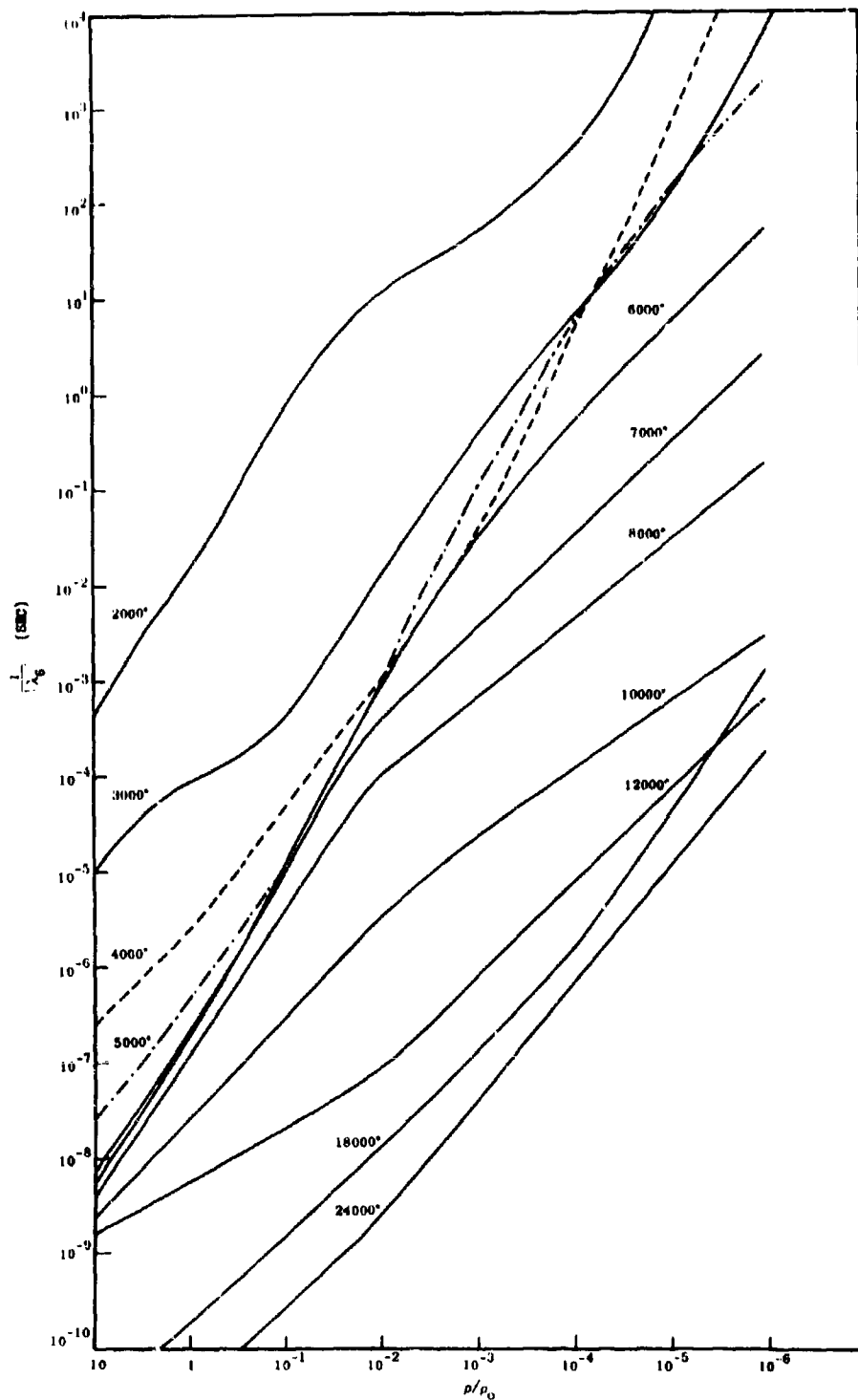


FIG. 6-1 COMPOSITION RELAXATION TIMES FOR AIR

## Chapter 7. ADIABATIC, NEAR-EQUILIBRIUM COOLING OF AIR

A general problem for radiation hydrodynamics is the ability of a system to maintain chemical equilibrium as conditions change. Strictly speaking, deviations from LTE are tied up with the manner in which the conditions change, and a rigorous treatment of any particular case requires simultaneous solution of all the equations of radiation hydrodynamics. We are interested in the development of a general set of criteria for use in such problems and so we consider the composition changes in a system with a superimposed variation of conditions. In our treatment, the chemical composition is decoupled from hydrodynamic effects, a separation which is approximately valid if the assumption of near-equilibrium holds. The criteria we find depend upon the breakdown of the consistency in our treatment.

### 7.1 The linear equations and their solution

For our purpose it is best to choose an imposed volume change on the system, since this can be completely defined. If we tried to create a volume change by specifying the pressure acting on the system or the temperature, for example, the case would be more difficult to treat. For the sake of concreteness, we can think of the system as contained in a thermally-insulated enclosure with a movable wall whose position can be changed by an unspecified mechanical device. Let us say that the volume is changed in such a way that the quantity  $\frac{1}{\rho} \frac{d\rho}{dt}$ , where  $\rho$  is the density, is equal to a previously-specified constant. The basic equation (6.4-5) becomes

$$\frac{d\vec{C}}{dt} = \left( \frac{1}{\rho} \frac{d\rho}{dt} \right) \vec{C} + A\vec{e} \quad (7.1-1)$$

where we have set the external source term  $\vec{Q}$  equal to  $\left( \frac{1}{\rho} \frac{d\rho}{dt} \right) \vec{C}$ .

Because the changing volume of the system induces changes in  $\vec{C}^0$ , the left

side of this equation cannot be developed as before. It is still, however, possible to relate this case to a soluble eigenvalue problem in our previous variable  $\bar{\delta}$ . Using

$$\bar{C} = C^0 \bar{\eta} = \bar{C}^0 + C^0 \bar{\epsilon} = \bar{C}^0 + (C^0)^{1/2} \bar{\delta} \quad (7.1-2)$$

we can obtain

$$\frac{d}{dt} \bar{\delta} = \left( \frac{1}{\rho} \frac{d\rho}{dt} - \frac{1}{C^0} \frac{dC^0}{dt} \right) (\bar{C}^0)^{1/2} + D \bar{\delta} \quad (7.1-3)$$

where

$$D = B + \frac{1}{\rho} \frac{d\rho}{dt} - \frac{1}{2C^0} \frac{dC^0}{dt} \quad (7.1-3a)$$

is a symmetric matrix. The matrix  $B$  is the same as introduced in Section 6.4.

Since our equations are valid only near equilibrium, we shall take

$$\frac{d}{dt} = \frac{dT}{dt} \left( \frac{\partial}{\partial T} \right)_{C^0} = \frac{dT}{dt} \left( \frac{\partial}{\partial T} \right)_S \quad (7.1-4)$$

where the subscripts  $C^0$  and  $S$  mean that the derivatives are taken for concentrations at equilibrium and at constant entropy respectively.

A solution to (7.1-3) can be obtained by introducing a matrix  $U$  such that

$$U^{-1} DU = \Lambda \quad (7.1-5)$$

where  $U^{-1}$  is the inverse of  $U$ , and  $\Lambda$  is a diagonal matrix whose

non-zero elements are the eigenvalues,  $\lambda_j$ , of  $D$ . (That  $U$  and  $U^{-1}$  exist follows from the fact that  $D$  is real and symmetric.) Multiplying (7.1-3) by  $U^{-1}$  and using (7.1-5), we obtain

$$\frac{d}{dt} (U^{-1} \vec{\delta}) = U^{-1} z \frac{dT}{dt} (\vec{C}^0)^{1/2} + (\Lambda + \frac{dU^{-1}}{dt} U) U^{-1} \vec{\delta} \quad (7.1-6)$$

where

$$z = \left( \frac{1}{\rho} \frac{d\rho}{dT} \right)_{C^0} - \left( \frac{1}{C^0} \frac{dC^0}{dT} \right)_{C^0} \quad (7.1-7)$$

If we restrict ourselves to very small times and take  $D$  (and thus  $\Lambda$ ,  $U$  and  $U^{-1}$ ) to be constant, the equations for the components of  $U^{-1} \vec{\delta}$ , Eqs. (7.1-6), decouple and can be integrated easily to give

$$(U^{-1} \vec{\delta})_j = e^{\lambda_j t} \int_0^t S_j e^{-\lambda_j t} dt \quad (7.1-8)$$

where

$$S_j = \left[ U^{-1} z \frac{dT}{dt} (\vec{C}^0)^{1/2} \right]_j \quad (7.1-9)$$

and where we have assumed the  $\delta_j$ 's to be zero at  $t = 0$ .

Before we can apply this solution to the specific case of air for a given value of  $dT/dt$ , we must compute the values of  $\left( \frac{1}{\rho} \frac{d\rho}{dT} \right)_{C^0}$  and  $\left( \frac{1}{C^0} \frac{dC^0}{dT} \right)_{C^0}$ . This is done in the next section.

## 7.2 Relation of temperature and density changes

The solution we are now considering is only valid for conditions near equilibrium, and so we need the explicit relationships satisfied by the quantities

$$\frac{1}{C_1^0} \left( \frac{\partial C_1^0}{\partial T} \right)_S \quad \text{and} \quad \frac{1}{p} \left( \frac{\partial p}{\partial T} \right)_S \quad i = 1, 2, 3, \dots, 8$$

At this point we shall explicitly deal with the case of air below  $6000^\circ\text{K}$ , discussed in Chapter 6. Since there are eight quantities to be determined, we shall need eight relations. The eight equations involve six chemical equilibrium and two conservation equations. The six chemical equilibrium equations are (deleting the superscript zero)

$$\frac{(N)^2}{(N_2)} = \frac{K_1}{p} \eta \quad ; \quad \frac{(O)^2}{(O_2)} = \frac{K_2}{p} \eta \quad (7.2-1a)$$

$$\frac{(N)(O)}{(NO)} = \frac{K_3}{p} \eta \quad ; \quad \frac{(O_2)(O)}{(O_3)} = \frac{K_4}{p} \eta \quad (7.2-1b)$$

$$\frac{(NO)(O)}{(NO_2)} = \frac{K_5}{p} \eta \quad ; \quad \frac{(N_2)(O)}{(N_2O)} = \frac{K_6}{p} \eta \quad (7.2-1c)$$

when  $\eta$  is now the total particle density and the  $K$ 's are functions of  $T$  only. The two conservation equations are

$$(N_2) + (O_2) + (NO) + (N) + (O) + (NO_2) + (N_2O) + (O_3) = \eta \quad (7.2-2)$$

(sum of individual particle concentrations equals total concentration),  
and

$$\frac{2(N_2) + (NO) + (N) + (NO_2) + 2(N_2O)}{2(O_2) + (NO) + (O) + 2(NO) + (N_2O) + 3(O_3)} = M \quad (7.2-3)$$

(ratio of total nitrogen atoms to oxygen atoms is a constant  $M$ ).

For any of the concentrations we can write

$$\frac{1}{C_1} \left( \frac{\partial C_1}{\partial T} \right)_S = \frac{1}{C_1} \left( \frac{\partial C_1}{\partial T} \right)_P + \frac{1}{C_1} \left( \frac{\partial C_1}{\partial p} \right)_T \left( \frac{\partial p}{\partial T} \right)_S \quad (7.2-4)$$

The expression for  $\left( \frac{\partial p}{\partial T} \right)_S$  is

$$\left( \frac{\partial p}{\partial T} \right)_S = - \left[ \left( \frac{\partial u}{\partial T} \right)_P - \frac{p}{\rho^2} \left( \frac{\partial \rho}{\partial T} \right)_P \right] / \left[ \left( \frac{\partial u}{\partial p} \right)_T - \frac{p}{\rho^2} \left( \frac{\partial \rho}{\partial p} \right)_T \right] \quad (7.2-5)$$

where  $u$  is the internal energy of the gas per unit mass. This can be written as

$$u = \frac{1}{\rho} \left[ \sum_1 \left\{ \gamma_1 kT C_1 + H_1^{\infty} C_1 \right\} \right] \quad (7.2-6)$$

where  $k$  is Boltzmann's constant, and  $\gamma_1$  and  $H_1^{\infty}$  are the internal energy coefficients and heats of formation for the  $i^{\text{th}}$  species and are known functions of  $T$  and  $p$ .

If we take  $\rho$  proportional to  $\sum_1 \mu_1 C_1$ , where  $\mu_1$  are the species molecular weights, we see that a computation of  $(\partial C_1 / \partial T)_P$  and  $(\partial C_1 / \partial p)_T$  will lead, via equations (7.2-4) to (7.2-6), to  $(\partial C_1 / \partial T)_S$ . To obtain these quantities we can differentiate appropriately equations (7.2-1) to (7.2-3), which give us sixteen equations. Using the fact that

$$p = \eta kT \quad (7.2-7)$$

and thus

$$\frac{1}{\eta} \left( \frac{\partial \eta}{\partial T} \right)_p = -\frac{1}{T} ; \quad \frac{1}{\eta} \left( \frac{\partial \eta}{\partial p} \right)_T = \frac{1}{p} \quad (7.2-8)$$

and the fact that

$$\left( \frac{\partial \ln (K_1/p)}{\partial T} \right)_p = \frac{(\text{enthalpy change in reaction})}{kT^2} \quad (7.2-9)$$

we can solve for the needed quantities. Once  $\left( \frac{\partial C_1}{\partial T} \right)_S$  is known,  $\frac{1}{p} \left( \frac{\partial p}{\partial T} \right)_S$  can be computed.

### 7.3 The relaxation process

We now return to the solution of (7.2-3), which was obtained in Equation (7.1-8). Taking  $D$  to be constant implies that

$$\frac{1}{C_j^0} \frac{dC_j^0}{dt} = \alpha_j = \text{constant} \quad (7.3-1)$$

and thus

$$C_j^0 = C_j^{00} e^{\alpha_j t} \quad (7.3-1a)$$

where  $C_j^{00}$  is the value of  $C_j^0$  at  $t=0$ . Using (7.3-1a) and the fact that  $U^{-1}$  is the matrix whose rows are the unit length eigenvectors of  $D$ , we can integrate (7.1-8) for any given  $T$ ,  $p$ , and  $dT/dt$ . If we take  $dT/dt$  sufficiently small and arrange the  $\lambda$ 's in order of descending absolute value, the first six eigenvalues,  $\lambda_1, \dots, \lambda_6$ , correspond to the non-zero eigenvalues of the  $B$  matrix. The remaining

two eigenvalues are not zero, but are of the order of  $\frac{1}{\rho} \frac{d\rho}{dt}$ .

A typical solution for one of the components of  $\vec{\delta}$  or  $\vec{c}$  behaves as follows. From  $t = 0$  to a time of the order of  $1/|\lambda_6|$ , the  $\epsilon_j$  (or  $\delta_j$ ) will in general increase as  $z_j \frac{dT}{dt} t$ . (If the species is in pseudo-equilibrium, it may deviate from this behavior, but not significantly.) At later times  $\epsilon_j$  becomes essentially constant, i.e., the concentration lags behind the equilibrium concentration by a constant amount. We shall denote this value of  $\epsilon_j$  or  $\delta_j$  by  $\epsilon_j^*$  or  $\delta_j^*$ . The region of constant  $\epsilon_j$  lasts for a finite time and is ended by an abrupt rise (or decrease) in  $\epsilon_j$ . As the absolute magnitude of  $dT/dt$  is increased, the behavior of  $\epsilon_j$  is essentially the same, except that the value of  $\epsilon_j^*$  is greater, being proportional to  $\frac{dT}{dt}$ , and the constant region is shortened in time.

We can understand this behavior better by taking only the terms in first order in  $t$  in Eq. (7.3-1a) and solving (7.1-3) in a manner analogous to the solution of the constant density and temperature problem carried out in Chapter 6. Eq. (7.1-3) becomes

$$\frac{d\vec{\delta}}{dt} = \left( I + \frac{\alpha}{2} t \right) \vec{W} + D \vec{\delta} \quad (7.3-2)$$

where

$$\vec{W} = z \frac{dT}{dt} (\vec{C}^{00})^{1/2} = \text{const.}, \quad I \text{ is the identity matrix, and}$$

$$\alpha = \begin{bmatrix} \alpha_1 & 0 & . & . & 0 \\ 0 & \alpha_2 & & & \\ . & & . & & \\ . & & & . & \\ 0 & & & & \alpha_8 \end{bmatrix}$$

By making the substitution

$$\vec{\delta} = \vec{\psi} - D^{-1} \left( I + \frac{\alpha}{2} t \right) \vec{W} - D^{-2} \frac{\alpha}{2} \vec{W} \quad (7.3-3)$$

we obtain

$$\frac{d\vec{\psi}}{dt} = D\vec{\psi} \quad (7.3-4)$$

the solution to which is

$$\vec{\psi} = \sum_{k=1}^{\delta} a_k \vec{\psi}^k e^{\lambda_k t} \quad (7.3-5)$$

where  $\vec{\psi}^k$  is the eigenvector of  $D$  corresponding to the eigenvalue  $\lambda_k$ .

Thus

$$\vec{\delta} = -D^{-1} \left( I + \frac{\alpha}{2} t \right) \vec{W} - D^{-2} \frac{\alpha}{2} \vec{W} + \sum_{k=1}^{\delta} a_k \vec{\psi}^k e^{\lambda_k t} \quad (7.3-6)$$

The  $a_k$ 's can be obtained by using the conditions at  $t=0$ . If we now assume that  $\frac{1}{|\lambda_6|} \ll t \ll \frac{1}{|\lambda_7|}$  we obtain for  $\delta_j$

$$\begin{aligned} \delta_j = & -(D^{-1} \vec{W} + D^{-2} \frac{\alpha}{2} \vec{W})_j + a_7 \psi_j^7 + a_8 \psi_j^8 \\ & + [a_7 \lambda_7 \psi_j^7 + a_8 \lambda_8 \psi_j^8 - (D^{-1} \frac{\alpha}{2} \vec{W})_j] t \end{aligned} \quad (7.3-7)$$

The quantities independent of  $t$  sum to the value of  $\delta_j^*$  which we obtained before. This value is proportional to  $dT/dt$ . At some time

the quantity depending on  $t$  becomes important, and the region of constant  $\delta_j$  is terminated. Because the actual value of  $\delta_j^*$ , which is given by

$$\delta_j^* = - (D^{-1} \vec{W} + D^{-2} \frac{\alpha}{2} \vec{W})_j + a_7 \psi_j^7 + a_8 \psi_j^8 \quad (7.3-8)$$

is much less than many of the terms of which it is comprised, the time dependent term can become important at times such that the quantities  $\lambda_7 t$ ,  $\lambda_8 t$  and all the  $\alpha_j t$ 's are still much less than unity.

An important property of this solution is that the values of  $\delta_j^*$  are independent of the initial values of the displacements, i.e., the same values of  $\delta_j^*$  would be attained even though the  $\delta_j$ 's at  $t=0$  were not zero. Using this fact we can obtain a solution for a particular problem involving large changes in density and temperature by dividing the expansion into intervals over which the changes in these quantities are small. The solution for the displacements would then be the  $\delta_j^*$ 's (or  $\epsilon_j^*$ 's) obtained in each interval. Of course, if any of the  $\epsilon_j^*$ 's become of the order of unity or greater, our assumption of linearity breaks down, and the solution is no longer valid.

#### 7.4 The criterion for LTE

In the previous section it was noted that the region in which  $\delta_j$  is equal to  $\delta_j^*$  becomes shorter as we increase the value of  $|dT/dt|$ . For each temperature and density there exists a value of  $|dT/dt|$  above which a region of constant  $\delta_j$  does not exist, i.e., the time dependent quantity in Eq. (7.3-7) is already important at times of the order of  $1/|\lambda_6|$ . In this case the concentrations cannot follow the equilibrium

concentrations as before. Just at what value of  $dT/dt$  this occurs cannot be defined without arbitrariness, but this is only a reflection of the fact that the distinction between near equilibrium and frozen conditions is itself somewhat arbitrary.

In general, the values of  $|dT/dt|$  above which equilibrium cannot be maintained, and which we shall call  $\dot{T}_e$ , will be different for each species. However, in the particular case of air below 6000°K all the species are, as we have noted in Chapter 6, rather closely coupled, i.e.,  $1/|\lambda_6|$  is the dominant chemical relaxation time for all the species. In addition, the values of  $\lambda_7$  and  $\lambda_8$  differ from each other only slightly in all cases. Thus, the value of  $\dot{T}_e$  is essentially the same for all species.

We have taken as our criterion a  $\dot{T}_e$  such that  $\delta_j$  differs from  $\delta_j^*$  by 5% at the value of  $t$  when it would differ from  $\delta_j^*$  by only 1% if the time dependent term in Eq. (7.3-7) were not present. This yields a value of  $\dot{T}_e$  such that

$$\left| \frac{[a_7 \lambda_7 \psi_j^7 + a_8 \lambda_8 \psi_j^8 - (D^{-1} \frac{\alpha}{2} \bar{W})_j] (4.6/\lambda_6)}{-(D^{-1} \bar{W} + D^{-2} \frac{\alpha}{2} \bar{W})_j + a_7 \psi_j^7 + a_8 \lambda_j^8} \right| = .05 \quad (7.4-1)$$

This choice of criterion was found to be equivalent in the actual cases to choosing  $\dot{T}_e$  such that

$$\left| \frac{\lambda_7}{\lambda_6} \right| \approx .01 \quad (7.4-2)$$

which would be the criterion obtained if all the  $\alpha$ 's had been taken as zero. This indicates that the variation of the source term in Eq. (7.1-3) over our chosen time intervals is not significant. The use of (7.4-2) rather than (7.4-1) greatly facilitated the computation of  $\dot{T}_e$ . The results are shown in Fig. 7-1 (solid lines) for the region below 6000°K.

The criterion for LTE for air at the higher temperatures is essentially the same as that for air below 6000°K, i.e., Eq. (7.4-2). The values of  $\lambda_6$  are those obtained in Section 6.8, the reciprocals of which are shown in Fig. 6-1. The values of  $\lambda_7$  were estimated by assuming

$$\lambda_7 \approx \frac{1}{\rho} \frac{d\rho}{dt} = \frac{1}{(\gamma_{\text{eff}} - 1)} \quad \frac{1}{T} \frac{dT}{dt} \quad (7.4-3)$$

where  $\gamma_{\text{eff}}$  is an effective adiabatic exponent and has values between unity and 5/3, depending on the degree of dissociation and ionization.

The estimates of  $\gamma_{\text{eff}}$  usually were between 1.05 and 1.3. The resulting expression for  $\dot{T}_e$  is

$$\dot{T}_e \approx 10^{-2} \lambda_6 (\gamma_{\text{eff}} - 1) T \quad (7.4-4)$$

The results for air above 6000°K are shown as dotted lines in Fig. 7-1.

They are rather approximate because of the uncertainty in  $\lambda_6$  and  $\gamma_{\text{eff}}$ , and also because a considerable amount of curve smoothing was done.

It would be well to note again that all the results in this and the preceding chapter were obtained under the assumption that the internal degrees of freedom are always in equilibrium. In the next three chapters

this assumption is examined and is found to break down at sufficiently low densities. When this happens the chemical rates may differ from those used and reverse rates may no longer be related to forward rates through the equilibrium constant. In these regions the criteria which are developed in Chapters 9 and 10 should supersede those developed here.

#### 7.5 Maintenance of LTE in cooling air

The usefulness of Fig. 7-1 depends upon the quantitative features of the problem of interest. Clearly it is most useful if the concentration of some small component of the air is important. Two types of problems can be mentioned as examples: (1) Air is heated by the bow shock of a rocket or missile and a certain amount of ionization is produced. As the air expands about the body and cools, it is of interest to know if the ionization can disappear according to LTE predictions. (2) Air is shock heated in an air blast of a nuclear weapon and nitrogen oxides are produced. As the air expands and cools, it is of interest to know if the  $\text{NO}_2$  remains in equilibrium.

We shall discuss this second problem in more detail. In Figs. 7-2 and 7-3, the solid curves show typical density and temperature variations with time of a spherical shell of air initially at a given distance from the origin of a nuclear blast wave (Hillendahl, 1965). We see at the peak of the temperature and density histories that the  $\text{NO}_2$  has more than sufficient time to form, since the relaxation time, from Fig. 6-1, is of the order of  $10^{-4}$  sec., and the time the gas remains between  $3200^\circ\text{K}$  and  $3250^\circ\text{K}$  is of the order of  $10^{-2}$  sec.

The rates of change of the temperature after passage of the shock are given in Table 7.1.

Table 7.1

## Rate of Change of Temperature During Expansion

Time sec.	Temperature °K	$ dT/dt $ K/sec.
$7.2 \times 10^{-2}$	3200	$1 \times 10^4$
$9.0 \times 10^{-2}$	3000	$9 \times 10^3$
$1.2 \times 10^{-1}$	2800	$7 \times 10^3$
$1.5 \times 10^{-1}$	2600	$6 \times 10^3$
$1.9 \times 10^{-1}$	2400	$4 \times 10^3$
$2.6 \times 10^{-1}$	2200	$2 \times 10^3$

We see that it is not until the temperature drops to about 2600°K that the value of  $|dT/dt|$  lies to the right of the curve in Fig. 7-1 for  $\rho/\rho_0 = 10^{-1}$ . Up until this time the  $\text{NO}_2$  has been able to remain in equilibrium with the temperature and density. At later times we infer that it no longer can and that the  $\text{NO}_2$  concentration will tend to freeze out. Since the equilibrium  $\text{NO}_2$  concentration has its maximum at about 3000°K at  $\rho/\rho_0 = 10^{-1}$  (Gilmore, 1966), we would expect the  $\text{NO}_2$  concentration to be significantly higher than its equilibrium value after a time of  $1.5 \times 10^{-1}$  sec. This non-equilibrium  $\text{NO}_2$  concentration can drastically effect the radiative characteristics of air at these temperatures.

The dotted lines in Fig. 7-2 and 7-3 show the temperature and density histories for the same blast wave but for a shell of air initially at a greater distance from the origin than before (Hillendahl, 1965). As before, the time the gas remains within 50 degrees of the peak temperature, 2330°K,

is of the order of 0.01 sec. The relaxation time from Fig. 6-1 is also about 0.01 sec., and thus the  $\text{NO}_2$  would still form, though perhaps not completely. This  $\text{NO}_2$  concentration freezes out as soon as the gas begins to expand, since the value of  $|dT/dt|$  is initially about  $6 \times 10^3 \text{ K/sec.}$ , which again is at  $2300^\circ\text{K.}$  to the right of the  $10^{-1}$  curve in Fig. 7-1.

As we consider gas shells which are initially at even further distances from the origin we quickly reach a point where the temperature behind the shock is too low for  $\text{NO}_2$  to have time to form at all. On the other hand, if we consider gas which is initially closer to the origin than that which we have discussed, we enter a region where the simple model of a shock wave followed by an expansion is no longer applicable. The energy release which gives rise ultimately to the shock wave is not confined to a point, but usually occurs over a finite volume. In this region the temperatures are too high during the times of interest for the equilibrium concentration of  $\text{NO}_2$  to be important. Thus, in general, we can expect that the  $\text{NO}_2$  concentration at any given time to have a maximum at some distance from the origin, and that this maximum will be significantly higher than that predicted on the basis of chemical equilibrium throughout. The use of our criterion would enable us to gain some quantitative information as to where and how large this maximum is.

#### References

Gilmore, F.R., The Equilibrium Thermodynamic Properties of High Temperature Air, Lockheed, Palo Alto (1966).

Hillendahl, R.W., Private Communication, LMSC (1965).

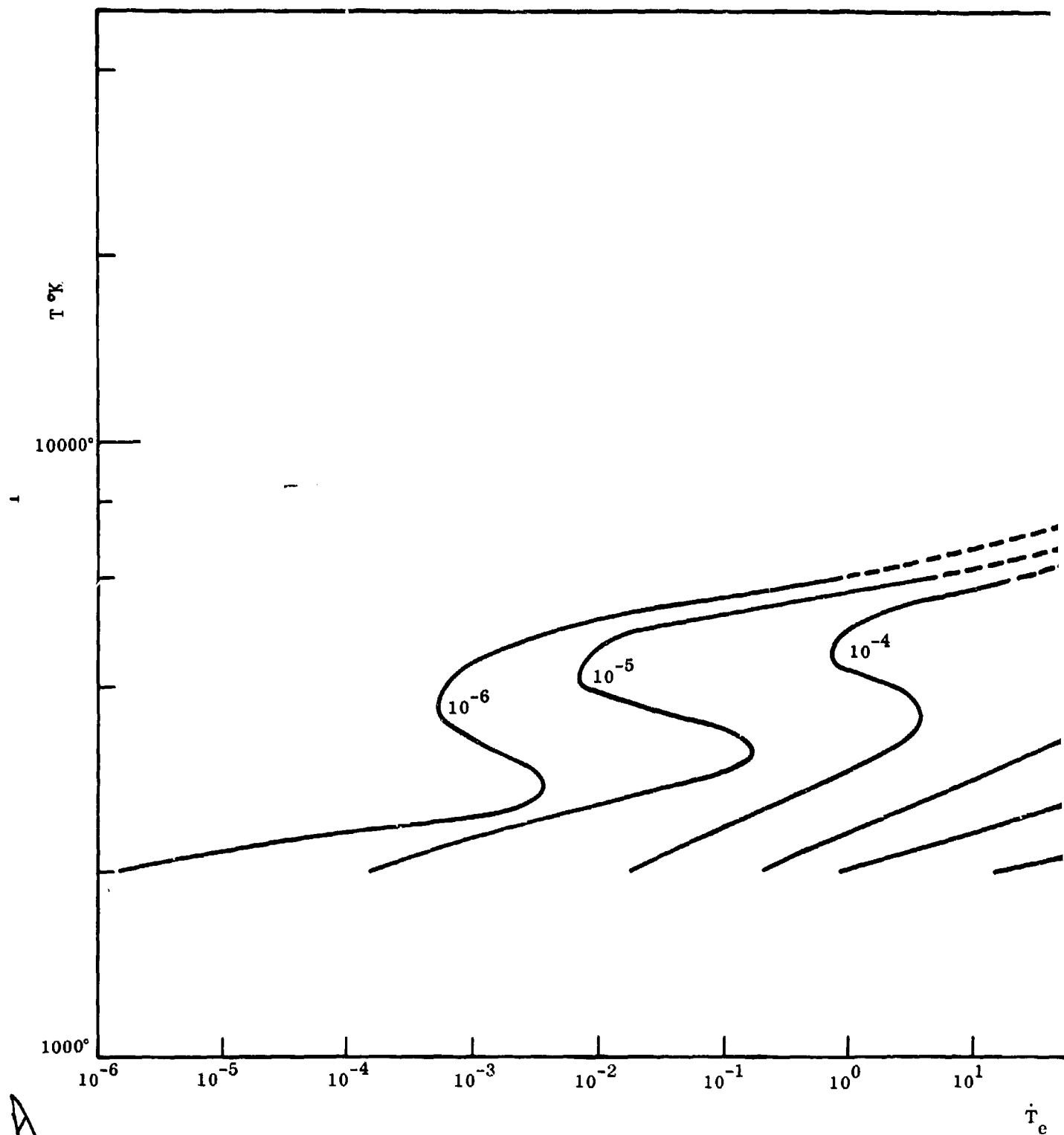
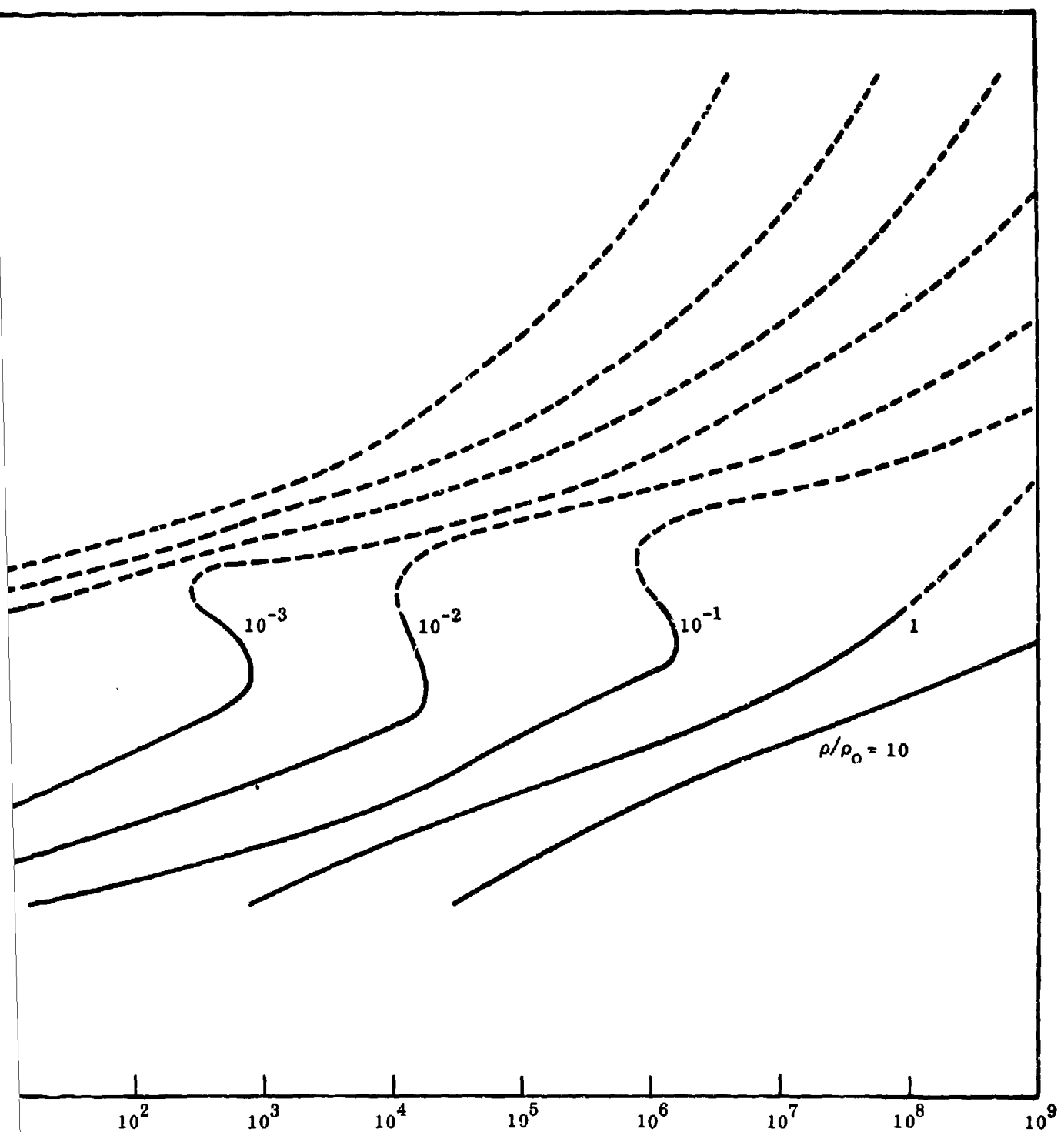


FIG. 7-1 LTE CRITERION,  $\dot{t}_e$



$T_e$  °K/SEC  
 $T_e$  , FOR AIR

B

**BLANK PAGE**

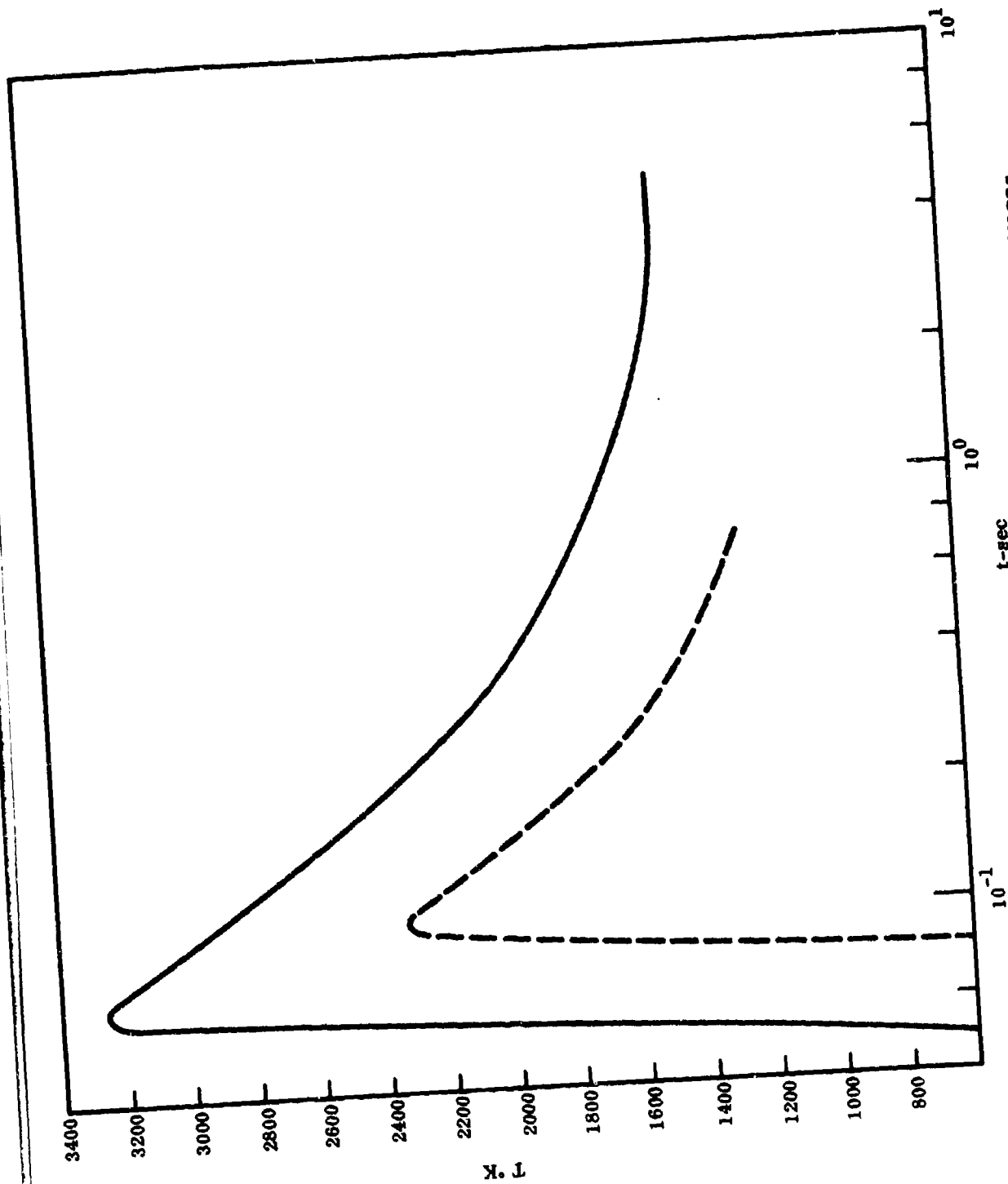


FIG. 7-2 TYPICAL TEMPERATURE HISTORIES FOR AIR AT TWO DISTANCES FROM SPHERICAL SHOCK WAVE ORIGIN

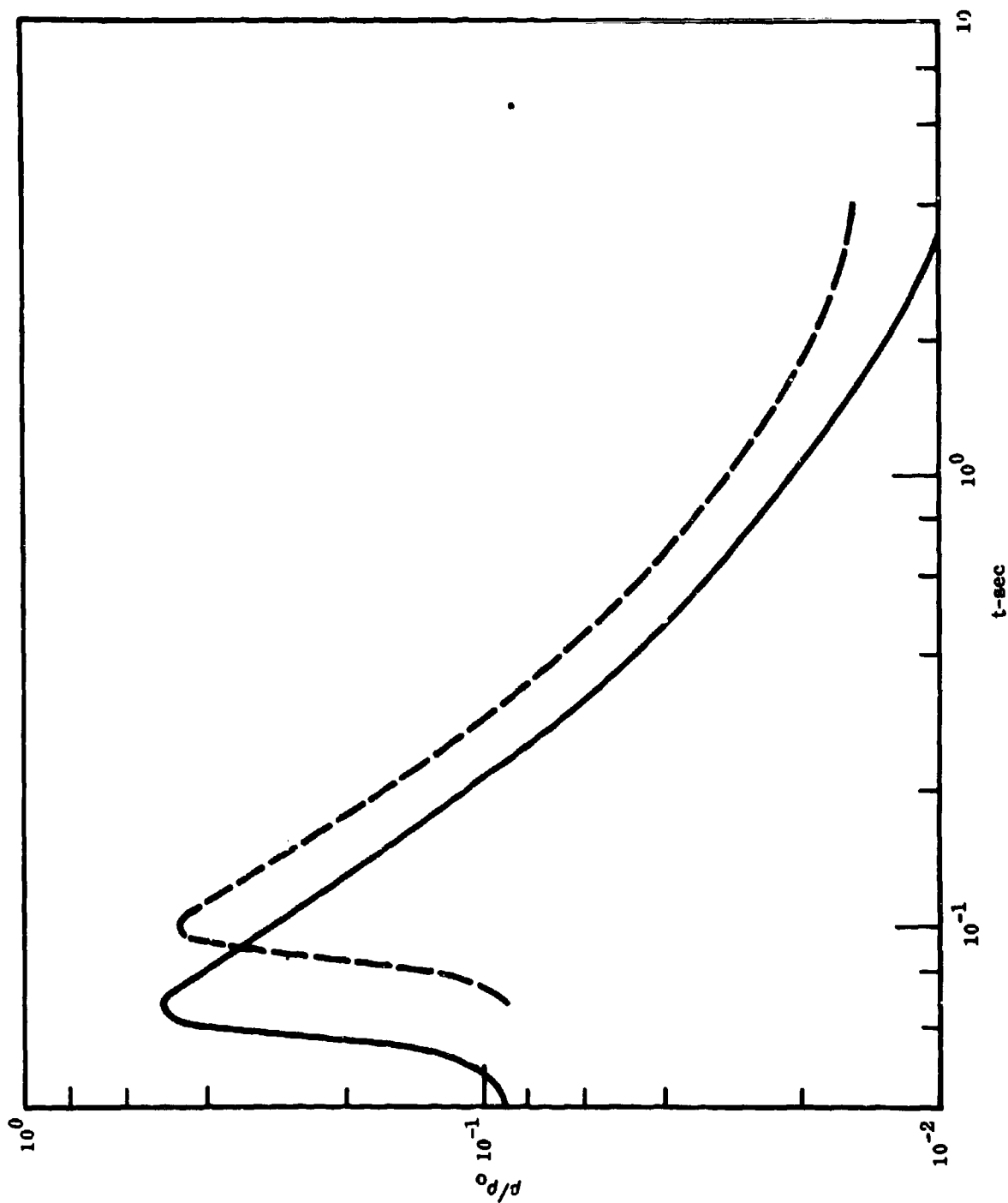


FIG. 7-3 TYPICAL DENSITY HISTORIES FOR AIR AT TWO DISTANCES FROM SPHERICAL SHOCK WAVE ORIGIN

## Chapter 8. NON-EQUILIBRIUM RADIATION TRANSPORT

### 8.1 Introduction

To calculate the radiative properties of a gas it is necessary that the occupation numbers of the various atomic states of the gas particles be known. If the gas is in LTE, the occupation numbers can be expressed in terms of the local temperature and atomic parameters by using standard statistical mechanics. The only parameters required are the energies and statistical weights of the atomic states. When LTE conditions do not prevail, determination of the occupation numbers becomes much more complicated. In general, the occupation numbers depend on the state of the radiation field, so the equations governing the atomic configuration of the gas and the transport of radiation must be solved simultaneously.

The problem of the coupled equations in the absence of LTE was first formulated by Milne (1930). During the next quarter of a century, the problem was largely ignored, however, until its astrophysical importance was emphasized in a series of papers by Thomas and Jefferies. In the past decade a large amount of work has gone into the implications of non-LTE radiative transport for both stars and laboratory plasmas. (For a discussion of this work and a complete bibliography, see Thomas, 1965, Thomas and Athay, 1961, and Smithsonian, 1965.)

With the advent of high altitude nuclear detonations, this work has more recently become of interest to those engaged in the study of weapons effects. In this chapter we give only a cursory introduction to the subject. The chapter was written without a great deal of reference to the literature,

and hence some differences in viewpoint and notation may be present. The papers of Cuperman et al. (Cuperman, Englemann, and Oxenius, 1963, 1964) were particularly helpful in preparing the present introduction.

To gain insight into the physical mechanisms involved, we adopt the simplest model which still contains the essential elements of the problem. The gas is assumed to be in a steady state, and to contain only one radiating species, whose atoms are denoted by  $X$ . These atoms have only one excited state, and the only collisions which populate this state are with electrons. The continuous radiation from the electrons is assumed to be negligible, so the only radiation present is the line arising from radiation by  $X$  atoms. Both electron and  $X$  densities are assumed to be uniform, and the electron energy distribution is assumed to be the equilibrium distribution corresponding to the uniform temperature  $T$ . In contrast to the oversimplified atomic model, however, the radiation field is treated in considerable detail.

A different type of non-LTE problem involving radiation is studied in Chapter 9. The problem considered there is the radiative cooling of a hot sphere of tenuous gas. In that work a realistic atomic model which includes multi-level atoms and electron-ion recombination is assumed, but the radiative transport is treated in a very approximate manner. In Chapter 10 some of the results of both Chapters 8 and 9 are applied to specific problems.

In the following pages, we first derive the transport equation without the assumption of equilibrium. The equation contains the occupation numbers of the atomic states, which in turn are shown to depend in general on the radiation intensity. The equation derived in this way is based on an incorrect treatment of photon scattering, but is nevertheless useful for obtaining approximate results.

Approximate solutions of the transport equations are found which show that, when the time between quenching collisions is long compared with the lifetime of an excited state, the rate of radiation of a hot gas is small compared with the value deduced under the assumption of equilibrium occupation numbers. This result is true even for radiation from a semi-infinite slab. An expression for the shape of the line radiated from a semi-infinite slab which shows the effects of scattering is also deduced.

## 8.2 The transport equation

The radiative transport equation governs the behavior of the radiation intensity  $I(\nu, \vec{n})$ , which is the energy per unit frequency per steradian crossing unit area normal to  $\vec{n}$  per unit time. The equation is conveniently written in terms of the Einstein coefficients  $B_{12}$ ,  $B_{21}$ , and  $A_{21}$  which describe the processes of absorption, induced emission, and spontaneous emission, respectively.

Let  $N_1$  and  $N_2$  denote the density of  $X$  atoms in the ground state and excited state. The rate of transitions from the ground state to the excited state resulting from photon absorption is

$$\left(\frac{dN_1}{dt}\right)_a = - \frac{B_{12}N_1}{4\pi} \iint I(\nu, \vec{n}) \varphi_\nu d\nu d\Omega = - B_{12}N_1 \int \bar{I}_\nu \varphi_\nu d\nu \quad (9.2-1)$$

where  $\bar{I}_\nu$  is the mean value of  $I(\nu, \vec{n})$  obtained by averaging over angles.

The rate of induced transitions from the excited state to the ground state is

$$\left(\frac{dN_2}{dt}\right)_i = - \frac{B_{21} N_2}{4\pi} \iint I(\nu, \Omega) \varphi_\nu d\nu d\Omega = - B_{21} N_2 \int \bar{I}_\nu \varphi_\nu d\nu \quad (8.2-2)$$

and the rate of spontaneous transitions downward is

$$\left(\frac{dN_2}{dt}\right)_s = - \frac{A_{21} N_2}{4\pi} \iint j_\nu d\nu d\Omega = - A_{21} N_2 \quad (8.2-3)$$

In these equations the integrals are extended over all angles and frequencies.

The quantities  $\varphi_\nu$ ,  $\psi_\nu$ , and  $j_\nu$  are line shape factors for the various processes, all normalized to unity, so that

$$\int \varphi_\nu d\nu = \int \psi_\nu d\nu = \int j_\nu d\nu = 1 \quad (8.2-4)$$

The last relation in Eq. (8.2-4) was used in obtaining the final form of Eq. (8.2-3).

The  $A$  and  $B$  coefficients satisfy the well known relationships

$$\frac{B_{21}}{B_{12}} = \frac{g_1}{g_2} \quad (8.2-5)$$

and

$$\frac{A_{21}}{B_{12}} = \frac{g_1}{g_2} \frac{2h\nu_0^3}{c^2} \quad (8.2-6)$$

where  $g_2$  and  $g_1$  are the statistical weights of the upper and lower states, respectively, and  $\nu_0$  is the frequency at the center of the line.

Now since each interaction has the result of adding or removing a photon of energy  $h\nu$  from the radiation field, the corresponding contributions to  $I_\nu(\nu, \vec{n})$  per unit length  $s$  measured in the direction  $\vec{n}$  are obtained from Eqs. (8.2-1, 8.2-2, and 8.2-3) by dropping the integrations and multiplying by  $h\nu$ . Thus

$$\frac{dI(\nu, \vec{n})}{ds} = - \frac{B_{12} N_1 h\nu \varphi_\nu I(\nu, \vec{n})}{4\pi} + \frac{B_{21} N_2 h\nu \psi_\nu I(\nu, \vec{n})}{4\pi} + \frac{A_{21} N_2 h\nu j_\nu}{4\pi} \quad (8.2-7)$$

In the following we shall ordinarily write  $I_\nu(s)$ , or simply  $I_\nu$  in place of  $I(\nu, \vec{n})$ , with the understanding that  $s$  refers to a definite direction of propagation and that the intensity at a point in general depends on the direction. In this notation, Eq. (8.2-7) becomes

$$\frac{dI_\nu}{ds} = - \frac{B_{12} N_1 h\nu \varphi_\nu I_\nu}{4\pi} + \frac{B_{21} N_2 h\nu \psi_\nu I_\nu}{4\pi} + \frac{A_{21} N_2 h\nu j_\nu}{4\pi} \quad (8.2-7')$$

To solve the transport equation, we require knowledge of  $N_1$  and  $N_2$ . In the special case of thermodynamic equilibrium,

$$\left(\frac{N_2}{N_1}\right)^{eq} = \frac{g_2}{g_1} e^{-h\nu_0/kT} = \frac{g_2}{g_1} e^{-\xi_0} \quad (8.2-8)$$

where we have introduced

$$\xi = h\nu/kT \quad (8.2-9)$$

Making use of Eq. (8.2-8) in Eq. (8.2-7), introducing the equilibrium radiation field

$$B_\nu = \frac{2h\nu^3}{c^2} \frac{1}{e^{h\nu/kT} - 1} \quad (8.2-10)$$

and assuming  $\varphi_\nu = \psi_\nu = I_\nu$ , we find that

$$\frac{dI_\nu}{ds} = - \frac{B_{12} \varphi_\nu N_1^{eq} h\nu (1 - e^{-\xi_0})}{4\pi} I_\nu + \frac{B_{12} \varphi_\nu N_1^{eq} h\nu (1 - e^{-\xi_0})}{4\pi} B_\nu \quad (8.2-11)$$

With the definitions

$$\mu_\nu = \frac{B_{12} \varphi_\nu N_1^{eq} h\nu}{4\pi} = \alpha \varphi_\nu \quad (8.2-12)$$

and

$$\mu'_v = \mu_v (1 - e^{-\xi_0}) = \alpha' \varphi_v \quad (8.2-12')$$

where  $\alpha$  is the line absorption coefficient

$$\alpha = \int \mu_v dv, \quad \alpha' = \alpha (1 - e^{-\xi_0}) \quad (8.2-13)$$

we obtain the well known transport equation for the equilibrium case

$$\frac{dI_v}{ds} = - \mu'_v (I_v - B_v) \quad (8.2-14)$$

### 8.3 Non-equilibrium occupation numbers

When the gas is not in equilibrium, Eq. (8.2-8) no longer holds, and a more general expression for the ratio of occupation numbers must be derived. In a steady state situation, such an expression can be found by setting the time derivatives of  $N_1$  and  $N_2$  equal to zero.

Denoting by  $i$  any one of the processes that produce transitions between the two atomic states, we note that any reaction which depopulates state 1 produces an equal increase in the population of state 2, and vice versa, so that

$$\left(\frac{dN_1}{dt}\right)_i = - \left(\frac{dN_2}{dt}\right)_i$$

The total derivative is obtained by summing over all reactions

$$\frac{dN_1}{dt} = - \frac{dN_2}{dt} = \sum_i \left(\frac{dN_1}{dt}\right)_i \quad (8.3-1)$$

The contributions to Eq. (8.3-1) from radiative processes have already been given in Eqs. (8.2-1, 8.2-2 and 8.2-3). In addition to these we must include the effects of transitions resulting from particle collisions. An atom can be raised from the ground state to the excited state by collision with another particle. If the frequency of such collisions is  $\eta_e$ , the resulting change in  $N_1$  is

$$\left(\frac{dN_1}{dt}\right)_e = - \eta_e N_1 \quad (8.3-2)$$

Similarly, an atom can make a non-radiative transition from the excited state to the ground state by the inverse process, which is called quenching.

Denoting the frequency of quenching collisions by  $\eta_q$ , we have

$$\left(\frac{dN_2}{dt}\right)_q = - \eta_q N_2 \quad (8.3-3)$$

When the gas is in equilibrium, it follows from detailed balance that the quenching and excitation rates are equal, so in that case

$$\frac{\eta_e}{\eta_q} = \left(\frac{N_2}{N_1}\right)^{eq} = \frac{g_2}{g_1} e^{-\epsilon_0} \quad (8.3-4)$$

For collisions with electrons, both  $\eta_e$  and  $\eta_q$  are proportional to the electron density, depend on the electron energy distribution, and are independent of  $N_1$  and  $N_2$ . It follows that Eq. (8.3-4) is valid regardless of whether the electron density and atomic populations have their equilibrium values, provided only that the electrons present are in a Maxwellian distribution, and that only electrons contribute to  $\eta_e$  and  $\eta_q$ . In the following we shall always

make these assumptions, and hence shall assume that Eq. (8.3-4) always holds.

Substituting Eqs. (8.2-1, 8.2-2, 8.2-3, 8.3-2 and 8.3-3) into Eq. (8.3-1), we obtain

$$\frac{dN_1}{dt} = -B_{12} N_1 \int \bar{I}_\nu \varphi_\nu d\nu + B_{21} N_2 \int \bar{I}_\nu \psi_\nu d\nu + A_{21} N_2 - \eta_e N_1 + \eta_q N_2 = 0 \quad (8.3-5)$$

which can be solved for  $N_2/N_1$  to yield

$$\frac{N_2}{N_1} = \frac{\eta_e + B_{12} \int \bar{I}_\nu \varphi_\nu d\nu}{\eta_q + A_{21} + B_{21} \int \bar{I}_\nu \psi_\nu d\nu} \quad (8.3-6)$$

For simplicity, we tentatively assume

$$\varphi_\nu = \psi_\nu \quad (8.3-7)$$

and also define the mean intensity in the neighborhood of  $\nu_0$  obtained by averaging over angle and frequency

$$J = \frac{1}{4\pi} \iint \bar{I}_\nu \varphi_\nu d\Omega d\nu = \int \bar{I}_\nu \varphi_\nu d\nu \quad (8.3-8)$$

Making use of Eqs. (8.3-7) and 8.3-8) in Eq. (8.3-6), we find

$$\frac{N_2}{N_1} = \frac{\eta_e + B_{12} J}{\eta_q + A_{21} + B_{21} J} \quad (8.3-9)$$

From Eq. (8.2-3) the lifetime against spontaneous emission is

$$\tau = A_{21}^{-1} \quad (8.3-10)$$

The rate of induced transitions, according to Eq. (8.2-2), is  $B_{21} J$ , and we are led to define a lifetime against induced emission

$$\tau_i = (B_{21} J)^{-1} \quad (8.3-11)$$

The overall lifetime  $\tau'$  satisfies

$$\frac{1}{\tau'} = \frac{1}{\tau_1} + \frac{1}{\tau} = A_{21} + B_{21} J \quad (8.3-12)$$

Substitution of Eqs. (8.3-12 and 8.3-4) into Eq. (8.3-9) yields, after some algebra

$$\frac{N_2}{N_1} = \frac{y}{1+y} \left[ \left( \frac{N_2}{N_1} \right)^{eq} + \frac{F(J)}{y} \right] \quad (8.3-13)$$

where we have introduced

$$y = \eta_q \tau' \quad (8.3-14)$$

and

$$F(J) = \frac{B_{12} J}{A_{21} + B_{21} J} \quad (8.3-15)$$

From Eq. (8.3-13) it is apparent that

$$\lim_{y \rightarrow \infty} \left( \frac{N_2}{N_1} \right) = \left( \frac{N_2}{N_1} \right)^{eq} \quad (8.3-16)$$

which means that for very large collision frequencies, the equilibrium population is maintained, regardless of the value of  $J$ . If  $y$  is zero or finite, however,  $N_2/N_1$  has its equilibrium value if and only if

$$F(J^{eq}) = \left(\frac{N_2}{N_1}\right)^{eq} = \frac{g_2}{g_1} e^{-\xi_0} \quad (8.3-17)$$

which in turn implies that

$$J^{eq} = \frac{2h\nu_0^3}{c^2} \frac{1}{e^{\xi_0} - 1} = B_{\nu_0} = B_0 \quad (8.3-18)$$

Thus we have shown not only that an average intensity equal to  $B_0$  is sufficient to insure the equilibrium population ratio, but also that in the absence of a high collision frequency, this condition is necessary.

#### 8.4 Non-equilibrium transport equation

Since the radiation intensity appears in Eq. (8.3-13), which determines  $N_2/N_1$ , while  $N_1$  and  $N_2$  also appear in Eq. (8.2-7), which governs  $I_\nu$ , these equations must in general be solved simultaneously. The approach to the problem of non-equilibrium radiation transport by solution of these coupled equations was originally introduced by Milne (1930) and extended by Thomas (see Thomas, 1965, for a bibliography) and his co-workers in the study of stellar line shapes and intensities.

The general transport equation (8.2-7) can be cast in a form similar to the equilibrium case (Eq. (8.2-14)) by writing

$$\frac{dI_v}{ds} = -\kappa_v (I_v - S_v) \quad (8.4-1)$$

which, assuming Eq. (8.3-7), is equivalent to Eq. (8.2-7) if

$$\kappa_v = \frac{(B_{12} N_1 - B_{21} N_2) \varphi_v h\nu}{4\pi} \quad (8.4-2)$$

and

$$S_v = \frac{A_{21} N_2}{B_{12} N_1 - B_{21} N_2} \frac{I_v}{\varphi_v} \quad (8.4-3)$$

Substitution of Eq. (8.3-9) into Eq. (8.4-2), and use of Eqs. (8.2-5, 8.3-4, 8.3-10 and 8.3-14) yields

$$\kappa_v = \frac{B_{12} N_1 h\nu \varphi_v}{4\pi} \frac{y}{1+y} \frac{1+z}{z} (1 - e^{-\xi_0}) \quad (8.4-4)$$

where we have introduced

$$z = \eta_Q \tau (1 - e^{-\xi_0}) \quad (8.4-5)$$

With the help of the same equations, together with Eqs. (8.2-6 and 8.2-10), Eq. (8.4-3) reduces to

$$S_v = \frac{I_v}{\varphi_v} \left( \frac{z}{1+z} B_v + \frac{1}{1+z} \right) \quad (8.4-6)$$

Comparison of Eq. (8.4-4) with Eq. (8.2-12) shows that

$$\kappa_v = \mu_v \frac{N_1}{N_1^{eq}} \frac{y}{1+y} \frac{1+z}{z} \quad (8.4-7)$$

Substituting Eqs. (8.4-6 and 8.4-7) in Eq. (8.4-1), we obtain for the transport equation

$$\frac{dI_v}{ds} = -\mu_v \frac{N_1}{N_1} \frac{y}{1+y} \frac{1+z}{z} \left[ I_v - \frac{j_v}{\varphi_v} \left( \frac{z}{1+z} B_v + \frac{1}{1+z} \right) \right] \quad (8.4-8)$$

In the limit of very large collision frequencies,  $y$  and  $z$  approach infinity,  $N_1$  goes to  $N_1^{eq}$ , and again assuming  $j_v$  goes to  $\varphi_v$ , we find that Eq. (8.4-8) goes to the equilibrium form Eq. (8.2-14).

Eq. (8.4-8) can be inferred in a more straightforward manner which does not involve calculation of  $N_2/N_1$ . In this method, one first recognizes that the right hand side of Eq. (8.2-7) contains contributions from absorption, induced emission, and spontaneous emission, so that

$$\frac{dI_v}{ds} = -a_v + i_v + q_v \quad (8.4-9)$$

Just as before, the absorption term is

$$a_v = \frac{h\nu}{4\pi} B_{12} N_1 \varphi_v I_v \quad (8.4-10)$$

In the steady state, the total rates of excitation and de-excitation are equal to each other and have the value

$$\frac{dN_2}{dt} = (B_{12} I + \eta_e) N_1 \quad (8.4-11)$$

The relative probabilities for de-excitation by quenching and emission into solid angle  $d\Omega$  and frequency interval  $dv$  by induced or spontaneous emission are  $\eta_q$ ,  $\frac{B_{21} I_\nu \nu dv d\Omega}{4\pi}$ , and  $\frac{A_{21}}{4\pi} j_\nu dv d\Omega$ , respectively. The total rate of de-excitation is then  $\eta_q + B_{21} J + A_{21}$ . Dividing the relative probabilities by the total rate gives a normalized probability.

Multiplication of Eq. (8.4-11) by  $h\nu$  and the normalized probabilities gives the corresponding term in Eq. (8.4-9). Thus

$$e'_\nu = \frac{h\nu}{4\pi} (B_{12} J + \eta_e) N_1 \frac{B_{21} I_\nu \nu dv d\Omega}{\eta_q + A_{21} + B_{21} J} \quad (8.4-12)$$

which is reduced by the methods previously employed to

$$e'_\nu = \frac{h\nu}{4\pi} B_{12} N_1 \varphi_\nu I_\nu \left[ 1 - \frac{y}{1+y} \frac{z+1}{z} (1 - e^{-\xi_0}) \right] \quad (8.4-13)$$

Similarly, for spontaneous emission

$$d_\nu = \frac{h\nu}{4\pi} (B_{12} J + \eta_e) N_1 \frac{A_{21} j_\nu}{\eta_q + A_{21} + B_{21} J} \quad (8.4-14)$$

which can be written

$$d_\nu = \frac{h\nu}{4\pi} B_{12} N_1 \varphi_\nu \left( \frac{j_\nu}{\varphi_\nu} \right) \left[ \frac{y}{1+y} (1 - e^{-\xi_0}) B_\nu + \frac{y}{1+y} \frac{(1 - e^{-\xi_0})}{z} J \right] \quad (8.4-15)$$

Substitution of Eqs. (8.4-10, 8.4-13, and 8.4-15) into Eq. (8.4-9) again yields Eq. (8.4-8).

The term proportional to  $J$  in Eq. (8.4-8) arises because of the finite probability that an atom which absorbs a photon reradiates before it has a quenching collision. In other words, this term gives the contribution of

scattering. From the way this term was derived, it is apparent that the preceding treatment is equivalent to assuming isotropic scattering with no correlation between the energy of the incoming and scattered photon. The energy distribution of scattered photons is determined by  $j_\nu$  and  $I_\nu$ , and does not depend on the energy of the absorbed photon.

In a gas where the collision frequency is very low, the assumption that absorption and re-emission are consecutive, independent processes is invalid. The process is actually one of resonant scattering, the scattered light is coherent with the incoming light, and a well-defined correlation exists between the incoming and scattered photon energies. Only when  $z \gg 1$  do these correlations vanish because of the high collision rate. However for  $z \gg 1$ , the scattering term in Eq. (8.4-8) becomes negligible, so that when scattering is important, correlations cannot in general be neglected. However, as shown by Hummer (1962) and others, neglect of correlation effects is often an adequate approximation because of Doppler redistribution of the scattered light.

For the time being we ignore the difficulties in the treatment of scattering, and assume Eq. (8.4-8). Later, in Section 8.9, we shall return to the discussion of this point.

#### 8.5 Collision limited radiation from an optically thin gas

The simplest application of the approximate transport Eq. (8.4-8) is the case of radiation from an optically thin slab of gas. If both the absorption and scattering terms in Eq. (8.4-8) are neglected, as they can be for a sufficiently thin slab of gas, the transport equation reduces to

$$\frac{dI_\nu}{ds} = -\mu_\nu' \frac{N_1}{N_1^{\text{eq}}} \frac{y}{1+y} B_\nu \quad (8.5-1)$$

where we have substituted

$$j_\nu = \varphi_\nu \quad (8.5-2)$$

in Eq. (8.4-8). . . In this case, use of Eq. (8.5-2) constitutes no approximation, however, since the radiation all results from spontaneous emission following excitation by collision with a continuous distribution of electron energies, in which case Eq. (8.5-2) can be shown to hold (Heitler, 1933).

In the absence of significant scattering or absorption, the coefficient of  $B_\nu$  in Eq. (8.5-1) is independent of position, and hence the equation can be integrated immediately. If no radiation is incident from outside on a slab of thickness  $L$ , the intensity leaving a face of the slab in the direction at angle  $\theta$  to the normal is

$$I_\nu = \frac{\mu'_\nu L}{\cos \theta} \frac{N_1}{N_1^{\text{eq}}} \frac{\gamma}{1 + \gamma} B_\nu \quad (8.5-3)$$

In the limit  $\gamma \gg 1$ ,  $N_1 \rightarrow N_1^{\text{eq}}$  and we have

$$I_\nu^{\text{eq}} = \frac{\mu'_\nu L B_\nu}{\cos \theta} \quad (8.5-4)$$

The total intensity obtained by integrating over the line is

$$I_L^{\text{eq}} = \int I_\nu^{\text{eq}} d\nu = \frac{\alpha' L B_0}{\cos \theta} \quad (8.5-5)$$

with  $\alpha'$  and  $B_0$  as defined in Eqs. (8.2-13 and 8.3-18).  $I_\nu$  can be written in

terms of  $I_V^{eq}$

$$I_V = \frac{y}{1+y} \frac{N_1}{N_1^{eq}} I_V^{eq} \quad (8.5-6)$$

and integrating over the line we obtain

$$I_L = \frac{y}{1+y} \frac{N_1}{N_1^{eq}} I_L^{eq} \quad (8.5-7)$$

In the limit  $y \rightarrow 0$ , virtually every excitation by collision results in emission of a photon. For an optically thin slab, the probability a photon escapes without being absorbed or scattered is nearly unity. Therefore, the power radiated per unit volume is just the rate of exciting collisions multiplied by the mean energy of a photon, or

$$\frac{dW_L}{dv} = \eta_e N_1 h\nu_0 \quad (8.5-8)$$

To show that this result is consistent with Eq. (8.5-7), we first calculate the power per unit area leaving one face of the slab

$$F_+ = 2\pi \int_0^\pi I_L \cos \theta \sin \theta d\theta = 2\pi \alpha' L B_0 \frac{y}{1+y} \frac{N_1}{N_1^{eq}} \quad (8.5-9)$$

The power per unit volume is obtained by adding the contribution of both faces and dividing by the thickness

$$\frac{dW_L}{dv} = 4\pi \alpha' \frac{y}{1+y} \frac{N_1}{N_1^{eq}} B_0 \quad (8.5-10)$$

With the help of Eqs. (8.2-6, 8.2-10, 8.2-12, 8.2-13, 8.3-4, 8.3-10 and 8.3-14) and the fact that induced emission is negligible and hence  $\tau' \simeq \tau$ , Eq. (8.5-10) is easily shown to be identical with the intuitive result Eq. (8.5-8).

Since the radiation rate in this case is determined by the collision frequency  $\eta_e$ , the radiation is said to be collision limited. Increasing  $\eta_e$  increases the radiation rate until  $y \gg 1$ , after which the volume radiation rate no longer increases, since the equilibrium concentration ratio has been attained. Further insight may be gained from Eq. (8.3-13), according to which

$$N_2 \simeq \frac{y}{1+y} \frac{N_1}{N_1^{\text{eq}}} N_2^{\text{eq}} \quad (8.5-11)$$

The reduction in radiation rate below the equilibrium value as given by Eq. (8.5-6) is seen to correspond to the reduction in population of the excited state in Eq. (8.5-11) by the same factor. The upper state is underpopulated because the low collision frequency cannot keep up with the rate of radiation.

The term "optically thin", upon which the assumption of Eq. (8.5-1) was based, has not yet been defined. The question naturally arises as to whether only absorption, or both absorption and scattering need be negligible. From Eq. (8.4-8), the condition for Eq. (8.5-1) to hold at all angles is

$$I_\nu \ll \frac{z}{1+z} B_\nu \simeq y \left(1 - e^{-\xi_0}\right) B_\nu \quad (8.5-12)$$

According to Eq. (8.5-3) this implies

$$\mu_v L \ll 1 \quad (8.5-13)$$

Since  $\mu_v$  contains contributions from both scattering and absorption, it follows that both must be negligible in the slab for the optically thin solution to hold. However in Sections 8.6 and 8.7 we shall show that the result Eq. (8.5-9) for the total flux remains valid for greater thicknesses, viz., for  $z^{1/2} \mu_v L \ll 1$ , but that the angular distribution is changed by scattering.

To obtain some idea of the conditions under which collision limiting is apt to occur, assume a quenching cross section

$$\sigma_q = 2.5 \times 10^{-16} \text{ cm}^2 \quad (8.5-14)$$

and electron velocity

$$v_e = 4 \times 10^7 \text{ cm/sec} \quad (8.5-15)$$

Then

$$\eta_q \simeq N_e \sigma v = 10^{-8} N_e \quad (8.5-16)$$

where  $N_e$  is the electron density. For an allowed transition,

$$\tau \simeq 10^{-8} \text{ sec} \quad (8.5-17)$$

hence

$$y \simeq \eta_q \tau \sim 10^{-16} N_e \quad (8.5-18)$$

so that  $y \ll 1$  implies that  $N_e \ll 10^{16} \text{ cm}^{-3}$ . A more detailed discussion of specific cases of collision limiting will be found in Chapter 10.

## 8.6 Radiation from a semi-infinite slab

As a second example of the application of Eq. (8.4-8) , we consider the radiation from a semi-infinite slab in which the electron temperature is assumed to be constant. For simplicity, we shall assume that all line shape factors are rectangular with width  $\delta$  , so that

$$I_\nu = \varphi_\nu = \psi_\nu = \begin{cases} \delta^{-1} & \text{if } \nu_0 - \frac{\delta}{2} < \nu < \nu_0 + \frac{\delta}{2} \\ 0 & \text{otherwise} \end{cases} \quad (8.6-1)$$

As a result of this assumption we lose all information as to the true shape of the radiated line, of course, but can still obtain useful estimates of the total intensity radiated in the line.

With Eq. (8.6-1), the transport equation becomes

$$\frac{dI_\nu}{ds} = -\kappa_\nu \left[ I_\nu - \frac{z}{1+z} B_\nu + \frac{I}{1+z} \right] \quad (8.6-2)$$

Since  $\kappa_\nu$  is proportional to  $\varphi_\nu$  , and otherwise independent of  $\nu$  , from Eqs. (8.6-1 and 8.6-2) it follows that the intensity is zero outside of the range  $\nu_0 \pm \delta/2$  , and constant within this range. Neglecting the variation of  $B_\nu$  across the line, we can drop the subscript  $\nu$  and write

$$\frac{dI}{ds} = -\kappa \left[ I - \frac{z}{1+z} B_0 - \frac{I}{1+z} \right] \quad (8.6-3)$$

In terms of a coordinate  $x$  perpendicular to the face of the slab and the angle  $\theta$  between  $s$  and the positive  $x$  direction, Eq. (8.6-3) can be rewritten

$$\cos \theta \frac{\partial I}{\partial x} = - \kappa \left[ I - \frac{2}{1+z} B_0 - \frac{I}{1+z} \right] \quad (8.6-4)$$

In spite of its apparent linearity, Eq. (8.6-4) is actually nonlinear because of the dependence of  $\kappa$  on  $y$ , which depends on  $\tau'$  and hence on  $I$  through  $J$ . The equation can be put in linear form by introducing the optical depth  $t$

$$t = \int_0^x \kappa \, dx \quad (8.6-5)$$

where the slab is assumed to extend to infinity in the negative  $x$  direction and to be bounded by a face at  $x = 0$ . The transport equation with  $t$  as one independent variable becomes

$$\cos \theta \frac{\partial I}{\partial t} = - \left[ I - \frac{2}{1+z} B_0 - \frac{I}{1+z} \right] \quad (8.6-6)$$

We now seek a solution of Eq. (8.6-6), in terms of an expansion in Legendre polynomials. Denoting  $\cos \theta$  by  $\zeta$ , we write

$$I = \sum_n f_n(t) P_n(\zeta) \quad (8.6-7)$$

Making use of the recursion relation

$$\zeta P_n(\zeta) = \frac{1}{2n+1} \left[ (n+1) P_{n+1}(\zeta) + n P_{n-1}(\zeta) \right] \quad (8.6-8)$$

and denoting differentiation with respect to  $t$  by a prime, we obtain

$$\sum_n \frac{1}{2n+1} \left[ (n+1) P_{n+1} + n P_{n-1} \right] f'_n = \frac{z}{1+z} B_0 + \frac{I}{1+z} - \sum_n f_n P_n \quad (8.6-9)$$

Multiplying Eq. (8.6-9) through by  $P_m(\zeta)$ , and integrating over  $\zeta$ , we obtain

$$\frac{m}{2m-1} f'_{m-1} + \frac{m+1}{2m+3} f'_{m+1} = \delta_{m0} \left( \frac{z}{1+z} B_0 + \frac{I}{1+z} \right) - f_m \quad (8.6-10)$$

The first three equations, obtained by setting  $m = 0, 1, 2$  in Eq. (8.6-10) are

$$f'_1 = -3 \left( f_0 - \frac{z}{1+z} B_0 - \frac{I}{1+z} \right) \quad (8.6-11)$$

$$f'_0 + \frac{2}{5} f'_2 = -f_1 \quad (8.6-12)$$

$$\frac{2}{3} f'_1 + \frac{3}{7} f'_3 = -f_2 \quad (8.6-13)$$

From Eqs. (8.3-8, 8.6-1 and 8.6-7) we also have

$$J = \frac{1}{2} \iint L_\nu \varphi_\nu d\zeta d\nu = \frac{1}{2\delta} \int_{\nu_0 - \frac{\delta}{2}}^{\nu_0 + \frac{\delta}{2}} \int_{-1}^1 \sum_n f_n(t) P_n(\zeta) d\zeta d\nu = f_0(t) \quad (8.6-14)$$

so that Eq. (8.6-11) becomes

$$f'_1 = -\frac{3z}{1+z} (f_0 - B_0) \quad (8.6-15)$$

One obvious solution to the system of equations is  $f_0 = B_0$ , with all other  $f_n = 0$ . Since this solution implies an isotropic radiation field, it

is not valid when boundaries are present. It is the correct solution in the case of an unbounded medium, however, and as shown below, is the asymptotic value approached in the deep interior of a bounded medium. It is also the correct solution for an isothermal optically thick medium in thermodynamic equilibrium.

To study the more general case where  $f_0 \neq B_0$ , we wish to truncate the series Eq. (8.6-7). If  $f_3'$  is neglected in Eq. (8.6-13), then  $f_2 = -2/3 f_1'$ , or from Eq. (8.6-15),  $f_2' = \frac{2z}{1+z} f_0'$ . For  $z \ll 1$ , the  $f_2'$  term in Eq. (8.6-12) can be neglected as higher order in  $z$  than the leading term. For  $z \gg 1$ , Eq. (8.3-13) shows that the atomic states have their equilibrium value, and hence we expect the intensity to be isotropic. Neglect of all except the first two terms in the expansion is therefore justified for both limiting cases of large and small  $z$ . We assume it is a good approximation for intermediate values as well, and keep only the first two terms in the series, i.e., we take

$$I = f_0(t) + f_1(t) \cos \theta \quad (8.6-16)$$

an assumption known to astrophysicists as the Eddington approximation.

The coupled equations to be solved are now

$$f_1' = -\frac{3z}{1+z} (f_0 - B_0) \quad (8.6-17)$$

$$f_0' = -f_1 \quad (8.6-18)$$

Differentiating Eq. (8.6-18) and substituting Eq. (8.6-17), we eliminate  $f_1$  to obtain

$$f_0'' = \frac{3z}{1+z} (f_0 - B_0) \quad (8.6-19)$$

The most general solution of Eq. (8.6-19) is

$$f_0 = C_1 e^w + C_2 e^{-w} + B_0 \quad (8.6-20)$$

where we have introduced the variable  $w$

$$w = \left( \frac{3x}{1+x} \right)^{1/2} t \quad (8.6-21)$$

Since  $f_0$  must remain finite as  $w \rightarrow -\infty$ ,  $C_2 = 0$  and

$$f_0 = C_1 e^w + B_0 \quad (8.6-22)$$

From Eq. (8.6-18) we find

$$f_1 = - \left( \frac{3x}{1+x} \right)^{1/2} C_1 e^w \quad (8.6-23)$$

Since  $w$  depends on  $f_0$  through  $x$ , Eq. (8.6-22) is actually a transcendental equation determining  $f_0$ . As shown below, however, a great deal of information can be extracted from the formal solution without actually solving the transcendental equation.

From Eqs. (8.6-22 and 8.6-23) it is apparent that as  $t \rightarrow -\infty$ ,  $f_0 \rightarrow B_0$ ,  $f_1 \rightarrow 0$ , and  $I \rightarrow B_0$ . Thus in the deep interior of the gas for any finite value of  $x$ , the intensity is isotropic and has its equilibrium value, regardless of the values of  $x$  and  $z$ . From the discussion following Eq. (8.3-18) we can infer that in this region the atomic states also have their equilibrium populations.

To evaluate  $C_1$ , we require that the flux entering the surface at  $x = 0$  be zero, and hence that

$$F_- = 2\pi \int_{-1}^0 I \zeta d\zeta = 2\pi \left[ -\frac{f_0(0)}{2} + \frac{f_1(0)}{3} \right] = 0 \quad (8.6-24)$$

from which it follows that

$$C_1 = - \frac{B_0}{1 + \frac{2}{3} \left( \frac{3x}{1+x} \right)^{1/2}} \quad (8.6-25)$$

The total intensity leaving the surface is

$$F_+ = 2\pi \int_0^1 I \zeta d\zeta = 2\pi \left[ \frac{f_0(0)}{2} + \frac{f_1(0)}{3} \right]$$

or

$$F_+ = 2\pi B_0 \frac{\frac{2}{3} \left( \frac{3x}{1+x} \right)^{1/2}}{1 + \frac{2}{3} \left( \frac{3x}{1+x} \right)^{1/2}} \quad (8.6-26)$$

In the special case  $x \rightarrow \infty$

$$\lim_{x \rightarrow \infty} F_+ = 1.07 \pi B_0 \quad (8.6-27)$$

For radiation from a blackbody

$$F_+ = 2\pi B_0 \int_0^1 \zeta d\zeta = \pi B_0 \quad (8.6-28)$$

According to Eq. (8.3-13), in the limit  $z \rightarrow \infty$  (which implies  $y \rightarrow \infty$ ) the atomic states have their equilibrium populations. Therefore the slab should radiate as a blackbody in the line. The result of our many approximations is thus an error of only seven per cent in this case.

For the case  $z \ll 1$ , Eq. (8.6-26)

$$F_+ \simeq 4\pi \left(\frac{z}{3}\right)^{1/2} B_0 \quad (8.6-29)$$

so that even for an infinitely thick medium, the radiated flux can be arbitrarily small compared with the blackbody value, in spite of the previously mentioned result that in the deep interior  $I \sim B_0$ .

A numerical solution to the problem treated above has been given by Chandrasekhar (1960) in discussing the Milne-Eddington problem. His result in our notation is

$$I(0, \zeta) = \left(\frac{z}{1+z}\right)^{1/2} H(\zeta) B_0 \quad (8.6-30)$$

where  $H(\zeta)$  is a function calculated numerically. The corresponding flux is

$$F_+ = 2\pi \left(\frac{z}{1+z}\right)^{1/2} B_0 \int_0^1 H(\zeta) \zeta d\zeta \quad (8.6-31)$$

The ratio of this to the result in Eq. (8.6-26) is

$$R = \left[ \frac{\sqrt{3}}{2} + \left(\frac{z}{1+z}\right)^{1/2} \right] \int_0^1 H(\zeta) \zeta d\zeta \quad (8.6-32)$$

From the values of  $\int_0^1 H(\zeta) \zeta d\zeta$  tabulated by Chandrasekhar in his Table XXXIII the value of  $R$  for various  $z$  can be calculated

Table 8-1 Ratio of Calculated Fluxes

$\frac{z}{1+z}$	$\int_0^1 H(\zeta) \zeta d\zeta$	$\left(\frac{z}{1+z}\right)^{1/2}$	$R$
0	1.155	0	1.000
0.025	0.964	0.158	0.987
0.05	0.902	0.223	0.983
0.10	0.825	0.316	0.975
0.30	0.679	0.548	0.960
0.50	0.603	0.707	0.949
0.80	0.533	0.895	0.944
1.00	0.500	1.000	0.933

The two calculations are thus seen to agree to within seven per cent over the entire range of  $z$  from zero to infinity. The neglect of all but the first two terms in Eq. (8.6-7) therefore appears to be justified for all  $z$ .

A simple physical interpretation of the result Eq. (8.6-29) for small  $z$  can be made as follows. From Eq. (8.6-3), the effective volume emission rate for  $z \ll 1$  is  $\kappa z B_0$ . The photons escaping from the surface of the slab tend to be emitted near the surface, since those emitted too far within are absorbed before they escape. If we assume that one half of all photons radiated in a slab of thickness  $L$  adjacent to the surface escape, and none from greater distances within, the radiated flux is

$$F_{\pm} = 2\pi \kappa z B_0 L \quad (8.6-33)$$

To estimate  $L$ , we observe that for small  $z$ , propagation of a photon is a random walk, since many scatterings occur before an absorption. The mean free path between collisions is  $\kappa^{-1}$ , and the probabilities of absorption and scattering are approximately  $z$  and  $1$ , respectively. Therefore a photon must make  $z^{-1}$  collisions on the average before being absorbed. The net distance travelled in a random walk after  $z^{-1}$  collisions with mean free path  $\kappa^{-1}$  is  $\kappa^{-1} \left(\frac{2}{z}\right)^{1/2}$ . Taking  $L$  to be the net distance travelled between absorbing collisions, we have

$$L = \kappa^{-1} \left(\frac{2}{z}\right)^{1/2} \quad (8.6-34)$$

With this value for  $L$ , Eq. (8.6-33) becomes

$$F_+ = 2\pi (2z)^{1/2} B_0 \quad (8.6-35)$$

which agrees with Eq. (8.6-29) except for a numerical factor of order unity. From this simple model, we can conclude that the decrease in the radiated flux results directly from scattering, which "traps" the radiation from deep inside and prevents its escape. In the absence of scattering, the blackbody result is obtained regardless of how small the absorption coefficient is, provided the gas is sufficiently thick.

## 8.7 Radiation from a finite slab

From the arguments in the preceding section we are led to expect that for a finite slab of thickness much greater than  $L$  the emergent flux approaches the value for a semi-infinite slab. This supposition is further

strengthened by Eqs. (8.6-22 and 8.6-23), according to which the intensity approaches its asymptotic value at points deeper within the slab than  $\kappa^{-1} \left( \frac{1+z}{3z} \right)^{1/2}$ .

In fact Eq. (8.6-20) is also the solution of Eqs. (8.6-17 and 8.6-18) for a finite slab, but now  $C_1$  and  $C_2$  are determined by the conditions that the inward flux vanish at both faces of the slab.

For a finite slab of thickness  $2\ell$  with faces at  $x = \pm \ell$ , it is easily shown that

$$f_0 = B_0 \left[ 1 - \frac{e^{w_0} + e^{-w_0}}{e^{w_0} + e^{-w_0} + \frac{2}{3} \left( \frac{3z}{1+z} \right)^{1/2} (e^{w_0} - e^{-w_0})} \right] \quad (8.7-1)$$

$$f_1 = B_0 \left( \frac{3z}{1+z} \right)^{1/2} \left[ \frac{e^{w_0} - e^{-w_0}}{e^{w_0} + e^{-w_0} + \frac{2}{3} \left( \frac{3z}{1+z} \right)^{1/2} (e^{w_0} - e^{-w_0})} \right] \quad (8.7-2)$$

where we have introduced

$$w_0 = \left( \frac{3z}{1+z} \right)^{1/2} t_0 = \left( \frac{3z}{1+z} \right)^{1/2} \int_0^\ell \kappa \, dx \quad (8.7-3)$$

For very large slab thicknesses, Eqs. (8.7-1 and 8.7-2) go over into the solutions for the semi-infinite slab. Furthermore, calculation of  $F_+$  yields

$$F_+ = 2\pi B_0 \frac{\frac{2}{3} \left( \frac{3z}{1+z} \right)^{1/2} \tanh w_0}{1 + \frac{2}{3} \left( \frac{3z}{1+z} \right)^{1/2} \tanh w_0} \quad (8.7-4)$$

which goes over into the forms Eqs. (8.5-9 and 8.6-26) for thin and thick slabs, respectively.

From Eq. (8.7-4) it is clear that the upper limit to the flux which can be radiated depends only on  $z$ . The thickness for which a particular value less than the upper limit is realized, however, depends not only on  $z$ , but on the magnitude of  $\kappa$  as well.

### 8.8 Spectrum of emitted radiation

A thorough discussion of line shapes is beyond the scope of this discussion. We shall, however, give a brief outline of a method of generalizing the procedure of Section 8.6 to obtain an approximate solution for  $I_\nu$ . The method consists of using the previously determined value of  $J$  as an approximation in Eq. (8.6-2). In place of  $t$ , a new independent variable  $t_\nu$  is introduced for each frequency

$$t_\nu = \int_0^x \kappa_\nu dx = (\varphi_\nu \delta) t \quad (8.8-1)$$

$I_\nu$  is again approximated by the first two terms in the expansion Eq. (8.6-7)

$$I_\nu = f_{0\nu} + f_{1\nu} \cos \theta \quad (8.8-2)$$

Using the same methods as before, a second order differential equation for  $f_{0\nu}$  is derived. Its solution for the semi-infinite slab is

$$f_{0\nu} = B_0 + C_\nu e^{\sqrt{3} t_\nu} + \frac{B_0 (\varphi \delta)^2}{z - (1+z) (\varphi \delta)^2} \frac{e^w}{1 + \frac{2}{3} \left( \frac{3z}{1+z} \right)^{1/2}} \quad (8.8-3)$$

$C_\nu$  is determined from the flux condition to be

$$C_\nu = - \frac{\sqrt{3} B_0}{2 + \sqrt{3}} \left\{ 1 + \frac{\frac{2}{3} (\varphi_\nu \delta) \left( \frac{3z}{1+z} \right)^{1/2} + (\varphi_\nu \delta)^2}{\left[ z - (1+z) (\varphi_\nu \delta)^2 \right] \left[ 1 + \frac{2}{3} \left( \frac{3z}{1+z} \right)^{1/2} \right]} \right\} \quad (8.8-4)$$

The emergent flux at frequency  $\nu$  is then

$$F_{+\nu} = \frac{4\pi B_0}{2\sqrt{3}} \left\{ 1 - \frac{1}{(1+z) \left[ 1 + \left( \frac{z}{1+z} \right)^{1/2} \frac{1}{\varphi_\nu \delta} \right] \left[ 1 + \frac{2}{3} \left( \frac{3z}{1+z} \right)^{1/2} \right]} \right\} \quad (8.8-5)$$

In the special case  $\varphi_\nu \delta = 1$ , Eq. (8.8-5) reduces to the previous result Eq. (8.5-26)

Furthermore, in the limit  $z \rightarrow \infty$ , we again obtain Eq. (8.6-27) for all  $\nu$  regardless of the value of  $\varphi_\nu$ , provided  $\varphi_\nu \neq 0$ .

For the special case  $z \ll 1$  and  $z^{1/2} \ll \varphi_\nu \delta$ ,

$$F_{+\nu} \simeq \frac{4\pi B_0 z^{1/2}}{2 + \sqrt{3}} \left( \frac{1}{\varphi_\nu \delta} + \frac{2}{\sqrt{3}} \right) \quad (8.8-6)$$

The flux is therefore a minimum at the center of the line, and increases monotonically on either side. At great distances from  $\nu_0$ , the flux asymptotically approaches its approximate blackbody value

$$\lim_{\varphi_\nu \rightarrow 0} F_{+\nu} = 1.07 \pi B_\nu \quad (8.8-7)$$

For a finite slab, Eq. (8.8-7) will hold only if the thickness of the slab at frequency  $\nu$  is great, i.e., if  $t_\nu \gg 1$ . The radiation from a thick but finite slab will be similar to that from the semi-infinite slab in the neighborhood of  $\nu_0$ , approaching (111) for large  $|\nu - \nu_0|$ , then decreasing again for  $|\nu - \nu_0|$  so large that  $t_\nu < 1$ . For still thinner slabs Eq. (8.8-7) will never be attained, and the spectrum will be a smoothly varying double-humped curve, with a minimum at  $\nu_0$  and maxima at frequencies such that  $t_\nu \sim 1$ . Finally for a very thin slab, optically thin even at  $\nu_0$ , the result of Section 8.5 will hold. The spectral distribution will just be  $\phi_\nu$ , and darkening of the center will be absent.

#### 8.9 Resonant scattering

The development in the preceding sections is based on the assumption that the excitation of an atom and the emission of a photon are consecutive, independent processes. According to this picture, an atom is always in either the ground state or the excited state. Atoms in the excited state may radiate and make a transition to the ground state. If they do, the character of the radiation is independent of the means by which the atom was excited. Thus, for example, we have assumed that the spectrum of radiated photons is  $j_\nu$ , regardless of whether the radiating atom was excited by collision with an electron or absorption of a photon.

In a very tenuous gas, the model which treats absorption and emission of energy as independent processes is not necessarily valid. For example, the process of absorption of a photon followed by emission of a second photon is actually one of resonant scattering, as previously noted. The physical distinction between the two processes lies in the fact that (in the system where the total momentum of photon plus atom is zero) the energy of the scattered

photon is precisely the same as that of the incoming photon, and the scattered beam is coherent with the incoming beam (Weisskopf, 1931; Heitler, 1944). If the process were one of absorption and independent emission, light scattered from a perfectly monochromatic beam would show a frequency spread in the zero-momentum frame, and the scattered light would be incoherent with the incoming beam. Similarly, as Heitler (1933, 1944) has shown, excitation of a collection of atoms by a beam of monoenergetic electrons gives rise to radiation with a frequency distribution which in general is different from the natural line profile.

Questions involving coherence and strict energy conservation pose no real problem in gases where the collision frequency is very high, i.e., in the limit  $y \rightarrow \infty$ ,  $z \rightarrow \infty$ . In this limit an atom undergoes many collisions during the time it is interacting with a photon. The result is that the photon is almost certainly absorbed rather than scattered, and even if scattering occurs, the coherence is destroyed by the collisions. According to Eqs. (8.4-12 and 8.4-14), in this limit the contribution of excitation by absorption to the emission terms becomes negligible, almost all of the emission resulting from collisional excitation. This is equivalent to saying that photon scattering is negligible. Thus the only radiation loss mechanism is true absorption, whereby energy is transferred from the radiation field to the electrons. The effects of collisions can then be taken into account in the (collision broadened) line profile  $\phi_\nu$ .

Similarly, the high collision frequency destroys strict energy conservation between incoming electrons and radiated photons in radiation resulting from collisional excitation. The collision broadened line will be radiated in both induced and spontaneous transitions, and hence  $j_\nu$  and  $\epsilon_\nu$  are

equal and equal to  $\phi_\nu$ . Since the limit  $\gamma \rightarrow \infty$  has already been shown to imply equilibrium concentrations, however, the foregoing considerations only serve to demonstrate that the assumption of independent emission and absorption processes is self-consistent in the equilibrium case, but sheds no light on the non-equilibrium problem.

When the collision frequency is very low, the total rate at which energy is being removed from that part of the radiation field at frequency  $\nu$  travelling in direction  $\Omega$  is still given by Eq. (8.4-10), but  $\phi_\nu$  is now the Doppler-broadened natural profile. Following the arguments of Heitler, we also conclude that for excitation by electrons with a continuous energy distribution extending well above  $h\nu_0$ , both spontaneous and induced emission from electron impact will have the same profile  $\phi_\nu$ . The correct contribution of collisions to the transport equation, therefore, is

$$\left(\frac{dI_\nu}{ds}\right)_{\text{coll}} = \frac{h\nu}{4\pi} \eta_e N_1 \frac{(A_{21} + B_{21} I_\nu)}{\eta_q + A_{21} + B_{21} J} \phi_\nu \quad (8.9-1)$$

which differs from the corresponding terms in Eqs. (8.4-12 and 8.4-14) only in that both  $\psi_\nu$  and  $j_\nu$  have been replaced by  $\phi_\nu$ .

The real difficulty in deriving the transport equation when collision frequencies are low arises from the terms previously treated as radiation resulting from excitation by photon absorption, since these terms actually describe resonant scattering. An accurate description cannot be made in terms of a line profile which is independent of the frequency of the "absorbed" radiation. In fact, the frequency of the "emitted" radiation is precisely equal to that of the "absorbed" in the zero-momentum frame of photon and atom.

The correct procedure consists of transforming an incident photon of frequency  $\nu'$  to a particular zero momentum frame in which its frequency is  $\nu''$ . If the number of ground state atoms with velocity corresponding to this frame is  $\delta N_1$ , the rate of scattering is  $B_{12} \delta N_1 \phi_{\nu''}^0$ , where  $\phi_{\nu}^0$  is the natural line profile. For a given differential cross section for resonant scattering, the angular distribution of scattered photons, all of frequency  $\nu''$  in this frame, is determined. By transforming back to the laboratory system, the angular distribution and frequency in that frame are found. Upon integration over all zero-momentum frames, i.e., over  $\delta N_1$ , the contribution to the intensity from light scattered from  $\nu', \Omega'$  is obtained. The total contribution of scattering to  $I(\nu, \Omega)$  is finally found by integrating over  $\nu'$  and  $\Omega'$ .

The result of these calculations is a scattering term in the transport equation of the form

$$\left( \frac{dI_{\nu}}{ds} \right)_{\text{scatt}} = \frac{h\nu}{4\pi} B_{12} N_1 \iint K(\nu\Omega, \nu'\Omega') I(\nu', \Omega') d\nu' d\Omega' \quad (8.9-2)$$

where the kernel  $K$  is also a functional of  $I_{\nu}$  and the atomic velocity distribution. The corresponding terms assumed in Eqs. (8.4-12 and 8.4-14) are equivalent to assuming that

$$K(\nu\Omega, \nu'\Omega') = \left( \frac{B_{21} I_{\nu} + A_{21} J_{\nu}}{\eta_q + A_{21} + B_{21} J} \right) \left( \frac{\phi_{\nu'}}{4\pi} \right) \quad (8.9-3)$$

which neglects correlation between initial and final frequencies and assumes isotropic scattering. These terms are also based on Eq. (8.3-7), which is not

strictly true when scattering is important.

The correct transport equation is

$$\frac{dI_\nu}{ds} = -a_\nu + \left(\frac{dI_\nu}{ds}\right)_{\text{coll}} + \left(\frac{dI_\nu}{ds}\right)_{\text{scatt}} \quad (8.9-4)$$

with the various terms given by Eqs. (8.4-10, 8.9-1 and 8.9-2). While no difficulty in principle exists in deriving the correct form for  $K(\nu\Omega, \nu'\Omega')$  we shall not attempt to do so here. Solutions of the correctly formulated transport equation would undoubtedly differ from the approximate solutions in detail, particularly with regard to spectral distributions, but are unlikely to differ qualitatively in gross characteristics.

#### 8.10 Summary and conclusions

On the basis of an approximate transport equation, we have shown that under conditions where the rate of radiation of a hot gas is limited by the frequency of exciting collisions, the rate of radiation from a collection of two level atoms is greatly reduced. For a thin sample of gas, the radiation is reduced by a factor of  $\sim \eta_q \tau$ , for  $\eta_q \tau \ll 1$ , where  $\eta_q$  is the frequency of quenching collisions and  $\tau$  is the lifetime of the excited state. The reduction factor given is relative to the radiation which would be emitted if the radiating atoms had their equilibrium occupation numbers.

For radiation from a semi-infinite slab the reduction is smaller, being of order  $z^{1/2}$ , where  $z \sim \eta_q \tau (1 - e^{-\frac{h\nu}{kT}})$ . This reduction is also relative to the flux to be expected if the atoms were in equilibrium, which for a semi-infinite medium is the corresponding blackbody value.

In both cases the decrease in intensity is associated with a decrease in the population of the excited state. In the case of the thick slab, the existence of scattering of light by the atoms plays an important role in determining the flux which escapes. The equations used in deducing these conclusions were shown to be based on an incorrect treatment of scattering. Nevertheless, the results are believed to be at least qualitatively correct, since the same equations appear to be capable of correctly predicting the qualitative characteristics of the radiated spectral distribution.

### References

- Chandrasekhar, S., p. 321 et seq., Radiative Transfer, Dover, 1960.
- Cuperman, S., F. Engelmann, and J. Oxenius, Phys. Fluids 6, 108, 1963;  
7, 428, 1964.
- Heitler, W., The Quantum Theory of Radiation, Oxford, 1944.
- Heitler, W., Z. Physik 82, 146, 1933.
- Hummer, D.G., Monthly Notice Roy. Astron. Soc. 125, 21, 1962.
- Smithsonian Astrophysical Observatory Special Report Number 174, Proceedings of the Second Harvard-Smithsonian Conference on Stellar Atmospheres, 1965.
- Milne, E.A., Handbuch der Astrophysik Vol. 3, Ch. 2, Springer, Berlin, 1930.
- Thomas, R.N., Non-Equilibrium Thermodynamics in the Presence of a Radiation Field, University of Colorado Press, 1965.
- Thomas, R.N. and R.G. Athay, Physics of the Solar Chromosphere, Interscience, 1961.
- Weisskopf, V., Ann. d. Phys. 9, 23, 1931.

## Chapter 9. RADIATION IN TENUOUS AIR AT HIGH TEMPERATURES

### 9.1 Introduction

For very hot and tenuous air the most rapid relaxation mechanism is radiative energy loss to the surroundings. Of course, the air densities and energy contents for which this is true depend somewhat on the size of the hot region. There is a strong tendency in such a gas cooling radiatively for the internal energy distribution to be shifted significantly from thermodynamic equilibrium. We are interested in this shifted energy distribution as well as the cooling rate and power radiated.

In this chapter we study the behavior of a sphere of hot gas cooling radiatively under non-LTE conditions. The treatment here differs essentially from the discussion of Chapter 8 in that the emphasis is placed on determining occupation numbers for the states of a realistic multi-level atom and its associated ions. The calculations make use of detailed atomic structure parameters and the best available cross sections, while treating radiative transport by crude approximations. In the preceding chapter the emphasis was reversed, an attempt being made there to treat the transport in some detail while using the highly unrealistic model of a two level atom with no ionization or recombination.

For definiteness we consider the behavior of a sphere of air about  $10^{-6}$  normal density with a radius of 5 km and a temperature of about  $24,000^{\circ}\text{K}$ . Hot air contains such a large number of different atomic and ionic species that

it is not yet feasible to carry out detailed calculations on air; however, to gain some insight into the problem we shall consider:

(1) The properties of a large sphere of hot hydrogen which contains only hydrogen atoms, protons and electrons.

(2) The properties of a large sphere of hot gas which initially contains only electrons and doubly-charged hydrogenic ions.

The former can be treated very easily; Bates et al. (1962) have considered recombination of such a system for both optically thin and optically thick conditions. A comparison of these calculations with available experimental data suggests that the accuracy of the calculations is quite good (Bates and Kingston, 1964).

The doubly-charged ion case, which is a better model for hot air than hydrogen is, cannot be treated so easily because recombination has only been calculated for optically thin conditions (Bates et al., 1962). We can, however, use the available calculations to estimate what happens under optically thick conditions.

When cross-section data become available for oxygen and nitrogen atoms and ions, these calculations can be extended to air, but of course, they will become more complicated because many more types of atoms and ions have to be considered.

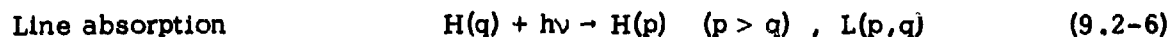
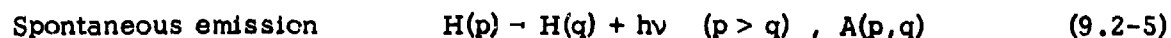
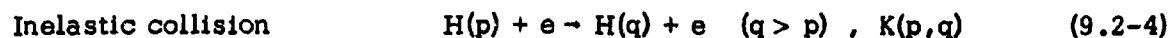
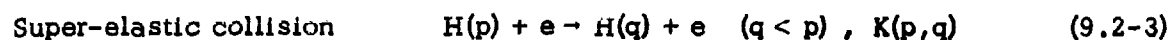
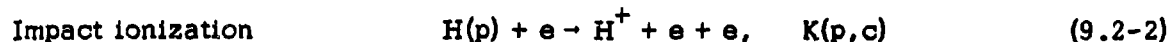
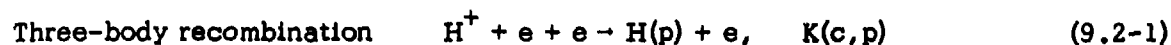
## 9.2 Properties of a large sphere of hot hydrogen

The main constituents of hot air at  $10^{-6}$  normal density and a temperature of  $24,000^{\circ}\text{K}$  are electrons and doubly ionized nitrogen and oxygen (Gilmore, 1955; Armstrong and Scheibe, 1964). If we assume that these ions are hydrogenic, then according to the scaling laws of Bates et al. (1962) ions and electrons

will recombine in a similar manner to protons and electrons at an electron density of  $10^{12}$  particles per cc and an electron temperature of about  $6,000^{\circ}\text{K}$ . Therefore, since we are interested in air at  $24,000^{\circ}\text{K}$ , we will concentrate our attention on hydrogen at an electron density of about  $10^{12}$  particles per cc and an electron temperature of  $6,000^{\circ}\text{K}$ .

### 9.2.1 Electron-ion recombination

In this discussion we will confine our attention to the recombination of electrons with protons (Bates et al., 1962). We write  $p, q \dots$  for the principal quantum numbers of the discrete levels and  $c$  for the continuum; we write  $n(p), \dots, n(q) \dots$  for the number densities of atoms in the levels indicated and  $n(c)$  for the number density of free electrons which we shall take equal to the number density of free protons. The reactions of this system and their reaction rate coefficients are as follows:



$$\text{Radiation recombination} \quad H^+ + e \rightarrow H(p) + h\nu, \beta(p) \quad (9.2-7)$$

$$\text{Photoionization} \quad H(p) + h\nu \rightarrow H^+ + e, \gamma(p) \quad (9.2-8)$$

In our treatment we neglect the effect of electronic transitions due to atom-atom and atom-proton collisions, and we also assume that the degenerate states of a level are populated according to their statistical weight.

With the exception of  $L(p, q)$  and  $\gamma(p)$ , all of the rate coefficients listed above depend only on atomic parameters, and are independent of the state of the radiation field. As discussed in Chapter 8, however, the radiation processes described by  $L$  and  $\gamma$  are complicated functions of line shapes and spectral distributions, and hence of the dimensions of the sphere as well.

In most cases we can ignore photoionization. Also, for most systems we can ignore all line absorption except for the resonance lines which can be strongly absorbed if the population of the ground state is large. Even to take proper account of these lines would be a complicated problem, and so we are forced to consider two limiting cases: 1) optically thin case: we assume that all the resonance radiation escapes from the plasma, and once it is emitted it does not interact with the plasma again; and 2) optically thick case: we assume that all the resonance radiation is reabsorbed before it escapes from the plasma. In practice we just put  $A(p, 1) = 0$  for all  $p$  in the optically thick calculations.

In terms of the rate coefficients defined above, the rate at which electrons build up in state  $p$  is given by

$$\dot{n}(p) = - \left\{ n(p) n(c) \left[ \sum_{q \neq p} K(p, q) + K(p, c) \right] + n(p) \sum_{q < p} A(p, q) \right\} \quad (9.2-9)$$

$$+ n^3(c) K(c, p) + n^2(c) \beta(p) + \sum_{q > p} n(q) A(q, p) + \sum_{q \neq p} n(c) n(q) K(q, p)$$

and the total recombination rate is given by

$$\dot{n}(c) = - \sum_{p=1}^{\infty} \dot{n}(p) \quad (9.2-10)$$

Since Eq. (9.2-9) applies to each of an infinite number of states, the recombination rate can only be determined by solving this infinite set of coupled differential equations. Fortunately, over a very large range of physical conditions the relaxation times associated with excited states are very much shorter than that associated with the ground state, and the populations of the excited states quickly adjust themselves so that

$$\dot{n}(p) = 0 \quad \text{for } p \neq 1 \quad (9.2-11)$$

and hence

$$\dot{n}(c) = - \dot{n}(1) \quad (9.2-12)$$

To determine  $\dot{n}(1)$  we must solve the infinite set of equations obtained from Eq. (9.2-9) by putting  $\dot{n}(p) = 0$  for all  $p \neq 1$ . This infinite set of simultaneous equations may be reduced to a finite set by using the fact that when  $p$  is large enough, the collisional rates to and from the continuum,  $F(p,c)$  and  $K(c,p)$ , are much larger than the radiative rates involving the  $p$  level. Therefore, for  $p$  greater than some limiting value,  $s$ , the relative values of the  $n(p)$  are those corresponding to equilibrium at the electron temperature  $T_e$ . The limiting value  $s$  is chosen so that

$n(s)$  is almost equal to  $n_E(s)$ , where

$$n_E(p) = n^2(c) p^2 \left\{ h^2 / 2\pi m k T_e \right\}^{3/2} \exp(I_p / k T_e) \quad (9.2-13)$$

is the number density of hydrogen atoms or hydrogenic ions in level  $p$  in Saha equilibrium at temperature  $T_e$  with free electrons and bare nuclei of number density  $n(c)$ , and  $I_p$  is the ionization potential of level  $p$ .

In the calculations we introduce the ratio

$$\rho(p) = n(p) / n_E(p) \quad (9.2-14)$$

which gives the extent to which the population deviates from equilibrium. Introducing this into Eq. (9.2-9) and using

$$\left. \begin{aligned} n_E(q) K(q, p) &= n_E(p) K(p, q) \\ n^2(c) K(c, p) &= n_E(p) K(p, c) \end{aligned} \right\} \quad (9.2-15)$$

we find that

$$\frac{\dot{n}(p)}{n_E(p)} = - \rho(p) \left[ n(c) (K(p, c) + \sum_{q \neq p} K(p, q)) + \sum_{q < p} A(p, q) \right] \quad (9.2-16)$$

$$+ \sum_{q \neq p} \rho(q) n(c) K(p, q) + \sum_{q > p} \rho(q) \frac{n_E(q)}{n_E(p)} A(q, p) + n(c) K(p, c) + \frac{n^2(c)}{n_E(p)} \beta(p)$$

TABLE R6 (CONT.). DIATOMIC SPECTROSCOPIC CONSTANTS

MOLEC.	STATE	T <sub>0</sub>	ω <sub>0</sub>	ω <sub>0</sub> X <sub>0</sub>	ω <sub>0</sub> Y <sub>0</sub>	ω <sub>0</sub> Z <sub>0</sub>	B <sub>0</sub>	a <sub>0</sub>	γ <sub>0</sub>	δ <sub>0</sub>
O <sub>2</sub>	X <sup>2</sup> Π <sub>g</sub>	-0.	1170.000	8.5000	-0.	-0.	1.18000	0.015000	-0.	-0.
O <sub>2</sub>	X <sup>2</sup> Σ <sub>g</sub> <sup>-</sup>	0.	1580.360	12.0730	5.460E-02	1.430E-03	1.44520	0.0153400	4.000E-04	1.300E-04
	a <sup>1</sup> Δ <sub>g</sub>	7882.4	1509.300	12.9000	-0.	-0.	1.42640	0.0171000	-0.	-0.
	b <sup>1</sup> Σ <sub>g</sub> <sup>+</sup>	13120.9	1432.690	13.9500	-1.075E-02	-0.	1.40042	0.0181700	-4.300E-05	-0.
	C <sup>3</sup> Δ <sub>u</sub>	34329.0	862.000	20.9000	-0.	-0.	0.96180	0.0262000	-0.	-0.
	A <sup>3</sup> Σ <sub>u</sub> <sup>+</sup>	35004.0	805.000	15.1500	3.300E-02	4.000E-02	0.91060	0.0142000	-9.700E-04	-0.
	c <sup>1</sup> Σ <sub>u</sub> <sup>-</sup>	36213.0	650.490	17.0360	-1.056E-01	7.440E-03	0.82610	0.0205500	-8.300E-04	-0.
	B <sup>2</sup> Σ <sub>u</sub> <sup>-</sup>	49337.6	710.000	10.9300	-5.000E-02	1.200E-02	0.81900	0.0110000	-8.300E-04	-0.
O <sub>2</sub> <sup>+</sup>	X <sup>2</sup> Π <sub>g</sub>	0.	1876.500	16.5300	-0.	-0.	1.67220	0.0198400	-0.	-0.
	a <sup>4</sup> Π <sub>u</sub>	32372.0	1035.690	10.3900	-0.	-0.	1.10466	0.0157500	-0.	-0.
	A <sup>2</sup> Π <sub>u</sub>	38205.0	899.000	13.7000	-0.	-0.	1.06170	0.0190600	-1.950E-04	-0.
	b <sup>4</sup> Σ <sub>g</sub> <sup>-</sup>	49039.0	1196.770	17.0900	-0.	-0.	1.28729	0.0220600	-0.	-0.
CO	X <sup>1</sup> Σ <sup>+</sup>	0.	2169.823	13.2939	1.150E-02	1.570E-05	1.93127	0.0175130	2.960E-06	-0.
	a <sup>3</sup> Π	48474.0	1743.550	14.4700	-0.	-0.	1.69110	0.0195000	-0.	-0.
	a' <sup>3</sup> Σ <sup>+</sup>	55353.9	1230.651	11.0130	7.378E-02	-1.150E-03	1.34530	0.0187200	2.050E-04	-0.
	d <sup>3</sup> Δ	60646.9	1152.580	7.2812	-1.125E-01	-0.	1.30990	0.0167700	-0.	-0.
	e <sup>3</sup> Σ <sup>-</sup>	63708.9	1113.167	9.5960	5.870E-03	-0.	1.28480	0.0181000	1.000E-04	-0.
	I <sup>1</sup> Σ <sup>-</sup>	64746.5	1515.610	17.2505	-0.	-0.	1.61160	0.0222900	-1.050E-04	-0.
	A <sup>1</sup> Π	65633.0	1063.800	9.5100	-0.	-0.	1.22600	0.0180000	-0.	-0.

**BLANK PAGE**

Putting  $\dot{n}(p) = 0$  for  $p \neq 1$  and putting  $\rho(p) = 1$  for  $p > s$  we find that

$$\rho(p) \left[ n(c) \left( K(p, c) + \sum_{q \neq p} K(p, q) \right) + \sum_{q < p} A(p, q) \right] - \sum_{\substack{q \neq p \\ \leq s}} \rho(q) n(c) K(p, q) - \sum_{\substack{q > p \\ \leq s}} \rho(q) \frac{n_E(q)}{n_E(p)} A(q, p) = n(c) \left[ \sum_{q > s} K(p, q) + K(p, c) \right] \quad (9.2-17)$$

$$+ \frac{n^2(c) \beta(p)}{n_E(p)} + \sum_{q > s} \frac{n_E(q)}{n_E(p)} A(q, p)$$

$$\text{for } 1 < p \leq s. \quad (9.2-18)$$

The solutions to this set of  $s-1$  linear equations for the  $\rho(p)$  may be expressed in terms of  $\rho(1)$  in the form

$$\rho(p) = r_0(p) + r_1(p) \rho(1) \quad (9.2-19)$$

where  $r_0(p)$  and  $r_1(p)$  are functions of  $n(c)$  and  $T_e$ .

The recombination rate is then given by

$$\dot{n}(c) = -\dot{n}(1) = -n(c)n_E(1) \left[ \sum_{\substack{q > 1 \\ \leq s}} \rho(q) K(1, q) + \sum_{q > s} K(1, q) + K(1, c) \right] \quad (9.2-20)$$

$$-n^2(c) \left[ \sum_{\substack{q > 1 \\ \leq s}} \rho(q) \frac{n_E(q)}{n^2(c)} A(q, 1) + \sum_{q > s} \frac{n_E(q)}{n^2(c)} A(q, 1) + \beta(1) \right] + n(c)n(1) \left[ K(1, c) + \sum_{q \neq 1} K(1, q) \right]$$

The first two terms in square brackets represent the rates of filling of the ground state by collisional deactivation and three-body recombination, and by cascading and radiative recombination. The third term represents the evacuation of the ground level by collisional excitation and ionization. Because of the form of Eq. (9.2-19) and Eq. (9.2-13) the above equation may be written

$$\dot{n}(c) = -\alpha n^2(c) + S n(1) n(c) \quad (9.2-21)$$

where  $\alpha$ , the effective recombination coefficient, and  $S$ , the ionization coefficient, are positive quantities dependent only on  $n(c)$ ,  $T_e$  and various atomic parameters. In highly ionized plasmas tenuous enough for radiative processes to be important the second term in Eq. (9.2-21) becomes negligible compared to the first term and can usually be ignored.

For hydrogen and hydrogenic ions the rates for all the optical transitions are known exactly, but the rates  $K(p, q)$ ,  $K(p, c)$  and  $K(c, p)$  for collisional processes are not well known. The simultaneous equations (9.2-17) have been solved and recombination rates calculated over a wide range of electron densities and temperatures by Bates et al. (1962), using classical cross sections for hydrogen and approximate quantal cross sections for hydrogenic ions. If it were not for the possible errors in these cross sections the calculations would be effectively exact within the specified limitations.

Bates et al. found that for hydrogenic ions it was possible to reduce the computational labor by taking advantage of certain scaling laws. These

laws were established by choosing the basic independent parameters to be reduced values of the electron temperature and number density of free electrons defined by

$$\Theta = T_e/Z^2, \quad \eta(c) = n(c)/Z^7 \quad (9.2-22)$$

where  $Z$  is the charge on the recombining nucleus. The electron recombination rate was found to be a unique function of the reduced variables. Thus a gas containing hydrogenic ions with charge  $Z = 2$  and electrons at a temperature of  $24,000^\circ\text{K}$  and density  $n(c) = 10^{14}$  will have the same electron recombination rate as hydrogen with an electron temperature  $T_e = 24,000/4 = 6,000^\circ\text{K}$  and electron density  $n(c) = 10^{14}/Z^7 \approx 10^{12}$ . Calculations of the effective recombination rate have not been carried out at  $6,000^\circ\text{K}$ , but results are available at  $4,000^\circ\text{K}$  and  $8,000^\circ\text{K}$ . These are compared with the radiative recombination rate as follows:

	$T_e = 4,000^\circ\text{K}$	$T_e = 8,000^\circ\text{K}$
$\alpha_{\text{coll-rad}}$	$3.4 \times 10^{-12} \text{ cm}^3 \text{ sec}^{-1}$	$6.8 \times 10^{-13} \text{ cm}^3 \text{ sec}^{-1}$
$\alpha_{\text{rad}}$	$7.9 \times 10^{-13} \text{ cm}^3 \text{ sec}^{-1}$	$4.6 \times 10^{-13} \text{ cm}^3 \text{ sec}^{-1}$

Here we have assumed that the plasma is so large that all the line radiation involving the ground state is trapped, i.e., that the plasma is optically thick to the resonance radiation.

### 9.2.2 Energy balance in a plasma

In a recombining plasma when we know the quasi-equilibrium of the various excited states from Eqs. (9.2-17), (9.2-13) and (9.2-14), we can, of course, determine the rate at which energy radiates from the plasma. The chief types of radiation from the plasma are (1) radiation from transitions from one bound state to another, (bound-bound transitions); (2) radiation from transitions of a free electron into a bound state, (free-bound transitions); (3) radiation from transitions from one free state to another free state, (free-free transitions).

The rate at which a recombining hydrogen plasma radiates energy has been calculated by Bates and Kingston (1963). At an electron density  $n(e) = 10^{12}$  they found that the power radiated,  $P$ , at  $4,000^\circ\text{K}$  was  $24 \text{ ergs/cm}^3 \text{ sec}$  and at  $8,000^\circ\text{K}$  was  $16 \text{ ergs/cm}^3 \text{ sec}$ . In accordance with the optically thick assumption, resonance lines were not included. This power,  $P$ , was made up from the contributions listed below:

	$P(T_e = 4,000)$	$P(T_e = 8,000)$
1. bound-bound	17	11
2. free-bound	6.9	4.9
3. free-free	<u>.1</u>	<u>.1</u>
Total	$24 \text{ ergs/cm}^3 \text{ sec}$	$16 \text{ ergs/cm}^3 \text{ sec}$

In a non-equilibrium plasma, when an electron recombines it not only radiates some of the potential energy of the plasma but also changes the kinetic energy. Processes (9.2-1) and (9.2-3) tend to increase the kinetic energy of the electrons, and (9.2-2), (9.2-4) and (9.2-7) tend to decrease

the kinetic energy of the electrons. If we have a system consisting only of electrons, protons and hydrogen atoms, we find that the rate of increase of kinetic energy of the electrons of temperature  $T_e$  and density  $n(c)$  is (Bates and Kingston, 1964)

$$\begin{aligned} \frac{d}{dt} \left\{ \frac{3}{2} n(c) k T_e \right\} = & \alpha n^2(c) I_1 - P - (T_e - T_i) \eta_{ei} n^2(c) \\ & - (T_e - T_a) \eta_{ea} n(c) n(l) - \mathcal{L}_e \end{aligned} \quad (9.2-23)$$

where  $k$  is the Boltzmann constant, the density of atoms is assumed equal to  $n(l)$ ,  $I_1$  is the ionization potential of the ground level,  $T_a$  and  $T_i$  are the kinetic temperatures of the atoms and ions respectively. The term  $(T_e - T_i) \eta_{ei} n^2(c)$  gives the rate at which electrons lose (or gain) energy from ions by elastic collisions,  $(T_e - T_a) \eta_{ea} n(l) n(c)$  gives the rate at which electrons lose (or gain) energy from atoms by elastic collisions, and  $\mathcal{L}_e$  is the loss of electron energy by diffusion to the surroundings. In the large dimensions considered here we can take  $\mathcal{L}_e = 0$ .

We may write Eq. (9.2-23) as

$$\frac{3}{2} n(c) k \frac{dT_e}{dt} = H_0 - (T_e - T_i) \eta_{ei} n^2(c) - (T_e - T_a) \eta_{ea} n(c) n(l) \quad (9.2-24)$$

where

$$H_0 = (I_1 + \frac{3}{2} k T_e) \alpha n^2(c) - P \quad (9.2-24a)$$

We find that  $H_0 = 5.5 \times 10^1 \text{ ergs/cm}^3 \text{ sec}$  at  $T_e = 4,000^\circ\text{K}$  and  $n(c) = 10^{12}$ , and  $H_0 = -2.1 \times 10^{-1} \text{ ergs/cm}^3 \text{ sec}$  at  $T_e = 8,000^\circ\text{K}$ .

We can also write down similar expressions for the atom temperature and ion temperature (Bates and Kingston, 1964). However, a solution of these three equations for general conditions is scarcely feasible, and we look for an approximate solution to Eq. (9.2-24). If  $T_i$  and  $T_a$  are fixed, we get such a solution, for when we consider Eq. (9.2-24) we see that  $H_0$  decreases rapidly with  $T_e$ , while if  $T_e > T_i$  and  $T_a$  the remainder of the expression grows more negative with increasing  $T_e$ . Fig. 9-1 shows the two opposing terms in Eq. (9.2-24).

These curves cross at the temperature  $T_e = T_S$ , and it can be shown that if  $T_e$  is displaced slightly from this point, it will return very rapidly. This temperature is given by the value of  $T_e$  such that

$$H_0 = (T_e - T_i)\eta_{ei} n^2(c) + (T_e - T_a)\eta_{ea} n(c) n(i) \quad (9.2-25)$$

If now  $T_e > T_i$  and  $T_e > T_a$ , the right hand side of Eq. (9.2-25) is always positive, and if the equation is to be satisfied,  $H_0$  must be positive. However, if we assume that all the radiation to the ground state is reabsorbed, at a given electron density there is always a temperature above which  $H_0$  becomes negative. For electron densities less than  $n(c) = 10^{13}$  this temperature is approximately  $8,000^\circ\text{K}$  and so  $T_S < 8,000^\circ$ . The assumption that  $T_e > T_i$  or  $T_a$  is probably correct for most plasmas, because the electrons receive the recombination energy which is not radiated out of the system, and since the atoms and ions receive their kinetic energy

from the electrons, they cannot have a temperature greater than the electron temperature.

The temperature given by  $H_0 = 0$  is an upper bound to  $T_S$ . However, when we examine the three terms in Eq. (9.2-24) at an electron density of  $n(c) = 10^{12}$  and  $T_e \simeq 8,000^\circ\text{K}$ , we find that as  $T_e$  decreases,  $H_0$  increases very rapidly, whereas the other two terms rapidly become less negative. It follows that  $T_S$  is only slightly less than  $8,000^\circ$ . A graph of the steady state electron temperature  $T_S$  is given in Fig. 9-2. Also plotted on this graph is the variation with density of the electron temperature,  $T_E$  for electrons in thermodynamic equilibrium with the atoms. These are plotted for two values of  $n(l) + n(c)$ . We see that the steady state temperature  $T_S$  is always above the temperature given by thermodynamic equilibrium conditions, except when the plasma is almost fully ionized.

These arguments are perfectly general as long as we can neglect diffusion and as long as  $T_e > T_i$  or  $T_a$ . They are also dependent on the fact that  $H_0$ , the energy that the electrons receive from recombination, can become negative. It is instructive to see why this term becomes negative. Consider a simplified model of hydrogen such that only the transitions shown in Fig. 9-3 are taken into account.

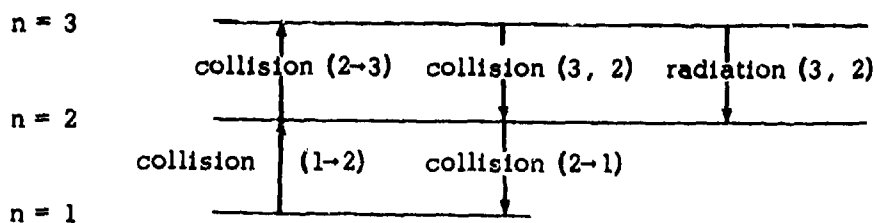


FIG. 9-3 SIMPLIFIED MODEL OF THE HYDROGEN ATOM

If an electron is to recombine, it must reach  $n = 1$ , and the only way it can do this is by having an electron collision from  $(2 \rightarrow 1)$ . Hence, the free electrons should gain the energy of this electron for each recombining electron, and since this is usually  $\gg kT_e$ , the electron temperature rises rapidly. However, as the electron temperature rises, the rate of collisions from  $(2 \rightarrow 3)$  becomes greater than the rate of collisions from  $(2 \rightarrow 1)$ , and an electron may be excited several times to level  $n = 3$  before recombining, since these electrons will then drop from  $(3 \rightarrow 2)$  by radiating the energy of the transition. We get an internal pumping system which is continually pumping energy from the continuum into excitation of electrons from state 2 to 3, which then radiates from 3 to 2. Hence, the electrons lose kinetic energy for every electron that recombines, and so the electron temperature will fall.

### 9.2.3 Results

If we assume that the electron temperature  $T_e$  is constant, it is not difficult to obtain the recombination rates at given electron densities (Bates et al., 1962), and these can then be used to obtain the variation of electron density with time. In a hydrogen plasma, the electron density  $n(c)$  equals the proton density, so Eq. (9.2-21) gives

$$\frac{d n(c)}{dt} = - \alpha n^2(c) \quad (9.2-26)$$

when the reionization term is neglected. The electron density  $n_t(c)$  at time  $t$  is then given by

$$\frac{1}{n_t(c)} = \frac{1}{n_0(c)} + \int_0^t \alpha dt \quad (9.2-27)$$

where  $n_0(c)$  is the electron density at  $t = 0$ . Since  $\alpha$  varies with  $n(c)$ , we must in general solve Eq. (9.2-27) numerically. However, for an optically thick hydrogen plasma (Bates et al., 1962) at  $T_e = 8,000^\circ\text{K}$  and  $n(c)$  in the range  $10^{14}$  to  $10^{10}$ , the recombination rate can be taken to be  $\approx 6.6 \times 10^{-13} \text{ cm}^3 \text{ sec}^{-1}$  without giving rise to serious error. For this case we have

$$\frac{1}{n_t(c)} = \frac{1}{n_0(c)} + 6.6 \times 10^{-13} t. \quad (9.2-28)$$

Fig. 9-4 shows the variation of electron density with time for three initial electron densities  $n(c) = 10^{13}$ ,  $10^{12}$  and  $10^{11}$ . Because of the form of Eq. (9.2-28) we find that all three initial densities can be given in the same graph by adjusting the scales of the graph. It should be noted that the present results are only applicable if reionization can be neglected. This is not the case, for example, if the density of free electrons is very much less than the density of neutral particles.

The rate at which energy is radiated from a plasma consisting only of hydrogen atoms, protons and electrons is also of interest. These rates for a recombining plasma have been calculated (Bates and Kingston, 1963) for a wide range of electron temperatures and densities. For an electron temperature of  $8,000^\circ\text{K}$  and electron densities in the range  $n(c) = 10^{14}$  to  $10^{10}$ , we find that the total rate at which energy is radiated is approximately

$$P = \frac{dE}{dt} = 1.6 \times 10^{-23} n^2(c) \text{ ergs/cm}^3 \text{ sec} \quad (9.2-29)$$

This rate of loss of energy by radiation is the sum of losses by bound-bound, free-bound, and free-free transitions. These contribute  $1.1 \times 10^{-23} n^2(c)$ ,  $4.9 \times 10^{-24} n^2(c)$ , and  $1.3 \times 10^{-25} n^2(c)$  ergs/cm<sup>3</sup> sec, respectively, to the total of  $1.6 \times 10^{-23} n^2(c)$ .

To calculate the rate at which energy is radiated at a given time we now require only the electron density at that time. From the time variation of electron density for various initial electron densities given in Fig. 9-4 we can readily construct Fig. 9-5, which gives the time variation of the rate at which radiation is emitted from a plasma for three initial electron densities  $n(c) = 10^{13}$ ,  $10^{12}$  and  $10^{11}$ . The rates for the three types of radiation: bound-bound, bound-free and free-free are given separately.

For an initial electron density of  $10^{12}$  the rate at which energy is radiated by bound-bound collisions drops by about a factor of three in 1 second and by about a factor of 20 in ten seconds. The amount of energy radiated from a plasma in a given time interval may be calculated from  $P$ . We can simplify the calculations greatly by noting that if  $T_s = T_a = T_i = 8,000^\circ\text{K}$ , and the number of atoms is not very much greater than the number of electrons and ions, then most of the energy loss in the plasma as it recombines is a loss in potential energy. The potential energy of the plasma is given by  $n(c) I_1$ , where  $I_1$  is the ionization potential of hydrogen ( $13.6 \text{ eV} = 2.18 \times 10^{-11}$  ergs). The loss of energy in a given time interval may then be obtained by multiplying the change in electron density in the time interval by  $I_1$ . For example, Fig. 9-4 shows that a system which has initially  $10^{12}$  electrons per cc, i.e., 21.8 ergs per cc, loses 1.3 ergs per cc in 0.1 seconds, 8.3 ergs per cc in 1 second and 19 ergs per cc in 10 seconds.

### 9.3 Model for sphere of hot air

The calculations carried out in the previous section are only applicable to a hydrogen-proton-electron plasma, but they should approximately describe the behavior of any large plasma consisting of singly charged ions and electrons. In order to obtain some ideas of how a large plasma of hot air decays with time, we now consider a plasma consisting initially of only doubly charged nuclei and electrons. This should be a good approximation to air at about 2 eV and  $10^{-6}$  normal density, which consists mainly of electrons and doubly charged ions of nitrogen and oxygen.

The problem of electron-ion recombination in a plasma which initially consists of doubly-charged ions and electrons has not previously been treated theoretically. Basically this problem is very similar to the problem of ion-electron recombination for singly charged ions. We must first write down equations similar to (9.2-9) for all levels of the neutral atom and singly charged ion and include all transitions between all states. From these we then obtain the quasi-equilibrium populations of the states from Eq. (9.2-17) and so calculate the total electron recombination rate to both atom and ion. However, if the ionization potential of the neutral atom is very much less than the ionization potential of the singly charged ion, the rate for electron recombination to the doubly-charged ions is very much greater than that for recombination to the singly-charged ions. We can therefore consider the recombination to the doubly-charged ion and the recombination to the singly-charged ion as completely independent processes.

Electron recombination to a singly-charged ion has already been considered in the previous section. Calculations of electron-ion recombination rates for doubly charged hydrogenic ions have been carried out (Bates et al., 1962;

McWhirter and Hearne, 1963). Unfortunately, these calculations are not applicable to large plasmas as the optically thin case only was considered, i.e., there was no absorption of radiation by ground state ions. We must therefore use the calculations on doubly-charged hydrogenic ions for optically thin conditions together with the calculations on singly charged ions for optically thin and thick conditions to infer the properties of electron recombination with a doubly-charged hydrogenic ion under optically thick conditions.

This can be done readily by making use of the reduced temperature and electron density introduced in Eq. (9.2-22). A further simplification results from the fact that for small electron densities, the multiply-charged hydrogenic ion calculations and the singly-charged ion calculations for optically thin conditions give very similar results (Bates et al., 1962). It seems therefore reasonable to expect that for optically thick conditions the results for electron recombination to a multiply charged ion and the results for electron-proton recombination will not differ appreciably, and so we can use the electron-proton results to obtain results for other values of  $Z$ .

If we now assume that a doubly-ionized hydrogenic ion recombines similarly to a singly-charged hydrogenic ion, and if we replace the electron density by  $n(c)/2^7$  and the electron temperature by  $T_S/2^2$ , we find that the steady state electron temperature is  $T_S \approx 2^2 \times 8,000^\circ\text{K}$ , i.e.,  $2^2$  times the temperature given in Fig. 9-2. The recombination rate (Bates et al., 1962) at an electron density  $n(c)$  is twice the recombination rate for electron-proton recombination at an electron density of  $n(c)/2^7$ . Under optically thick conditions this will give a recombination rate of  $\alpha = 2 \times 6.6^{-13} \text{ cm}^3 \text{ sec}^{-1}$  for  $n(c)$  from  $10^{16}$  to  $10^{12}$ .

If we denote the number density of electrons, doubly charged ions, singly charged ions, and neutral atoms by  $n(c)$ ,  $n(N^{++})$ ,  $n(N^+)$ , and  $n(N)$  respectively, then for a plasma which has no net charge and initially consists of only doubly-charged ions of density  $n_0(N^{++})$  and electrons of density  $2n_0(N^{++})$  we have

$$n(N^{++}) + n(N^+) + n(N) = n_0(N^{++}) \quad (9.3-1)$$

and  $2n(N) + n(N^+) + n(c) = 2n_0(N^{++}) \quad (9.3-2)$

with  $\dot{n}(N^{++}) = -\alpha_1 n(c) n(N^{++}) \quad (9.3-3)$

$$\dot{n}(N^+) = -\dot{n}(N^{++}) - \dot{n}(N) \quad (9.3-4)$$

$$\dot{n}(N) = \alpha_2 n(c) n(N^+) \quad (9.3-5)$$

and also  $\dot{n}(c) = \dot{n}(N^{++}) - \dot{n}(N) \quad (9.3-6)$

where  $\alpha_1$  and  $\alpha_2$  are the electron-ion recombination rates for recombination with doubly and singly charged ions, respectively. To solve these equations for  $n(N^{++})$ ,  $n(N^+)$ ,  $n(N)$  and  $n(c)$  is a formidable task which can be greatly simplified by noting that if

$T_E \approx 32,000^\circ K$ ,  $\alpha_1$  is then about 20 times greater than  $\alpha_2$  so that the rate at which neutral atoms are formed is very much smaller than the rate at which singly charged ions are formed, and we can therefore initially neglect  $n(N)$ .

Hence, we have

$$n(N^{++}) + n(N^+) = n_o(N^{++}); \quad (9.3-7)$$

$$n(N^+) + n(c) = 2 n_o(N^{++}) \quad (9.3-8)$$

$$\dot{n}(N^{++}) = -\alpha_1 n(c) n(N^{++}) \quad (9.3-9)$$

$$= -\alpha_1 n(N^{++}) [n_o(N^{++}) + n(N^{++})]$$

and therefore

$$\int_{n_o(N^{++})}^{n(N^{++})} \frac{dn(N^{++})}{n(N^{++}) [n_o(N^{++}) + n(N^{++})]} = - \int_0^t \alpha_1 dt$$

$$\therefore \frac{1}{n_o(N^{++})} \left\{ \log_e \left[ \frac{n_o(N^{++})}{n(N^{++})} \right] - \log_e \left[ \frac{2 n_o(N^{++})}{(n_o(N^{++}) + n(N^{++}))} \right] \right\} = + \int_0^t \alpha_1 dt, \quad (9.3-10)$$

$$\therefore n(N^{++}) = \frac{n_o(N^{++})}{\left[ 2 e^{[n_o(N^{++}) \int_0^t \alpha_1 dt]} - 1 \right]}$$

If  $\alpha_1$  is constant, we have

$$n(N^{++}) = \frac{n_0(N^{++})}{2 e^{n_0(N^{++}) \alpha_1 t} - 1} \quad (9.3-11)$$

Taking  $\alpha_1 = 2 \times 6.6 \times 10^{-13} \text{ cm}^3 \text{ sec}^{-1} = 1.32 \times 10^{-12} \text{ cm}^3 \text{ sec}^{-1}$ , we plot in Fig. 9-6 the decay of doubly charged ions for initial ion densities  $n_0(N^{++}) = 10^{14}$ ,  $10^{13}$  and  $10^{12}$ . Because of the form of Eq. (9.3-11) these may all be plotted on the one graph by adjusting the scales used. The electron density may then be found from

$$n(e) = n_0(N^{++}) + n(N^{++}) \quad (9.3-12)$$

Most of the energy in a plasma consisting of doubly charged ions and electrons is in the form of potential energy. For a hydrogenic system this energy is given by

$$E = I_1 n(N^+) + (I_1 + 2^2 I_1) n(N^{++}) \quad (9.3-13)$$

where  $I_1$  is the ionization potential of hydrogen and  $2^2 I_1$  is the ionization potential of a hydrogenic ion of charge 2. Using Eq. (9.3-1) with  $n(N) = 0$  we have

$$E = I_1 n_0(N^{++}) + 4I_1 n(N^{++}) \quad (9.3-14)$$

The loss of energy from the plasma may then be obtained from the loss of  $N^{++}$  ions from the plasma.

As time progresses the number of  $N^{++}$  ions will become very much less than the  $N^+$  ions, and the  $N^+$  ions will begin to compete with the  $N^{++}$  ions for the electrons. When this happens, our basic assumption that  $n(N)$  may be neglected becomes invalid. Also when  $n(N)$  begins to become important, we can no longer treat the electron recombination to the doubly and singly charged ions as independent processes, and we must carry out recombination calculations which take full account of transitions between all atomic and ionic energy levels. In this transition region where the plasma is changing from domination by doubly-charged ions to domination by singly-charged ions, the electron temperature must also drop and tend to the equilibrium temperature for a singly-charged ion plasma. A full treatment of this transition region would be very difficult because of the variation of electron temperature and the fact that we have to consider the variations of  $n(c)$ ,  $n(N^{++})$ ,  $n(N^+)$  and  $n(N)$  simultaneously.

Since the recombination rate to the  $N^{++}$  ions increases very rapidly as  $T_s$  decreases, it seems likely that as the plasma becomes dominated by electron recombination to  $N^+$  and the temperature drops, the  $N^{++}$  ions will rapidly be converted to  $N^+$  ions. We will then reach a region which will be dominated by electron recombination to  $N^+$  and will follow the pattern described in the previous section.

#### 9.4 Conclusions

Though most of the previous discussion applied strictly to a hydrogenic plasma, certain general conclusions about the behavior of air at high temperatures can be derived. Some of these conclusions have been explicitly stated already.

We would primarily like to develop a criterion which would indicate when the assumption of LTE fails, and a method of calculating the power radiated in the absence of LTE. An obvious criterion can be obtained from Eq. (9.2-21), which is that LTE fails when the ionization term becomes much smaller than the recombination term, or

$$S \ll \frac{\alpha n(c)}{n(1)} \quad (9.4-1)$$

This however is not a useful criterion since the detailed problem always has to be solved, i.e.,  $n(1)$  has to be obtained before Eq. (9.4-1) can be used. In addition a steady state may occur, in which  $n(1) = \alpha n(c)/S$  but where the populations and radiation are non-LTE. A more suitable criterion is

$$S \ll \frac{\alpha n(c)}{n_E(1)} \quad (9.4-2)$$

which is just the condition which results when radiative processes become important (Bates et al., 1962). It should be noted that the inequality (9.4-2) does not imply that all collisions are unimportant. In fact, collisional recombination and ionization, represented by Eqs. (9.2-1) and (9.2-2), involving states near the continuum are important well into the non-LTE regime.

The approximate values of the electron density below which Eq. (9.4-2) is satisfied are as follows:

- $10^{16} \text{ cm}^{-3}$  - hydrogen ion plasma, optically thin
- $10^{14} \text{ cm}^{-3}$  - pseudo-alkali ion plasma (ground state inaccessible), optically thin
- $10^{14} \text{ cm}^{-3}$  - hydrogen ion plasma, optically thick in resonance lines
- $10^{18} \text{ cm}^{-3}$  - hydrogenic ion plasma,  $Z = 2$ , optically thin

The values of  $S$ ,  $\alpha$ , and  $n_E(1)$  used in determining these conditions were taken from Bates et al. (1962).

The type of non-LTE considered in this chapter is characterized by an overabundance of free electrons and ions, and a deficiency of neutral particles. In such a situation the plasma recombines in the manner described above. The radiative energy loss during the decay of the plasma is essentially equal to the loss of the potential stored as ionization energy. Under these conditions the radiative loss is greater than the loss would be from an LTE plasma with the same energy content. This is in contrast to the collision limited non-LTE case discussed in Chapters 8 and 10 where the radiative loss is lower than the LTE value.

During the major part of the decay the electron temperature remains approximately constant. It is only when recombination to singly ionized atoms becomes competitive with that to doubly ionized atoms or when the density of neutral particles is much greater than the density of free electrons that the electron temperature can vary appreciably.

Finally it should be mentioned that although the emphasis here is on the decay of plasmas, the analysis on which the results are based is also of direct relevance in connection with the growth of plasmas (Bates, et al., 1962), such as in the case of cold air suddenly shocked to a high temperature.

## REFERENCES

- Armstrong, B. H., and M. Scheibe, Equilibrium Occupation Numbers and Species Concentrations for Air, Nitrogen and Oxygen to 24,000°K, Report 6-74-64-33, LMSC, June (1964).
- Bates, D. R., A. E. Kingston and R. W. P. McWhirter, Proc. Roy. Soc. A 267, 297 (1962) and 270, 155 (1962).
- Bates, D. R., and A. E. Kingston, in Planetary and Space Sciences, 11, ed. D. R. Bates, Pergamon Press, New York (1963).
- Bates, D. R., and A. E. Kingston, Proc. Roy. Soc. A 279, 10 (1964).
- Gilmore, F. R., Equilibrium Composition and Thermodynamic Properties of Air to 24,000°K, RM-1543, The RAND Corp., Santa Monica, Calif. (1955). An updated version of this work is also contained in the volume written by Gilmore for the Thermal Radiation Handbook.
- McWhirter, R. W. P., and A. G. Hearne, Proc. Roy. Soc. 82, 651 (1963).

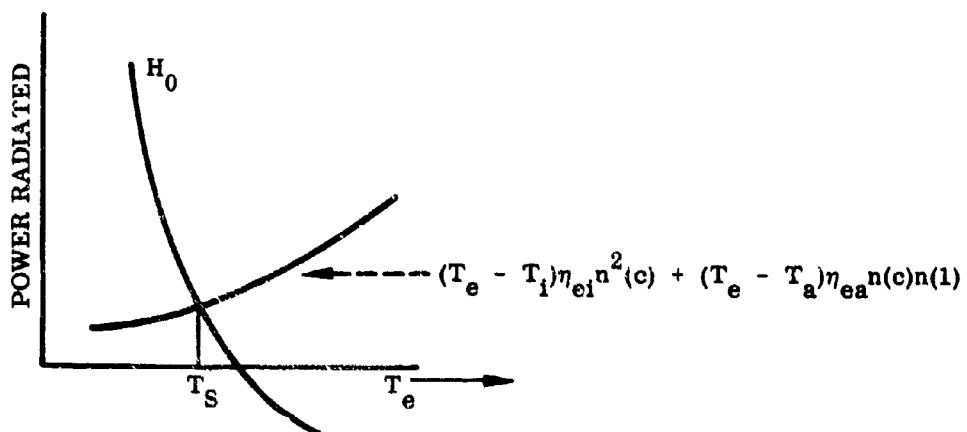


FIG. 9-1 ELECTRON ENERGY CHANGE BY RADIATION AND RECOMBINATION,  $H_0$ , AND BY ELASTIC COLLISIONS

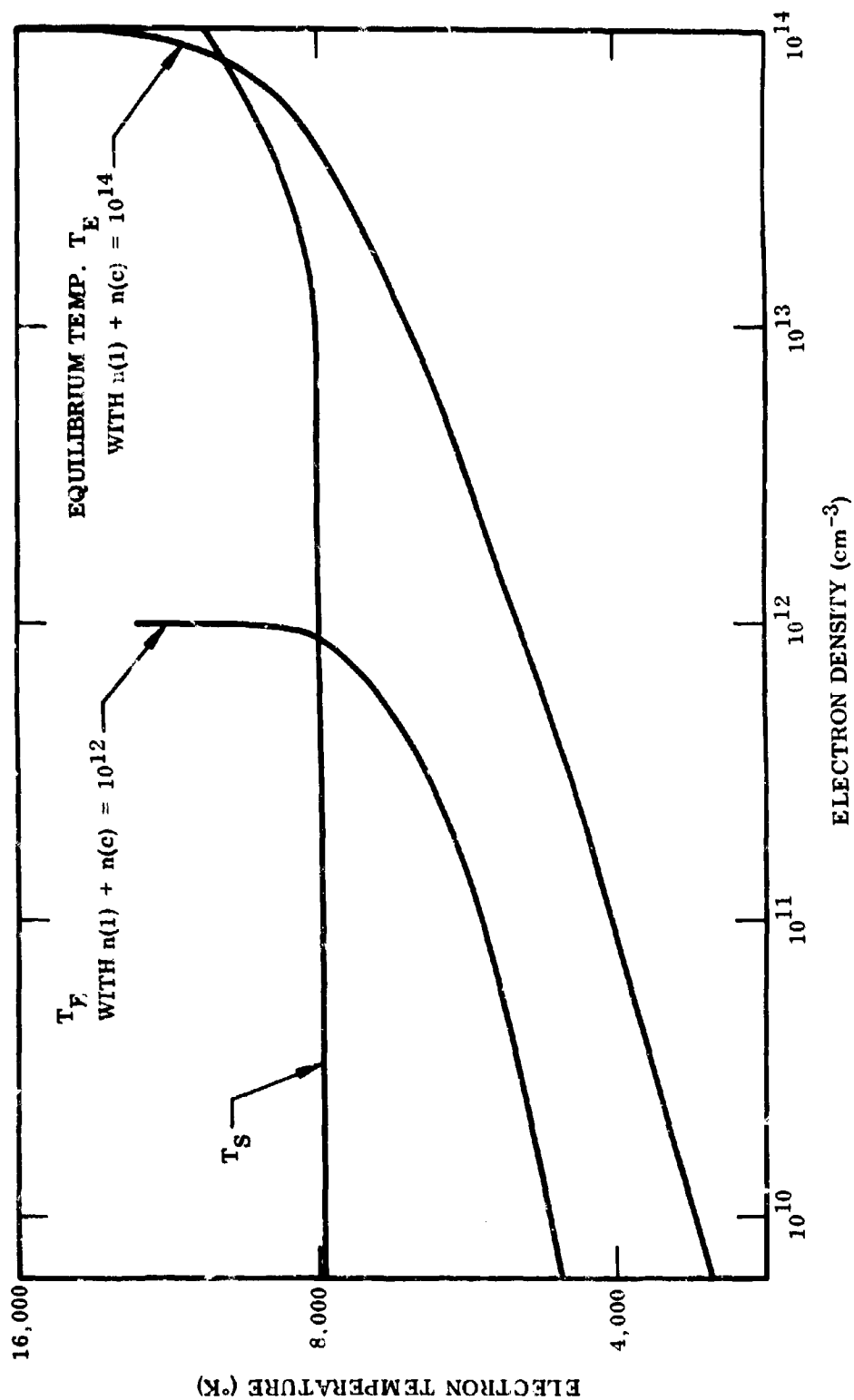


FIG. 9-2 STEADY STATE ELECTRON TEMPERATURE,  $T_s$ , AND THE THERMODYNAMIC EQUILIBRIUM TEMPERATURE,  $T_E$ .

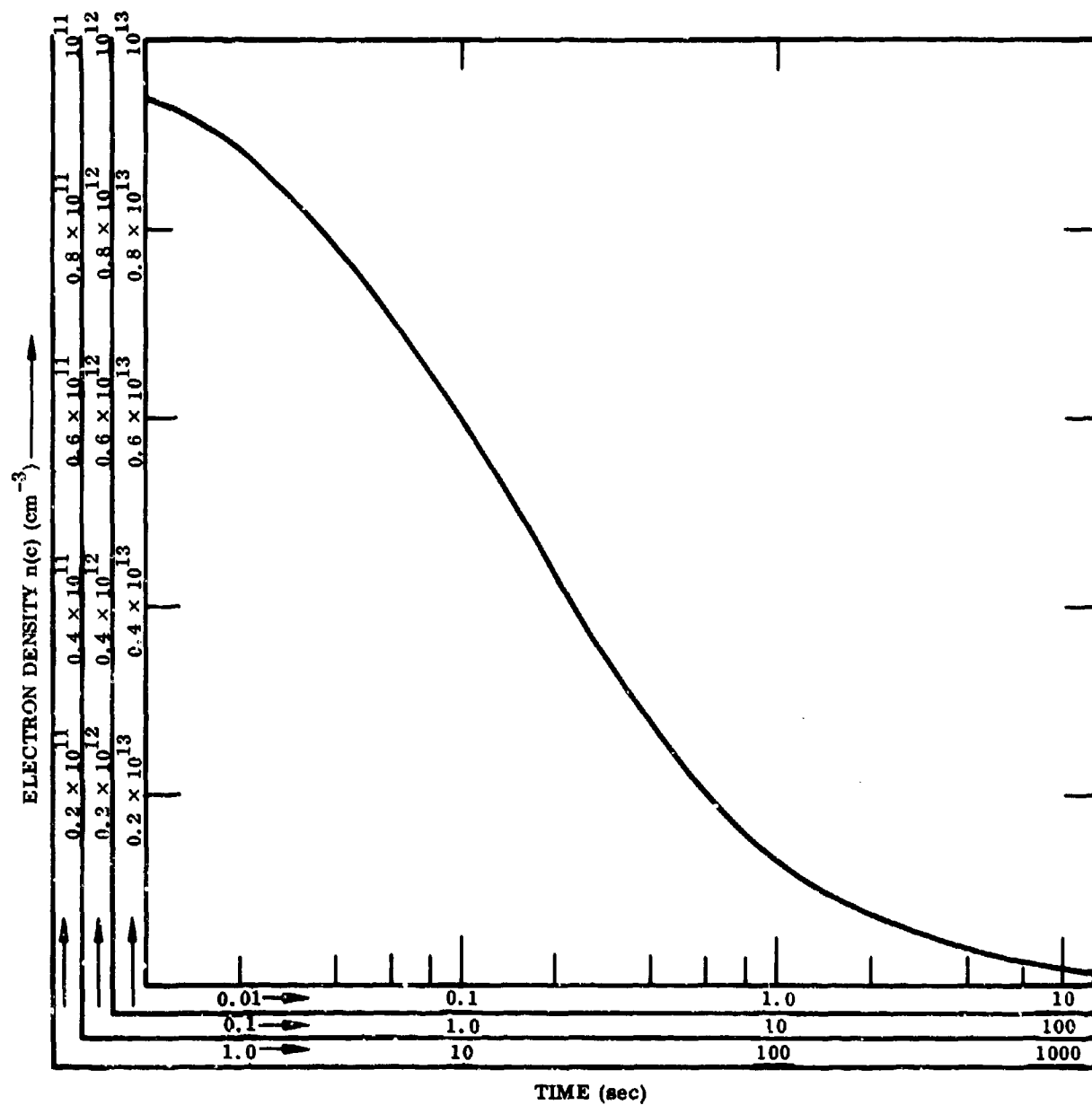


FIG. 9-4 THE VARIATION OF ELECTRON DENSITY WITH TIME IN A LARGE  
 $\text{H} - \text{H}^+ - e$  PLASMA FOR INITIAL ELECTRON DENSITIES OF  
 $n(c) = 10^{11}$ ,  $10^{12}$  and  $10^{13}$   $\text{cm}^{-3}$

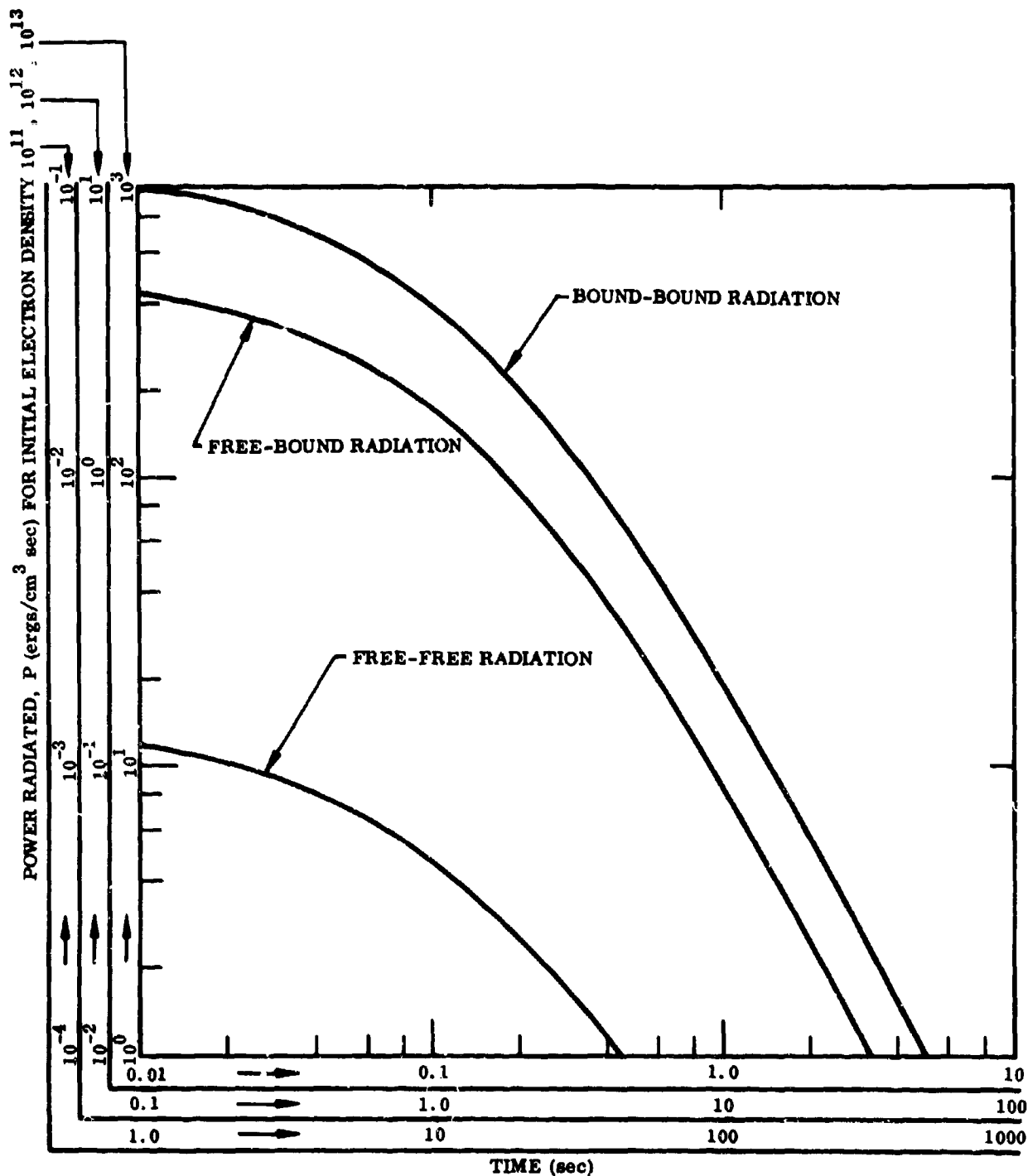


FIG. 9-5 THE RATE,  $p$ , AT WHICH A LARGE  $H - H^+ - e$  PLASMA RADIATES ENERGY AS A FUNCTION OF TIME, FOR INITIAL ELECTRON DENSITIES OF  $n(e) = 10^{11}$ ,  $10^{12}$  and  $10^{13} \text{ cm}^{-3}$ .

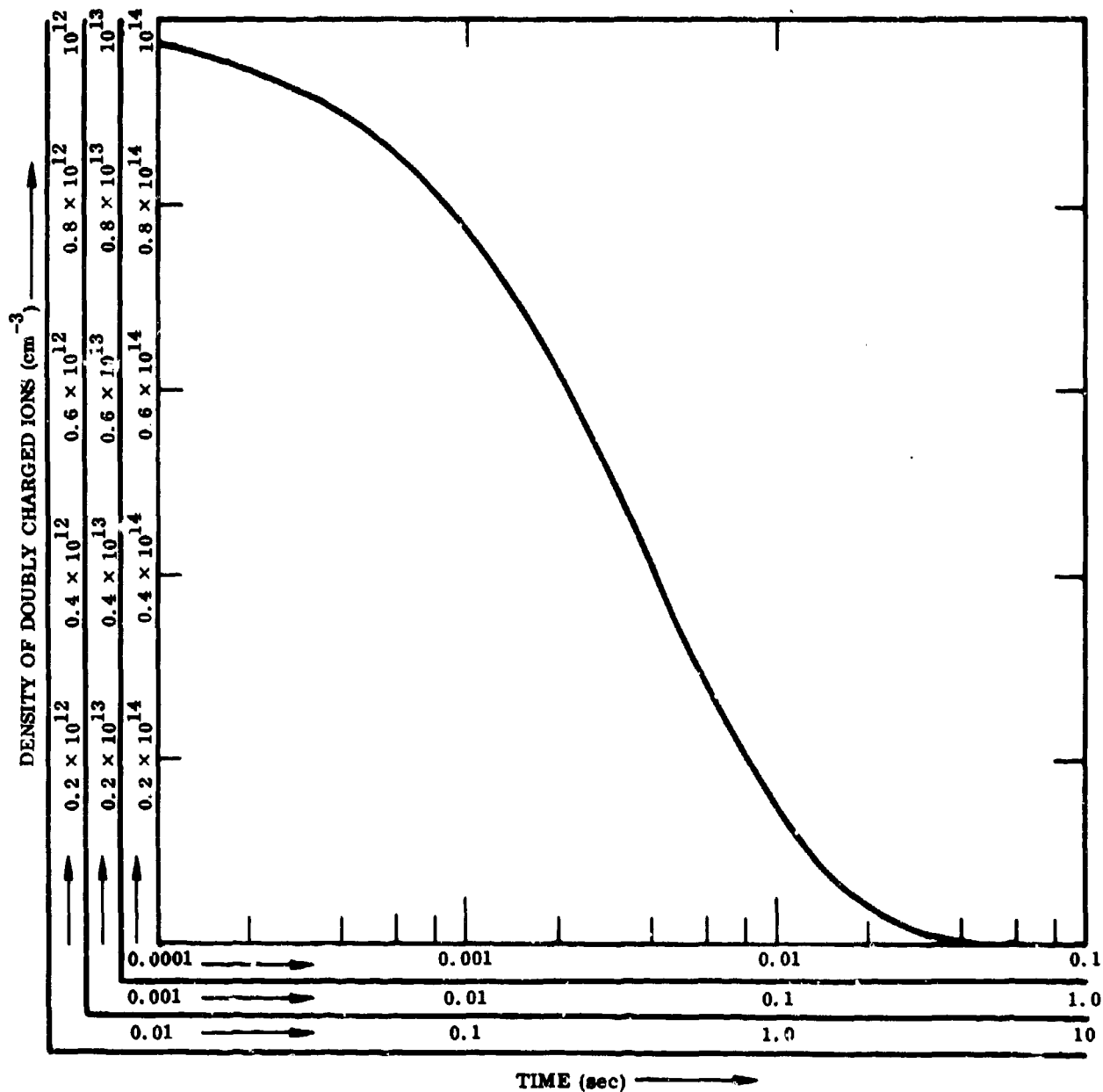


FIG. 9-6 THE VARIATION OF DOUBLY CHARGED ION DENSITY,  $n(N^{++})$ , with TIME IN A LARGE  $N^{++} - N^+ - e$  PLASMA FOR INITIAL ION DENSITIES OF  $n(N^{++}) = 10^{12}$ ,  $10^{13}$  and  $10^{14}$   $\text{cm}^{-3}$ .

## Chapter 10. RADIATION OF TENUOUS AIR WITH CONTAMINANTS AT LOW TEMPERATURES

In this chapter we deal with non-equilibrium radiation of air at low temperatures, i.e., primarily below  $6000^{\circ}\text{K}$ , and at low densities. We are considering systems smaller in dimension than the radiative mean free path and under such conditions a Boltzmann distribution among the excited electronic state populations at a definable temperature can only be maintained if collision excitation and de-excitation mechanisms are dominant and are in balance. If the density of the air is low enough, radiative processes will compete with the collision processes, and the excited state populations can deviate significantly from those predicted by LTE. This in turn will drastically affect the radiative properties of the air.

In the following sections we shall discuss radiation from the usual air species and also from impurities which may be found in hot air under a variety of circumstances. In order to see why these impurities may be important, we must first examine some of the general radiative properties of air at low temperatures.

### 10.1 Radiation of air at low temperatures

At low temperatures, where emission of radiation by free-free, free-bound, and bound-bound transitions of ionized air species becomes small, the main radiative contributions in air are from the molecular band and atomic line spectra of the neutral species. For an optically thin gas, the intensity of a given line or band is proportional to the number of atoms or molecules in the electronic state from which the radiative transition

occurs. With the further assumption of LTE, we have that

$$N_1 = N_0 \frac{g_1}{g_0} e^{-E_1/kT} \quad (10.1-1)$$

where  $N_0$  and  $N_1$  are the populations in the ground state and the  $i^{\text{th}}$  excited state respectively,  $g_0$  and  $g_1$  are the statistical weights of these states, and  $E_1$  is the energy of  $i^{\text{th}}$  state above that of the ground state. Thus, in the region where  $E_1 \gg kT$ , the population and the radiation arising from this state decreases very rapidly with decreasing  $T$ .

All the strong transitions in the air species originate from levels which are fairly high above the ground states. The (0,0) transition of the  $N_2$  - First Positive system originates in a state 7.4 eV above the ground state. The equilibrium population of this state decreases about six orders of magnitude from 6000°K to 3000°K, and another six orders of magnitude from 3000°K to 2000°K. The strongest bands of the  $O_2$  Schumann-Runge system originate in an electronic state 6.2 eV above ground level. For NO, the lowest excited electronic levels lie 5.5 and 5.1 eV above ground level and give rise respectively to the  $\beta$  and  $\gamma$  systems. The atomic lines, whose small number makes their contribution insignificant relative to the molecular lines, are subject to the same considerations. It is primarily for these reasons that the equilibrium radiation from pure air, at least in the visible region of the spectrum, decreases so rapidly as the temperature is decreased below about 6000°K (Breene and Nardone, 1962). At 3000°K the emissivity of air is almost entirely due to the NO vibration-

rotation spectra, which lies in the infrared part of the spectrum. (Breene and Nardone, 1962).

In the light of these facts, it is easy to see how the presence of a small amount of impurities which have low-lying excited states can dominate the radiative properties of low temperature equilibrium air. The impurities which are likely to be the most effective in this regard are metallic atoms and monoxides. The dissociation energy of  $N_2$  is comparatively high and impurity nitrides are not likely to be present in any significant amounts. The metallic monoxides, giving rise to band spectra, are particularly important. Unfortunately, information concerning their band systems is very scanty. A summary, compiled by R. W. Nicholls, is given in Appendix B.

## 10.2 Collisional excitation mechanisms

We shall consider three possible collision mechanisms which can excite an atom or molecule  $X$  to a state  $X^*$  :



where  $N_2(v')$  and  $N_2(v'')$  denote nitrogen molecules in  $v'$  and  $v''$  vibrational levels,  $M$  is any atom or molecule, and  $e$  is any electron with enough kinetic energy to excite  $X$ . For reactions such as (10.2-1) and (10.2-3), the number of exciting collisions per sec per  $X$  atom

is given by

$$\eta_e = N \int_0^\infty \sigma_e(u) f(u) u du = N \overline{u \sigma_e} \quad (10.2-4)$$

where  $N$  is the number density of the impacting particle,  $u$  is its velocity,  $f(u)$  is its velocity distribution (assumed always to be Maxwellian), and  $\sigma_e$  is the excitation cross section. Since the impacting particle must have kinetic energy at least equal to the excitation energy  $E$ , the integrand is non-zero only for

$$u \geq \left( \frac{2E}{\mu} \right)^{1/2}$$

where  $\mu$  is the reduced mass of the system. For a reaction of type (10.2-2), where the excitation energy is obtained from and must be less than or equal to the vibrational energy (neglecting rotational effects), we have

$$\eta_e = \sum_{v' \geq v'_0} N_{v'} (u \sigma_e)_{v'} = \sum_{v' \geq v'_0} \frac{N}{Q_{vib}} e^{-\frac{E_{vib}}{kT}} (u \sigma_e)_{v'} \quad (10.2-5)$$

where  $N_{v'}$  is the number density in the  $v'$  vibrational level,  $v'_0$  is the level which has the energy  $E_{vib}$  which is equal to  $E$ , and  $Q_{vib}$  is the vibrational partition function. If we assume that  $u \sigma_e$  is the same for each of the vibrational states in the sum and that the vibrational levels are equally spaced and infinite in number, we obtain (Herzberg, 1950)

$$\eta_e = N e^{-E/kT} \overline{u \sigma_e} \quad (10.2-6)$$

In all cases the number of de-exciting, or quenching collisions per sec per atom,  $\eta_q$ , is obtained by detailed balance from  $\eta_e$ . The two rate coefficients are related by

$$\eta_e = \eta_q \left( \frac{N_2}{N_1} \right)^{eq.} \quad (10.2-7)$$

where  $\left( \frac{N_2}{N_1} \right)^{eq.}$  is the equilibrium ratio of the population of the  $X^*$  state to that of the  $X$  state as defined by Eq. (10.1-1).

Reaction (10.2-3) can be eliminated on the basis of its anticipated negligibly small cross section. Although no actual cross sections are available for this type of excitation, they should be of the same general magnitude as the ionization cross sections for similar collisions. Recent measurements (Utterback and Miller, 1960) on the ionization of  $N_2$  by fast  $N_2$  molecules down to energies of 5 eV above threshold give a cross section decreasing to  $10^{-20} \text{ cm}^2$  at the lowest energy. At low temperatures, these cross sections would yield an excitation rate which is negligible compared to reaction (10.2-1) or (10.2-2).

An expression for the rate of excitation by reaction (10.2-1), i.e., electron impact when  $X$  is a neutral atom and the transition is optically allowed is given by (Allen, 1963)

$$\overline{u\sigma_e} = 10^{-6} \frac{f}{E_{ev}^{3/2}} e^{-E/kT} \text{ cm}^3/\text{sec} \quad (10.2-8)$$

where  $f$  and  $E_{ev}$  are the oscillator strength and energy in eV of the transition. This expression was obtained assuming  $E/kT \gg 1$ , but it

can be used to obtain the excitation rate to within a factor of two as long as  $E/kT > 0.5$ . The corresponding quenching rate is given by

$$\overline{u\sigma_q} = 10^{-6} \frac{g_1}{g_2} \frac{f}{E_{ev}^{3/2}} \text{ cm}^3/\text{sec.} \quad (10.2-9)$$

Applying the formula to the quenching of the sodium D lines we have

$$\overline{u\sigma_q} = 10^{-7} \text{ cm}^3/\text{sec.}$$

The value of the quenching cross section,  $\sigma_q$ , is usually very strongly dependent on the energy of the impacting particle. We can define, however, a  $\overline{\sigma_q}$  such that

$$\overline{\sigma_q} = \frac{\overline{u\sigma_q}}{\overline{u}} \quad (10.2-10)$$

where

$$\overline{u} = \sqrt{\frac{3kT}{\pi m}} \text{ cm/sec.}$$

and  $m$  is the mass of the electron. For the sodium D lines, at  $300^\circ\text{K}$ ,  $\overline{\sigma_q} = 10^{-14} \text{ cm}^2$ . The sodium D lines are discussed mainly because this is the system for which the most data are available. Using the experimental cross section data (Seaton, 1962) and performing a rough integration over a Maxwellian distribution of velocities, good agreement was obtained with the excitation rate given by Eq. (10.2-8). We shall use Eqs. (10.2-8) and (10.2-9) also when  $X$  is a diatomic molecule. The magnitude of the cross sections implied by the use of such a formula are consistent with the limited

data available for this type of excitation (McDaniel, 1964).

Very little is known about reactions of the type (10.2-2). Various experiments have been performed on the quenching of resonance radiation of several types of atoms by  $N_2$ . In the case of sodium, the observed quenching is in all probability due to the reverse of reaction (10.2-2). Using the experimental data for sodium (Mitchell and Zemansky, 1961; Norrish and Smith, 1940; Brehm, et al, 1961) we obtain in the range of  $300^\circ K$  to  $3000^\circ K$

$$\bar{u}_{\sigma_e} \approx 10^{-9} \text{ cm}^3/\text{sec} \quad (10.2-11)$$

This yields a value of  $\bar{\sigma}_q \approx 5 \times 10^{-15}$  at  $300^\circ K$ .

Even less is known when  $X$  in reaction (10.2-2) is a molecule. Recent measurements (Sheridan, et al, 1964) of the quenching of the (2,0) band of the  $N_2^+$  Meinel system by  $N_2$  gave a cross section of about  $10^{-14} \text{ cm}^2$ . However, since only the (2,0) band was observed, the transition may have involved only a vibrational de-excitation. Measurements of the quenching of what is probably the  $N_2^+$  First Negative System in air and possibly also the  $N_2$  Second Positive System (Grün, 1958) yielded

$$Q = \frac{1}{1 + p/11.5} \quad (10.2-12)$$

where  $Q$  is the ratio of radiation emitted to that which would have been emitted without quenching, and  $p$  is the pressure in mm Hg at a temperature of  $300^\circ K$ . If we identify Eq. (10.2-12) with the Stern-Volmer formula (Mitchell and Zemansky, 1961)

$$Q = \frac{1}{1 + \tau \eta_q} \quad (10.2-13)$$

where  $\tau$  is the radiative lifetime, we obtain

$$\frac{p}{11.5} = \tau \eta_q = \tau N_q \overline{\sigma}_q \quad (10.2-14)$$

where  $N_q$  is the number density of quenching particles. Using  $\tau = 6.6 \times 10^{-8}$  sec (Bennett and Dalby, 1959),  $\bar{u} = 0.7 \times 10^5$  cm/sec,  $p \approx 11.5$  mm Hg, and the fact that the transition involves levels with the same weights, we obtain  $\overline{\sigma}_q = \overline{\sigma}_e = 5 \times 10^{-11}$  and  $\overline{\sigma}_q = \overline{\sigma}_e = 7 \times 10^{-16}$  cm<sup>2</sup> if we assume that  $N_2$  is responsible for the quenching. If  $O_2$  is responsible, the cross sections are a factor of four higher. The work of Davidson and O'Neil (1964) indicates that  $O_2$  is about twenty times more efficient than  $N_2$  in quenching the  $N_2$  First and Second Positive Systems in air but no different for  $N_2^+$  First Negative. In both experiments, however, the bulk of the energy of the electron beam used to excite the radiation is deposited in the sample of gas. Under such conditions in air, a complicated time-dependent chemical composition results. Thus, the use of these air results to obtain specific quenching cross sections is unreliable.

For the case of pure nitrogen, the situation is somewhat better. Davidson and O'Neil (1964) obtain a value of  $\overline{\sigma}_q \approx 10^{-15}$  cm<sup>2</sup> for the quenching of  $N_2^+$  First Negative radiation by  $N_2$  molecules. Their data suggest a somewhat smaller value for the  $N_2$  First and Second Positive radiation. Fowler and Holzberlein obtain  $\overline{\sigma}_q$ 's of  $2 \times 10^{-14}$  and  $2 \times 10^{-15}$  cm<sup>2</sup> for the  $N_2^+$  First Negative and the  $N_2$  Second Positive systems respectively. In all of these experiments there is uncertainty concerning what is the actual quenching reaction.

At high degrees of ionization, electron impact will be the dominant mechanism of excitation and quenching. Below 6000°K, excitation of the Na D lines, for example, by molecular vibrational energy transfer becomes dominant when the electron density drops to about  $3 \times 10^{-3}$  that of the

molecular density. The point at which electron impact is no longer dominant for other radiating systems depends on the specific cross sections, but very likely is not significantly different from the sodium value.

### 10.3 Collision limiting of radiation

We now consider the ability of the collision processes discussed above to maintain a Boltzmann distribution among the radiating electronic levels of a tenuous sample of contaminated air. This gas is assumed to be, unless stated otherwise, optically thin to the radiation in question. In addition, it is assumed that no external source of radiation is present.

For such a system only collisional excitation, de-excitation and radiative de-excitation between two states, 1 and 2, of any species are important. From Eqs. (8.3-9), (8.3-10), and (10.2-7) (neglecting terms due to absorption and induced emission), we have

$$\frac{N_2}{N_1} = \frac{\eta_e}{\eta_q + A_{21}} = \frac{\eta_e \tau}{1 + \eta_q \tau} = \left( \frac{N_2}{N_1} \right)^{\text{eq.}} \frac{\eta_q \tau}{1 + \eta_q \tau} \quad (10.3-1)$$

where  $A_{21}$  is the Einstein transition probability. The condition for the equilibrium ratio is that  $\eta_q \tau$  is much greater than unity; if  $\eta_q \tau$  is of the order unity, the population ratio will deviate from equilibrium. If  $\eta_q \tau \ll 1$  and  $N_1$  is the ground state, the population of the excited state,  $N_2$ , is reduced by a factor  $\eta_q \tau$  from its equilibrium value. The radiation arising from this state, in the optically thin case, is given by

$$I_{\text{em}} = N_2 h \nu A_{21} \text{ ergs/cm}^3\text{-sec} \quad (10.3-2)$$

where  $h\nu = E_{21}$ . This, too, is reduced below its equilibrium value by the factor  $\eta_q \tau$ . Using Eqs. (10.3-1), (10.3-2) and the assumption that  $\eta_q \tau \ll 1$ , we obtain

$$I_{em} = N_1 h\nu \eta_e \text{ ergs/cm}^3\text{-sec} \quad (10.3-3)$$

where  $h\nu = E_{21}$ . This is the same result obtained in Chapter 8, i.e., that every excitation results in an emission of a photon.

When the conditions of collision limiting of radiation exist in a gas, the radiation can no longer be characterized by the temperature (defined by the particle velocity distribution), density and the various Einstein coefficients or oscillator strengths of the transitions. The radiation can then be obtained only when the rates of all processes which are significant in exciting and quenching the radiation are known. To determine when these conditions exist in air at low temperatures for a particular transition, we shall define a concentration of electrons or molecules,  $N_c$ , such that

$$N_c = \frac{1}{\overline{\sigma}_q \tau} \quad (10.3-4)$$

We shall consider cases in which either the molecules or electrons, but not both, are the important quenchers. Thus,  $N_c$  is the concentration at which  $\eta_q \tau = 1$ . If the actual concentration of electrons or molecules is less than the corresponding value of  $N_c$ , the radiation will be considered collision limited. For electron de-excitation we shall use the rate given by Eq. (10.2-11). For quenching by molecules we shall take

$$\overline{\sigma}_q = 3 \times 10^{-10} \text{ cm}^2/\text{sec.}$$

Expressing  $\tau$  in terms of the  $f$  number and wavelength,  $\lambda$ , in cm, we obtain

$$\tau = \frac{3}{2} \frac{\lambda^2}{f} \frac{g_2}{g_1} \text{ sec.} \quad (10.3-5)$$

Thus, for electron de-excitation,

$$N_C \text{ (electrons)} = 6.7 \times 10^5 \frac{E_{\text{ev}}^{3/2}}{\lambda^2} \quad (10.3-6)$$

and for molecular quenching, with  $g_1 = g_2$ ,

$$N_C \text{ (molecules)} = 2.2 \times 10^9 \frac{f}{\lambda^2} \quad (10.3-7)$$

The wavelength range of principal interest is between the near ultraviolet and the near infrared. Some calculated values of  $N_C$  are shown in Table 10.1.

Table 10.1		
$\lambda$ (Angstroms)	$N_C$ (electrons)	$N_C$ (molecules)
2500	$1.2 \times 10^{16}$	$3.5 \times 10^{18} f$
5000	$1.0 \times 10^{15}$	$8.7 \times 10^{17} f$
7500	$2.5 \times 10^{14}$	$3.8 \times 10^{17} f$
10000	$9.3 \times 10^{13}$	$2.2 \times 10^{17} f$

The dominant transitions arising from neutral air species ( $O_2$  Schumann-Runge,  $N_2$  First and Second Positive,  $NO$   $\beta$  and  $\gamma$ )

and most important line and impurity radiation have  $f$  numbers of 0.001 and greater. Thus, at 3000°K, for example, we can expect non-LTE for the excited state populations and radiation when the electron density and molecular concentrations fall below about  $10^{14} \text{ cm}^{-3}$ . This corresponds to density ratios,  $\rho/\rho_0 \leq 10^{-4}$ , if we assume at most single ionization. If the degree of dissociation is large and the degree of ionization is small, the radiation will be collision limited at even higher densities, particularly if the  $f$  number is large.

When the radiating species is an ion such as  $\text{N}_2^+$  rather than a neutral atom or molecule the electron excitation rate (Allen, 1963) and molecular excitation rate (see Chapter 3) are in general an order of magnitude larger and collision limiting occurs at a lower density than for neutrals.

An interesting consequence of the type of non-equilibrium we have discussed here concerns the radiation arising from forbidden transitions. The excitation cross sections for electron impact excitation of selected forbidden transitions given in Allen, (1964), imply a rate coefficient,  $U\sigma_q$ , the order of  $10^{-10} \text{ cm}^3/\text{sec}$ . Since the lifetimes of these forbidden lines are very long, one second or more, this radiation would be in equilibrium at much lower densities than the allowed radiation. At these densities the forbidden radiation would be greatly enhanced relative to the allowed transitions, and recourse to non-thermal excitation mechanisms may not be necessary to explain the observance of such situations, particularly in gases of large dimensions.

In the foregoing treatment it was assumed that the population of vibrational levels of the molecules was in equilibrium at the kinetic temperature of the particles. This situation will not always hold, since the population

of vibrational levels is subject to the same considerations we have discussed for the populations of electronic states. The lifetimes of the vibrational states are much longer, however, than the allowed electronic transitions. A typical lifetime of a vibrational state is about 1 second (Penner, 1959). As in the case of the metastable electronic levels, the populations of vibrational states should remain in equilibrium to much lower densities than the allowed electronic populations. Another consideration is that, in the case of a gas which has cooled from a higher temperature, the vibrational degrees of freedom have not had time to relax. The population of vibrational states may have a Boltzmann-type distribution, but corresponding to a higher temperature than the temperature of translational degrees of freedom. Still another related consideration is whether the Maxwellian temperature of the electrons is the same as that of the radiating particles.

Although we have dealt with optically thin gases only, it was shown in Chapter 8 that similar considerations apply to the optically thick case. No matter how large the dimensions of the sample of air, if the time between quenching collisions is longer than the radiative lifetime of an excited state, the radiation from this state will be reduced from its equilibrium value.

#### 10.4 Excitation by electron recombination

Heretofore we have discussed only thermal excitation. Two examples of other types of reactions which involve the creation or destruction of an excited electronic state are





For reaction (10.4-2), when  $X$  is sodium and  $Y$  and  $Z$  are hydrogen atoms, a rate coefficient of  $2 \times 10^{-32} \text{ cm}^6/\text{sec}$  has been measured (Padley and Sugden, 1958). This is probably a typical value for either reaction. In an un-ionized and fully dissociated gas, these reactions could become dominant for excitation of electronic states.

In a gas which has been expanded and cooled from an initial fully ionized state the most important non-thermal excitation mechanism is electron recombination. The various collisional and radiative processes involved have been discussed in detail in Chapter 9. The rates of recombination have been computed for hydrogen and pseudo-alkali plasmas and are expressed as two-body rates (Bates, Kingston, and McWhirter, 1962).

As an example of the importance of the collisional-radiative mechanism, let us consider air which has expanded and cooled to  $2000^\circ\text{K}$  and a density of  $10^{-7} \rho_0$  from a fully ionized state. We shall further assume that molecules have not had time to form but that electron recombination has reduced the electron density to a value of  $5 \times 10^9 \text{ cm}^{-3}$ . This would correspond to a degree of ionization of about  $10^{-3}$ . The equilibrium radiation rate from air at  $2000^\circ\text{K}$  and  $\rho = 10^{-7} \rho_0$  in the visible photographic region of the spectrum ( $4000 - 6500 \text{ \AA}$ ) is about  $10^{-14} \text{ watts/cm}^3$  which was obtained by extrapolation from the values given by Gilmore (1964). Since practically all this radiation is from molecular species which we have assumed are not present and since, from Table 10.1, we would expect the radiation to be severely collision limited, the actual radiative rate would be

many orders of magnitude lower.

Now let us consider the effect of electron recombination. The numerical results of the last chapter do not apply since the number of neutrals is too large compared to the electrons. If we assume, however, that each recombination results in the production of one photon in the visible photographic region we obtain a radiation rate of about  $3 \times 10^{-11}$  watts/cm<sup>3</sup>, where we have taken the air atoms to be hydrogenic and the recombination coefficient,  $\alpha$ , equal to  $3.5 \times 10^{-12}$  (Bates, et al, 1962). If one were to try to estimate the temperature from the observed radiation using the assumption of LTE the value obtained would be too high. Here, as in the previous chapter, the populations of excited states are determined by the electron density, which is well above its equilibrium value. The Maxwellian temperature of the particles is not important as regards the radiation since thermal excitation and quenching are not important.

In the case of the recombination and radiation from the contaminants in air the situation is somewhat different. Since the number density of the impurity atoms is much smaller than the density of air atoms the electron density and electron temperature are determined by the air recombination as described in Chapter 9 at least until the degree of air ionization becomes small. During this time the electron temperature,  $T_e$ , is about 8000°K, if oxygen and nitrogen can be considered hydrogenic. The recombination of the impurity ions is governed by the equation

$$\frac{dI^+}{dt} = -\alpha' X^+ n_e + S' X n_e \quad (10.4-3)$$

where  $X$  and  $X^+$  are the number densities of the impurity neutrals and ions,  $n_e$  is the electron density, and  $\alpha'$  and  $S'$  are the recombination and ionization coefficients corresponding to the particular impurity species. Bates, et al (1962) have computed  $\alpha'$  and  $S'$  for a pseudo-alkali species with an ionization potential of 3.9 eV by using hydrogen with the ground state rendered inaccessible. The values of  $\alpha'$  are not significantly different from the hydrogenic values, but the values of  $S'$ , for 4000°K and 8000°K are very much greater than the hydrogenic values. If we set Eq. (10.4-3) equal to zero we obtain for the steady state condition

$$\frac{X^+}{X} = \frac{S'}{\alpha'} \quad (10.4-4)$$

until the value of  $S'/\alpha'$  becomes of the order unity or less no appreciable recombination can take place. For the pseudo-alkali species this does not occur, for all values of  $n_e$ , until the electron temperature falls below 4000°K. Thus the impurity ionization will not begin to disappear until most of the air has recombined. If we assume that roughly

$$S' \propto \exp \left( - \frac{I_p}{kT_e} \right) \quad (10.4-5)$$

where  $I_p$  is the impurity ionization potential, then the above conclusion would hold for any impurity with  $I_p < 8$  eV. The radiation arising from these impurities would be proportional to the various ion densities as well as to the electron density.

#### 10.5 Conclusions

The principal conclusion we can reach from the various considerations of thermal and non-thermal excitation is that in low density (i.e.,  $\frac{p}{p_0} < 10^{-3}$ ) and low temperature air (i.e.,  $T < 6000^\circ\text{K}$ ), the assumption of LTE excited state populations is not justified. In any particular case the rate of radiation must be calculated in a detailed manner taking into account all mechanisms which create or destroy the radiating states. Of particular importance will be the radiation arising from electron recombination. Here, as in the equilibrium case, metallic impurities will be of greater importance than their relative concentrations would indicate.

### References

- Allen, C.W., *Astrophysical Quantities*, The Athlone Press, London (1963).
- Bates, D.R., A.E. Kingston and R.W.P. McWhirter, *Proc. Roy. Soc. A* 267, 297 (1962) and 270, 155 (1962).
- Bennett, R.G. and F.W. Dalby, *J. Chem. Phys.* 31, 434 (1959).
- Breene, R.G., and M.C. Nardone, *J. Quant. Spect.* 2, 272 (1962).
- Brehm, B., W. Demtröder, O. Osberghaus, and H. Ehrhardt, *Second Conference on the Physics of Electronic and Atomic Collisions*, Univ. of Colorado (1961).
- Davidson, G. and R. O'Neill, *J. Chem. Phys.* 41, 3946 (1964).
- Fowler, R.G. and T.M. Holzberlein, *J. Chem. Phys.* 45, 1123 (1966).
- Gilmore, F.R., *Approximate Radiation Properties of Air Between 2000 and 8000°K*, RM-3997-ARPA, The RAND Corp., Santa Monica, Calif. (1964).
- Grün, A.E., *Can. Jour. Phys.* 36, 858 (1958).
- McDaniel, E.W., *Collision Phenomena in Ionized Gases*, John Wiley and Sons, New York (1964).
- Mitchell, A.C.G., and M.W. Zemansky, *Resonance Radiation and Excited Atoms*, Cambridge Univ. Press, London (1961).
- Norrish, R.G.W. and W.M. Smith, *Proc. Roy. Soc. A* 176, 295 (1940).
- Padley, P.J. and T.M. Sugden, *Proc. Roy. Soc. A* 248, 248 (1958).
- Penner, S.S., *Quantitative Molecular Spectroscopy and Gas Emissivities*, Addison-Wesley, Reading, Mass. (1959).
- Seaton, M.J., *Atomic and Molecular Processes*, ed. by D.R. Bates, Academic Press, New York (1962).
- Sheridan, W.F., O. Oldenberg, and N.P. Carleton, *Atomic Collision Processes*, *Proceedings of the 3rd Conference on Electronic and Atomic Collisions*, ed. by M.R.C. McDowell, North-Holland Publishing Co., Amsterdam (1964).
- Utterback, N.G. and G.H. Miller, *Proceedings of the Atomic and Molecular Beams Conference*, Univ. of Denver (1960).

## APPENDIX A. - The Approach to Equilibrium of a Displaced System

The approach of a displaced system to equilibrium has been a topic of great interest since the earliest days of statistical mechanics. It was first considered by Boltzmann and the proposition that displaced systems do indeed approach the correct statistical equilibrium described by statistical mechanics is usually called the "Boltzmann H-Theorem". The feature of the discussion presented here is that chemical reactions and radiation are explicitly considered. Most discussions are so very general that the working machinery of statistical thermodynamics is not used, or they are limited to energy distribution displacements of systems. For a more rigorous treatment of the H-Theorem the work of Tolman (1938) should be consulted. Reviews of statistical mechanics which present the most modern point of view on the H-Theorem have been given by Cohen (1962) and de Boer and Uhlenbeck (1962).

In Chapter 6 a rigorous proof is presented that systems with small displacements from equilibrium approach the equilibrium state, a conclusion which depends upon the linearity of the equations for such systems. The displacements of this treatment are arbitrarily large.

Consider the function  $H$  defined as

$$-H = \sum_{s,j} \ln \frac{g_{sj}^{N_{sj}}}{N_{sj}!} + \sum_v \ln \frac{(g_v + N_v)!}{g_v! N_v!} \quad (A1.)$$

The first term on the RHS of Eq. (A1.) gives the contribution of the material particles, and the second term gives the contribution of the radiation. The quantities  $g_{sj}$  and  $g_v$  give the number of states within small energy intervals (or frequency intervals) sometimes called "cells." These expressions arise from the requirement that

$$-H = \ln W \quad (A2.)$$

where  $W$  is the total number of possible arrangements of the particles (or photons) in the accessible cells. The second expression on the RHS of Eq. (A1.) recognizes the boson character of the photon; we have dropped unity as small in comparison with  $g_v^*$ . For the equilibrium state  $-H$  reduces to  $S/k$ , the entropy divided by the Boltzmann constant.

---

\* The expression for bosons is more properly

$$W = \frac{(g_v + N_v - 1)!}{N_v! (g_v - 1)!}$$

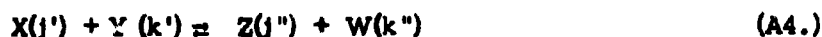
but the unity is always dropped.

Consider the rate of change of  $-H$  as the occupations of states change because of the natural time development of the system

$$\frac{d}{dt} (-H) = \sum_{sj} \frac{dN_{sj}}{dt} \ln \frac{g_{sj}}{N_{sj}} + \sum_v \frac{dN_v}{dt} \ln \frac{g_v + N_v}{N_v} \quad (A3.)$$

The Stirling approximation for the factorials has been made to obtain Eq. (A3.) from Eq. (A1.).

The only changes which can occur result from collision processes of the particles and absorption and emission of photons. We can write the summations of Eq. (A1.) in terms of the radiative and non-radiative processes of the system. Consider first a bimolecular non-radiative process



which has a forward rate constant  $k_{xy}^{j'k'}$  and a reverse rate constant  $k_{xy}^{j''k''}$ .

Thus we have that

$$-\frac{dN_{xj'}}{dt} = -\frac{dN_{yk'}}{dt} = \frac{dN_{zj''}}{dt} = \frac{dN_{wk''}}{dt} = k_{xy}^{j'k'} N_{xj'} N_{yk'} - k_{xy}^{j''k''} N_{zj''} N_{wk''} \quad (A5.)$$

This process contributes four terms to  $\frac{d}{dt} (-H)$ , and they combine as

$$(k_{xy}^{j'k'} N_{xj'} N_{yk'} - k_{xy}^{j''k''} N_{zj''} N_{wk''}) \ln \frac{g_{xj'} g_{yk'} N_{zj''} N_{wk''}}{g_{zj''} g_{wk''} N_{xj'} N_{yk'}} \quad (A6.)$$

Let us introduce the equilibrium concentration,

$$N_{xj}^0 = g_{xj} e^{-\alpha_x E_{xj}/kT} \quad (A7.)$$

the equilibrium constant,

$$K_{xy}^{j'k'} = \frac{k_{xy}^{j'k'}}{k_{xy}^{j''k''}} = \frac{N_{zj}^0 N_{wk}^0}{N_{xj}^0 N_{yk}^0} = \frac{g_{zj} g_{wk}}{g_{xj} g_{yk}} \quad (A8.)$$

and the relative concentrations,

$$\eta_{xj} = \frac{N_{xj}}{N_{xj}^0}, \text{ etc.} \quad (A9.)$$

In Eq. (A8.) we have used conservation of energy and free energy, which is valid for all collision processes. Using Eqs. (A7.), (A8.) and (A9.) we can write Eq. (A6.) as

$$-k_{xy}^{j'k'} N_{xj}^0 N_{yk}^0 (\eta_{xj} \eta_{yk} - \eta_{zj} \eta_{wk}) \ln \frac{\eta_{zj} \eta_{wk}}{\eta_{xj} \eta_{yk}} \quad (A10.)$$

We note that Eq. (A10.) is a quantity which can only be positive. The bracket and logarithm terms have opposite signs, and so one of them must be negative, combining with the negative sign in front to give a positive definite quantity. No values of the  $\eta$ 's are excluded, and thus the displacement from equilibrium can be quite arbitrary. The contribution of each non-radiative collision processes must be of the form of Eq. (A10.). As a result of such processes the quantity  $-H$  can only increase.

Now let us consider radiative processes. We shall neglect scattering, and so the only process of interest is

$$X_{j'} = X_{j''} + h\nu \quad (A11.)$$

For this radiative process we have

$$-\frac{dN_{xj'}}{dt} = \frac{dN_{xj''}}{dt} = \frac{dN_\nu}{dt} = AN_{xj'}(N_\nu + g_\nu) - BN_{xj''}N_\nu \quad (A12.)$$

where the A and B are the Einstein coefficients. This process contributes three terms to  $\frac{d}{dt}(-H)$  and they combine to give

$$-\left[AN_{xj'}(N_\nu + g_\nu) - BN_{xj''}N_\nu\right] \ln \frac{g_{xj'}}{g_{xj''}} \frac{N_\nu N_{xj''}}{(g_\nu + N_\nu) N_{xj'}} \quad (A13.)$$

It can be shown that the Einstein coefficients satisfy the relationship

$$\frac{A}{B} = \frac{N_{xj''}^0}{N_{xj'}^0} \frac{N_\nu^0}{N_\nu^0 + g_\nu} = \frac{g_{xj''}}{g_{xj'}} \quad (A14.)$$

Using Eqs. (A14.), (A7.) and the relations

$$N_\nu^0 = g_\nu (e^u - 1)^{-1} \quad (A15.)$$

$$\eta_\nu = N_\nu / N_\nu^0 \quad (A16.)$$

where

$$u = h\nu/kT \quad (A17.)$$

we get for the contribution to  $\frac{d}{dt}(-H)$  of process (Eq. (A11.))

$$- BN_{xj}^0 N_v^0 \left[ \eta_{xj} \{ 1 + (\eta_v - 1)e^{-u} \} - \eta_{xj} \eta_v \right] \ln \frac{\eta_{xj} \eta_v}{\eta_{xj} \{ 1 + (\eta_v - 1)e^{-u} \}} \quad (A18.)$$

As before, this is a term which can only be positive.

We find, therefore, that as a result of all processes by which the occupation numbers of a displaced system can change

$$\frac{d}{dt}(-H) > 0 \quad (A19.)$$

The alternative to the increase in  $-H$  is that its rate of change is zero, and this occurs when all  $\eta$ 's for matter particles and photons are unity. It is customary to identify the maximum value of  $-H$  with  $S/k$ , and the statistical calculation of the properties of air is consistent with this procedure (Gillmore, 1966).

It should be noted that the reaction rates used in this section are average rates and not instantaneous rates. This is, of course, the standard procedure used in reaction kinetics. The theorem demonstrated here shows that  $-H$  increases on the average if it changes at all. There can, of course, be instantaneous decreases in its value.

### References

- Cohen, E.G.D., Fundamental Problems in Statistical Mechanics, North Holland Publishing Co., Amsterdam (1962).
- de Boer, J. and Uhlenbeck, G.E., Studies in Statistical Mechanics, Vol. 1, North Holland Publishing Co., Amsterdam (1962).
- Gilmore, F.R., The Equilibrium Thermodynamic Properties of Air, Lockheed, Palo Alto (1966).
- Tolman, R.C., The Principles of Statistical Mechanics, Oxford University Press, London (1938).

## APPENDIX B. - Table of the States and Spectra of the Metallic Monoxides

In the following table, the known energy levels, transitions, and wavelength ranges are reviewed for the monoxides which have levels low enough to be abundantly excited below  $6000^{\circ}\text{K}$ , and which radiate in the visible and near infrared regions of the spectrum. It should be stressed that this summary reviews only the gross spectroscopy of the oxides. In only a few cases have vibrational and rotational analyses of the band been made and definitive vibrational and rotational constants been derived. There is still much discussion of the identity of many of the electronic states, the transition assignments, and the relative certainty of many of the term values. Virtually nothing is known about the absolute transition probabilities of these bands and very little about the relative emission intensities within these band systems.

Conspicuously absent are the monoxides of the alkali metal ( $\text{LiO}$ ,  $\text{NaO}$ ,  $\text{KO}$ , etc.). Spectra of these monoxides have never been reported in the literature, and a search for such spectra by shock excitation of higher alkali oxides was unsuccessful.

Table of the States and Spectra of the Monoxides

Column 1 gives the molecule and its ground state, where known. Columns 2 and 3 give the higher states and energies. Columns 4 and 5 are the initial and final states of the transition whose name is given in Column 6. Columns 7 and 8 give the maximum initial and final vibrational transitions, and Column 9 the wavelengths of the transition.

<u>Molecule</u>	<u>State</u>	<u>Energy</u>	<u>F.S.</u>	<u>System</u>	<u>v'</u>	<u>v''</u>	<u>Wave Lengths</u>
<u>AlO</u> ( <sup>2</sup> Σ)	A <sup>2</sup> Σ	2.56	X	Green	7	7	5424 - 4374
	B(?)	4.1	X	Violet	2	1	3112 - 2500
<u>BeO</u> ( <sup>1</sup> Σ)	A <sup>1</sup> Π	1.18	X	Red 1	9	2	11600 - 5600
	B <sup>1</sup> Σ <sup>+</sup>	2.63	X	Blue-Green	7	5	5495 - 4180
			A	Red 2	7	4	11600 - 4750
	C(Σ?)	4.85	A	Harvey-Bell	1	0	3485 - 3247
	D <sup>1</sup> Π	5.1	A	Bengtsson	1	2	3368 - 3134
<u>BiO</u> ( <sup>2</sup> Σ)	A <sup>2</sup> Σ	1.78	X	Red	8	5	8282 - 5564
	B <sup>2</sup> Π	3.46	X	Violet	5	0	3577 - 3173
	C <sup>2</sup> Π	5.4	X	Ultra-Violet	2	2	2637 - 2440
<u>CaO</u> ( <sup>1</sup> Σ)	A <sup>1</sup> Σ	0.94	X	Red	5	3	9229 - 7308
	B <sup>1</sup> H	3.2	X	Blue	-	-	4519 - 3373
	C <sup>1</sup> Σ	3.6	X	Ultra-Violet	3	3	3753 - 3287
	?	-	-	Far I.R.	-	-	10533 - 9193
<u>CeO</u>	A	1.56	X	-	-	-	8396 - 7380
X(?)	B	1.73	X	-	-	-	6847 - 7716
X <sup>1</sup> (?)	A <sup>1</sup>	2.56	X <sup>1</sup>	-	-	-	4863 - 4683
	B <sup>1</sup>	2.6	X <sup>1</sup>	-	-	-	4792 - 4614

<u>Molecule</u>	<u>State</u>	<u>Energy</u>	<u>F.S.</u>	<u>System</u>	<u>v'</u>	<u>v''</u>	<u>Wave Lengths</u>
<u>CuO</u> ( <sup>2</sup> Σ <sup>+</sup> )	A <sup>2</sup> Σ <sup>+</sup>	2.03	X	Orange	-	-	6547 - 5827
	B	2.6	X	Green	-	-	5344 - 5237
	C	?	X	Violet	-	-	5392 - 4197
<u>CrO</u> ( <sup>5</sup> Π?)	A( <sup>5</sup> Π?)	2.05	X	Green	4	4	6891 - 5168
<u>FeO</u>	A	0.62	X	Far I.R.	-	-	~ 2μ
	B	2.1	X	Orange	-	-	6650 - 5289
	C	2.1	X	Orange	-	-	6650 - 5289
	D	2.23	X	I.R.	-	-	9408 - 6700
			X	Orange	-	-	6650 - 5287
	E	2.76	X	Violet	-	-	4292 - 4386
<u>LaO</u> ( <sup>2</sup> Σ)	A <sup>2</sup> Π	1.6	X	Red	2	3	8526 - 6994
	B <sup>2</sup> Σ	2.22	X	Yellow	3	5	6243 - 5778
	C <sup>2</sup> Π	2.82	X	Blue	3	3	4594 - 4348
	D	3.5	X	Ultra-Violet	-	-	3710 - 3457
	F	3.5	X	Ultra-Violet	-	-	3710 - 3457
<u>MgO</u> ( <sup>1</sup> Σ)	A <sup>1</sup> Π	0.445	X	Far I.R.	-	-	~ 2.8μ
	B <sup>1</sup> Σ	2.48	Z	Red	3	2	5581 - 5286
			X	Green	7	7	5206 - 4801
	C <sup>1</sup> Σ	3.84	A	Violet	1	1	3762 - 3820
<u>MnO</u>	A	2.2	X	-	5	6	6556 - 5050
<u>NiO</u>	A	1.57	X	I.R.	4	6	9195 - 7910
	B	2.04	X	Red	3	3	6605 - 5529
	a	?	-	-	-	-	-
	b	a+2.68	a	Blue	7	2	4849 - 4145

<u>Molecule</u>	<u>State</u>	<u>Energy</u>	<u>F.S.</u>	<u>System</u>	<u>v'</u>	<u>v''</u>	<u>Wave Lengths</u>
<u>ScO</u> ( <sup>2</sup> Σ)	A <sup>2</sup> Π	2.06	X	Red	6	5	7300 - 5740
	B <sup>2</sup> Σ	2.48	X	Blue	4	2	5330 - 4500
<u>SnO</u> ( <sup>1</sup> Σ)	A <sup>1</sup> Σ	1.45	X	I.R.	3	3	10427 - 7861
	B <sup>1</sup> Π	3.1	X	Blue	2	7	4692 - 3897
	C <sup>1</sup> Σ	3.5	X	Ultra-Violet	3	1	3587 - 3336
<u>TaO</u>	?	?	-	-	-	-	9920 - 3625
<u>TiO</u>	A <sup>3</sup> Δ	1.75	X	γ-Red	4	5	7948 - 6215
	B	2	X	Orange-Red	2	1	6629 - 5849
X <sup>3</sup> Π	C <sup>3</sup> Π	2.4	X	α-Blue-Green	4	5	6214.9 - 4762.1
a <sup>1</sup> Δ	a <sup>1</sup> Σ	a+1.1	-	-	-	-	-
	b <sup>1</sup> Π	a+1.4	a <sup>1</sup>	I.R.-2	1	1	11302 - 10025
			a	I.R.-1	3	3	9094 - 8859
	c <sup>1</sup> Σ	a+2.2	a	β-Orange	4	4	5733 - 5597
<u>VO</u> ( <sup>2</sup> Δ)	A <sup>2</sup> Δ	2.16	X	-	3	6	8643 - 5010
	B(?)	1.56	X	-	-	-	8666 - 7334
<u>WO</u>	-	-	-	-	-	-	4110 - 7743
<u>ZnO</u>	-	-	-	-	-	-	9500 - 7600

### References and Comments for Monoxides Table

- AlO The best known system - the green system - has been vibrationally analyzed and some bands have been studied experimentally.
- Lagerqvist, Nilsson and Borrow, Ark. Fys. 12, 543 (1957)  
Pomeroy, Phys. Rev. 29, 59 (1927)  
Shimauchi, Science of Light 7, 101 (1958)  
Cohen and Rosen, Mem. Soc. Roy. Sci. Liege, 405 (1941)
- BeO BeO is the first member of the alkaline earth oxides, all of which (BeO, MgO, CaO, SrO, BaO) exhibit similar energy level arrays. They have been studied by Lagerqvist, et al, spectroscopically and have also received attention from the thermochemists. There is great doubt that  $X^1\Sigma^+$  is the ground state since it does not dissociate into ground state atoms. There are also triplet systems observed, six bands at 3247<sup>0</sup>A and six at 3357. The states are unknown.
- A. Lagerqvist, Band Spectrum of BeO (Thesis, Stockholm, 1948)
- BiO Scavi, Acts Phys. Hungar 6, 73 (1956)  
Bridge and Howell, Proc. Phys. Soc. 67, 44 (1954)
- CaO Hulthen and Lagerqvist, Ark. Fys. 2, 471 (1951)  
Lagerqvist, Ark. Fys. 8, 83 (1954)  
Meggers, J. Res. N.B.S. 10, 669 (1933)
- CeO Poor vibrational analyses, nothing known of states.
- Watson, Phys. Rev. 53, 639 (1938)
- CuO Vaguely understood systems, with no dependable vibrational analysis.
- Absolute position of C is unknown.
- Loomis and Watson, Phys. Rev. 48, 280 (1935)  
Guentsch, Ark. Mat. Astr. Fys. A 33, No. 2 (1946)

- CrO Character of electronic states is unknown.  
Ninomiya, J. Phys. Soc. Japan 10, 829 (1955)
- FeO Vibrational analyses very fragmentary. No specifications of electronic states. The ground state may not be X.  
A. G. Gaydon, Ph.D. Thesis, London 1937  
Delseneme and Rosen, Bull. Soc. Roy. Liege 70 (1945)
- LaO Meggers and Wheeler, J. Res. N.B.S. 6, 239 (1931)  
Hautecler and Rosen, Bull. Acad. Roy. Liege 45, 790 (1959)
- MnO Fragments of other systems, including suspected triplet transitions reported. The ground state may not be  $^1\Sigma$ , but  $^3\Sigma$ , a few  $1000\text{ cm}^{-1}$  below it. See discussion in second reference below.  
Brewer, Trajmar and Berg, Astrophys. J. 135, 955 (1962)  
Brewer and Trajmar, J. Chem. Phys. 36, 1585 (1962)
- MnO No knowledge of the electronic states.  
Das Salma, Zeit. f. Phys. 157, 98 (1959)
- NiO No definitive knowledge of the electronic states.  
Mulet and Rosen, Bull. Soc. Roy. Liege, 382 (1945)
- ScO Meggers and Wheeler, J. Res. N.B.S. 6, 239 (1931)
- SrO The ground state may not be X.  
Almqvist and Lagerqvist, Ark. Fys. 1, 477 (1949); 2, 233 (1950); 8, 481 (1954)
- TaO Bands reported between 9920 and 3625. Nothing known of electronic transitions.  
Premaswarup, Ind. J. Phys. 29, 109 (1955); Nature 180, 602 (1957)
- TiO There is doubt as to the identify of the ground state. Singlets and Triplets are seen in absorption. Relative position of a and X is not known.  
Phillips, Astrophys. J. 111, 314 (1950); 114, 152 (1951)  
Pettersson, Ark. Fys. 16, 185 (1959); Naturwiss. 48, 128 (1961)

VO Lagerqvist and Selin, Ark. Fys. 11, 429 (1959); 12, 553 (1957)

WO A number of unanalyzed bands between 4110 and 7743.

Gatteren and Krishnamurty, Nature 169, 543 (1952)

Vittocher and Krishnamurty, Arv. Sci. 23, 57 (1954)

ZrO Triplet bands in yellow, green and blue. Singlet bands in ultra-violet. Unanalyzed and unassigned bands in IR (9500-7600 Å).

Afaf, Proc. Phys. Soc. A 63, 1156 (1950)

Akerlind, Ark. Fys. 11, 395 (1956)

Lagerqvist, Uhler and Barrow, Ark. Fys. 8, 281 (1954)

Uhler and Akerlind, Ark. Fys. 10, 431 (1956)

UNCLASSIFIED

Security Classification

## DOCUMENT CONTROL DATA - R &amp; D

(Security classification of title, body of abstract and indexing annotation must be entered when the overall report is classified)

1. ORIGINATING ACTIVITY (Corporate author)		2a. REPORT SECURITY CLASSIFICATION	
Lockheed Missiles & Space Company		Unclassified	
3. REPORT TITLE		2b. GROUP	
THERMAL RADIATION PHENOMENA VOL. 4 EXCITATION AND NON-EQUILIBRIUM PHENOMENA IN AIR			
4. DESCRIPTIVE NOTES (Type of report and inclusive dates)			
Final Report, 4th out of a series of 6.			
5. AUTHOR(S) (First name, middle initial, last name)			
Rolf K. Landshoff and John L. Magee			
6. REPORT DATE	7a. TOTAL NO. OF PAGES	7b. NO. OF REFS	
November, 1967	295	210	
8a. CONTRACT OR GRANT NO.	8b. ORIGINATOR'S REPORT NUMBER(S)		
DA-49-146-XZ-198	DASA 1917-4		
A. PROJECT NO.	8c. OTHER REPORT NO(S) (Any other numbers that may be assigned this report)		
	3-27-67-1 Vol. 4		
9. DISTRIBUTION STATEMENT			
Distribution of this document is unlimited.			
11. SUPPLEMENTARY NOTES		12. SPONSORING MILITARY ACTIVITY	
		Defense Atomic Support Agency Washington, D.C. 20305	
13. ABSTRACT			
<p>The report deals with excitation and non-equilibrium phenomena in air that has been subjected to a large amount of radiation. The following topics are covered; Absorption and scattering of X-rays and gamma rays in air. Collisions of ions and electrons with air molecules. Secondary processes following this excitation. This includes the creation of various chemical species. X-ray heating and shock heating of air with special reference to very high energy densities. The approach to composition equilibrium in low and high temperature air. Adiabatic, near equilibrium cooling of air and the formulation of a criterion for local thermodynamic equilibrium. Non-equilibrium radiative transport and its effect on the total amount and the spectrum of emitted radiation. Radiation in tenuous air at high temperatures. Radiation in tenuous air with contaminants at low temperatures. The report has two appendices. One discusses mathematical aspects of the approach to equilibrium of a displaced system. The other one presents a table of the states and spectra of the Metallic Monoxides.</p>			

DD FORM 1473

REPLACES DD FORM 1473, 1 JAN 64, WHICH IS OBSOLETE FOR ARMY USE.

UNCLASSIFIED  
Security Classification

UNCLASSIFIED

Security Classification

KEY WORDS	LINK A		LINK B		LINK C	
	ROLE	WT	ROLE	WT	ROLE	WT
excitation						
non-equilibrium						
irradiated air						
X-rays						
ions						
electrons						
collisions						
absorption						
heating						
cooling						
relaxation						
chemical composition of irradiated air						
radiative transport						
strong shocks						
electron recombination						

UNCLASSIFIED

Security Classification